



On the Energy Efficiency of Cooperative Wireless Networks

Ph.D. Dissertation by

Jesús Gómez Vilardebó

Advisor: Prof. Ana I. Pérez Neira

**Department of Signal Theory and Communications
Universitat Politècnica de Catalunya (UPC)**

Dissertation Submitted, June 2009

© Copyright by Jesús Gómez Vilardebó 2009

All rights reserved

A mis padres, hermana y a Ester

Summary

The aim of this dissertation is the study of cooperative communications in wireless networks. In cooperative networks, each user transmits its own data and also aids the communication of other users. User cooperation is particularly attractive for the wireless medium, where every user listens to the transmission of other users.

The main benefit of user cooperation in wireless networks is, probably, its efficacy to combat the wireless channel impairments. *Path loss* and *shadowing* effects are overcome using *intermediate nodes*, with better channel conditions, to retransmit the received signal to the destination. Further, the *channel fading* effect can be also mitigated by means of cooperative *spatial diversity* (the information arrives at the destination through multiple independent paths). These benefits result in an increase of the users spectral efficiency and/or savings on the overall network power resource.

Besides these gains, the simple idea of cooperation expands enormously the communication possibilities, compared to classical communications. For instance, in cooperative networks the interference caused by a source terminal on its neighbor nodes can be seen as a useful signal and used to aid the communication of other nodes. Cooperation also changes the classical idea of the channel as a simple link between a source and a destination. If users cooperate, then any node that serves as a relay becomes an element of the channel, just as reflecting obstacles that cause signal fading. Thus, the channel is no more one link but the network itself. Due to these new possibilities, the design of cooperative networks has motivated new problems at all the levels of the communication protocol stack.

In this dissertation, we address these problems by analyzing the energy efficient regime of different cooperative communication systems. In particular, we are interested in studying, the spectral efficiency as a function of the transmitted power per information bit relative to the noise spectral level. Obtaining the spectral efficiency for all values of energy per bit is usually unfeasible. Instead, if the energy efficient regime coincides with the low power regime, the communication strategy can be well characterized by computing two fundamental metrics: the minimum energy that we need to dedicate to each transmitted bit to have a reliable communication or, equivalently, the maximum rate that can be achieved per unit energy (RPE) and also the slope of the spectral efficiency at the point of minimum energy per bit. This slope indicates

the bandwidth efficiency.

Throughout the dissertation it is assumed an average total network power to be shared with all users. According to the channel magnitudes and phases, which we assume constant and available at all network nodes, the total power is optimally allocated among users and transmission intervals to maximize the RPE and the slope of the spectral efficiency.

We consider three basic cooperative channels: the single relay channel, the two-user cooperative multiple access channel, and the multi-hop multiple relay channel. These channels capture the essence of user cooperation and serve as primary building blocks for cooperation on a larger scale. Even for the simplest one, the relay channel, the capacity is not known today. Therefore, we mainly focus on studying spectral efficiencies achievable with decode and forward (DF) protocols and capacity upper bounds derived with the cut-set bound. In these cases, the low power analysis is a useful tool to study the energy efficiency of the communication system.

Firstly, we study the single relay channel, where a source communicates with a destination aided by a dedicated relay. For this channel, we analyze the benefits associated with different capabilities at terminals, such as: *i)* the *phase synchronization* between the source and the relay, that allows terminals to transmit signals that add coherently at the destination; *ii)* the *full duplex* (FD) capability at the relay, that allows the relay to receive and transmit simultaneously in the same band; and *iii)* the *channel access via superposition*, that jointly with a receiver able to cope with inter-user interference, allows the source and the relay to transmit simultaneously. The synchronism benefit can be observed by computing the maximum RPE. If the relay can not work in FD mode, the relay works in *half duplex* (HD) mode and the transmission and reception channels are orthogonal, e.g. time-division; Likewise, if superposition channel access is not possible, then the transmission must be orthogonal. In both situations, the resultant bandwidth inefficiencies can be observed by computing the slope of the spectral efficiency.

For the relay channel, we also study the energy efficient regime using other forwarding protocols, such as *amplify and forward* or *compress and forward*, and extend the energy efficiency analysis to ergodic fading channels, in order to assess the impact of the channel fading statistics.

Secondly, we investigate the two-user cooperative multiple access channel, where two nodes cooperate with each other in transmitting information to a common destination. The gains provided by the same terminal capabilities considered for the relay channel are revisited here. In addition, we study the gains provided by jointly coding, via superposition, the own generated data and the cooperative data, instead of transmitting them as separated data flows. We design new coding schemes to accommodate the HD/FD modes, the superposition/orthogonal channel access and the joint coding and data flow separation.

Finally, we consider the extension of the relay channel to the multi-hop multiple-relay channel, where a source communicates with a destination aided by several relay nodes that listen to all the transmissions. In this case, we restrict the analysis to asynchronous and orthogonal trans-

missions. Although we only consider DF-like protocols, several coding schemes are possible depending on: *i*) whether all the relays decode the source message (*allcast*) or only the destination (*unicast*), and depending on *ii*) whether nodes use multiple received signals to decoded the message (*accumulative*) or only one signal (*non-accumulative*). For each of these possibilities, we design a different multi-terminal coding strategy and compute the maximum RPE. By maximizing the RPE, we provide a joint solution to a set of problems traditionally belonging to different layers: power allocation (physical), relay selection, and routing (network). Among all the possibilities, we find solutions for distributed scenarios.

Resum

L'objectiu d'aquesta tesi és l'estudi de les comunicacions cooperatives sense fils. En xarxes de comunicacions cooperatives, cadascun dels usuaris transmet la seva pròpia informació però també assisteix les comunicacions dels altres usuaris. La cooperació entre usuaris és particularment interessant pel medi sense fils, on tots i cadascun dels usuaris rep el senyal transmès pels altres usuaris.

El principal guany que proporciona la cooperació entre usuaris en xarxes sense fils és probablement l'eficàcia amb la que és capaç de combatre els danys causats pel canal radio. Les pèrdues degudes a la *propagació* del senyal, així com les pèrdues pel *blocatge* del senyal causades pel obstacles físics poden ser contrarestades utilitzant *nodes intermedis*, amb millor condicions de canal, que retransmeten el senyal rebut cap al node destí. A més, l'efecte dels *esvaïments* del canal deguts a la propagació multi-camí del senyal, pot ser disminuït mitjançant la cooperació, gràcies a la *diversitat en l'espai* (la informació arriba al destí mitjançant múltiples camins independents). Aquests beneficis es tradueixen en una major eficiència espectral per cada usuari, així com en un estalvi en l'energia utilitzada a tota la xarxa.

A més d'aquests guanys, la simple idea de cooperar expandeix enormement les possibilitats de la comunicació en comparació a les que existeixen en les comunicacions clàssiques. Per exemple, la interferència causada per una font en els nodes veïns pot ésser considerada en xarxes cooperatives, com a senyal útil i utilitzada per assistir la comunicació entre altres usuaris. A més, la cooperació canvia la idea clàssica del canal com a una simple connexió entre en node font i el node destí. Així doncs, si els usuaris cooperen, qualsevol node que serveix com a retransmissor es converteix en un element més del canal, de la mateixa manera que els obstacles reflecteixen el senyal transmès, causant els esvaïments del senyal. Com a conseqüència, el canal ja no és únicament una simple connexió si no que esdevé la xarxa en si mateixa. A causa d'aquestes noves possibilitats, el disseny de xarxes cooperatives ha motivat nous problemes a tots els nivells de la pila dels protocols de comunicacions.

En aquesta tesi, ens apropem a aquest problemes mitjançant l'estudi de sistemes de comunicació cooperatius funcionant en el règim d'eficiència energètica. En particular, estem interessats en estudiar l'eficiència espectral en funció de la potència dedicada per cada bit d'informació i normalitzada pel nivell espectral de soroll. Obtenir l'eficiència espectral per cada valor

d'energia dedicada per bit no és sempre possible. En canvi, si el règim d'eficiència energètica coincideix amb el règim de baixa potència, l'estratègia de comunicació pot ser ben caracteritzada calculant dos mètriques fonamentals: la mínima energia que és necessari dedicar a cada bit per tal d'establir una comunicació sense errors, o equivalentment, la màxima taxa de bits que es pot aconseguir per unitat d'energia (RPE) i el pendent de l'eficiència espectral com a funció de l'energia per bit en el punt de mínima energia per bit. Aquest pendent determina l'eficiència en l'ús que se'n fa de l'ample de banda espectral.

A tota la tesis s'assumeix una quantitat total de potència mitja compartida per tots els usuaris de la xarxa. D'acord amb les magnituds dels canals, que es consideren constants i conegudes per tots els nodes de la xarxa, la potència total és distribuïda de manera òptima entre els usuaris i els diferents intervals de transmissió, per tal de maximitzar el RPE i el pendent de l'eficiència espectral.

L'estudi considera separatament tres canals bàsics de comunicació amb cooperació: el canal amb únic retransmissor, el canal d'accés múltiple amb dos usuaris cooperatius, i el canal amb múltiples retransmissors i múltiples salts. Aquests canals capturen l'essència de la cooperació entre usuaris i serveixen com a blocs fonamentals per a la construcció de sistemes cooperatius a gran escala.

Ni tan sols pel més simple d'aquest canals (un únic retransmissor), la capacitat és coneguda. En aquest treball ens centrem en estudiar l'eficiència espectral que es pot aconseguir utilitzant el protocol de *descodificar i retransmetre* (DF) i el límit superior sobre la capacitat que estableix el *cut-set* límit. En aquests casos, l'anàlisi del règim de baixa potència és especialment útil per estudiar l'eficiència energètica.

En primer lloc estudiem el canal amb un únic retransmissor on un node font es comunica amb node destí amb l'ajuda d'un retransmissor totalment dedicat. Per aquest canal estudiem el benefici en termes d'eficiència energètica associat a diferents funcionalitats als terminals, com ara: i) la *sincronització en fase* entre la font i el retransmissor, que permet que els terminals enviïn senyals que es sumen de forma coherent al destí, ii) el mode *full duplex* (FD) al retransmissor, que permet que aquest rebi i transmeti de forma simultània en la mateixa banda; i iii) l'accés al canal mitjançant la *superposició* de senyals, que juntament amb un receptor capaç de tenir en compte l'interferència entre-usuaris, permet que la font i el retransmissor transmetin simultàniament. El benefici de sincronisme pot ser observat obtenint el màxim RPE. Si el retransmissor no és capaç de treballar en el mode FD aquest treballa en el mode *half duplex* (HD) i els canals de transmissió i recepció son ortogonals, e.g. divisió temporal; de la mateixa manera, si l'accés al canal per superposició no és possible, les transmissions entre la font i el retransmissor han de ser ortogonals. Les ineficiències espectrals, que resulten d'aquestes dos últimes limitacions poden ser observades obtenint el pendent de l'eficiència espectral.

Per aquest canal amb un únic retransmissor, també estudiem el règim d'eficiència energètica

que es pot obtenir utilitzant altres protocols de retransmissions, diferents a DF, com ara *amplificar i retransmetre* o *comprimir i retransmetre*. També, ampliem l'anàlisi per tal de considerar canals amb esvaïments ergòdics i avaluem l'impacte de l'estadística del canal en l'eficiència energètica.

En segon lloc, investiguem el canal d'accés múltiple amb dos usuaris cooperatius, a on dos nodes cooperen entre ells per transmetre informació cap a un node destí comú. Els guanys que proporcionen les habilitats esmentades anteriorment són novament estudiades per aquest escenari. A més a més, estudiem els guanys que proporciona la *codificació conjunta*, mitjançant superposició, de la informació pròpia i la informació cooperativa. Aquesta codificació permet considerar les dues informacions com a un únic flux, en comptes de com a fluxos separats d'informació i transmetent-les simultàniament en lloc de mitjançant canals ortogonals. Per aquest canal, dissenyem nous esquemes de comunicació per tal d'incloure: els modes HD o FD, l'accés al canal per superposició o mitjançant transmissions ortogonals i la codificació conjunta o mitjançant fluxos d'informació separats.

En últim lloc, considerem l'extensió del canal amb un únic retransmissor a canals amb múltiples retransmissors i amb múltiples salts, a on un node font es comunica amb un node destí amb l'ajuda de diversos retransmissors. Per aquest escenari l'anàlisi es limita a transmissions asíncrones i ortogonals. Tot i que únicament considerem protocols del tipus DF, diversos esquemes de codificació són possibles en funció de si: *i*) tots els retransmissors han de descodificar el missatge transmès per la font (*allcast*) o únicament el destí (*unicast*), *ii*) els nodes utilitzen els múltiples senyals rebuts per descodificar el missatge (*acumulatiu*) o únicament una senyal (*no acumulatiu*). Per cadascun d'aquests requisits i/o habilitats dissenyem diferents estratègies de codificació i obtenim el màxim RPE. Maximitzant el RPE, també obtenim la solució conjunta a problemes que tradicionalment pertanyen a diferents nivells de la comunicació: assignació de potència (*nivell físic*), selecció de nodes retransmissors i ruta cap al destí (*nivell de xarxa*). De entre totes les possibilitats, intentem trobar solucions vàlides per escenaris distribuïts.

Acknowledgments

El balance de estos últimos 4 años que culminan ahora con la finalización de la tesis no pueden ser más positivos. Esto es así, no tengo ninguna duda, gracias a los viejos y nuevos conocidos, compañeros y amigos que me han rodeado y tanto me han aportado estos años.

En primer lugar quisiera agradecer a mi directora de tesis Ana Pérez el apoyo y la confianza puesta en mi desde el inicio de esta aventura. Siempre he encontrado en ella facilidades y soluciones prácticas a cualesquiera fueran mis preocupaciones o dudas.

También quisiera agradecer a Miguel Ángel Lagunas y Simó Aliana, en representación del CTTC por permitirme realizar la tesis en el marco del programa de becas doctorales del CTTC. En el CTTC me he sentido enormemente privilegiado, no sólo por la cantidad de facilidades y calidad de las personas que me he encontrado, sino también por las experiencias personales que me ha brindado. Gracias al CTTC he podido presentar mi trabajo en conferencias internacionales y atender a presentaciones de expertos en lugares fantásticos. Por todo esto estoy inmensamente agradecido.

Mención especial merecen las personas que han aceptado revisar la tesis y los trabajos previos para conferencias o revistas. Muchas gracias Aitor por introducirme al "relay channel" , a David y Javibi por su paciencia y compañía, y a Fran, Miquel y Toni por su generosa acogida.

También quisiera recordar las personas que me han hecho pasar momentos inolvidables durante este tiempo ya fuera en los descansos, en la comida, o durante los largos trayectos en tren. Muchas gracias Ana Maria, Bego, Daniel, Fermín, Javier Arribas, Jesús Alonso, Lluís Ventura, Pavel y Ricardo así como a mis compañeros de despacho, doctorándose, el equipo de fútbol y demás compañeros del CTTC.

Finalmente, quiero agradecer a Xavi su generosa y duradera amistad y dedicar esta tesis a mis padres y hermana por su continuo apoyo y motivación y a mi esposa Ester por darme tanto amor, hacerme tan feliz y sobretodo por estar siempre a mi lado recordándose con su ejemplo y compañía lo que es realmente importante en la vida.

Contents

1	Introduction	1
1.1	Motivation	1
1.1.1	Benefits	1
1.1.2	Drawbacks	3
1.2	Objectives and Scope	5
1.2.1	Performance Metric	6
1.2.2	Assumptions	7
1.3	Thesis Outline	10
2	Background	15
2.1	The Low Power Regime Analysis	15
2.1.1	Direct Transmission	17
2.1.2	Multiple Input Multiple Output Channel	20
2.1.3	Multiple Access Channel	21
2.1.4	The Broadcast Channel	23
2.2	Coding Techniques for Multi-Terminal Networks	24
2.2.1	Parallel Channel Decoding: Repetition vs Independent coding	25
2.2.2	Superposition Encoding	25
2.2.3	Dirty Paper Coding	26
2.2.4	Multiplexing Encoding	26
2.2.5	Regular vs Irregular Encoding and Joint vs Successive Decoding	27

2.2.6	Block Markov Coding	28
3	The Relay Channel	31
3.1	Related Work and Contributions	32
3.2	Channel Model	35
3.3	Relay Channel Capacity Bounds	36
3.3.1	The Full Duplex Relay Channel	36
3.3.2	The Half Duplex Relay Channel	38
3.4	The Energy Efficiency Analysis	39
3.4.1	The Relay Channel	39
3.4.2	The Energy Efficient and the Low Power Regime	40
3.5	Maximum Rate Per Energy	43
3.6	Slope of the Spectral Efficiency	45
3.7	Numerical Results	49
3.7.1	Terminal Capabilities	49
3.7.2	Resource Allocation	51
3.7.3	Relay Position	52
3.8	Extension to Ergodic Fading Channels	54
3.8.1	Ergodic Capacity Bounds	54
3.8.2	The Energy Efficiency Analysis	55
3.8.3	Maximum Rate Per Energy	56
3.8.4	Slope of the Spectral Efficiency	57
3.8.5	Numerical Results	61
3.8.6	Conclusions	62
3.9	Extension to Non-Regenerative Relaying Techniques	63
3.9.1	Spectral Efficiency	63
3.9.2	Time Sharing On-Off	64

3.9.3	Generalized Time-Sharing Strategy	66
3.9.4	Comparison with Regenerative Strategies	67
3.10	Chapter Summary and Conclusions	67
3.A	Derivatives of the Rate Constraints	69
4	Cooperative Multiple Access Channel	71
4.1	Related Work and Contributions	72
4.1.1	MAC	72
4.1.2	RC	72
4.1.3	CMAC	73
4.2	Channel Model	75
4.3	The Energy Efficiency Analysis	76
4.4	Cooperative Multiple-Access Channel with FS	79
4.4.1	Rate Region	79
4.4.2	Maximum Rates Per Energy	80
4.4.3	Slope Region of Spectral Efficiencies	82
4.5	Rate Regions for the CMAC with Joint Coding	86
4.5.1	Coding for the Flow-Separation Strategy	86
4.5.2	Joint Coding with Full Duplex Operation	87
4.5.3	Joint Coding with Half Duplex Operation	90
4.5.4	Joint Coding with TDMA	94
4.5.5	Summary of Cooperative Configurations	96
4.6	Maximum Rates Per Energy	96
4.6.1	Preliminaries	97
4.6.2	Joint Coding with Full Duplex Operation	99
4.6.3	Joint Coding with Half Duplex Operation	100
4.6.4	Joint Coding with TDMA	102

4.7	The Slope Region	103
4.7.1	Preliminaries	104
4.7.2	Joint Coding with Full Duplex Operation	105
4.7.3	Joint Coding with Half Duplex Operation	107
4.7.4	Joint Coding with TDMA	111
4.8	Numerical Results	113
4.9	Chapter Summary and Conclusions	116
4.A	Derivatives of the Rate Constraints	117
5	The Multiple Relay Multi-Hop Channel	119
5.1	Related Work and Contributions	121
5.2	Network Model	124
5.3	The Energy Efficiency Analysis	125
5.4	Two-Hop Multiple Relay Network	127
5.4.1	Decode and Forward	127
5.4.2	Cut-Set Bound	129
5.5	Traditional Multi-Hop Network	131
5.6	Allcast Multi-Hop Relay Network	132
5.7	Unicast Cooperative Multi-Hop Network	136
5.7.1	One-Relay Network	136
5.7.2	Multi-Hop Multiple Relay Network	137
5.8	Upper Bound for Regenerative Networks	141
5.9	Cut-Set Bound for Multi-Hop Networks	143
5.10	Simulation Results	148
5.11	Conclusions	149
5.A	Optimality of the Routing Algorithms	151
5.B	Proof of Remark 5.2	152

5.C	Auxiliary Results for Proof of Theorem 5.8	152
5.C.1	Proof of Lemma 5.1	153
5.C.2	Primal KKT Condition	153
6	Conclusions	155
6.1	Future Work	158
6.1.1	Studied Scenarios	158
6.1.2	New Scenarios	160
	Bibliography	163

List of Figures

2.1	Spectral efficiencies of the AWGN channel and the Rayleigh flat fading channel with and without receiver knowledge of fading coefficients [1].	19
2.2	Spectral efficiencies for direct transmissions with Gaussian inputs, QPSK, and BPSK in the AWGN channel [1].	19
2.3	Slope regions in the Gaussian multiaccess channel with TDMA and superposition.	23
3.1	Scenario description.	36
3.2	Relay near the destination at coordinates (0.75,0.25). Approximate and exact rate (bits/s/Hz) versus $\frac{E_b}{N_0}$ (dB) for full duplex, half duplex, orthogonal, and direct transmission.	49
3.3	Relay near the source at coordinates (0.25,0.25). Approximate and exact rate (bits/s/Hz) versus $\frac{E_b}{N_0}$ (dB) for full duplex, half duplex, orthogonal with optimal or linear power allocation, and direct transmission.	50
3.4	Maximum RPE versus source to relay distance. Source and Destination are located at $d = 0$ and $d = 1$ respectively.	51
3.5	Slope versus source to relay distance. Source and Destination are located at $d = 0$ and $d = 1$ respectively.	52
3.6	Maximum slope versus source to relay distance, for different resource allocation assumptions.	53
3.7	Relay selection. Rate as a function of the $\frac{E_b}{N_0}$ for HD nodes.	53
3.8	Maximum slope versus source to relay distance over Rayleigh fading $\kappa = 2$	61
3.9	Maximum slope versus the kurtosis of the channel coefficients at $d = 2/3$. For a relay in FD and HD modes with DF and different resource allocation polices.	62

3.10 Achievable rate as a function of the total power, $R(E)$ for AF and ON-OFF AF.	65
3.11 Achievable rate as a function of the $\frac{E_b}{N_0}$, $R\left(\frac{E_b}{N_0}\right)$ for AF and ON-OFF AF. . . .	66
3.12 Maximum RPE as a function of the relay position for CB, DF, CF and AF. . . .	67
3.13 Total power at which the maximum RPE is achieved for AF and CF.	68
4.1 Cooperative multiple-access channel model (CMAC).	75
4.2 Power allocation among sources. User 2 cooperates with user 1 in HD mode. .	76
4.3 Computation of the boundary points of the rate region.	77
4.4 Power allocation among flows.	79
4.5 Maximum RPE pairs for the FS-CMAC with sync./async. transmissions.	81
4.6 Slope regions in the FS-CMAC with asynchronous transmissions.	85
4.7 Slope regions if both users cooperate.	113
4.8 Slope regions if only user 2 cooperates.	114
4.9 Slope regions if only user 1 cooperates.	115
4.10 Slope regions if no user cooperates.	116
5.1 Two-relay network model.	124
5.2 Two-hop multiple relay network model.	127
5.3 Two-relay TMH network model.	131
5.4 Two-relay UCMH network model.	136
5.5 $\Pr(\eta/\eta_{DT} > G)$ for all the cooperative strategies studied in a scenario with 5 nodes (up to 4 hops) with a density of nodes of 1 <i>nodes/m</i> ²	148
5.6 Gain ratio $G = \eta/\eta_{DT}$ as a function of the density of nodes ρ for a given $\Pr(\eta/\eta_{DF} > G) = 0.5$ and a fixed number of nodes $N = 5$	149
5.7 The gain ratio G as a function of the number of nodes N , for a given $\Pr(\eta/\eta_{DT} > G) =$ 0.5 and $\rho = 1$	150

List of Tables

1.1	Communication scenarios and studies addressed for the RC in Chapter 3.	10
1.2	Communication scenarios and studies addressed for the two-user cooperative multiple access channel in Chapter 4.	12
1.3	Communication scenarios and studies addressed for the multiple relay multi-hop network in Chapter 5.	13
2.1	Block Markov coding scheme for the full duplex relay channel.	29
3.1	Scenarios depending on the terminal constraints.	32
3.2	Low power metrics found in the literature depending on the nodes capabilities.	33
4.1	Terminal constraints for RC, MAC and CMAC.	72
4.2	BMC scheme for the FD relay channel.	86
4.3	Coding scheme for the HD relay channel.	86
4.4	BMC construction for the CMAC with JC and FD nodes.	87
4.5	Cooperative configurations for the CMAC with JC and FD terminals.	89
4.6	Transmission strategy for the CMAC with JC and HD users if only user 2 cooperates.	91
4.7	Transmission strategy for the CMAC with JC and HD users if both users cooperate.	92
4.8	Transmission strategy for the CMAC with TD and FD users.	94
4.9	Summary of transmission strategies.	96

5.1	Multi-hop multiple relay transmission strategies depending on the terminals capabilities and decoding requirements.	123
5.2	Allcast relay selection and ordering algorithm.	135
5.3	TMH and UCMH: Relay selection and ordering algorithm.	140
5.4	CB upper bound: Relay selection and ordering algorithm.	145

Glossary

ACMH	Allcast cooperative multi-hop
AF	Amplify and forward
AWGN	Additive white Gaussian noise
BC	Broadcast channel
BMC	Block Markov coding
CF	Compress and forward
CB	Cut-set bound
CDF	Cumulative density function
CMAC	Cooperative Multiple access channel
CMH	Cooperative Multi-hop
CSI	Channel state information
DF	Decode and forward
DT	Direct transmission
FD	Full duplex
FS	Flow separation
HD	Half duplex
JC	Joint coding
KKT	Karush-Kuhn-Tucker
MAC	Multiple access channel
MIMO	Multiple-input-multiple-output
OT	Orthogonal transmissions
RC	Relay channel
RPE	Rate per energy
SNR	Signal-to-noise ratio
TDMA	Time division multiple access
TMH	Traditional Multi-hop
UCMH	Unicast cooperative multi-hop

Notation

\mathbf{x}	Vector notation
$[\mathbf{x}]_i$	Element i -th in the vector \mathbf{x}
$ \mathbf{x} $	Length of the vector \mathbf{x}
π	Ordered set of nodes (the route from node $[\pi]_1$ to node $[\pi]_{ \pi }$)
π_i	Route from node $[\pi]_i$ to node $[\pi]_{ \pi }$
\mathcal{X}	Set notation
\mathcal{X}^C	Complementary set of \mathcal{X}
\mathbb{R}	The real numbers
\mathbb{C}	The complex numbers
\mathbf{y}	Match-filter output
\mathbf{x}	Transmitted signal, space-time symbols
\mathbf{n}	Additive noise vector
snr	Signal to noise ratio
$\mathcal{CN}(\mu, \sigma^2)$	Complex Gaussian distribution with mean μ and variance σ^2
N_0	Noise spectral density power
$\frac{E_b}{N_0}$	Energy per bit normalized by the noise spectral level
$\frac{E_b}{N_0 \min}$	Minimum energy per bit normalized by the noise spectral level
S	Slope of the spectral efficiency vs $\frac{E_b}{N_0}$ in dB at $\frac{E_b}{N_0} = \frac{E_b}{N_0 \min}$
η	Maximum rate per energy normalized by the noise spectral level N_0
T	Transmission time slot period
W	Bandwidth
P	Power
τ_j	Time-sharing fraction
ρ	Correlation
s.t.	Subject to
w.r.t.	With respect to
i.i.d	Independently, identically distributed
r.v.	Random variable
$\ \mathbf{X}\ $	Norm of matrix \mathbf{X}
$\ \mathbf{X}\ _2$	2-norm of matrix \mathbf{X}
$E[x]$	Expectation of x

Pr	Probability
$p(x)$	Probability density function of random variable x
$H(x)$	Differential entropy: $\int p(x) \log_2 p(x) dx$
$I(x; y)$	Differential mutual information: $\int p(x, y) \log_2 \frac{p(x, y)}{p(x)p(y)} dx dy$
max	Operator that takes the maximum of functions or vectors
min	Operator that takes the minimum of functions or vectors
\dot{x}	First order derivative of x
\ddot{x}	Second order derivative of x

Chapter 1

Introduction

1.1 Motivation

The aim of this dissertation is the study of cooperative communications in wireless networks. In cooperative networks, each user transmits data as well as acts as a cooperative agent for other users. User cooperation is particularly attractive for the wireless medium, since every user listens to the transmission of other users. Compared to classical wireless communications, the simple idea of cooperation expands enormously the communication possibilities.

The main benefits and drawbacks of cooperation are detailed below.

1.1.1 Benefits

Most of the benefits of cooperation are in the physical layer and can be measured using link quality metric arguments such as spectral efficiency and reliability:

- Cooperative communications combat wireless channel impairments (path loss, shadowing and fading):
 - Path loss is caused by the dissipation of the power radiated by the transmitter with

the distance d as well as effects of the propagation channel, characterized by a channel attenuation exponent ν . If the transmitted power is P , then the received power at a distance d is $Pd^{-\nu}$. This attenuation makes long-range point to point communication impractical. The use of relay nodes as intermediate repeaters or boosters can overcome this problem by enhancing the signal quality at each hop. For instance, repeaters are currently employed in cellular system to increase the cell coverage [2].

- Shadowing is caused by obstacles between the transmitter and the receiver that absorb power. If the obstacle absorbs all the power, then the signal is blocked. However, if there is a relay node with line-of-sight to the source and also to the destination, then the shadowing problem can be overcome.
- Signal fading is caused by the constructive and destructive addition of multi-path signal components at the receiver antenna. The channel variations due to path loss and shadowing occur over relatively large distances, (large-scale propagation effects). Contrary, the channel variations due to multi-path occur over very short distances, on the order of the signal wavelength (small-scale propagation effects). Signal fading arising from multi-path propagation can be mitigated through the use of diversity [3]. Spatial or multiple-antenna diversity techniques, such as space-time coding [4–7], that consist of coding the transmitted message across different antennas and channel uses, are particularly attractive because they can be easily combined with other forms of diversity without sacrificing additional degrees of freedom in time or frequency. To efficiently combat the multi-path fading, non-cooperative terminals need antennas to be spaced at least $\lambda/4$ apart, where λ is the wavelength. For many terminals (e.g. mobile telephones, WLAN cards), this means that only 1 or 2 antennas are realistic. Instead, by means of relaying, spatial diversity is obtained by using a collection of distributed antennas belonging to multiple terminals and forming a virtual antenna array (VAA) through physical layer coding and signal processing [8]. This form of space diversity is referred to as *cooperative diversity* and is extensively studied in [2, 9–11] among others.
- Beamforming gains can be obtained if transmitters have channel knowledge and can synchronize their transmissions [12, 13]. Then, multiple transmitters concentrate its power onto a desired spatial direction increasing the received signal quality at the intended receiver and reducing the interference onto any other node.
- Cooperative communications save power and computational resources. Sharing power and computation efforts with neighboring nodes can lead to saving of overall network resources. For instance, the increment in spectral efficiency due to e.g. diversity gains, can be converted into a reduction of the transmitted power.

In addition, cooperation can simplify the network design at the cost of more complicated links. The idea is that cooperation allows us to rethink the network layer of a multi-hop communication system, which consist of routing over a large number of simple links, by routing only over a smaller number of more complicated cooperative links [14].

1.1.2 Drawbacks

As shown in previous subsection, user cooperation can simplify the network design, decreases computational efforts and overcome the hardware size limitations associated with placing multiple antennas at a single terminal. However, most of the benefits of user cooperation require new capabilities and further complexity at terminals [15]. The main capabilities and increments in complexity are discussed below:

- Relay protocols. First, we have to take into account the additional hardware and processing capabilities required to forwarding data. The specific capabilities depend strongly on the relay protocol. There are mainly three relay protocols from which the source and the relay nodes can share their resources to achieve the highest spectral efficiency possible:
 - Decode and forward (DF): The relay decodes the source transmission and then retransmits the decoded signal [16].
 - Compress and forward (CF): The relay may not be able to decode the source signal, but nonetheless it has an independent observation of the source signal that can aid in decoding at the destination. Therefore, the relay sends an estimate of the source transmission to the destination [16].
 - Amplify and forward (AF): This is an important special case of the above strategy where the estimate of the source transmission is simply the signal received by the relay, scaled up or down before retransmission [9, 17].
- The full duplex (FD) capability allows the relay to receive and transmit simultaneously in the same band. Then, the signal transmitted by the relay interferes with the received signal. In theory, it is possible for the relay to cancel out this interference because it is known. Radio-frequency techniques making this possible can be found in [18, 19]. In practice, however, any error in interference cancelation due to inaccurate knowledge of device characteristics or due to the effects of quantization and finite-precision processing can be catastrophic because the transmitted signal is typically 100-150dB stronger than the received signal [9]. While FD operation in general can be difficult to implement, it is more feasible in the low energy regime, since interference between signals is less of an issue. If FD operation is not possible, then nodes are said to work in half duplex (HD), which consists of relays transmitting and receiving using different degrees of freedom,

with the consequent loss in spectral efficiency [20,21]. Orthogonality between the transmitted and received signals can be in time-domain, in frequency domain, or by using any set of signals that are orthogonal over the time-frequency plane. HD relaying has been accepted as a practical form of relaying that has potential for implantation in near future.

- Channel state information (CSI) at the receivers allows the receiver to use coherent detection and optimal combining of multiple received signals. Usually, it is assumed that CSI is known at the receiver, otherwise, the capacity is significantly penalized [22, 23]. Decoding without channel knowledge is possible using differential space-time codes [24, 25]. However, these codes have a 3dB penalization.
- CSI at the transmitters allows to allocate, efficiently, the resources: power and bandwidth. The transmitters may obtain local CSI in two ways: *i*) via receiver estimation and feedback to the transmitter or *ii*) for system operating in time-division duplex (TDD) mode, the transmitter can exploit channel reciprocity and make channel measurement based on the signal received along the opposite link. In multi-user networks and, in particular, in cooperative wireless networks, the resources can belong to the network and thus, are shared with all the users. Then, instead of local CSI only, terminals may require global CSI. In that case, user terminals know all the CSI in the network. To obtain this global CSI, several questions arise: *i*) how can the feedback channel be organized, *ii*) can we find channel metrics that reduce the amount of feedback? *iii*) is there any cooperative strategy with good performance and low channel feedback requirements?
- The synchronization among users transmission is the possibility that different user terminals transmit signals that add coherently or destructively at the destination. In point-to-point communications with multiple antennas per terminal, this capability is the responsible for obtaining beamforming gains. However, in multi-user communication antennas belong to separate terminals. Then, to obtain the beamforming gain, terminals must be synchronized. It is relatively straightforward to obtain symbol (timing) synchronization between different user terminals; however, carrier synchronization requires phase-locking-separated microwave oscillators, which is very challenging in practical systems [26]. Additionally, global and complete CSI is needed (magnitude and phase). The channel phases are needed to synchronize transmissions and the channel magnitudes are needed to allocate efficiently the total network energy among users. Overall seems highly unrealistic. Left by themselves, the drift of the oscillators makes synchronization impossible. However, some distributed carrier synchronization and channel feedback techniques are currently available. An excellent overview of the state of the art can be found in [27].
- More complex coding/decoding schemes are needed;
 - To allow simultaneous transmissions of multiple independent users to a single des-

mination. This is solved only in part with multiple access channel coding, e.g. time-division or superposition coding. In cooperative scenarios, the basic multiple access channel (MAC) is the one from a source and its relay to a destination. In this case, simultaneous transmissions over all the transmission interval are only allowed if, additionally, the relay has FD capability and block Markov coding is used [28], which is difficult to implement with practical codes [29].

- To allow the simultaneous transmission of multiple independent messages from a single user terminal. This is solved only in part with broadcast channel coding. In cooperative networks, terminals may need to transmit, simultaneously, the own generated and the relayed data. To that end, joint encoding techniques are needed. Joint encoding can be done with multiplexing coding or superposition coding. Multiplexed codes are difficult to build, see [30]. With superposition coding, for each joint encoded message, a different and independent codebook is needed.
- The decoding of jointly encoded messages or simultaneously received signals requires high complexity receivers. In the later case, user terminals are said to be *accumulative* (AC), if are able to use multiple received signals to decode the source message.
- Security reasons: users' data has to be encrypted before transmission. Then, a relay node can detect its partner's transmitted data without understanding the information being sent.

1.2 Objectives and Scope

The existence of terminals with relay capabilities in a network, as previously discussed, promises benefits to the overall network. However, the design of these networks has motivated new problems at all the levels of the communication protocol stack [31]. In non-cooperative wireless communication, the physical layer is only responsible for communicating information from one node to another. Compared to classical communications, the simple idea of cooperation expands enormously the communication possibilities. For instance, the interference caused by a source terminal on its neighbor nodes is seen in cooperative networks as a signal useful to aid the communication of other nodes. Cooperation also changes the classical idea of the channel as a simple link between a source and a destination. If users cooperate, then any node that serves as a relay becomes an element of the channel, just as reflecting obstacles that cause signal fading, and thus the channel is no more one link but the network itself. The simplest and oldest form of user-cooperation is perhaps *multi-hopping*, which consists of a chain of point-to-point links from the source to the destination. Each node in this chain, communicates only with the nodes that are one hop away. Multi-hopping is probably the cooperation strategy more widely implemented today. For example, this principle underlies the widely used Zigbee

standard [32] for low-rate, low-power networking. However, multi-hopping is clearly suboptimal in a wireless environment since every node in the chain can only listen to the previous transmission.

In this dissertation, we address the analysis and design of cooperative communication systems in the energy efficient regime:

- **Analysis:** We provide a unified and practical framework to analyze and compare the energy efficiency of various transmission strategies in wireless networks. We discuss the gains provided by different user capabilities and increments in complexity at terminals.
- **Design:** By optimizing cooperative networks in the energy efficient regime, we find joint solution to a set of *design problems* that traditionally belong to different layers: power allocation (physical), relay selection, and routing (network). Applications of them on real systems might require a more careful examination of relevant *observables*, i.e., channel gain, traffic, etc., and controllable *parameters*, i.e., route, transmission power, transmission rate, cooperative diversity scheme, etc., [33]. Nevertheless, the solutions found can be used as a starting point for developing practical solutions for relay channels.

Whether or not cooperation pays off, however, depends on what perspective the network is seen in, and on what is the objective of the network. The performance metric and assumptions taken in this dissertation are detail below.

1.2.1 Performance Metric

One of the main concerns in wireless networks especially in low-rate, low-power networks, such as sensory or Zigbee networks [32] is power consumption [34,35]. The users in these networks have limited energy sources (batteries) and, thus, need to use power efficiently. We only consider the power consumption due to transmission and not due to computation. However, we should mention that, at low signal to noise (SNR) (where many wireless networks usually operate at) the circuit energy consumption might be important, as pointed out in [36–38].

Our analysis is mainly focused on studying the spectral efficiency $C \left(\frac{E_b}{N_0} \right)$ of cooperative wireless communication systems. In particular, we are interested in its behavior as a function of the transmitted power per information bit relative to the noise spectral level $\left(\frac{E_b}{N_0} \right)$.

In the energy efficient regime, there are two metrics of special interest [1]:

- The maximum rate per energy (RPE) or, equivalently, the minimum energy per bit $\left(\frac{E_b}{N_0} \min \right)$ is the most relevant point in the spectral efficiency curve.

- In most of the communication systems, the minimum values of energy per bit are obtained in the limit of low power or infinite bandwidth and therefore imply zero spectral efficiency $C\left(\frac{E_b}{N_0}\right) = 0$. Consequently, in those cases, the $\left(\frac{E_b}{N_0}\right)$ gives no indication about the bandwidth-power tradeoff in the channel and the key performance measure is the slope (S) of the spectral efficiency vs $\left(\frac{E_b}{N_0}\right)$ at $\frac{E_b}{N_0} = \frac{E_b}{N_0 \min}$. This metric determines the bandwidth efficiency of the communication system.

It is shown in [1] that the spectral efficiency (bits/s/Hz) as a function of the $\frac{E_b}{N_0}$ (dB) can be approximated in the low power regime by

$$C\left(\frac{E_b}{N_0}\right) \Big|_{\frac{E_b}{N_0} \text{ dB} \rightarrow \frac{E_b}{N_0 \min} \text{ dB}} \approx \frac{S}{10 \log_{10} 2} \left(\frac{E_b}{N_0} \Big|_{\text{dB}} - \frac{E_b}{N_0 \min} \Big|_{\text{dB}} \right) \quad (1.1)$$

Tools to compute $\frac{E_b}{N_0 \min}$ and S valid for almost any communication scheme are derived in [1]. Further details and examples are given in Chapter 2.

In this dissertation, the maximum RPE is used to: determine the benefits of synchronizing transmissions, solve the optimal energy allocation and select the best nodes and routes. Instead, the slope (S) is used to: determine the performance losses due to the HD limitation and the time-division channel access.

1.2.2 Assumptions

Relays can be placed in infrastructure networks to enhance the coverage and the spectral efficiency [39]. Nevertheless, our main focus is on infrastructureless networks [2] which are usually characterized by an homogenous node configuration; all terminals develop similar tasks and have similar limitations or capabilities. Examples of these networks are: wireless ad-hoc networks, sensor networks or mesh networks. Examples of its applications are: wireless LAN (e.g IEEE 802.11) and MAN (e.g DARPA's GLOMO), home networks (e.g., HomeRF), device networks (e.g., Bluetooth), and sensor networks (e.g., SmartDust, WINS).

We assume that terminals are equipped with a single antenna and that the channel input signaling is Gaussian. The later choice is optimal for several communications channels over additive white Gaussian noise (AWGN) not subject to fading as: the point-to-point [40], the MIMO [13] and the relay channel (RC) with DF [28]. In addition, assuming Gaussian input signalling allows us to consider signal interferences simply as additive Gaussian noise, which is useful to find close form spectral efficiency expressions [40].

Besides these general assumptions, our studies are limited to the following considerations:

- **Relaying Protocols:** The capacity of the general RC is not known even today. Moreover, there is no single forwarding strategy known that works best for the general RC. We

mainly focus on regenerative relaying protocols, like DF, to study achievable rates and the cut-set bound (CB) to study rate upper bounds. In some scenarios non-regenerative strategies, such as AF or CF can offer a better energy efficiency than DF. However, it is not reached in the low energy regime [30]. Moreover, in the low energy regime these non-regenerative strategies can never improve DF. The CB [16, p. 445] is a very useful tool for bounding the capacity of any communication system. The CB is analogous to the well-known max-flow min-cut theorem [41]. It states that the rate of information flow across any cut (boundary) that divides the set of nodes in a network in two parts (the transmitter and receiver sides) cannot exceed the mutual information between the channel inputs on the transmitter side and the channel outputs on the receiver side conditioned on the knowledge of inputs on the receiver side.

- **“Network” resource constraints:** It is considered that the resources belong to the network and are optimized among user terminals. In particular, we assume a “network” sum power constraint. This constraint is motivated by the sensor network framework, where nodes are viewed as a part of a unique more complex agent, rather than as individual free-agents. Taking the individual power constraint into account would just complicate the solution without giving further insight. The sum power constraint allows us to compare the multi-terminal performance with the traditional single hop (direct transmission) channel model used as a base of reference. In addition, although the power allocation with a sum power constraint can result in an uneven power consumption among the nodes or in a solution where the individual node power consumption is above what the node is physically capable of, if we consider channel variations, this is averaged out; furthermore, if all nodes at sometimes or other act as source-destination pairs, the power consumption can be expected to be fairly distributed.
- **Channel Model:** We limit our analysis to the AWGN channel. The channel is assumed to remain constant over all the transmission and is frequency flat. The results we obtain here can be used as a first step towards the study of more involved time-varying channels. To study time varying channels properly, we would need to know in advance, the time-scale of the communication and the tolerance of the target application, which can be very challenging in mobile wireless networks [31].

The extension of our result to fading channels is possible. The two main types of time-varying channels depending on the time-scale of the communication are:

- Fast fading channels: in this case, the transmitter can take advantage of the variations in the channel conditions using time diversity to help increase robustness of the communication to a temporary deep fade. Although a deep fade may temporarily erase some of the information transmitted, the use of an error-correcting code coupled with successfully transmitted bits during other time instances (interleaving) can allow for the erased bits to be recovered. For this channel, instead of the

spectral efficiency with constant channels it is more appropriate the study of the *ergodic spectral efficiency*. The spectral efficiency as well as the power constraint are averaged over many coherence time periods. Each time slot is assumed to be large enough so that the randomness of the communication can be averaged: additive noise, fading, mobility. This can result in significant delay. The ergodic capacity in the low energy regime has been studied in [42] for the (MAC), Broadcast channel (BC) and interference channel (IC) and in [43] for the RC.

- Slow fading channels: in this case, it is not possible to use time diversity because the transmitter sees only a single realization of the channel within its delay constraint. A deep fade therefore lasts the entire duration of transmission and cannot be mitigated using coding. Then, no coding across channel states is done and the length of the codes might be of the length of the coherence time of the channel (block fading model) [40]. In this case, it is more appropriate the study of the *outage spectral efficiency* and/or *outage probability* [13, 44]. The outage spectral efficiency is there defined as

$$R_0 = \arg \max_R \Pr (C \geq R) > p \quad (1.2)$$

where C is the spectral efficiency for a fixed realization of the channel. Thus, the outage spectral efficiency R_0 is the $(1 - p)$ percentile of the random variable C . Likewise, the outage maximum RPE can be computed as

$$\eta_0 = \arg \max_{\eta} P (\eta_C \geq \eta) > p \quad (1.3)$$

where η_C is the maximum RPE of the spectral efficiency C for a fixed realization of the channel. This metric is computed to study the low energy regime for the two-user cooperative MAC in [45] and for the RC and the two-hop RC in [46], there η_0 is referred to as ϵ -outage capacity per unit energy C_ϵ .

- **Degree of channel state information:**

We assume CSI known at the receivers. Thus, unlike opportunistic approaches [47], we consider that the set of relays involved in the transmission is known in advance and that the receiver uses coherent detection. Decoding without CSI is possible using differential space-time codes [24, 25]. However, these codes have a 3dB penalization.

We also assume CSI at the transmitters. Works assuming no CSI at the transmitters [45, 46] are mainly focused on the spatial diversity gains of cooperation in multi-path fading channels. Instead, in this dissertation, we focus on the gains of user cooperation due to an efficient use of the available network resources (bandwidth and energy). We assume that the CSI is globally known at all network nodes. The relays are optimally selected and ordered, and the resources are optimally allocated among terminals according to the channel state. Traffic or fairness issues are not addressed.

Table 1.1: Communication scenarios and studies addressed for the RC in Chapter 3.

Relay channel	
Relay Protocols	DF/AF/CF/CB
Terminals capabilities	full-duplex, synchronism, channel access via superposition
Metric	maximum RPE and slope for constant and ergodic channels
Solutions to	resource allocation and relay selection

It may be difficult to implement resource allocation solutions in practice. Specially, in the low power or energy efficient regime where even the channel estimation at the receiver is challenging. However, the approach taken in this dissertation allows us to obtain simple resource allocation solutions that likely work properly for any power regime.

The degree of CSI is related to the assumed channel model. The extension of our results to fading channels is possible taking into account that:

- For fast fading channels, the transmitters can not track the short-term fluctuation of the channels (which are considered ergodic) but can track the long term variation in average mainly due to mobility or shadowing. Thus, in this case, we can assume that the receivers have perfect CSI while transmitters only have statistical information of the channels; namely, the mean and the variance.
- For slow fading channels, if CSI is known at the transmitters and we have a delay tolerant applications, the resources can be allocated not only among user but also over time. The optimal power allocation over time is usually a “water-filling” solution. The intuition behind water-filling is to take advantage of good channel conditions: when channel conditions are good, more power is sent over the channel. As channel quality degrades, less power is sent over the channel. When the instantaneous channel falls below the cutoff value, the channel is not used. This scenario is addressed in [20] for the RC and in [48] for the cooperative MAC.

1.3 Thesis Outline

In Chapter 3, we address the study of the relay channel. In the RC, a source communicates with a destination assisted by a dedicated relay. This channel captures the essence of user cooperation and serves as one of the primary building blocks for cooperation on a larger scale. The different communication scenarios and studies addressed are detailed in the following and summarized in Table 1.1:

- We first find simple conditions to determine that the low power regime is the energy efficient regime for the rate bounds obtained with DF and the CB. The conditions found

are sufficiently general to determine the energy efficient regime of more involved scenarios such as the cooperative multiple access channel in Chapter 4 or the multiple relay multi-hop channel in Chapter 5.

- We obtain the maximum RPE and the slope of spectral efficiency for different single relay scenarios with different capabilities at terminals.
- Using these metrics, we discuss the energy and bandwidth efficiency gains associated with different capabilities at the terminals, such as: the phase synchronization between the source and relay transmissions, the FD capability at the relay, and the source-relay access to the channel via superposition instead of time-division.
- Throughout the energy efficiency study, we also obtain the optimal resource allocation in the energy efficient regime. In addition, we motivate the use of the power efficiency metrics (η and S) for relay selection.
- We extend these results to ergodic fading channels, in order to assess the impact of the channel fading distribution.
- Finally, we also extend the study to non-regenerative forwarding strategies such as AF or CF. In those cases, we restrict the analysis to showing that the energy efficient regime and the low power regime do not coincide. We show that this problem is only partially overcome by a simple time-sharing strategy. Then, the low power regime is the energy efficient regime, but the low power tools are useful no more.

The results of Chapter 3 are published in part on:

- **J. Gómez-Vilardebó** and Ana I. Pérez-Neira, “Energy Efficient Communications over a Relay Channel”, submitted to IEEE Trans. Wireless Commun., Apr., 2009.
- **J. Gómez-Vilardebó** and Ana I. Pérez-Neira, “The Energy Efficiency of The Ergodic Fading Relay Channel” in Proc. of European Signal Processing Conference (EUSIPCO), Ago. 2009.
- **J. Gómez-Vilardebó** and Ana I. Pérez-Neira, “Duplexing and Synchronism for Energy Efficient Communication over a Relay Channel” in Proc. of IEEE International Symposium on Information Theory (ISIT), July 2008.

In Chapter 4, we investigate the two-user cooperative multiple access channel (CMAC). In this scenario, two user terminals cooperate with each other in transmitting information to a common destination. The different communication scenarios and studies addressed are detailed in the following and summarized in Table 1.2.

Table 1.2: Communication scenarios and studies addressed for the two-user cooperative multiple access channel in Chapter 4.

Cooperative MAC	
Relay Protocols	DF
Terminals capabilities	full duplex, synchronism, superposition, joint coding
Metric	maximum RPE pair and slope region for constant channels
Solutions to	resource allocation, user selection

- We focus on the DF relay protocols only and design new coding schemes to accommodate the HD/FD modes, the superposition/orthogonal channel access and the joint coding and separation of data flows.
- Provided that, in this case, the energy efficient regime is the low power regime, low power analysis tools [1] are used to study the maximum rate per energy region and the slope region of spectral efficiencies as a function of the energy per bit.
- The gains provided by the terminal capabilities considered for the RC are revisited here. In addition, we study the gains given by jointly coding, via superposition, the own generated data and the cooperative data, instead of transmitting them as separated data flows.

The results of Chapter 4 are published in part on:

- **J. Gómez-Vilardebó** and Ana I. Pérez-Neira, “Energy Efficiency in Cooperative Users Communications”, submitted to IEEE Trans. Inform. Theory, Oct. 2008.
- **J. Gómez-Vilardebó** and Ana. I. Pérez-Neira, “Duplexing and Synchronism for Energy Efficient Source Cooperation”, in Proc. of IEEE 8th Workshop on Signal Processing Advances for Wireless Communications (SPAWC), July 2008.

In Chapter 5, we consider the extension of the RC to the multi-hop multiple-relay channel. This channel consist of a single source communicating with a single destination assisted by several relay nodes that listen to all the transmissions. The multiple-relay channel is the next step towards the analysis of more involved multi-user cooperative networks. This channel includes, as a special case, the two-hop multiple relay channel where relays only listen to the source but not to the other relays. In this case, see Table 1.3, we conduct only the first-order analysis of the spectral efficiency (maximum RPE). The slope of the spectral efficiency (second-order) is not addressed. The slope was useful in previous chapters to study the gains provided by, e.g. transmitting simultaneously or FD capabilities. However, each of the multi-hop strategy analyzed here obtains different maximum RPE and thus, can not be compared in terms of the slope.

Table 1.3: Communication scenarios and studies addressed for the multiple relay multi-hop network in Chapter 5.

	Two-Hops and Multi-hop Multiple Relay Networks
Assumptions	asynchronous, orthogonal transmissions
Relay Protocols	DF/CB
Capabilities	Allcat/Unicast Accumulative/Non accumulative
Metric	maximum RPE
Solutions to	resource allocation, route, and best multi-terminal coding

In addition, we restrict the analysis to asynchronous and orthogonal transmissions. We show in Chapter 3 that, if transmissions are asynchronous, the use of simultaneous transmissions does not increase the maximum RPE, even in the case of using FD terminals, and thus orthogonal transmissions are optimal in the maximum RPE sense.

- Although we only consider DF-like protocols, several coding schemes are possible depending on whether all the relays decode the source message (*allcast*) or only the destination (*unicast*), and depending on whether terminals use multiple received signals (*accumulative*) or just one signal (*non-accumulative*) to decoded the message. For each of these possibilities, we design different multi-terminal coding strategies.
- By maximizing the RPE, we provide a joint solution to a set of problems traditionally belonging to different layers: energy allocation (physical), relay selection, and routing (network). Among all the possibilities, we find solution for distributed scenarios.

The results of Chapter 5 are published in part on:

- **J. Gómez-Vilardebó** and A. I. Pérez-Neira, “Bounds on Maximum Rate-Per-Energy for Orthogonal AWGN Multiple-Relay Channels”, IEEE Trans. Wireless Commun., vol. 7, no. 11, pp 4238-4247, Nov 2008.
- **J. Gómez-Vilardebó**, A. I. Pérez-Neira, “Bounds on Maximum Rate-Per-Unit-Energy for Networks with Regenerative Relays”, in Proc of IEEE Global Telecommunications Conference, (GLOBECOM), pp. 3863-3867, Nov. 2007.
- **J. Gómez-Vilardebó**, A. I. Pérez-Neira, “An Achievable Rate per Unit Energy for Multiple Relay Networks”, in Proc. of IEEE 8th Workshop on Signal Processing Advances for Wireless Communications (SPAWC), June 2007.
- **J. Gómez-Vilardebó**, A. I. Pérez-Neira, “Energy Allocation, Relay Selection and Ordering in Orthogonal Relay Networks”, in Proc. of the Asilomar Conference on Signals, Systems and Computers, Oct. 2006.

- **J. Gómez-Vilardebó**, A. I. Pérez-Neira, “Optimal Energy Allocation, Relay Selection and Ordering in Orthogonal Relay Networks”, In Proc. International Symposium on Wireless Communication Systems (ISWCS). Sept. 2006.
- **J. Gómez-Vilardebó**, A. I. Pérez-Neira, “Upper Bound on Outage Capacity of Orthogonal Relay Networks”, in Proc. IEEE International Workshop on Signal Processing Advances for Wireless Communications (SPAWC), July 2006.

During the elaboration of this dissertation, the author has been involved in different projects and collaborations. From those works, several papers have been published that are not contained in the dissertation. The topics include: practical coding for multi-source cooperation, design of cross-layer access protocols for cooperation, and cooperative communication for satellite diversity among others.

- A. Cano, **J. Gómez-Vilardebó**, A.I. Pérez-Neira, and G. B. Giannakis, “High-Rate Distributed Multi-Source Cooperation Using Complex-Field Coding”, in Proc. of Intl. Conf. on Acoustics, Speech and Signal Processing , Apr. 2009.
- **J. Gómez-Vilardebó** , J. Alonso-Zárate, C. Verikoukis, A. I. Pérez-Neira, L. Alonso, “Cooperation On Demand Protocols for Wireless Networks”, in Proc. IEEE Personal Indoor and Mobile Radio Communications (PIMRC), Sept. 2007.
- J. Alonso-Zárate, **J. Gómez-Vilardebó**, C. Verikoukis, L. Alonso, A. I. Pérez-Neira, “Performance Evaluation of a Cooperative Scheme for Wireless Networks”, in Proc. IEEE Personal Indoor and Mobile Radio Communications (PIMRC). Sept. 2006.
- **J. Gómez-Vilardebó** , A. I. Pérez-Neira, M. Lagunas, “Average Rate Behavior for Cooperative Diversity in Wireless Networks”, in Proc. IEEE International Symposium on Circuits and Systems (ISCAS). May 2006.
- A. I. Pérez-Neira, C. Ibars, J. Serra, A. Del Coso, **J. Gómez-Vilardebó** , M. Caus, “MIMO Applicability to Satellite Networks”, in Proc. of 10th International Workshop on Signal Processing for Space Communications (SPSC), Oct. 2008.
- K.P. Liolis, **J. Gómez-Vilardebó**, E. Casini, and A. I. Pérez-Neira, “On the statistical modeling of MIMO land mobile satellite channels: a consolidated approach”, in Proc. of the International Communications Satellite Systems Conference (ICSSC), June 2009.
- M. Jiang, F. Rubio, Y. Wang, **J. Gómez-Vilardebó** , D. Yuan, “User Selection for Maximum Sum-Rate in Multi-User and MISO System with Evolutionary Algorithm”, in Proc. of the 1st IEEE International Workshop on Cross Layer Design, Sept. 2007.

Chapter 2

Background

In this chapter, we introduce the low power analysis of the spectral efficiency at the low power regime. Also, we review coding methods used to derive achievable rates for wireless networks, as these are repeatedly used throughout the dissertation.

2.1 The Low Power Regime Analysis

When studying the energy efficiency of a communication system, we aim at determining the spectral efficiency $C\left(\frac{E_b}{N_0}\right)$ (bits per second per hertz) as a function of the transmitted energy per information bit relative to the noise spectral level $\frac{E_b}{N_0}$.

The low power analysis was introduced by Verdú in [1] to analyze the spectral efficiency. The tools developed there have been successfully employed to study the energy efficient regime of several communication schemes [1, 42, 49]. This analysis is valid for any communication scheme where the number of information bits b transmitted per received dimension m is small. The number of receiver dimensions, for a continuous-time channel with effective duration and bandwidth of T and B is $m = TB$. This is because, passing the received signal through an orthonormal transformation with $m = TB$ complex dimensions is sufficient to preserve all the information (asymptotically). Then, the number of bits per received dimension is $\frac{b}{m}$, [16].

Consequently, the low power analysis is valid when: *i*) the data rate (b/s) is transmitted through a very large bandwidth (wideband regime) or *ii*) a given bandwidth is used to transmit a very small data rate.

To find $C\left(\frac{E_b}{N_0}\right)$, usually it is convenient to place a constraint, not on E_b directly, but on the energy transmitted per symbol P , or equivalent on the SNR. Then instead of $C\left(\frac{E_b}{N_0}\right)$, what we have is the spectral efficiency $C(\text{SNR})^1$ as a function of the signal to noise ratio SNR with the following relation

$$\text{SNR} = \frac{P}{mN_0}, \quad (2.1a)$$

$$= \frac{P}{N_0} \frac{b}{m}, \quad (2.1b)$$

$$= \frac{E_b}{N_0} C(\text{SNR}). \quad (2.1c)$$

If the spectral efficiency $C(\text{SNR}) = \frac{b}{m}$ in bits per dimension is a monotonically increasing concave function, according to (2.1c), the minimum values of energy per bit $\frac{E_b}{N_0 \min}$ are obtained in the low SNR regime and can be computed as

$$\frac{E_b}{N_0 \min} = \lim_{\text{SNR} \rightarrow 0} \frac{\text{SNR}}{C(\text{SNR})}, \quad (2.2a)$$

$$= \frac{\log_e 2}{\dot{C}(0)} \quad (2.2b)$$

where $\dot{C}(0)$ is the derivative at 0 of $C(\text{SNR})$ computed in nats/s.

Note that, the $\frac{E_b}{N_0 \min}$ is obtained in the limit of infinite bandwidth or zero power $\text{SNR} \rightarrow 0$, and therefore imply zero spectral efficiency $C(0) = 0$. Thus $\frac{E_b}{N_0 \min}$ gives no indication about the *bandwidth-power* tradeoff in the channel. Then, the key performance measure is the slope S of the spectral efficiency vs $\frac{E_b}{N_0}$ curve (bit/s/Hz/3 dB) at $\frac{E_b}{N_0} = \frac{E_b}{N_0 \min}$ defined as

$$S \triangleq \lim_{\frac{E_b}{N_0} \rightarrow \frac{E_b}{N_0 \min}} \frac{C\left(\frac{E_b}{N_0}\right)}{\left|\frac{E_b}{N_0}\right|_{dB} - \left|\frac{E_b}{N_0 \min}\right|_{dB}} 10 \log_{10} 2. \quad (2.3)$$

By using the second-order Taylor expansion of the spectral efficiency it was shown in [1] that the slope can be computed as

$$S = \frac{2 \left[\dot{C}(0)\right]^2}{-\ddot{C}(0)} \quad (2.4)$$

where $\ddot{C}(0)$ is the second-order derivative at 0 of $C(\text{SNR})$ computed in nats/s.

¹The choice of C and \mathbf{C} avoids the abuse of notation that assigns the same symbol to the spectral efficiency function of SNR and $\frac{E_b}{N_0}$.

2.1. The Low Power Regime Analysis

By simple observation of (2.3), it is direct that at the low energy regime, the spectral efficiency (bits/s/Hz) as a function of the $\frac{E_b}{N_0}$ (dB) can be approximated by

$$C\left(\frac{E_b}{N_0}\right) \Big|_{\frac{E_b}{N_0}|_{dB} \rightarrow \frac{E_b}{N_{0\min}}|_{dB}} = \frac{S}{10 \log_{10} 2} \left(\frac{E_b}{N_0} \Big|_{dB} - \frac{E_b}{N_{0\min}} \Big|_{dB} \right). \quad (2.5)$$

By using this result, and $\frac{E_b}{N_0} = \frac{P}{N_0 R}$ the required bandwidth for a system to achieve rate R with power P is

$$B = \frac{R}{C\left(\frac{E_b}{N_0}\right)}, \quad (2.6a)$$

$$= \frac{R}{S} \frac{3\text{dB}}{\frac{P}{N_0 R} \Big|_{dB} - \frac{E_b}{N_{0\min}} \Big|_{dB}}. \quad (2.6b)$$

In the following, we summarize some results for non-cooperative channels. We assume additive white Gaussian noise (AWGN) channels and consider a discrete-time channel model $m = 1$, unless otherwise indicated.

2.1.1 Direct Transmission

In the case of a single user white Gaussian noise channel, the received signal is

$$y = \sqrt{\beta}x + n \quad (2.7)$$

where β is a deterministic constant, n is a complex Gaussian noise with zero mean and variance

$$E[|n|^2] = \sigma^2 = N_0 \quad (2.8)$$

and x is the input signal subject to the power constraint

$$E[|x|^2] \leq P = \text{SNR}\sigma^2. \quad (2.9)$$

It was shown in [50] that Gaussian inputs achieve the capacity of this channel

$$C(\text{SNR}) = \log(1 + \beta \text{SNR}). \quad (2.10)$$

According to (2.2), the $\frac{E_b}{N_{0\min}}$ is give by

$$\frac{E_b}{N_{0\min}} = \frac{\log_e 2}{\dot{C}(0)} = \frac{\log_e 2}{\beta} \quad (2.11)$$

and using (2.4) the slope of the spectral efficiency is

$$S = 2 \text{ b/s/Hz}/(3 \text{ dB}). \quad (2.12)$$

Instead, if we consider the channel coefficient β as a random variable and the transmission time slot large enough so that the channel fading process is ergodic then, the ergodic spectral efficiency is

$$C(\text{SNR}) = \mathbb{E}[\log(1 + \beta \text{SNR})]. \quad (2.13)$$

Then, using (2.2) and (2.4) we obtain

$$\frac{E_b}{N_{0 \min}} = \frac{\log_e 2}{\mathbb{E}[\beta]}, \quad (2.14a)$$

$$S = \frac{2}{\kappa_\beta} \quad (2.14b)$$

where $\kappa_\beta = \frac{\mathbb{E}[\beta^2]}{(\mathbb{E}[\beta])^2}$ is the kurtosis of the channel fading amplitude $\sqrt{\beta}$. By Jensen's inequality, $\kappa_\beta \geq 1$. The kurtosis quantifies the peakiness of the fading amplitude. As an example, if β is assumed exponentially-distributed ($\sqrt{\beta}$ is Rayleigh) and thus $\kappa_\beta = 2$. Consequently, according to (2.6), a system operating over a ergodic Rayleigh fading channel needs

$$\frac{B_{Ray} - B_{Const}}{B_{Const}} \times 100 = \left(\frac{S_{Const}}{S_{Ray}} - 1 \right) \times 100 = 100\% \quad (2.14c)$$

more of the minimum bandwidth required for a system operating over a constant channel ($\kappa_\beta = 1$) for the same rate R and transmitted power P .

Computing only the $\frac{E_b}{N_{0 \min}}$ can lead to misleading interpretations about the behavior of the spectral efficiency. The study conducted in [1] demonstrates some of them:

- **Impact of the channel statistic:** The same $\frac{E_b}{N_{0 \min}}$ is achieved for any fading channel as long as the background noise is Gaussian. Contrary, the computation of the slope reveals that the bandwidth required to send a given data rate depends on the kurtosis of the channel amplitude. The Fig. 2.1 [1] illustrates that when the fading coefficients are known at the receiver, the bandwidth required by Rayleigh fading is twice the bandwidth required in the absence of fading.
- **Channel state information:** The $\frac{E_b}{N_{0 \min}}$ can be achieved even if the transmitter nor the receiver have any information about the channel. Again, the impact of the channel state information (CSI) is also revealed by the computation of the slope. The Fig. 2.1 [1] shows that, the bandwidth penalty due to lack of channel knowledge is equal to a factor of 1000 at $\frac{E_b}{N_0} = 1.25$ dB, and goes to infinity as we move closer to $\frac{E_b}{N_{0 \min}}$.
- **Optimal signaling:** The $\frac{E_b}{N_{0 \min}}$ can be achieved with on-off signaling. However, the computation of the slope shows that the on-off signaling obtains $S = 0.3238$ (b/s/Hz/3dB) while binary phase shift keying (BPSK) achieves a slope equal to 1 and quadrature phase shift keying (QPSK) approaches the optimal $S = 2$. Consequently, on-off signaling requires 509% the minimum bandwidth for the same rate and transmitted power. The Figure 2.2 [1] illustrates this result.

2.1. The Low Power Regime Analysis

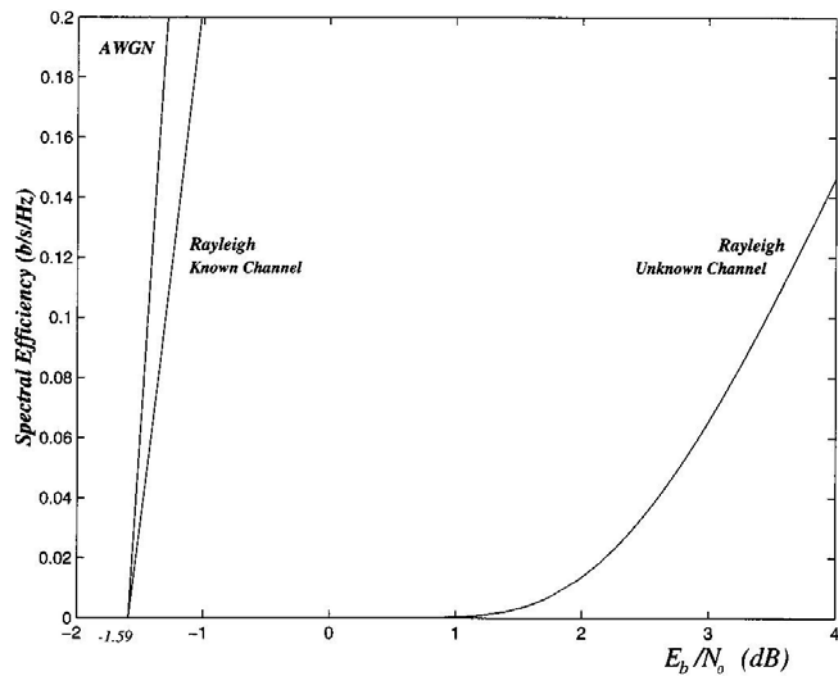


Figure 2.1: Spectral efficiencies of the AWGN channel and the Rayleigh flat fading channel with and without receiver knowledge of fading coefficients [1].

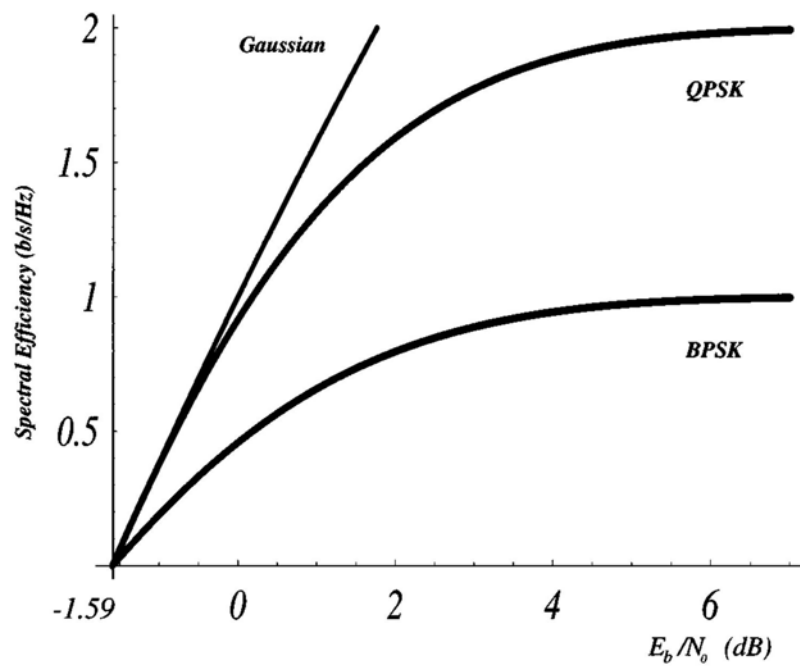


Figure 2.2: Spectral efficiencies for direct transmissions with Gaussian inputs, QPSK, and BPSK in the AWGN channel [1].

2.1.2 Multiple Input Multiple Output Channel

Consider a MIMO channel, this channel encompasses channels that incorporate features such as multi-element antennas, frequency-selective fading, multi-access, and crosstalk.

The received signal is

$$\mathbf{y} = \mathbf{H}\mathbf{x} + \mathbf{n} \quad (2.15)$$

where the noise components are independent and satisfy

$$\mathbb{E} [\|\mathbf{n}\|^2] = mN_0. \quad (2.16)$$

In this case, we only show the results for ergodic fading channels. \mathbf{H} is an $m \times n$ complex matrix whose random coefficients have finite second moments. The energy transmitted per symbol vector is $\mathbb{E} [\|\mathbf{x}\|^2]$ and

$$\text{SNR} = \frac{\mathbb{E} [\|\mathbf{x}\|^2]}{\mathbb{E} [\|\mathbf{n}\|^2]}. \quad (2.17)$$

If \mathbf{H} is random, we assume that it is stationary and ergodic, so that averaging capacity expressions over \mathbf{H} has operational significance.

Suppose that the receiver knows the $m \times n$ matrix \mathbf{H} , but the transmitter has no knowledge of the channel matrix (or its statistics). Then transmit antennas are fed by independent equal-power streams. In that case, the spectral efficiency is

$$C(\text{SNR}) = \mathbb{E} \left[\log \det \left(I + \frac{m}{n} \mathbf{H}^H \mathbf{H} \text{SNR} \right) \right] \quad (2.18)$$

The low power metrics were computed in [1]. The minimum energy per bit is given by

$$\frac{E_b}{N_{0 \min}} = \frac{n \log_e 2}{\text{trace} (\mathbb{E} [\mathbf{H}^H \mathbf{H}])} \quad (2.19)$$

the corresponding slope is

$$S = \frac{2 (\text{trace} (\mathbb{E} [\mathbf{H}^H \mathbf{H}]))^2}{m \text{trace} (\mathbb{E} [(\mathbf{H}^H \mathbf{H})^2])}. \quad (2.20)$$

If the entries of \mathbf{H} are independent zero-mean random variables with variance ζ^2 , then it can be checked that

$$\frac{E_b}{N_{0 \min}} = \frac{\log_e 2}{m\zeta^2} \quad (2.21)$$

and

$$S = \frac{2n}{\kappa(|H_{ij}|) + m + n - 2} \text{ b/s/Hz/(3 dB)/receive antenna}. \quad (2.22)$$

Furthermore, if the channel coefficient are complex Gaussian random variables, $|H_{ij}|$ follows the Rayleigh distribution whose kurtosis is equal to 2. Then the slope is

$$S = \frac{2nm}{m + n} \text{ b/s/Hz/(3 dB)}. \quad (2.23)$$

The spectral efficiency can thus be approximated by

$$C = \frac{2}{3.01} \frac{nm}{m+n} \left(10 \log_{10} \frac{E_b}{N_0} + 1.59 \right) \text{ b/s/Hz.} \quad (2.24)$$

This result reveals how the spectral efficiency is affected by the number of transmit and receive antennas. While the $\frac{E_b}{N_0 \min}$ does not depend on the number of transmit antennas, suppose that we fix the number of receive antennas m and the power and the data rate, then a system with one transmit antenna requires $(m+1)/2$ times the bandwidth of a system with m transmit antennas.

This metric is also employed in [1] to study the impact of different CSI at the transmitter and the receiver and in [49] to study the impact of the correlation between the element in \mathbf{H} .

2.1.3 Multiple Access Channel

The low power regime for the multiple access channel (MAC) and BC is studied in [42]. The low power metrics $\frac{E_b}{N_0 \min}$ and the slope S are computed therein to assess the suboptimality of time-division with respect to superposition transmissions.

For the MAC, consider the complex-valued channel

$$y = \beta_1 x_1 + \beta_2 x_2 + n \quad (2.25)$$

where n is a complex gaussian noise with zero mean and variance given by (2.8); β_1 and β_2 are deterministic complex scalars. The channel inputs x_1 and x_2 are constrained to satisfy

$$\mathbb{E} [|x_i|^2] \leq P_i = \text{SNR}_i \sigma^2, i \in \{1, 2\}. \quad (2.26)$$

The capacity region is achieved by superposition [16]

$$\begin{aligned} \{ R_1 &\leq \log(1 + \beta_1 \text{SNR}_1) \\ R_2 &\leq \log(1 + \beta_2 \text{SNR}_2) \\ R_1 + R_2 &\leq \log(1 + \beta_1 \text{SNR}_1 + \beta_2 \text{SNR}_2) \} \end{aligned} \quad (2.27)$$

In contrast, time-division multiple access (TDMA) achieves the region described as the union of rectangles as

$$\bigcup_{0 \leq \tau \leq 1} \left\{ \begin{aligned} R_1 &\leq \tau \log \left(1 + \beta_1 \frac{\text{SNR}_1}{\tau} \right) \\ R_2 &\leq (1 - \tau) \log \left(1 + \beta_2 \frac{\text{SNR}_2}{1 - \tau} \right) \end{aligned} \right\} \quad (2.28)$$

where the parameter τ is equal to the fraction of time that user 1 is active.

Define the transmitted energy per information bit relative to the noise spectral level of user $i \in \{1, 2\}$ as

$$\frac{E_i}{N_0} = \frac{\text{SNR}_i}{R_i}. \quad (2.29)$$

By enforcing the constraint $R_1 = \theta R_2$, we can move over all the point of the boundary of the rate region.

In [42], it is found that both superposition and time-division achieves the minimum energies per information bit for the MAC, equal to

$$\frac{E_i}{N_{0 \min}} = \frac{\log_e 2}{\beta_i}, i \in \{1, 2\} \quad (2.30)$$

for all $\theta = R_1/R_2$.

The slope region achieved by superposition depends on θ and is given by

$$\mathcal{S}(\theta) = \left\{ (\mathcal{S}_1, \mathcal{S}_2) : 0 \leq \mathcal{S}_1 \leq 2, 0 \leq \mathcal{S}_2 \leq 2 \right. \quad (2.31)$$

$$\left. \frac{1}{2} \leq \left(\frac{\theta}{1+\theta} \right)^2 \frac{1}{\mathcal{S}_1} + \left(\frac{1}{1+\theta} \right)^2 \frac{1}{\mathcal{S}_2} \right\}. \quad (2.32)$$

Instead, the multi-access slope region achieved by TDMA is

$$\mathcal{S}(\theta) = \{(\mathcal{S}_1, \mathcal{S}_2) : 0 \leq \mathcal{S}_1 \leq 2, 0 \leq \mathcal{S}_2 \leq 2, \mathcal{S}_1 + \mathcal{S}_2 \leq 2\}. \quad (2.33)$$

The slope region $\mathcal{S}(\theta)$ contains the slope pairs $(\mathcal{S}_1, \mathcal{S}_2) \in \mathcal{S}(\theta)$ at which the rates or (spectral efficiencies) of both users can increase simultaneously at $\frac{E_i}{N_0} = \frac{E_i}{N_{0 \min}}$. Initially, the slope pair depends on the specific point of the rate region studied, which is determined by θ . However, for the TDMA case, as can be observed in (2.33), the region of slopes is the same at any point in the rate region. As for the single user case, the slope determines the bandwidth efficiency of the system.

Figure 2.3 shows these two regions at different points of the rate region θ . We see, that the triangular region achieved by TDMA is markedly suboptimal compared to the superposition curves. Only if superposition is used both users can achieve slopes that are arbitrarily close to the single user slope provided that, the power are sufficiently unbalanced.

The extension of these results to ergodic channels is also conducted in [42]. There it is found that the slope region achieved by superposition depends on θ and is given by

$$\mathcal{S}(\theta) = \left\{ (\mathcal{S}_1, \mathcal{S}_2) : 0 \leq \mathcal{S}_1 \leq \bar{\mathcal{S}}_1, 0 \leq \mathcal{S}_2 \leq \bar{\mathcal{S}}_2, \right. \quad (2.34)$$

$$\left. 1 \leq \theta \left(\frac{1}{\mathcal{S}_1} - \frac{1}{\bar{\mathcal{S}}_1} \right) + \frac{1}{\theta} \left(\frac{1}{\mathcal{S}_2} - \frac{1}{\bar{\mathcal{S}}_2} \right) \right\}.$$

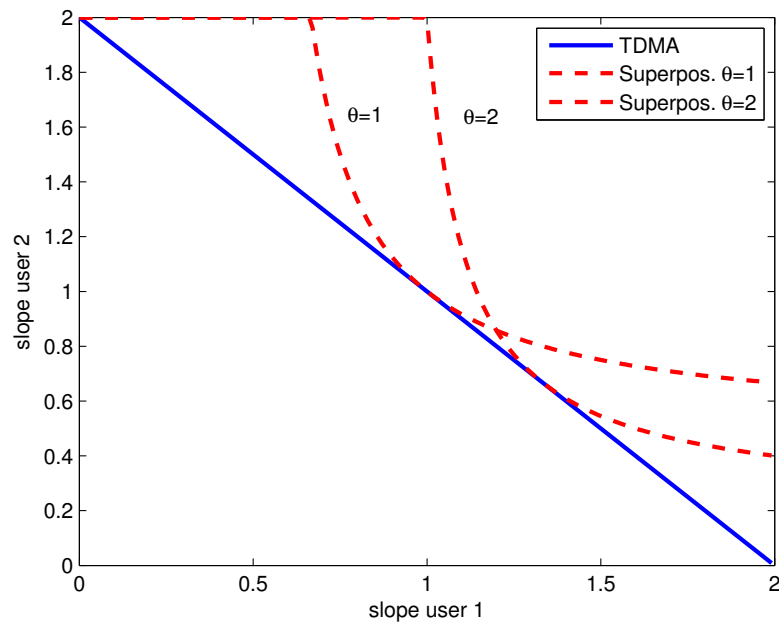


Figure 2.3: Slope regions in the Gaussian multiaccess channel with TDMA and superposition.

Instead, the multi-access slope region achieved by TDMA is

$$\mathcal{S}(\theta) = \left\{ (\mathcal{S}_1, \mathcal{S}_2) : 0 \leq \mathcal{S}_1, 0 \leq \mathcal{S}_2, \frac{\mathcal{S}_1}{\bar{\mathcal{S}}_1} + \frac{\mathcal{S}_2}{\bar{\mathcal{S}}_2} \leq 1 \right\} \quad (2.35)$$

where $\bar{\mathcal{S}}_i, i = \{1, 2\}$ is the slope of the coherent single-user fading channel given in (2.14b)

$$\bar{\mathcal{S}}_i = \frac{2}{\kappa\beta_i}. \quad (2.36)$$

2.1.4 The Broadcast Channel

Consider the two-user Gaussian broadcast channel (BC) where users 1 and 2 receive the same signal from the transmitter embedded in independent Gaussian noise

$$y_1 = \beta_1 x + n_1, \quad (2.37a)$$

$$y_2 = \beta_2 x + n_2 \quad (2.37b)$$

where β_1 and β_2 are deterministic and x, n_i satisfy

$$\mathbb{E}[|x|^2] \leq P, \quad (2.38a)$$

$$\mathbb{E}[|n_i|^2] \leq \sigma^2, i \in \{1, 2\}. \quad (2.38b)$$

In this case, the SNR is defined as

$$\text{SNR}_i = \frac{P}{\sigma^2} \quad (2.39)$$

and the transmitted energies per bit as

$$\frac{E_i}{N_0} = \frac{\text{SNR}_i}{R_i}. \quad (2.40)$$

Let us assume $\beta_1 > \beta_2$, the capacity region of this channel (achieved by superposition and stripping) is equal to [16]

$$\bigcup_{0 \leq \alpha \leq 1} \left\{ \begin{aligned} R_1 &\leq \log(1 + \alpha\beta_1\text{SNR}) \\ R_2 &\leq \log\left(1 + \frac{(1 - \alpha)\beta_2\text{SNR}}{\alpha\beta_2\text{SNR} + 1}\right) \end{aligned} \right\} \quad (2.41)$$

whereas the region achievable by TDMA is [16]

$$\bigcup_{0 \leq \alpha \leq 1} \left\{ \begin{aligned} R_1 &\leq \alpha \log(1 + \beta_1\text{SNR}) \\ R_2 &\leq (1 - \alpha) \log(1 + \beta_2\text{SNR}) \end{aligned} \right\}. \quad (2.42)$$

By enforcing the constraint $R_1 = \theta R_2$ to move over all the point of the boundary of the rate region. The minimum energies per bit achievable by both TDMA and superposition are

$$\frac{E_1}{N_{0 \min}} = \left(\frac{1}{\beta_1} + \frac{1}{\theta\beta_2} \right) \log_e 2, \quad (2.43a)$$

$$\frac{E_2}{N_{0 \min}} = \left(\frac{1}{\beta_2} + \frac{\theta}{\beta_1} \right) \log_e 2. \quad (2.43b)$$

The broadcast slope region achieved by TDMA is

$$\mathcal{S}(\theta) = \left\{ (\mathcal{S}_1, \mathcal{S}_2) : 0 \leq \mathcal{S}_1 \leq \frac{2\theta}{1 + \theta}, 0 \leq \mathcal{S}_2 \leq \frac{2}{1 + \theta} \right\}. \quad (2.44)$$

The broadcast slope region achieved by superposition is

$$\mathcal{S}(\theta) = \left\{ (\mathcal{S}_1, \mathcal{S}_2) : \begin{aligned} 0 \leq \mathcal{S}_1 &\leq \frac{2\theta(\theta + \beta_1/\beta_2)}{\theta^2 + 2\theta + \beta_1\beta_2} \\ 0 \leq \mathcal{S}_2 &\leq \frac{2(\theta + \beta_1/\beta_2)}{\theta^2 + 2\theta + \beta_1/\beta_2} \end{aligned} \right\}. \quad (2.45)$$

The extension of the above results to the case of BC subject to fading known to the receiver only is not as straightforward as for the MAC. The capacity region of general BCs is still an open problem, and only inner and outer bounds are available.

2.2 Coding Techniques for Multi-Terminal Networks

This dissertation is focussed in studying the information-theory limits. These limits are a necessary step into more practical strategies. We review here the coding methods used to derive achievable rates.

For all the techniques and scenarios, we assume random codebooks $\mathcal{X}_l(\cdot)$ with 2^{nR_l} codewords, where R_l is the rate of the code and $n \rightarrow \infty$ is the length of the codewords, which are generated independent and identically distributed *i.i.d* from a Gaussian distribution $\mathcal{X}_l(\cdot) \sim \mathcal{CN}(0, P_l)$. At the receiver, we consider joint typical decoding [16].

2.2.1 Parallel Channel Decoding: Repetition vs Independent coding

Consider the following two AWGN channels with the same capacity $C = \log(1 + P)$

$$y_1 = x_1 + n_1, \quad (2.46a)$$

$$y_2 = x_2 + n_2 \quad (2.46b)$$

where inputs x_1 and x_2 are of the same power constraint P , and noise n_1 and n_2 are of variance 1. The efficient usage of these two channels together is to let them transmit independently and then combine the rates afterwards. In this way, we can achieve any rate up to $2C = 2\log(1 + P)$. However, if we use the same codebook $\mathcal{X}_1 = \mathcal{X}_2$ at both channels and set $x_1 = x_2$, the best we can achieve is only up to $\log(1 + 2P) < 2C$. The reason is that, in the decoding process, when the simultaneous typicality check of the independent received signals is carried out, the decoding error arising from different *parallel channels* are independent of each other only if the codebooks are also independent.

The *parallel channel decoding* argument [51] can be extended to other channels. Suppose a destination receives a message ω from two parallel Gaussian channels of capacity C_1 and C_2 , using independent Gaussian codebooks $\mathcal{X}_1, \mathcal{X}_2$ of the same rate R . Then, the rate bound is the sum of the rates in each channel [16, Sec. 10.4].

$$R \leq C_1 + C_2. \quad (2.47)$$

We use this argument to justify the rate regions of the cooperative MAC in Chapter 4.

2.2.2 Superposition Encoding

Suppose a transmitter wants to transmit two messages $\omega_1 \in \{1, \dots, 2^{nR_1}\}$ and $\omega_2 \in \{1, \dots, 2^{nR_2}\}$. The transmitter assigns a random (Gaussian) code to each message, denoted as $x_1(\omega_1)$ and $x_2(\omega_2)$ with

$$\mathbb{E}[|x_i|^2] \leq P_i, i \in \{1, 2\} \quad (2.48)$$

and transmits the superposition of both messages. The signal received at destination is then

$$y = x_1 + x_2 + n. \quad (2.49)$$

By successive interference cancelation (SIC) and joint typicality decoding, the receiver can decode first ω_1 considering $x_2(\omega_2)$ as Gaussian noise if

$$R_1 \leq \log \left(1 + \frac{P_1}{1 + P_2} \right). \quad (2.50)$$

It then subtracts x_1 from the received signal and decodes x_2 ; it can do so if

$$R_2 \leq \log(1 + P_2). \quad (2.51)$$

The sum rate, thus satisfy the channel capacity

$$R_1 + R_2 \leq \log(1 + P_1 + P_2). \quad (2.52)$$

For the BC, this simple technique is able to achieve any point of the capacity region [16, Section 14.1.3]. For the MAC, considering that x_1 and x_2 are transmitted by different sources and are added at the receiver antenna, the SIC at the receivers is also able to achieve any point of the capacity region.

2.2.3 Dirty Paper Coding

Consider an AWGN channel with interference. The received signal is

$$y = x + s + n \quad (2.53)$$

where x is the transmitted signal with power P , s the interference with power Q , and n white Gaussian noise with power 1. If the receiver knows the interference perfectly the channel capacity is the same as if there was no interference, $C = \log(1 + P)$. In [52], Costa proved that if the receiver does not know the interference, while on the other hand the transmitter knows the interference perfectly (noncausally), then rate is still $C = \log(1 + P)$. This is possible through “binning” at the transmitter, and has become known as “dirty-paper coding” (DPC) because it models a transmitter which attempts to encode information on a piece of paper partially corrupted by dirt that is seen at the transmitter but it is not known at the receiver.

For the BC, this technique is able to achieve any point of the capacity region. Opposite to superposition coding for which the processing effort is done at the receivers, dirty paper coding centralizes the processing at the transmitter. Furthermore, DPC has been extended to give the full capacity region of a multiple-antenna BC [22].

2.2.4 Multiplexing Encoding

Multiplexing encoding allows a single codeword x to convey different kinds of information depending on the side information the receiver has. Suppose the transmitter wants to transmit

two messages $\omega_1 \in \{1, \dots, 2^{nR_1}\}$ and $\omega_2 \in \{1, \dots, 2^{nR_2}\}$. The transmitter makes a table with 2^{nR_1} rows and 2^{nR_2} columns, and assigns a random (Gaussian) code to each entry in the table, denoted as $x(\omega_1, \omega_2)$. A receiver can decode both ω_1 and ω_2 if the channel capacity $C > R_1 + R_2$. If it knows ω_1 , in advance, it can decode ω_2 if $C > R_2$ simply by only searching the row corresponding to ω_1 , and similarly if it knows ω_2 . This can be extended to more messages, and this simple technique plays a key role in cooperation and network coding [2].

2.2.5 Regular vs Irregular Encoding and Joint vs Successive Decoding

Suppose two transmitters want (e.g. a source and its regenerative relay) to transmit the same message $\omega \in \{1, \dots, 2^{nR}\}$ to a destination. For the simplicity of the exposition, let us assume that transmissions are over parallel channels.

The first transmitter assigns a random (Gaussian) code to each of the 2^{nR_1} messages $R_1 = R$, denoted as $x_1(\omega)$ with $E[|x_1|^2] \leq P_1$. The signal received at destination from source 1 is

$$y_1 = x_1 + n_1. \quad (2.54)$$

There are several options for the coding at the second transmitter and the decoding process at the destination:

- *Regular encoding with joint typicality decoding.* The second transmitter assigns also an independent random (Gaussian) code to each of the 2^{nR_2} messages $R_2 = R$, denoted as $x_2(\omega)$ with $E[|x_2|^2] \leq P_2$. The destination receives

$$y_2 = x_2 + n_2. \quad (2.55)$$

By joint typicality decoding, the destination can decode w making use of both received signals y_1 and y_2 if

$$R \leq \log(1 + P_1) + \log(1 + P_2). \quad (2.56)$$

- *Irregular encoding with successive decoding.* Consider a uniform random partition of the source 1 codebook into 2^{nR_2} bins $\{S_1, S_2, \dots, S_{2^{nR_2}}\}$ of size $2^{n(R_1 - R_2)}$. The transmitter 2 assigns a random (Gaussian) code to each of the 2^{nR_2} bins, denoted as $x_2(u)$ with $E[|x_2|^2] \leq P_2$. Transmitter 2 sends to the destination the index u associated with the bin containing the codeword transmitted by user 1 $x_1(w)$. Destination starts the decoding of the original message w , by first decoding s from y_2 . This is possible if

$$R_2 \leq \log(1 + P_2). \quad (2.57)$$

Upon decoding u , the destination now attempts to decode w from y_1 . There are $2^{n(R_1 - R_2)}$ possible w messages inside the bin indexed by u . Therefore, the decoding of w is successful if R_1 and R_2 satisfy

$$R_1 - R_2 \leq \log(1 + P_1). \quad (2.58)$$

The group of inequalities (2.57) and (2.58) results in the following achievable rate

$$R = R_1 \leq \log(1 + P_1) + \log(1 + P_2). \quad (2.59)$$

- *Irregular encoding with joint decoding.* The encoding at transmitter 2 is the same as in the previous case. However, in this case assume that the destination is not able to decode u directly, or equivalently

$$R_2 > \log(1 + P_2). \quad (2.60)$$

Destination can still, obtain w , by first *soft-decoding* u . It forms a list Φ of all likely u messages for which $x_2(u)$ and y_2 are jointly typical. The list Φ contains $2^{n\tilde{R}_2}$ candidates for u provided that

$$R_2 - \tilde{R}_2 \leq \log(1 + P_2). \quad (2.61)$$

Each element of Φ corresponds to a bin of x_1 codewords of size $2^{R_1 - R_2}$. Therefore, Φ restricts w to be inside a bin of size $2^{n(R_1 - R_2 + \tilde{R}_2)}$. Hence, the destination can successfully decode w from y_1 given that

$$R_1 - R_2 + \tilde{R}_2 \leq \log(1 + P_1). \quad (2.62)$$

Combining (2.61) and (2.62) the destination can decode w if

$$R = R_1 \leq \log(1 + P_1) + \log(1 + P_2). \quad (2.63)$$

Joint decoding along with irregular encoding combines the benefits of irregular encoding and regular encoding by providing rate flexibility for the second transmitter. In successive decoding along with irregular encoding, the second source rate R_2 must satisfy (2.57). On the other hand in joint decoding with regular encoding [53], the second transmitter messages has to be equal to the source message, which restricts $R_2 = R_1$. The combination of joint decoding and irregular encoding allows the second transmitter messages to have any rate R_2 satisfying $\log(1 + P_2) \leq R_2 \leq R_1$. This flexibility in choosing the rate R_2 is the key to extend multirelay decode and forward beyond the multihop scheme [54].

In addition, “binning” or parity forwarding bears a resemblance to network coding [55]. In both schemes, the intermediate nodes forward parities, instead of replicating decoded messages.

2.2.6 Block Markov Coding

Various Markov encoding and decoding techniques are often proposed for specific channels, e.g., the MAC with feedback, the relay channel (RC), the MAC with cribbing encoders [28, 56, 57]. This techniques often yield the same achievable rates for point-to-point and the RC. However, in general, in more complicated networks, different Markov encoding and decoding

Table 2.1: Block Markov coding scheme for the full duplex relay channel.

FD	Block 1	Block 2	Block 3	Block 4
Source	$x^R(\omega[1])$	$x^R(\omega[2])$	$x^R(\omega[3])$	$x^R(1)$
Relay	$x^C(1)$	$x^C(\omega[1])$	$x^C(\omega[2])$	$x^C(\omega[3])$

techniques yield different achievable rates and have various trade-offs in terms of delay and complexity.

We focus on the RC. For the full duplex RC, block Markov coding was introduced in [28]. This coding scheme allows the relay to retransmit the source message without requiring additional channel uses. The source divides the message into B blocks $\omega[1], \dots, \omega[B]$, with $\omega[b] \in 2^{nR}$ and encodes each block separately. For the RC, the encoding strategy is illustrated in Table 4.2. The source and the relay use different codebooks: $\mathcal{X}^R(\cdot), \mathcal{X}^C(\cdot)$. The source transmits the sequence of blocks $x^R(\omega[1]), \dots, x^R(\omega[B])$. Assume the relay node decodes $\omega[b]$ during block b . It then transmits $\omega[b]$ during block $b + 1$ using the random codebook $\mathcal{X}^C(\cdot)$. The whole transmission of B messages therefore uses $B + 1$ blocks. We thus have an overall rate of $R_W = \frac{RB}{B+1}$, when $B \rightarrow \infty$ this still yields a rate of R . The decoding at the destination has different possibilities, all using several or all of its available output blocks. In the original work, [28], list decoding was used for decoding. This was simplified in [58] using the backward decoding introduced in [57], but actually a simpler argument based on parallel (Gaussian) channels due to Valenti [51], see Subsection 2.2.1.

Chapter 3

The Relay Channel

In wireless networks, cooperation among users has shown to increase data rates and to provide energy savings [2,59]. However, these gains might come at the cost of additional capabilities at nodes such as, distributed synchronization, distributed channel state information (CSI), duplexing, etc. This chapter analyzes the energy efficiency gains associated with different capabilities at terminals. We restrict our analysis to the relay channel (RC) under additive white Gaussian noise (AWGN). In the RC, a source communicates with a destination assisted by a dedicated relay. This channel captures the essence of cooperative multi-hopping and serves as the primary building block for cooperation on a larger scale. The main terminal capabilities discussed are detailed below and summarized in Table 3.1:

- *Channel access*: Equivalently to the multiple access channel (MAC), within the RC two nodes share the same medium. If the receiver is able to cope with inter-user interference, then both nodes can transmit simultaneously. If not, orthogonal transmissions (OT) must be put in place, as e.g. time-division multiplexing.
- *Duplexing*: The full duplex (FD) capability at a relay allows it to receive and transmit simultaneously in the same band. In such a case, the signal transmitted by the relay interferes with its own received signal. In theory, it is possible for the relay to cancel out this interference because it is known [18, 19]. In practice, however, any error in interference cancelation (e.g. due to quantization and finite-precision processing effects)

Table 3.1: Scenarios depending on the terminal constraints.

Channel Access	Orthogonal	Simultaneous	
Duplexing	—	HD	FD
Synchronism	Async.	Sync./Async.	Sync./Async.

can be catastrophic because the transmitted signal is typically 100-150dB stronger than the received signal [9]. If FD operation is not possible, the relay works in half duplex (HD) mode, which consists of a relay transmitting and receiving using different degrees of freedom.

- *Synchronization*: In the RC, the source terminal knows, partially or completely, the signal transmitted by the relay. If, additionally, local oscillators are synchronized and the phases of the channels between the source and the destination and between the relay and the destination are known, the transmitted signals can add coherently at the receiver. It is relatively easy to obtain symbol (timing) synchronization; however, carrier synchronization requires phase-locking-separated microwave oscillators, which is very challenging in practice [26]. This seems highly unrealistic. Left by themselves, the drift of the oscillators makes synchronization impossible. However, some distributed carrier synchronization and channel feedback techniques are currently available. An excellent overview of the state of the art can be found in [27].

This chapter is focused on the study of the spectral efficiency $C\left(\frac{E_b}{N_0}\right)$ as a function of the transmitted energy per information bit relative to the noise spectral level $\frac{E_b}{N_0}$. In the energy efficient regime, there are two metrics of special interest [1]: The maximum rate per energy (RPE) or, equivalently, the minimum energy per bit $\frac{E_b}{N_{0\min}}$ is the most relevant point in the spectral efficiency curve. However, in most of the communication systems, the minimum values of energy per bit are obtained in the limit of low power or infinite bandwidth and therefore imply zero spectral efficiency $C\left(\frac{E_b}{N_{0\min}}\right) = 0$. Consequently, in those cases, the $\frac{E_b}{N_{0\min}}$ gives no indication about the bandwidth-power tradeoff in the channel and the key performance measure is the slope S of the spectral efficiency vs $\frac{E_b}{N_0}$ at $\frac{E_b}{N_0} = \frac{E_b}{N_{0\min}}$. This metric determines the bandwidth efficiency of the communication system. Tools to compute $\frac{E_b}{N_{0\min}}$ and S are derived in [1]. These tools have been successfully employed to study the energy efficient regime of several communication schemes [1, 42, 49].

3.1 Related Work and Contributions

The relay channel was introduced by Cover, El Gamal and Van der Meulen in [28, 62]. However, the capacity remains still unknown. We here focus on the capacity lower-bounds obtained

Table 3.2: Low power metrics found in the literature depending on the nodes capabilities.

DF and CB	Const./Erg.	$\eta/\bar{\eta}$	S_L/\bar{S}_L	S/\bar{S}
FD	Async.	[60]/ [61]	[61]	[*]
	Sync.	[60]/ [61]	[*]/[?]	[*]/[?]
OT or HD'	Async.	[60] / [61]	[61]	[*]
HD	Async.	[*]	[*]	[*]
	Sync.	[*]/[?]	[*]/[?]	[*]/[?]

with *decode and forward* (DF) and the upper bounds obtained with the *cut-set bound* (CB) in [28]. The study of the energy efficiency for the RC under AGWN with DF and the CB was initiated in [60] for constant channels and was extended in [61] to ergodic fading channels. The scenarios addressed there are detailed in the following and summarized in Table 3.2. The [*] stands for the new cases addressed in this chapter and [?] stands for the cases not available in the literature. The maximum RPE and the slope are denoted as η and S for constant channels and as $\bar{\eta}/\bar{S}$ for ergodic fading channels. As S_L/\bar{S}_L we denote the slopes obtained when the power allocated to the terminals, as a function of the total power, is restricted to be linear.

In [60] authors assumed perfect CSI at the transmitters and computed the maximum RPE for two scenarios:

- i) simultaneous and synchronous transmissions from the source and a FD relay and
- ii) orthogonal transmissions from the source and a HD relay.

These results were extended in [61] to ergodic fading channels assuming only statistical CSI at the transmitters, namely the mean and the variance. In this case, the authors computed not only the maximum RPE but also the slope. The same two scenarios were addressed. For the case of simulations transmission with a FD relay, it was shown that, asynchronous transmissions are optimal in terms of maximum RPE whenever the complex channel coefficients between the source and the destination and between the relay and the destination have zero mean, or equivalently the channel does not have a constant component. The optimal resource allocation and the maximum RPE were shown to have close form expressions only in those cases and thus, the slope was only computed for the asynchronous case *ii*) For a relay in HD mode, the relaying strategy presented in [61, eq. 48], denoted by HD', generalizes the one addressed in [60] by letting the source to transmit during the relay transmission period a synchronous signal. However, only the results for the OT case were reported.

In these works, the computation of the maximum RPE has been useful to demonstrate the sub-optimality of the orthogonal channel access a HD relay against simultaneous and synchronous transmissions with a FD relay, see also [63]. The case of synchronous transmission with a HD relay has not been addressed in the literature and thus, from those analysis the gains of FD

and synchronous capabilities cannot be separated. For asynchronous transmissions, FD and HD terminals obtain the same maximum RPE. In this case, the computation of the slope reveals the suboptimality of the HD mode with respect FD mode as well as the impact of the channel fading statistics.

These works have been extended to other forwarding protocols. The bounds on the maximum RPE obtained in [60] were extended in [64] to include side-information and linear relaying strategies. As argued in [30], although in some scenarios these techniques can offer a better maximum RPE, it is not obtained in the low power regime. In fact, in the low power regime these strategies can never improve DF. Likewise, the results presented in [61] were extended in [43] to include also the *amplify and forward* scheme. Other works studying the spectral efficiency gains of cooperation at the low power regime are [30,46,59]. In these works, no channel knowledge at the transmitters is assumed. Then, instead of studying the spectral efficiency as a function of the total network power, the outage capacity over Rayleigh fading channels is addressed.

In this work, we extend these previous results in two main directions:

- Firstly, we allow the resources: transmitted power and the transmission interval fractions, to be any function of the total transmitted power. In previous works, the power allocation was restricted to be a linear function of the total power and the transmission interval fractions were assumed independent of the total power. We show here, that although the maximum RPE is not affected by these limitations, the slope of the spectral efficiency can be increased.
- Secondly, for the HD scenario, we consider the bounds on the capacity presented in [20, Propositions 1 and 2], which improve the ones studied in [60] and [43], by letting the source to transmit during the relay transmission period, not only a synchronous signals but also new information.

We organize our contributions as follows:

- Given that the resources can now be any function of the total power, we first ensure that the low power metrics can still be employed to study the energy efficiency of the system. We find simple conditions to determine that low power regime is the energy efficient regime for the rate bounds obtained with DF and CB. These conditions are sufficiently general to determine the energy efficient regime of more involved scenarios such as the cooperative multiple access channel in Chapter 4 or the multiple relay multi-hop channel in Chapter 5.
- Then, we assess the impact on the energy efficiency of several terminals capabilities, such as: the transmission synchronization, the full duplex mode operation and the superposition channel access. To that end, we compute, assuming constant channels, the maximum

RPE and the slope of the spectral efficiency for different scenarios, that depend on these nodes capabilities.

- Then, numerical results are presented to validate the results and to motivate the use of the energy efficiency metrics to design the network.
- The analysis is then extended to ergodic fading channels. In this case, we only consider asynchronous transmissions. As shown in [43], the synchronous capability is only useful if the channel has a constant component.
- We also extend the study to non-regenerative forwarding strategies such as amplify and forward (AF) or compress and forward (CF). In those cases, we restrict the analysis to show that the energy efficient regime and the low power regime do not coincide. We show that this problem is only partially overcome by a simple time-sharing strategy. Then, the low power regime is the energy efficient regime but the low power tools are useful no more.

The remainder of the chapter is organized as follows. First, the channel model is presented in Section 4.2. The rate lower bounds with decode and forward and upper bounds with the CB for the AWGN relay channel under duplexing and synchronism constraints are presented in a unified manner in Section 3.3. In Section 3.4, the study of the energy efficient regime is particularized to the RC. In subsequent sections, we address the energy efficiency analysis. Section 3.5 is devoted to the maximum RPE and Section 4.7 is devoted to the maximum slope. Numerical results are presented in Section 3.7. The extension to ergodic fading channels is conducted in Section 3.8 and the extension to non-regenerative forwarding strategies is conducted in Section 3.9. Finally, conclusions are drawn in Section 4.9.

3.2 Channel Model

Consider the AWGN relay channel model depicted in Fig. 4.1. If the relay works in HD mode or if the source and the relay use orthogonal transmissions to access to the channel, then the channel degrees of freedom (time/bandwidth) must be shared and assigned. Without loss of generality, hereafter, we consider a fixed total bandwidth and assign the transmission time degree of freedom. Thus, the total transmission period is divided into two intervals $j \in \{1, 2\}$. The source transmits to the relay and destination in the first interval $j = 1$ while, in the second interval $j = 2$, both (HD case) or only the relay (OT case) transmit to the destination. In FD mode, there is only one channel and the index j is dropped. The received signals during the interval j at the relay Y_{2j} and at the destination Y_{0j} are given by

$$\begin{aligned} Y_{2j} &= \sqrt{\alpha_{12}}X_{1j} + Z_{2j}, \\ Y_{0j} &= \sqrt{\beta_1}X_{1j} + \sqrt{\beta_2}X_{2j} + Z_{0j}. \end{aligned} \tag{3.1}$$

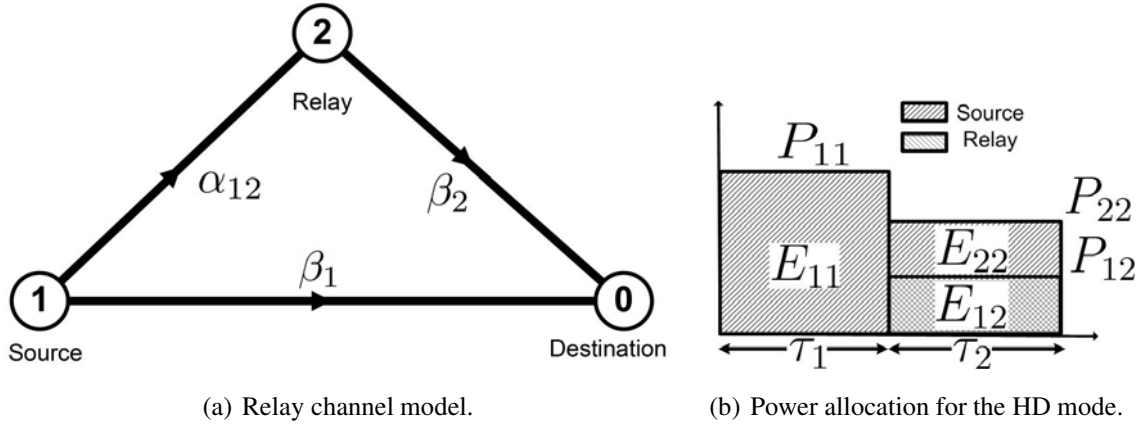


Figure 3.1: Scenario description.

We assume, without claim of optimality, that the signals transmitted by the source X_{1j} and the relay X_{2j} are Gaussian distributed with power P_{1j} , P_{2j} , respectively. The noise processes at the relay Z_{2j} and at the destination Z_{0j} are complex independent white Gaussian, each one with zero mean and unit variance $E[|Z_{ij}|^2] = N_0 = 1$. The channel gain from the source to the relay is denoted by α_{12} , from the source to destination by β_1 , and from the relay to destination by β_2 . Each orthogonal transmission uses a fraction $\tau_j T$ out of the total transmission period T , with $\sum_{j \in \{1,2\}} \tau_j = 1$. The power allocated to node $l \in \{1, 2\}$ during the interval j is denoted as $E_{lj} = \tau_j P_{lj}$. Notice that E_{lj} is still power, (not energy) since τ_j is a time-sharing factor. An example of the power allocation for the HD case is depicted in Fig. 3.1(b).

3.3 Relay Channel Capacity Bounds

The optimal relaying strategy for the relay channel is still unknown and only rate lower and upper bounds on the capacity exist. The energy efficiency analysis conducted in this work considers DF for rate lower bounds and the CB for rate upper bounds.

3.3.1 The Full Duplex Relay Channel

In this case, the capacity bounds under AWGN obtained with the CB and DF can be found in [28, Theorem 5]¹. Without entering into the details of the transmission strategies, we here mention the powers and transmissions involved. Out of the total source power E_1 , a portion E_1^A is used by the source to inject new information to the channel, not known at the relay, using an asynchronous signal X_1^A . The relay assists the communication by transmitting the signal X_2

¹The notation used here and the notation used in [28, Theorem 5] are related as $E_1^A = \rho P_1$, $E_1^S = (1 - \rho) P_1$ and $E_2 = P_2$.

3.3. Relay Channel Capacity Bounds

with power E_2 . Superposed, only if transmissions are synchronous, the source dedicates the rest of the power E_1^S to transmit coherently with the relay the signal $X_1^S = \sqrt{E_1^S} \frac{X_2}{\sqrt{E_2}}$. Then, the source transmitted signal is $X_1 = X_1^A + X_1^S$ and has power $E_1 = E_1^S + E_1^A$. Note that, the correlation between the source and relay transmitted signal is

$$\rho = \frac{(\mathbb{E}[X_1 X_2])^2}{\mathbb{E}[|X_1|^2] \mathbb{E}[|X_2|^2]} = \frac{E_1^S}{E_1}. \quad (3.2)$$

If only asynchronous transmission are possible, then $E_1^S = 0$. Finally, the capacity bounds obtained with DF and the CB for some fixed power allocation vector $\mathbf{E} = [E_1^A, E_1^S, E_2]$ can be written in a unified manner as follows

$$R_F(\mathbf{E}) = \min(\log(1 + g_1(\mathbf{E})), \log(1 + g_2(\mathbf{E}))), \quad (3.3a)$$

$$g_1(\mathbf{E}) = \hat{\alpha}_{12} E_1^A, \quad (3.3b)$$

$$g_2(\mathbf{E}) = \beta_1 E_1^A + \left(\sqrt{\beta_1 E_1^S} + \sqrt{\beta_2 E_2} \right)^2 \quad (3.3c)$$

with $\hat{\alpha}_{12} = \alpha_{12}$ for DF and $\hat{\alpha}_{12} = \alpha_{12} + \beta_1$ for the CB.

To obtain maximum rate R^* for all E , we need to maximize $R_F(\mathbf{E})$ while satisfying the total power constraint $E_1^A + E_1^S + E_2 = E$. This is possible in close form. First, for synchronous transmissions, let us denote $E^R = E_1^S + E_2$. The coherent term $\left(\sqrt{\beta_1 E_1^S} + \sqrt{\beta_2 E_2} \right)^2$ is maximized at

$$E_1^S = \frac{\beta_1 E^R}{\beta_1 + \beta_2}, \quad E_2 = \frac{\beta_2 E^R}{\beta_1 + \beta_2} \quad (3.4)$$

and thus $g_2(\mathbf{E}) = \beta_1 E_1^A + \hat{\beta}_2 E^R$ with $\hat{\beta}_2 = \beta_2 + \beta_1$. Note that, for asynchronous transmissions, $E_1^S = 0$ and we can simply replace $\hat{\beta}_2 = \beta_2$ in $g_2(\mathbf{E})$. Second, note that the logarithm term can be omitted and we only need to maximize the minimum between $g_1(\mathbf{E})$ and $g_2(\mathbf{E})$ as

$$\begin{aligned} \max_{E_1^A, E^R} \min & \left(\hat{\alpha}_{12} E_1^A, \beta_1 E_1^A + \hat{\beta}_2 E^R \right) \\ & E_1^A + E^R = E, \\ & 0 \leq E_1^A, E^R. \end{aligned} \quad (3.5)$$

Solving this linear problem, the optimal power allocation can be shown to be (see [63])

$$E_1^A = \frac{\hat{\beta}_2}{\hat{\beta}_2 + \hat{\alpha}_{12} - \beta_1} E, \quad E^R = \frac{\hat{\alpha}_{12} - \beta_1}{\hat{\beta}_2 + \hat{\alpha}_{12} - \beta_1} E \quad \text{if } \hat{\beta}_2, \hat{\alpha}_{12} > \beta_1 \quad (3.6)$$

otherwise ($\hat{\beta}_2 < \beta_1$ or $\hat{\alpha}_{12} < \beta_1$) the direct transmission from the source to the destination is better than relaying. Substituting this solution into (3.3) the resultant rate function is

$$R^*(E) = \log(1 + \beta_{FD} E) \quad (3.7)$$

with

$$\beta_{FD} = \begin{cases} \frac{\hat{\alpha}_{12} \hat{\beta}_2}{\hat{\alpha}_{12} + \hat{\beta}_2 - \beta_1} & \text{if } \hat{\alpha}_{12}, \hat{\beta}_2 > \beta_1, \\ \beta_1 & \text{otherwise.} \end{cases} \quad (3.8)$$

3.3.2 The Half Duplex Relay Channel

In this case, the capacity bounds under AWGN obtained with the CB and DF can be found in [20]². We assume a fixed transmission slot structure, where all terminals known in advance which modes (receive or transmit) every terminal is using. By dropping this assumption, it was shown in [65] that a random mode strategy achieves better rates than the fixed transmission slot strategy, and that non-Gaussian input distributions achieve better rates than Gaussian ones. However, we do not consider this possibility.

The communication is divided into two transmission intervals. During the first interval a fraction τ_1 of the total transmission time is used. In this interval, the source transmits alone, and thus asynchronously, the signal X_{11} with power P_{11} . The total amount of transmitted power is $E_{11} = \tau_1 P_{11}$. In the second interval, the relay dedicates the fraction of power $E_{22} = \tau_2 P_{22}$ to transmit the signal X_{22} with power P_{22} . Meanwhile, the source transmits, simultaneously, an asynchronous signal X_{12}^A with power P_{12}^A and the coherent signal $X_{12}^S = \sqrt{P_{12}^S} \frac{X_{22}}{\sqrt{P_{22}}}$ with power P_{12}^S . Then, the source transmitted signal is $X_{12} = X_{12}^A + X_{12}^S$ and uses the fraction of power $E_{12} = E_{12}^S + E_{12}^A$. The correlation between the source and relay transmitted signals in the second transmission interval is

$$\rho = \frac{(\mathbb{E}[X_{12}X_{22}])^2}{\mathbb{E}[|X_{12}|^2] \mathbb{E}[|X_{22}|^2]} = \frac{E_{12}^S}{E_{12}} = \frac{P_{12}^S}{P_{12}}. \quad (3.9)$$

If only asynchronous transmissions are possible, then $E_{12}^S = 0$. For OT, additionally, we force $E_{12}^A = 0$. Finally, the capacity bounds obtained with DF and the CB for some fixed power allocation vector $\mathbf{E} = [E_{11}, E_{12}^A, E_{12}^S, E_{22}]$ and time-sharing factor $\boldsymbol{\tau} = [\tau_1, \tau_2]$ is

$$R_F(\boldsymbol{\tau}, \mathbf{E}) = \min_{i \in \{1,2\}} C_i(\boldsymbol{\tau}, \mathbf{E}) \quad (3.10)$$

with

$$C_i(\boldsymbol{\tau}, \mathbf{E}) = \sum_{j=1}^2 \tau_j \log \left(1 + \frac{g_{ji}(\mathbf{E})}{\tau_j} \right) \quad (3.11)$$

and

$$g_{11}(\mathbf{E}) = \hat{\alpha}_{12} E_{11}, \quad g_{21}(\mathbf{E}) = \beta_1 E_{12}^A, \quad (3.12a)$$

$$g_{12}(\mathbf{E}) = \beta_1 E_{11}, \quad g_{22}(\mathbf{E}) = \beta_1 E_{12}^A + \left(\sqrt{\beta_1 E_{12}^S} + \sqrt{\beta_2 E_{22}} \right)^2 \quad (3.12b)$$

with $\hat{\alpha}_{12} = \alpha_{12}$ for DF, $\hat{\alpha}_{12} = \alpha_{12} + \beta_1$ for the CB.

To obtain the maximum rate R^* for all E , we need to maximize $R_F(\boldsymbol{\tau}, \mathbf{E})$ while satisfying the resource allocation constraints $E_{11} + E_{12}^A + E_{12}^S + E_{22} = E$ and $\tau_1 + \tau_2 = 1$. For the

²The notation used here and the notation used in [20] are related as $P_{12}^S = \rho P_1^{(2)}$, $P_{12}^A = (1 - \rho) P_1^{(2)}$ and $P_{22} = P_2$.

HD relay channel, this is not possible in close form. However, for synchronous transmissions we can simplify the coherent term. Let us denote $E^R = E_{22} + E_{12}^S$, then the coherent term $\left(\sqrt{\beta_1 E_{12}^S} + \sqrt{\beta_2 E_{22}}\right)^2$ is maximized at

$$E_{12}^S = \frac{\beta_1 E^R}{\beta_1 + \beta_2}, \quad E_{22} = \frac{\beta_2 E^R}{\beta_1 + \beta_2} \quad (3.13)$$

and thus $g_{22}(\mathbf{E}) = \beta_1 E_{12}^A + \hat{\beta}_2 E^R$ with $\hat{\beta}_2 = \beta_2 + \beta_1$ for synchronous and $\hat{\beta}_2 = \beta_2$ for asynchronous transmissions. Finally, $R^*(E)$ is found by solving

$$R^*(E) = \max_{\boldsymbol{\tau}, \mathbf{E}} \min_{i \in \{1,2\}} C_i(\boldsymbol{\tau}, \mathbf{E}) \quad (3.14a)$$

$$\tau_1 + \tau_2 = 1, \quad \tau_1, \tau_2 \geq 0, \quad (3.14b)$$

$$E_{11} + E_{12}^A + E^R = E, \quad E_{11}, E_{12}^A, E^R \geq 0. \quad (3.14c)$$

3.4 The Energy Efficiency Analysis

The low power analysis developed in [1] and introduced in Chapter 2 is utilized hereafter to study the energy efficient regime for the RC. First, we particularize the low power analysis to the AWGN relay channel. Then, we discuss the validity of the low power analysis to study the energy efficiency of this communication system.

3.4.1 The Relay Channel

Unlike the single-user case, for the RC there are different definitions for the energy per bit. These definitions depend on the considered energy cost of the communication and to whom the energy belongs. In this work, we consider that the energy belongs to the “network” and is optimally allocated among nodes. Then, the network energy per bit is defined as $E_b \triangleq \frac{E}{R(E)}$, where E is the sum energy $E = \sum_{l \in \{1,2\}} \sum_{j \in \{1,2\}} E_{lj}$ and $R(E)$ is the spectral efficiency in bits³.

We define the rate per total network energy normalized by the noise spectral level as

$$RPE \triangleq N_0 \log_e 2 \frac{R(E)}{E}. \quad (3.15)$$

If the energy efficient regime is the low power regime, it was shown in [1] that the minimum energy per bit normalized by the noise spectral level is given by $\frac{E_b}{N_0 \min} = \frac{\log_e 2}{\dot{R}(0)}$ where $\dot{R}(0)$ is computed in nats. Then, the maximum RPE (η) can be obtained as

$$\eta = \frac{\log_e 2}{\frac{E_b}{N_0 \min}} = \dot{R}(0) \quad (3.16)$$

³We replace the $\text{SNR} = \frac{E}{N_0}$ by the total power E , since we consider that the noise has unit variance $N_0 = 1$.

The slope of the spectral efficiency as a function of the $\frac{E_b}{N_0}$ was shown in [1] to be

$$S = \frac{2 \left[\dot{R}(0) \right]^2}{-\ddot{R}(0)}. \quad (3.17)$$

Then, the spectral efficiency can be approximated as [1]

$$R \left(\frac{E_b}{N_0} \right) \Big|_{\frac{E_b}{N_0} |_{dB} \rightarrow \frac{E_b}{N_{0 \min}} |_{dB}} \approx \frac{S}{10 \log_{10} 2} \left(\frac{E_b}{N_0} \Big|_{dB} - \frac{E_b}{N_{0 \min}} \Big|_{dB} \right). \quad (3.18)$$

Hereafter, unless otherwise indicated, all the logarithms are in base 2, i.e., all the rates (also referred to as spectral efficiencies) R are in bits per second per hertz. Nevertheless, the derivatives of the rates with respect to the power E , $\dot{R}(E)$ and $\ddot{R}(E)$ are computed in nats.

3.4.2 The Energy Efficient and the Low Power Regime

To study the energy efficiency of a communication system with rate $R(E)$ by using the low power tools presented above we need to ensure that the energy efficient regime is the low power regime, which is not always true. It was shown in [60] that for a rate function $R(E)$ that: *i*) satisfies $R(0) = 0$, increases monotonically with E and, *ii*) is concave for all E . Then, the energy efficient regime is the low power regime $E = 0$. This result, was used there to obtain bounds on the maximum RPE for the relay channel with DF and the CB. In particular, authors considered two scenarios: a FD relay with synchronous transmissions and a HD relay with orthogonal transmissions from the source and the relay. In that work, the rate function was of the type (3.14) but, the power allocation among nodes $\mathbf{E}(E)$ was restricted to be linear in the total power E . In addition, for the OT scenario, the time-sharing factors were fixed to $\tau_1 = \tau_2 = \frac{1}{2}$. In that case, the conditions above mentioned are satisfied and the energy efficient regime is the low power regime.

For the FD relay channel, as shown in the previous section, the optimal power allocation solution for each E is indeed a linear function of the total E , (see 3.6). However, for the more general HD relay channel and also for the ergodic fading relay channel, conducted next, the optimal power allocation is not necessarily linear in E and the time-sharing factors τ may dependent on E .

We consider that the resource allocation solution to (3.14) can be any pair of differentiable functions of E , $\tau(E)$ and $\mathbf{E}(E)$. In that case, it is direct to show that condition (*i*) is satisfied. However, the concavity condition is difficult to prove. Instead, in the following proposition, we found an alternative condition.

Proposition 3.1 *Consider a communication scheme with a rate function $R(E)$. If the function $R(E)$: i) satisfies $R(0) = 0$, increases monotonically and ii) is bounded, for all E , by the*

3.4. The Energy Efficiency Analysis

first-order Taylor series approximation of the rate function at $E = 0$ ($R(E) \leq \dot{R}(0) E$). Then, the minimum energy per bit is obtained in the low power regime $E = 0$.

Furthermore, if condition i) is satisfied then, condition ii) is necessary and sufficient, namely if the maximum RPE is obtained at $E = 0$, then the spectral efficiency satisfies ($R(E) \leq \dot{R}(0) E$).

Proof: If $R(0) = 0$, then as E goes to 0, $\lim_{E \rightarrow 0} \frac{R(E)}{E} = \dot{R}(0)$. If the $R(E)$ satisfies $\frac{R(E)}{E} \leq \dot{R}(0)$ (condition ii), then clearly the maximum rate per energy ($\frac{R(E)}{E}$) is reached at $E = 0$.

The sufficiency of condition ii) given condition i) is direct. If $\max \frac{R(E)}{E} = \lim_{E \rightarrow 0} \frac{R(E)}{E}$, then given that $\frac{R(E)}{E} < \max \frac{R(E)}{E}$ condition i) forces $\frac{R(E)}{E} < \lim_{E \rightarrow 0} \frac{R(E)}{E} = \dot{R}(0)$. ■

Using the condition ii) of Proposition 3.1, we can show that the rate function $R^*(E)$ for HD nodes defined in (3.14) obtains the maximum RPE in the low power regime. In fact, here, we consider a generalized version of this rate function by assuming up to L rate constrains C_i $i \in \{1, 2, \dots, L\}$ and T orthogonal intervals $j = \{1, 2, \dots, T\}$. Then, this result is also valid the rate functions obtained for other cooperative scenario such as the cooperative multiple access channel in Chapter 4 or the multiple relay multi-hop channel in Chapter 5.

First, we state the notation used as it is used, repeatedly, in all this chapter:

As we said before, we consider that the resource allocation solution to (3.14) can be any pair of differentiable functions of E $\boldsymbol{\tau}(E)$ and $\mathbf{E}(E)$. In fact, as we see later on, we only require right differentiability at $E = 0$.

- The vector of time-sharing factors and its first-order derivative evaluate at $E = 0$ are denoted as $\mathbf{t} \triangleq \boldsymbol{\tau}(0)$ and $\dot{\mathbf{t}} \triangleq \dot{\boldsymbol{\tau}}(0)$, respectively.
- The first and second-order derivatives of the power allocation vectors evaluated at $E = 0$ are denoted as $\dot{\mathbf{e}} \triangleq \dot{\mathbf{E}}(0)$ and $\ddot{\mathbf{e}} \triangleq \ddot{\mathbf{E}}(0)$, respectively.
- After substituting $\boldsymbol{\tau}(E)$ and $\mathbf{E}(E)$ into (3.10), (3.11) and (3.12), we define
 - The rate as a function of E as $R(E) \triangleq R_F(\boldsymbol{\tau}(E), \mathbf{E}(E))$.
 - The functions $C_i(\boldsymbol{\tau}, \mathbf{E})$ in (3.11) as a function of E as $C_{E_i}(E) \triangleq C_i(\boldsymbol{\tau}(E), \mathbf{E}(E))$.
 - The functions $g_{ji}(\mathbf{E})$ in (3.12) as a function of E as $g_{E_{ji}}(E) \triangleq g_{ji}(\mathbf{E}(E))$.

To use the condition ii), we need first to compute $\dot{R}^*(0)$. Using the above definitions, the rate as a function of E is given by

$$R(E) \triangleq R_F(\boldsymbol{\tau}(E), \mathbf{E}(E)), \quad (3.19a)$$

$$= \min_{i \in \{1, \dots, L\}} C_{E_i}(E). \quad (3.19b)$$

To satisfy the total and positive power conditions in (3.14c), the functions $C_{E_i}(E)$ for all i must coincide at $E = 0$, namely $C_{E_1}(0) = C_{E_2}(0) = 0$. Nevertheless, each one increases as $\dot{C}_{E_i}(0)$ and consequently, $\dot{R}(0)$ is given by

$$\dot{R}(0) = \min_{i \in \{1, \dots, L\}} \dot{C}_{E_i}(0). \quad (3.20)$$

In Appendix 3.A, for any C_i defined as in (3.10), we obtain the derivatives of the rate constraints $C_{E_i}(E)$ at $E = 0$, as

$$\dot{C}_{E_i}(0) = \sum_{j=1}^T \dot{g}_{E_{ji}}(0). \quad (3.21)$$

Notice that, the functions $\dot{g}_{E_{ji}}(0)$ and $\dot{C}_{E_i}(0)$ only depend on $\dot{\mathbf{e}}$, namely $\dot{g}_{E_{ji}}(\dot{\mathbf{e}})$ and $\dot{C}_{E_i}(\dot{\mathbf{e}})$. To find $\dot{R}^*(0)$, we only need to maximize (3.20) over $\dot{\mathbf{e}}$ as

$$\dot{R}^*(0) = \max_{\dot{\mathbf{e}}} \min_{i \in \{1, \dots, L\}} \dot{C}_{E_i}(\dot{\mathbf{e}}) \quad (3.22a)$$

$$\sum_{\forall j} [\dot{\mathbf{e}}]_j = 1, \quad (3.22b)$$

$$[\dot{\mathbf{e}}]_j \geq 0 \quad \forall j \quad (3.22c)$$

with $\dot{C}_{E_i}(\dot{\mathbf{e}})$ in (3.21) and, where $[\mathbf{x}]_j$ denotes the j -th element in the vector \mathbf{x} . The constraints (3.22b) and (3.22c) are given by the the total power and positive power constraints in (3.14c).

Now using the definition of $R^*(E)$ in (3.14), the following inequalities hold (for simplicity, we omit the resource constraints)

$$R^*(E) = \max_{\boldsymbol{\tau}, \mathbf{E}} \min_{i \in \{1, L\}} C_i(\boldsymbol{\tau}, \mathbf{E}) \quad \forall E, \quad (3.23a)$$

$$\leq \max_{\mathbf{E}} \min_{i \in \{1, L\}} \sum_{j=1}^T g_{ji}(\mathbf{E}) \quad \forall E, \quad (3.23b)$$

$$= \max_{\dot{\mathbf{e}}} \min_{i \in \{1, L\}} \sum_{j=1}^T \dot{g}_{E_{ji}}(\dot{\mathbf{e}}) E \quad (3.23c)$$

$$= E \max_{\dot{\mathbf{e}}} \min_{i \in \{1, L\}} \dot{C}_{E_i}(\dot{\mathbf{e}}), \quad (3.23d)$$

$$= \dot{R}^*(0) E \quad (3.23e)$$

The inequality (3.23b) follows from the concavity of the function $\log(1+x)$. To obtain the equality (3.23c), note that we only consider functions $g_{ji}(\mathbf{E})$ that are linear in the elements of \mathbf{E} . Then, the power allocation function that maximizes (3.23b) can only be linear in E . By substituting the linear power allocation $\mathbf{E} = \dot{\mathbf{e}}E$ into $g_{ji}(\mathbf{E})$ it is satisfied that $g_{ji}(\dot{\mathbf{e}}E) = \dot{g}_{E_{ji}}(\dot{\mathbf{e}}) E$ and we can write (3.23c). Finally, equality (3.23d) follows from (3.21) and (3.23e) follows from (3.22).

From (3.23e) it is clear that condition *ii*) in Proposition 3.1 is satisfied and thus, the low power regime and energy efficient regime coincide for any rate function of the type of (3.14).

3.5 Maximum Rate Per Energy

The simple inspection of the rate expressions in (3.7) and (3.14) reveals that for the relay channel the energy efficiency analysis with DF and the CB, under asynchronous or synchronous transmissions, can be carried out together just replacing $\hat{\alpha}_{12}$ and $\hat{\beta}_2$ appropriately.

For the FD relay channel, the bounds on the maximum RPE with DF and the CB were obtained in [60] assuming synchronous transmissions. The bounds for the asynchronous case can be determined using the results in [61] for ergodic fading channels. These results can be easily derived using the close form rate expression in (3.7) and the maximum RPE definition in (3.16) as

$$\eta_{FD} = \dot{R}^*(0) = \beta_{FD} \quad (3.24)$$

with β_{FD} defined as in (3.26).

For the HD relay channel, the bounds on the maximum RPE with DF and the CB were also studied in [60]. The HD limitation was introduced by forcing orthogonal transmissions from the source and the relay to the destination or, equivalently, forcing $E_{12}^A = 0$ and $E_{12}^S = 0$ in (3.14). Consequently, only the asynchronous case was solved. The maximum RPE bounds obtained coincide with the ones for the asynchronous FD case. Thus, no further gains are expected by studying the enhanced transmission strategy presented in [20]. For the synchronous case, $E_{12}^S \neq 0$, recently, in [66] authors analyzed the low and the high signal to noise ratio (SNR) regimes. There, the broadcast and the multiple access flows were optimized separately. The bounds on the maximum RPE found, were

$$\eta_{HD,FS} = \frac{\hat{\alpha}_{12}\hat{\beta}_2}{\hat{\alpha}_{12} + \hat{\beta}_2} \quad (3.25)$$

with $\hat{\beta}_2 = \beta_2 + \beta_1$ and $\hat{\alpha}_{12} = \alpha_{12}$ for the asynchronous case and $\hat{\alpha}_{12} = \alpha_{12} + \beta_1$ for the synchronous case. Here, we show that if both flows are considered together, the maximum RPE with a HD relay improves that in [66], and, even attains the bounds obtained for a FD relay, as occurs with asynchronous transmissions. The next theorem summarizes these results.

Theorem 3.1 *For the relay channel with synchronous or asynchronous transmissions, the bounds on the maximum RPE using DF for the lower bounds and the CB for the upper bounds, with a HD relay (η_{HD}) or with a FD relay (η_{FD}) satisfy $\eta_{HD} = \eta_{FD} = \beta_{FD}$ with*

$$\beta_{FD} = \begin{cases} \frac{\hat{\alpha}_{12}\hat{\beta}_2}{\hat{\alpha}_{12} + \hat{\beta}_2 - \beta_1} & \text{if } \hat{\alpha}_{12}, \hat{\beta}_2 > \beta_1, \\ \beta_1 & \text{otherwise.} \end{cases} \quad (3.26)$$

with $\hat{\alpha}_{12} = \alpha_{12}$ for DF, $\hat{\alpha}_{12} = \alpha_{12} + \beta_1$ for the CB, $\hat{\beta}_2 = \beta_2$ for asynchronous and $\hat{\beta}_2 = \beta_2 + \beta_1$ for synchronous transmissions.

Proof: We already know the maximum RPE obtained by a relay in FD and OT modes, thus in this proof we only address the strategy presented in [20] for HD nodes. Let us consider the rate $R^*(E)$ as defined in (3.14). Given that the low power regime is the energy efficient regime, to obtain the maximum RPE $\eta = \dot{R}^*(0)$, we only need to solve the problem in (3.22).

Taking derivatives of $g_{E_{ji}}(E)$ in (3.12) at $E = 0$ and substituting them into (3.21), we obtain

$$\dot{C}_{E_1}(\dot{\mathbf{e}}) = \dot{g}_{E_{11}}(\dot{\mathbf{e}}) + \dot{g}_{E_{21}}(\dot{\mathbf{e}}) = \hat{\alpha}_{12}\dot{e}_{11} + \beta_1\dot{e}_{12}^A, \quad (3.27a)$$

$$\dot{C}_{E_2}(\dot{\mathbf{e}}) = \dot{g}_{E_{12}}(\dot{\mathbf{e}}) + \dot{g}_{E_{22}}(\dot{\mathbf{e}}) = \beta_1\dot{e}_{11} + \beta_1\dot{e}_{12}^A + \hat{\beta}_2\dot{e}^R. \quad (3.27b)$$

Substituting (3.27) into (3.22), and solving the resultant problem over $\dot{\mathbf{e}} = [\dot{e}_{11}, \dot{e}_{12}^A, \dot{e}^R]$, we obtain the result in Theorem 3.1:

- If $\hat{\alpha}_{12} \leq \beta_1$ or $\hat{\beta}_2 \leq \beta_1$ only the source transmits, then $\dot{e}_{12}^{A*} = 1$, $\dot{e}_{11}^* = 0$, $\dot{e}^{R*} = 0$ and

$$\eta_{HD} = \dot{R}^*(0) = \dot{C}_{E_1}(\dot{\mathbf{e}}^*) = \dot{C}_{E_2}(\dot{\mathbf{e}}^*) = \beta_1. \quad (3.28)$$

- Otherwise, the relay transmits, then $\dot{e}_{11}^* = \frac{\hat{\beta}_2}{\hat{\alpha}_{12} + \hat{\beta}_2 - \beta_1}$, $\dot{e}_{12}^{A*} = 0$, $\dot{e}^{R*} = \frac{\hat{\alpha}_{12} - \beta_1}{\hat{\alpha}_{12} + \hat{\beta}_2 - \beta_1}$ and

$$\eta_{HD} = \dot{R}^*(0) = \dot{C}_{E_1}(\dot{\mathbf{e}}^*) = \dot{C}_{E_2}(\dot{\mathbf{e}}^*) = \frac{\hat{\alpha}_{12}\hat{\beta}_2}{\hat{\alpha}_{12} + \hat{\beta}_2 - \beta_1}. \quad (3.29)$$

For completeness, as we need them to compute the slope of the spectral efficiency in the next section, we provide here the solution to the first-order derivative of the functions $g_{E_{ji}}^*(E)$ evaluated at $E = 0$:

$\dot{g}_{E_{11}}^*(0)$	$\dot{g}_{E_{21}}^*(0)$	$\dot{g}_{E_{12}}^*(0)$	$\dot{g}_{E_{22}}^*(0)$	If $\hat{\alpha}_{12} \leq \beta_1$ or $\hat{\beta}_2 \leq \beta_1$ otherwise	(3.30)
0	η	0	η		
η	0	$\frac{\beta_1}{\alpha_{12}}\eta$	$\eta\left(1 - \frac{\beta_1}{\alpha_{12}}\right)$		

■

Theorem 3.1 shows that for the DF or the CB rate lower/upper bounds, the duplexity capability does not impact on the maximum RPE, regardless of the synchronism capability.

- For *synchronous* transmissions, the HD mode is sufficient to obtain the maximum RPE. The reason is that HD nodes can compensate the channel division limitation by transmitting fully correlated signals during the second interval. For FD nodes, given that there is not channel division, the synchronism gain can never be totally achieved since new (no correlated) information is continuously injected to the channel.
- For *asynchronous* transmissions, orthogonal transmissions are sufficient to obtain the maximum RPE.

3.6 Slope of the Spectral Efficiency

The study of the maximum RPE has not revealed the potential gain of FD capabilities at the relays. The same maximum RPE is obtained with a HD relay. Moreover, obtaining the maximum RPE is possible even without optimizing the time-sharing factors τ_1 and τ_2 and just considering a linear dependence of the power allocation with respect to the total power, i.e. $\mathbf{E}(E) = \dot{e}E$. Thus, we turn our attention to the analysis of the slope. This metric allows us to compare transmission schemes with equal maximum RPE.

The study of the slope of the spectral efficiency with FD and HD relays was first addressed in [61] for ergodic fading channels. The slope was only obtained for the asynchronous case and the power allocation was restricted to be linear in E . For the case of constant channels, we solve the synchronous case and show that the slope can be enhanced by removing the linear power allocation assumption. The next theorem summarizes the obtained results.

Theorem 3.2 *For a relay in FD mode, the slope of the spectral efficiency does not depend on the channel gains nor on the synchronism capabilities and is $S_{FD} = 2$. For HD nodes, the slope is given by $S_{HD} = 2$ if $\hat{\beta}_2 < \beta_1$ or $\hat{\alpha}_{12} < \beta_1$ (direct transmission is better), otherwise*

$$S_{HD} = \frac{2 \left(1 + \frac{\hat{\beta}_2 - \beta_1}{\hat{\alpha}_{12}}\right)}{\left(\sqrt{\frac{\hat{\beta}_2 - \beta_1}{\hat{\alpha}_{12}} + \left(\frac{\beta_1}{\hat{\alpha}_{12}}\right)^2} + \sqrt{\left(1 - \frac{\beta_1}{\hat{\alpha}_{12}}\right)^2}\right)^2}. \quad (3.31)$$

For a relay in FD mode, the optimal power allocation is linear in E , see (3.6). For HD nodes, if the power allocation is restricted to be linear in E but the time-sharing factors τ_1 and τ_2 are optimally assigned, the slope is $S_{HD_e} = 1 + \frac{\beta_1}{\alpha_{12}}$. Instead, if the time-sharing factors are fixed $\tau_1 = \tau_2 = \frac{1}{2}$ but the power is optimally allocated, then

$$S_{HD_\tau} = \frac{1}{1 + 2 \left(\frac{\eta}{\alpha_{12}} - 1\right) \left(\frac{\beta_1}{\alpha_{12}}\right)}. \quad (3.32)$$

Finally, if, both, the powers are restricted to be linear in E and the time-sharing factors are fixed to $\tau_1 = \tau_2 = \frac{1}{2}$, the slope decreases to $S_{HD_{\tau,e}} = 1$. Note that, in all these cases, the maximum RPE is unchanged.

Proof: The slope of the spectral efficiency is computed as $S \triangleq \frac{2[\dot{R}^*(0)]^2}{-\ddot{R}^*(0)}$. The first-order derivative $\dot{R}^*(0)$ was already computed in the previous section, see (3.28) and (3.29), and thus, we only need to obtain $\ddot{R}^*(0)$. For a relay in FD mode, we know that $\dot{R}^*(0) = \beta_{FD}$, see (3.24). By computing $\ddot{R}^*(E)$ analytically we obtain $\ddot{R}^*(0) = (\beta_{FD})^2$. Then, the slope is $S = 2$. For a relay in HD mode, let us consider $R(E)$ as defined in (3.19) where the resource allocation can be any pair of functions $\tau(E)$ and the definitions of C_{E_i} and $g_{E_{j_i}}$

previously introduced. The rate constraints $C_{E_i}(E) = C_i(\tau(E), E(E))$ are functions of E that coincide at $E = 0$, namely $C_{E_1}(0) = C_{E_2}(0) = 0$ and, as shown in the previous section, both increase as $\dot{R}^*(0) = \dot{C}_{E_1}(0) = \dot{C}_{E_2}(0)$. Consequently, $\ddot{R}(0)$ can be computed as $\ddot{R}(0) = \min_{i \in \{1,2\}} \ddot{C}_{E_i}(0)$.

In Appendix 3.A, for any C_i defined as in (3.10), we obtain the second-order derivative of the rate constraints $C_{E_i}(E)$ as

$$\ddot{C}_{E_i}(0) = \sum_{j=1}^2 \ddot{g}_{E_{ji}}(0) - \frac{(\dot{g}_{E_{ji}}(0))^2}{t_j}. \quad (3.33)$$

Taking second-order derivatives of the function $g_{E_{ji}}(E)$ in (3.12) at $E = 0$ and substituting them into (3.33), we obtain

$$\ddot{C}_{E_1}(0) = -\frac{(\dot{g}_{E_{11}}^*(0))^2}{t_1} - \frac{(\dot{g}_{E_{21}}^*(0))^2}{t_2} + \hat{\alpha}_{12}\ddot{e}_{11} + \beta_1\ddot{e}_{12}^A, \quad (3.34a)$$

$$\ddot{C}_{E_2}(0) = -\frac{(\dot{g}_{E_{12}}^*(0))^2}{t_1} - \frac{(\dot{g}_{E_{22}}^*(0))^2}{t_2} + \beta_1\ddot{e}_{11} + \beta_1\ddot{e}_{12}^A + \hat{\beta}_2\ddot{e}^R. \quad (3.34b)$$

In (3.34), we have already particularized the solution to $\dot{g}_{E_{ij}}^*(0)$ found in (3.30). Notice that given (3.34), it is clear that $\ddot{C}_{E_i}(0)$ only depends on \ddot{e} and \mathbf{t} , namely $\ddot{C}_{E_i}(\ddot{e}, \mathbf{t})$.

To find $\ddot{R}^*(0)$, we only need to solve the following problem over \ddot{e} and \mathbf{t}

$$\ddot{R}^*(0) = \max_{\ddot{e}, \mathbf{t}} \min_{i \in \{1,2\}} \ddot{C}_{E_i}(\ddot{e}, \mathbf{t}) \quad (3.35a)$$

$$t_1 + t_2 = 1, \quad t_1, t_2 \geq 0, \quad (3.35b)$$

$$\ddot{e}_{11} + \ddot{e}_{12}^A + \ddot{e}^R = 0, \quad (3.35c)$$

$$\begin{aligned} \ddot{e}_{11}, \ddot{e}^R &\geq 0 && \text{if } \hat{\alpha}_{12} \leq \beta_1 \text{ or } \hat{\beta}_2 \leq \beta_1, \\ \ddot{e}_{12}^A &\geq 0 && \text{otherwise.} \end{aligned} \quad (3.35d)$$

The constraints in (3.35b) are those in (3.14b) evaluated at $E = 0$. The constraint (3.35c) on \ddot{e} is obtained by taking the second-order derivative of the total power constraint in (3.14c). The constraints (3.35d) are due to the positive power constraint in (3.14c). Notice that if any element j of \ddot{e} , satisfies $\dot{e}_j = 0$, then E_j satisfies⁴ $\lim_{E \rightarrow 0} E_j(E) = \frac{\ddot{e}_j}{2}E^2 + o(E^3)$. Consequently, the positive power constraint ($E_j(E) > 0$) forces $\ddot{e}_j \geq 0$.

To solve this problem, we consider the two possible values for $\dot{g}_{E_{ij}}^*(0)$ found in (3.30):

If $\hat{\alpha}_{12} \leq \beta_1$ or $\hat{\beta}_2 \leq \beta_1$, after including the total power constraint $\ddot{e}_{12}^A = -(\ddot{e}_{11} + \ddot{e}^R)$ and $\dot{g}_{E_{i,j}}^*(0)$ obtained in (3.30) into $\ddot{C}_{E_i}(\ddot{e}, \mathbf{t})$, we get

$$\ddot{C}_{E_1}(\ddot{e}, \mathbf{t}) = -\frac{(\eta)^2}{t_2} - (\beta_1 - \hat{\alpha}_{12})\ddot{e}_{11} - \beta_1\ddot{e}^R, \quad (3.36a)$$

$$\ddot{C}_{E_2}(\ddot{e}, \mathbf{t}) = -\frac{(\eta)^2}{t_2} - (\beta_1 - \hat{\beta}_2)\ddot{e}^R \quad (3.36b)$$

⁴ $o(E^i)$ is a function that satisfies $\frac{o(E^i)}{E^{i-1}} \xrightarrow{E \rightarrow 0} 0$.

3.6. Slope of the Spectral Efficiency

with $\eta = \eta_{HD}$. Since $\ddot{e}_{11}, \ddot{e}^R \geq 0$, both rate constraints are maximized at $\ddot{e}_{11}^* = \ddot{e}^{R*} = 0$ and $t_2^* = 1$. Then $\ddot{R}^*(0) = \ddot{C}_1(\ddot{\mathbf{e}}^*, \mathbf{t}^*) = \ddot{C}_2(\ddot{\mathbf{e}}^*, \mathbf{t}^*) = -(\eta)^2$ and the slope is $S_{HD} = 2$.

Otherwise, if $\beta_1 \leq \hat{\alpha}_{12}, \hat{\beta}_2$ by including the total power constraint $\ddot{e}^R = -(\ddot{e}_{11} + \ddot{e}_{12}^A)$ into (3.34), we get

$$\ddot{C}_{E_1}(\ddot{\mathbf{e}}, \mathbf{t}) = -\frac{(\dot{g}_{E_{11}}^*(0))^2}{t_1} - \frac{(\dot{g}_{E_{21}}^*(0))^2}{t_2} + \hat{\alpha}_{12}\ddot{e}_{11} + \beta_1\ddot{e}_{12}^A, \quad (3.37a)$$

$$\ddot{C}_{E_2}(\ddot{\mathbf{e}}, \mathbf{t}) = -\frac{(\dot{g}_{E_{12}}^*(0))^2}{t_1} - \frac{(\dot{g}_{E_{22}}^*(0))^2}{t_2} - (\hat{\beta}_2 - \beta_1)\ddot{e}_{11} - (\hat{\beta}_2 - \beta_1)\ddot{e}_{12}^A. \quad (3.37b)$$

We substitute (3.37) into (3.35) and then solve the resultant problem, first over $\ddot{e}_{11}, \ddot{e}_{12}^A$ assuming constant \mathbf{t} . Note that (3.37a) linearly increases with \ddot{e}_{11} and \ddot{e}_{12}^A whereas (3.37b) linearly decreases with both \ddot{e}_{11} and \ddot{e}_{12}^A . Consequently, (3.35) is maximized in the equality of (3.37a) and (3.37b) at

$$\ddot{e}_{12}^{A*} = 0, \ddot{e}^{R*} = -\ddot{e}_{11}^*, \quad (3.38a)$$

$$\hat{\alpha}_{12}\frac{\hat{\beta}_2}{\eta}\ddot{e}_{11}^* = \frac{(\dot{g}_{E_{11}}^*(0))^2 - (\dot{g}_{E_{12}}^*(0))^2}{t_1} - \frac{(\dot{g}_{E_{22}}^*(0))^2}{t_2}. \quad (3.38b)$$

Then,

$$\ddot{R}^*(0) = \ddot{C}_{E_1}(\ddot{\mathbf{e}}^*, \mathbf{t}) = \ddot{C}_{E_2}(\ddot{\mathbf{e}}^*, \mathbf{t}) = -\frac{(\Psi_1)^2}{t_1} - \frac{(\Psi_2)^2}{t_2} \quad (3.39)$$

with $(\Psi_1)^2 = \left(1 - \frac{\eta}{\hat{\beta}_2}\right) (\dot{g}_{E_{11}}^*(0))^2 + \frac{\eta}{\hat{\beta}_2} (\dot{g}_{E_{12}}^*(0))^2$ and $(\Psi_2)^2 = \frac{\eta}{\hat{\beta}_2} (\dot{g}_{E_{22}}^*(0))^2$.

Maximizing (3.39) over \mathbf{t} , we get

$$\frac{1}{t_1^*} = 1 + \frac{\Psi_2}{\Psi_1}, \quad \frac{1}{t_2^*} = 1 + \frac{\Psi_1}{\Psi_2}. \quad (3.40)$$

Notice that since $(\Psi_1, \Psi_2 \geq 0)$, then \mathbf{t}^* satisfies the constraints in (3.35b). Substituting (3.40) into (3.39) yields $\ddot{R}^*(0) = -(\Psi_1 + \Psi_2)^2$ and the slope is (3.31).

Instead, if the power allocation is restricted to be linear in E , $E_{11} = \dot{e}_{11}^*E$, $E_{12} = 0$, and $E_{22} = \dot{e}_{22}^*E$, then substituting $\ddot{e}_{11}^* = \ddot{e}_{12}^* = \ddot{e}_{22}^* = 0$ into (3.37) and optimizing (3.35) only with respect to \mathbf{t} , we obtain $t_1^* = \frac{\alpha_{12} + \beta_1}{2\alpha_{12}}$, $t_2^* = \frac{\alpha_{12} - \beta_1}{2\alpha_{12}}$. Notice that since $\alpha_{12} > \beta_1$, t_1^* and t_2^* always satisfy the constraints in (3.35b). Then, $\ddot{R}^*(0) = \ddot{C}_{E_1}(\mathbf{0}, \mathbf{t}^*) = \ddot{C}_{E_2}(\mathbf{0}, \mathbf{t}^*) = -\frac{2\alpha_{12}}{\alpha_{12} + \beta_1}(\eta)^2$ and the slope is $S_{HD_e} = 1 + \frac{\beta_1}{\alpha_{12}}$.

Consider, now, that the time-sharing factors are fixed (independent of the channel gains) $\mathbf{t}_0 = [\frac{1}{2}, \frac{1}{2}]$ but the energies $\ddot{\mathbf{e}}$ are optimally allocated. It is direct from (3.39) that

$$\ddot{R}^*(\mathbf{t}_0) = -2(\Psi_1)^2 - 2(\Psi_2)^2 \quad (3.41)$$

and the slope is (3.32).

Finally, consider that, the power allocation is linear and the time-sharing factors are fixed $\mathbf{t} = \mathbf{t}_0$. In this case, we have

$$\ddot{C}_{E_1}(\mathbf{0}, \mathbf{t}) = -2(\eta)^2, \quad (3.42a)$$

$$\ddot{C}_{E_2}(\mathbf{0}, \mathbf{t}) = -2(\eta)^2 \frac{(\beta_1)^2 + (\alpha_{12} - \beta_1)^2}{(\alpha_{12})^2} \quad (3.42b)$$

and $\ddot{R}^*(0) = \min_{i \in \{1,2\}} \ddot{C}_{E_i}(\mathbf{0}, \mathbf{t}) = \ddot{C}_{E_1}(\mathbf{0}, \mathbf{t})$, then the slope is $S_{HD\tau,e} = \frac{2(\eta)^2}{-C_1} = 1$. ■

The following conclusions can be extracted from the result in Theorem 3.2.

- The duplexity constraint clearly impacts on the slope.
- If the relay works in HD mode, the use of fixed time-sharing factors or a linear power assumption decreases the slope. See numerical results below.
- If the relay works in HD mode and the transmission are asynchronous, no gain is obtained by transmitting simultaneously from the source and the relay to the destination. In this case, the orthogonal channel access is optimal for the energy efficient and low power regime.
- The DF strategy for HD nodes presented in [20] reduces to a *full decode and forward* one in the energy efficient regime. For relays in FD mode, it was shown in [64] that for the AWGN channel, the *generalized decode and forward* strategy [28, Theorem 7], where the relay is only required to decode a part of the source message, reduces the *full decode and forward* strategy studied in this chapter, where the relay node is either required to fully decode the message transmitted by the sender or is not used at all. For relays in HD mode, the DF strategy analyzed here considers that the relay is not required to decode the source message, entirely (*partial decode and forward*). During the relay transmission interval, the source transmits information directly to the destination, which is thus, not listened to at the relay. To this signal the source dedicates the power E_{12}^A . However, we have shown that in the energy efficiency regime, this strategy also reduces to a *full decode and forward* one. We have found that, the power dedicated to transmit new information from the source in the second interval E_{12}^A , satisfies $\lim_{E \rightarrow 0} E_{12}^A(E) = o(E^3)$, since after optimal resource allocation $\dot{e}_{12}^A = \ddot{e}_{12}^A = 0$.

For synchronous transmission, this result implies that in the second interval only the coherent signal is transmitted from the source, note that $E_{12}(E) = E_{12}^A(E) + E_{12}^S(E)$, and thus, $E_{12}(E) = \dot{e}_{12}^S E + \frac{\ddot{e}_{12}^S}{2} E^2 + o(E^3)$. For asynchronous transmissions, where $E_{12}^S = 0$, this result implies that the source does not transmit simultaneously with the relay $\lim_{E \rightarrow 0} E_{12}(E) = o(E^3)$.

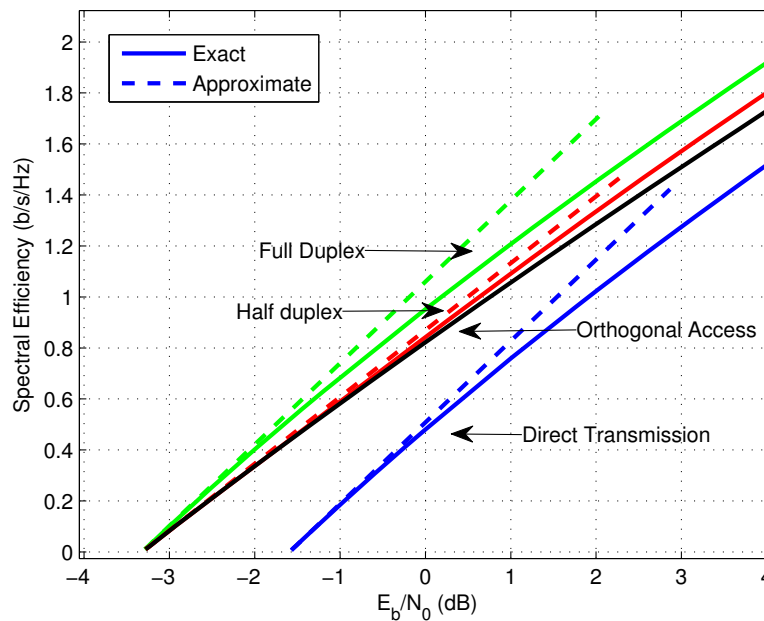


Figure 3.2: Relay near the destination at coordinates (0.75,0.25). Approximate and exact rate (bits/s/Hz) versus $\frac{E_b}{N_0}$ (dB) for full duplex, half duplex, orthogonal, and direct transmission.

3.7 Numerical Results

In this section, we present numerical results to validate the low power approximation of the spectral efficiency and to discuss the energy efficiency gains of the terminal capabilities considered: synchronization, duplexing and simultaneous channel access). Additionally, we discuss the performance losses incurred by the suboptimal resource allocation solutions considered in Thm. 3.2 for HD nodes and motivate the use of the energy efficiency metrics for relay selection.

In simulations we consider distance dependent channel gains with a pathloss exponent $\nu = 2$ and $\beta_1 = 1$. The source and the destination are located in a plane at coordinates (0,0) and (0,1), respectively.

3.7.1 Terminal Capabilities

First, we investigate the gap between the low power approximation and the exact spectral efficiency curve. The spectral efficiency can be approximated as (3.18), the exact $R\left(\frac{E_b}{N_0}\right)$ is here obtained by exhaustive search of the optimal resources allocation. In Fig. 3.2 and 3.3, we show the spectral efficiency curves for DF with *asynchronous* transmissions if the relay is near the destination or near the source. As pointed out also in [61], if the spectral efficiency is less than 0.3 b/s/Hz the gap between the approximate and exact curves is small in all the studied cases.

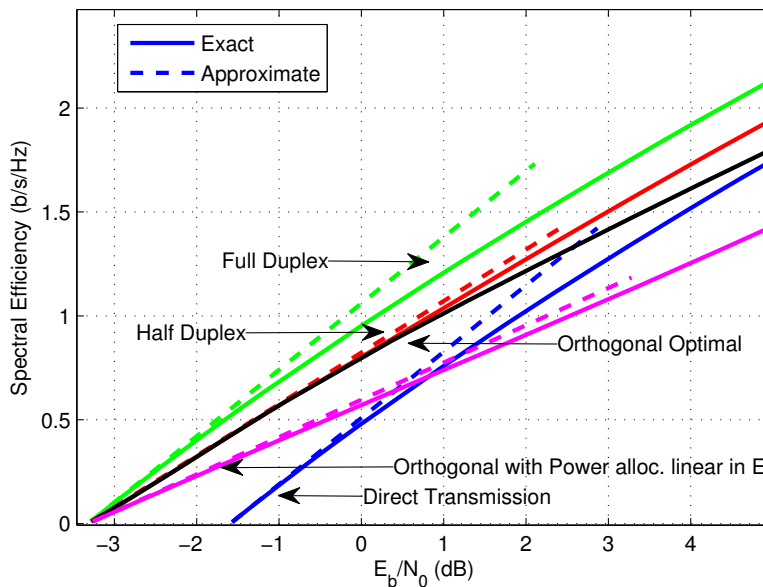


Figure 3.3: Relay near the source at coordinates (0.25,0.25). Approximate and exact rate (bits/s/Hz) versus $\frac{E_b}{N_0}$ (dB) for full duplex, half duplex, orthogonal with optimal or linear power allocation, and direct transmission.

Next, we study the impact on the energy efficiency of the terminal capabilities considered:

The channel access. By forcing the source and the relay transmissions to be orthogonal, neither the synchronism nor the full duplex capabilities are used. However, we have seen that if *asynchronous* and HD transmissions are assumed, then the *orthogonal channel access* is optimal in terms of both, the maximum RPE and the slope. This result is verified in Fig. 3.2. Notice that the exact curves for HD nodes and with the orthogonal channel access increase with the same slope.

Synchronism. This gain is observed computing the maximum RPE. We have found that this metric is independent of the duplexing capability at the relay. In Fig. 3.7.1, we depict the maximum RPE with DF and the CB, for asynchronous and synchronous transmissions as a function of the source to relay position $(d, 0)$, then $\alpha_{12} = |d|^{-\nu}$ and $\beta_2 = |1 - d|^{-\nu}$. We observe that synchronism (in yellow) provides important gains if the relay is near to the source, even if the relay is farther than the source from the destination (negative axes). However, synchronism provides negligible gains if the relay is near to the destination.

This effect is dual to the gap between the CB and DF. In Fig. 3.7.1, we observe that the gap between CB (dashed lines) and DF (solid lines) is only important if the relay is near to the destination, even if the relay is farther than the destination from the source ($d > 1$). However, the CB is very close to the DF strategy if the relay is near to the source.

Duplexing. This gain is observed computing the slope of the spectral efficiency (S). This

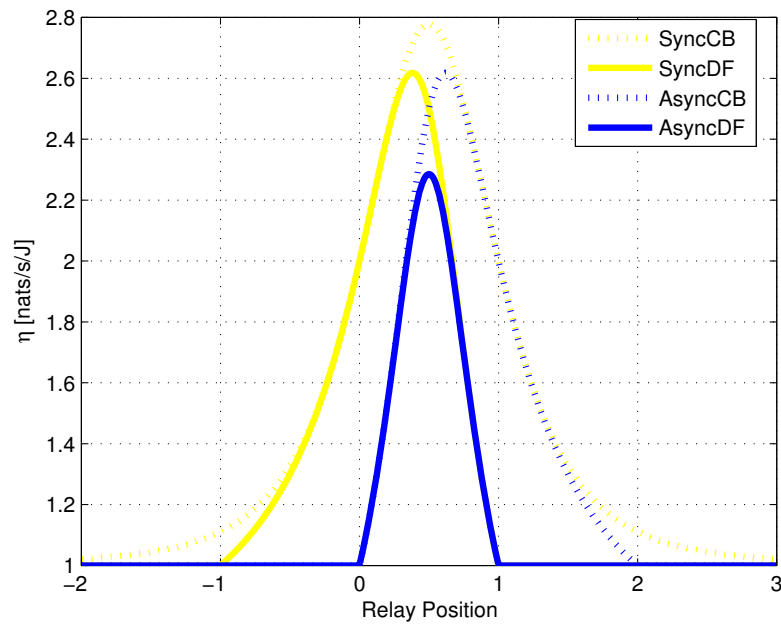


Figure 3.4: Maximum RPE versus source to relay distance. Source and Destination are located at $d = 0$ and $d = 1$ respectively.

metric determines the bandwidth efficiency. The required bandwidth for a system to achieve a rate R with power E is [1]

$$B = \frac{R}{S} \frac{3\text{dB}}{\frac{E}{N_0 R}|_{\text{dB}} - \frac{E_b}{N_0 \text{min}}|_{\text{dB}}}. \quad (3.43)$$

For FD nodes with DF or the CB, the slope is always $S_{FD} = 2$ regardless of the synchronism capability or the relay position.

For HD nodes, in Fig. 3.7.1 we depict the slope as a function of the relay position $(d, 0)$ for all the studied scenarios. We can see that, if the relay is near to the middle point between the source and the destination, the HD mode requires approximately $\left(\frac{B_{HD}-B_{FD}}{B_{FD}} \times 100 = \left(\frac{S_{FD}}{S_{HD}} - 1\right) \times 100 = 50\%\right)$ more of the minimum bandwidth needed with a FD relay for the same rate and transmitted power.

3.7.2 Resource Allocation

For FD nodes, the optimal power allocation is a linear function of the total power E . For HD nodes, the optimal power allocation is not linear in E and, in addition, the time-sharing factors τ_1 and τ_2 must be allocated. The performance losses incurred by the suboptimal resource considered in Thm. 3.2 for HD nodes, are studied in terms of the slope in Fig. 3.6. It is shown that fixing $\tau_1 = \tau_2 = \frac{1}{2}$ is a good solution only if the relay is in the middle point between the source and the destination. Likewise, the linear power allocation is a good solution if the

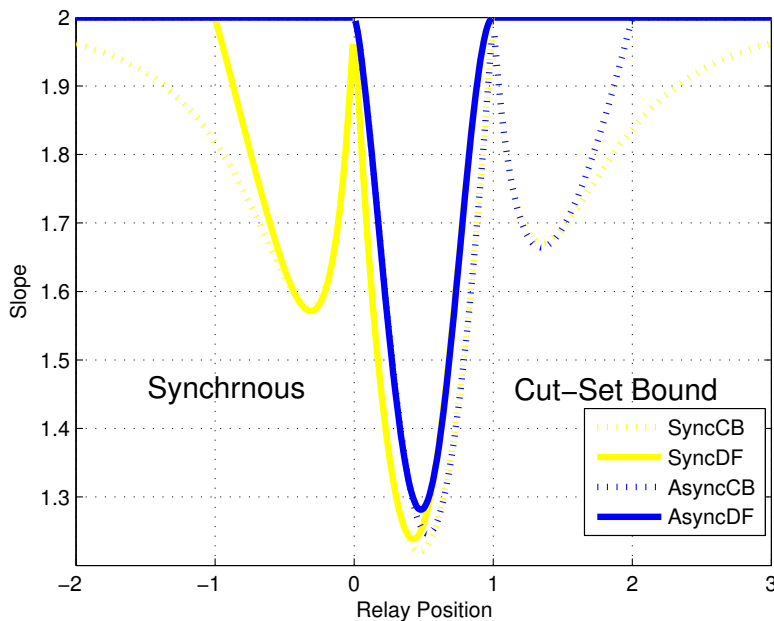


Figure 3.5: Slope versus source to relay distance. Source and Destination are located at $d = 0$ and $d = 1$ respectively.

relay is near to the destination. However, all the suboptimal resource allocation solutions fail if the relay is near to the source, see Fig. 3.3. As an example, at $d = 0$ the linear power assumption taken in [61] requires (100%) more of the minimum bandwidth needed without the linear power constraint for the same rate and transmitted power.

3.7.3 Relay Position

For a relay in FD mode, the rate as a function of the total power is obtained in close form in (3.7) as $R(E) = \log(1 + \eta_{FD}E)$. From this expression it is direct that we can choose the best relay in the network as the one with largest η . Instead, for a relay in HD mode, we only have the low power regime approximation for the rate $R(E)$. In Fig. 3.7, we study the feasibility of using the low power metrics η or equivalently $\frac{E_b}{N_0 \min}$ and S to select the best relay. There we consider a network with one source at coordinates (0,0), one destination at (1,0) and three potential relays at (0.25,0.25), at (0.5,0.25) and (0.75,0.25). Fig. 3.7 depicts the exact numerical computation of the rate as a function of the $\frac{E_b}{N_0}$ for each of these relays. In all considered range for $\frac{E_b}{N_0}$, the evaluation of η or $\frac{E_b}{N_0 \min}$ is sufficient to choose the best relay.

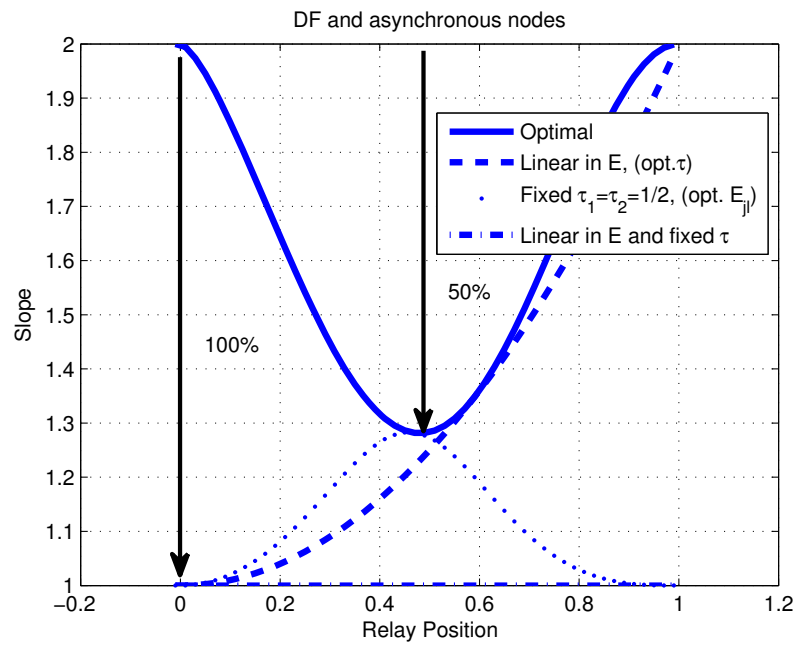


Figure 3.6: Maximum slope versus source to relay distance, for different resource allocation assumptions.

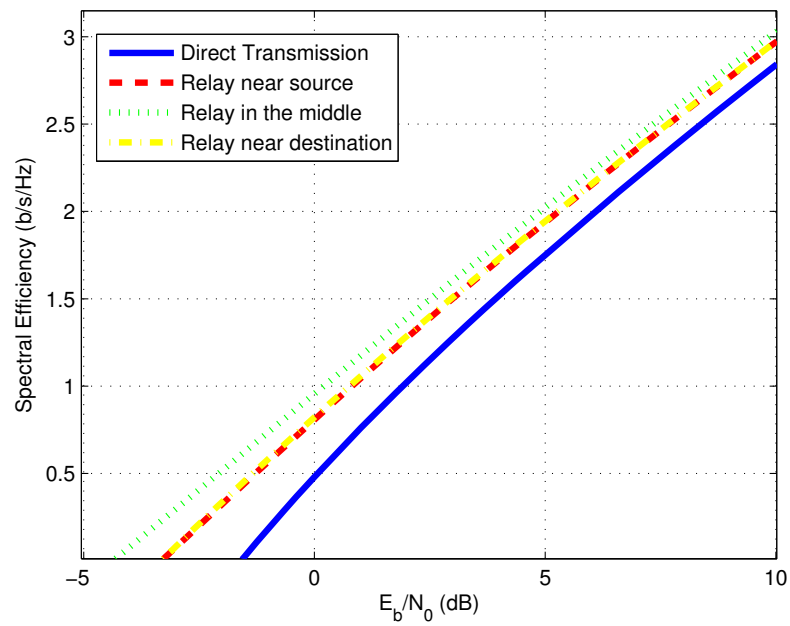


Figure 3.7: Relay selection. Rate as a function of the $\frac{E_b}{N_0}$ for HD nodes.

3.8 Extension to Ergodic Fading Channels

In this section, we extend the previous analysis to the ergodic fading channel. The study addresses both FD and HD terminals. Again, we investigate the achievable rate with DF and the capacity upper bound with the CB. The maximum rate per energy and the slope of the spectral efficiency with the energy per bit are computed to assess the impact of: *i*) the duplexing capabilities, *ii*) the resource allocation and *iii*) the channel fading distribution.

The low power analysis of several communication schemes over ergodic fading can be found in the literature. For instance, the direct transmission with single or multiple antennas was studied in [1]. The multiple access, broadcast and interference channels were conducted in [42]. The relay channel under ergodic fading was first considered in [61]. There, the ergodic capacity bounds with DF and the CB, with FD terminals or with orthogonal transmission were studied. The results were extended in [43] to also include *amplify and forward*.

In this section, we provide more insight into those results by studying the HD scenario. In the HD scenario, contrary to the OT scenario, the source is allowed to transmit during the relay transmission interval. Furthermore, we allow the resource allocation functions to be any differentiable function of the total power. In all these previous works, the power allocated to each node was restricted to be a linear function of the total power. Whereas, in the low power regime, we show later on that the HD mode does not provide any gain with respect to OT, the linear power allocation assumption results on an inefficient use of the bandwidth.

3.8.1 Ergodic Capacity Bounds

Let us consider channel coefficients $\alpha_{1,2}$, β_1 , β_2 to be independent random variables. Each time slot is assumed to be large enough so that the channel fading processes are ergodic. The receiver has perfect channel information while transmitters (source and relay) only have statistical information of the channel; namely, the mean $E[\alpha_{1,2}]$, $E[\beta_1]$, $E[\beta_2]$ and the variance $E[(\alpha_{1,2})^2]$, $E[(\beta_1)^2]$, $E[(\beta_2)^2]$. We only consider the case of asynchronous transmissions. For this case, close form solution to the low power regime metrics can be found. Furthermore, as shown in [61], under ergodic fading, the synchronous case reduces to the asynchronous case if the channel components have zero mean, (the channel has not a constant component).

The expressions for the ergodic capacity bounds with DF and the CB for the relay channel in FD or HD modes simply boil down to expressions (3.3) and (3.10), respectively, where each of the rate constrains C_i is averaged with respect to the channel gains $\alpha_{1,2}$, β_1 , β_2 . We assume hereafter that the channel gains have finite second moments.

The rate bounds for HD and FD modes under some fixed resource allocation vectors $\boldsymbol{\tau}$, \mathbf{E} can

be found in [28] and [20], respectively. We write them in a unified manner as

$$R_F(\boldsymbol{\tau}, \mathbf{E}) = \min_{i \in \{1,2\}} C_i(\boldsymbol{\tau}, \mathbf{E}) \quad (3.44)$$

with

$$C_i(\boldsymbol{\tau}, \mathbf{E}) = \mathbb{E} \left[\sum_{j=1}^2 \tau_j \log \left(1 + \frac{g_{ji}(\mathbf{E})}{\tau_j} \right) \right]. \quad (3.45)$$

For the FD mode, the power allocation vector is $\mathbf{E} = [E_1, E_2]$, the vector of time-sharing factors is $\boldsymbol{\tau} = [1, 0]$ and the functions $g_i, i \in \{1, 2\}$ are given by

$$g_1(\mathbf{E}) = \hat{\alpha}_{12} E_1, \quad (3.46a)$$

$$g_2(\mathbf{E}) = \beta_1 E_1 + \beta_2 E_2. \quad (3.46b)$$

with $\hat{\alpha}_{12} = \alpha_{12}$ for DF and $\hat{\alpha}_{12} = \alpha_{12} + \beta_1$ for the CB.

For the HD mode, the power allocation vector is $\mathbf{E} = [E_{11}, E_{12}, E_{22}]$ and the vector of time-sharing factors is $\boldsymbol{\tau} = [\tau_1, \tau_2]$. In this case, $g_{i,j}(\mathbf{E}), i, j \in \{1, 2\}$ are given by

$$\begin{aligned} g_{11}(\mathbf{E}) &= \hat{\alpha}_{12} E_{11}, & g_{21}(\mathbf{E}) &= \beta_1 E_{12}, \\ g_{12}(\mathbf{E}) &= \beta_1 E_{11}, & g_{22}(\mathbf{E}) &= \beta_1 E_{12} + \beta_2 E_{22}. \end{aligned} \quad (3.47)$$

3.8.2 The Energy Efficiency Analysis

To obtain the low power metrics $\bar{\eta}$ and \bar{S} , we need to compute the first and second-order derivatives at $E = 0$ of the rate $R^*(E)$. However, the rate $R^*(E)$ is only available as the solution to the following problem for all E

$$R^*(E) = \max_{\boldsymbol{\tau}, \mathbf{E}} \min_{i \in \{1,2\}} C_i(\boldsymbol{\tau}, \mathbf{E}) \quad (3.48a)$$

$$\tau_1 + \tau_2 = 1, \quad \tau_1, \tau_2 \geq 0, \quad (3.48b)$$

$$\sum_{\forall j} [\mathbf{E}]_j = E, \quad [\mathbf{E}]_j \geq 0, \forall j. \quad (3.48c)$$

where $[\mathbf{x}]_j$ denotes the j -th element in vector \mathbf{x} .

We are unable to find, explicitly, the pair $(\boldsymbol{\tau}, \mathbf{E})$ that maximizes the rate in (3.48) for all E . Therefore, we can not directly compute the derivatives of $R^*(E)$ at $E = 0$.

To compute these derivatives, we assume that the resources allocation solution for all E are any differentiable function $\boldsymbol{\tau}(E)$ and $\mathbf{E}(E)$ and define $\dot{\mathbf{e}} \triangleq \dot{\mathbf{E}}(0)$, $\ddot{\mathbf{e}} \triangleq \ddot{\mathbf{E}}(0)$ and $\mathbf{t} \triangleq \boldsymbol{\tau}(0)$. Then, the first and second-order derivatives of the rate constraints in (3.45) as a function total power E , $C_{E_i}(E) = C_i(\boldsymbol{\tau}(E), \mathbf{E}(E))$ evaluated at $E = 0$ can be obtained by taking expectation to

the derivatives of the rate limits given in Appendix 3.A (equations (3.91) and (3.93)) as

$$\dot{C}_{E_i}(E)|_{E=0} = \sum_{j=1}^2 \mathbb{E} [g_{E_{ji}}(\dot{\mathbf{e}})], \quad (3.49a)$$

$$\ddot{C}_{E_i}(E)|_{E=0} = \sum_{j=1}^2 \mathbb{E} [\ddot{g}_{E_{ji}}(\dot{\mathbf{e}}, \ddot{\mathbf{e}})] - \frac{\mathbb{E} [(\dot{g}_{E_{ji}}(\dot{\mathbf{e}}))^2]}{t_j} \quad (3.49b)$$

with $g_{E_{ji}}(E) = g_{ji}(\mathbf{E}(E))$. Notice that given (3.49) it is clear that $\dot{C}_{E_i}(E)|_{E=0} = \dot{C}_{E_i}(\dot{\mathbf{e}})$ and $\dot{g}_{E_{ji}}(0) = \dot{g}_{E_{ji}}(\dot{\mathbf{e}})$ only depend on $\dot{\mathbf{e}}$ whereas $\ddot{g}_{E_{ji}}(0) = \ddot{g}_{E_{ji}}(\dot{\mathbf{e}}, \ddot{\mathbf{e}})$ and $\ddot{C}_{E_i}(E)|_{E=0} = \ddot{C}_{E_i}(\dot{\mathbf{e}}, \ddot{\mathbf{e}}, \mathbf{t})$ only depends on $\dot{\mathbf{e}}, \ddot{\mathbf{e}}$ and \mathbf{t} . To find $\dot{R}^*(0)$ we only need to solve the following problem over $\dot{\mathbf{e}}$

$$\dot{R}^*(0) = \max_{\dot{\mathbf{e}}} \min_{i \in \{1,2\}} \dot{C}_{E_i}(\dot{\mathbf{e}}) \quad (3.50a)$$

$$\sum_{\forall j} [\dot{\mathbf{e}}]_j = \mathbf{1}, [\dot{\mathbf{e}}]_j \geq 0, \forall j \quad (3.50b)$$

where the constraints (3.50b) on $\dot{\mathbf{e}}$ are due to the constraints in (3.48c).

After solving (3.50) we know $\dot{\mathbf{e}}^*$, thus $\ddot{C}_{E_i}(0) = \ddot{C}_{E_i}(\mathbf{t}, \ddot{\mathbf{e}})$ only depends on $\ddot{\mathbf{e}}$ and \mathbf{t} . The second derivative $\ddot{R}^*(0)$ can be obtained solving the following problem over $\ddot{\mathbf{e}}$ and \mathbf{t}

$$\ddot{R}^*(0) = \max_{\ddot{\mathbf{e}}, \mathbf{t}} \min_{i \in \{1,2\}} \ddot{C}_{E_i}(\ddot{\mathbf{e}}, \mathbf{t}) \quad (3.51a)$$

$$t_1 + t_2 = 1, t_1, t_2 \geq 0, \quad (3.51b)$$

$$\sum_{\forall j} [\ddot{\mathbf{e}}]_j = \mathbf{0}, [\ddot{\mathbf{e}}]_j \geq 0 \quad \text{if } [\dot{\mathbf{e}}]_j = 0. \quad (3.51c)$$

where the constraints (3.51b) on \mathbf{t} are found evaluating the constraints in (3.48b) at $E = 0$ and the constraints on $\ddot{\mathbf{e}}$ (3.51c) are found by computing the second-order derivative of the constraints in (3.48c) at $E = 0$.

3.8.3 Maximum Rate Per Energy

To obtain $\bar{\eta} = \dot{R}^*(0)$, we need to solve the problem in (3.50).

For a relay in FD mode, substituting the functions g_{E_i} in (3.46) into (3.49a), the first-order derivative of the rate constraints at $E = 0$ read

$$\dot{C}_{E_1}(\dot{\mathbf{e}}) = \mathbb{E} [\dot{g}_{E_1}(\dot{\mathbf{e}})] = \mathbb{E} [\hat{\alpha}_{12}] \dot{e}_1, \quad (3.52a)$$

$$\dot{C}_{E_2}(\dot{\mathbf{e}}) = \mathbb{E} [\dot{g}_{E_2}(\dot{\mathbf{e}})] = \mathbb{E} [\beta_1] \dot{e}_1 + \mathbb{E} [\beta_2] \dot{e}_2. \quad (3.52b)$$

By substituting (3.52) into (3.50), and solving the resultant problem over \dot{e}_1, \dot{e}_2 , we obtain

$$\dot{e}_1^* = \frac{\mathbb{E} [\beta_2]}{\mathbb{E} [\beta_2] + \mathbb{E} [\hat{\alpha}_{12}] - \mathbb{E} [\beta_1]}, \quad (3.53a)$$

$$\dot{e}_2^* = \frac{\mathbb{E} [\hat{\alpha}_{12}] - \mathbb{E} [\beta_1]}{\mathbb{E} [\beta_2] + \mathbb{E} [\hat{\alpha}_{12}] - \mathbb{E} [\beta_1]} \quad (3.53b)$$

if $E[\hat{\alpha}_{12}], E[\beta_2] > E[\beta_1]$, otherwise the relay is not used $\dot{e}_1^* = 1$ and $\dot{e}_2^* = 0$.

For a relay in HD mode, substituting the functions $g_{E_{ij}}$ in (3.47) into (3.49a), the first-order derivative of the rate constraints at $E = 0$ read

$$\dot{C}_{E_1}(\dot{\mathbf{e}}) = E[\hat{\alpha}_{12}] \dot{e}_{11} + E[\beta_1] \dot{e}_{12}, \quad (3.54a)$$

$$\dot{C}_{E_2}(\dot{\mathbf{e}}) = E[\beta_1] \dot{e}_{11} + E[\beta_1] \dot{e}_{12} + E[\hat{\beta}_2] \dot{e}_{22}. \quad (3.54b)$$

Substituting (3.54) into (3.50), and solving the resultant problem over \dot{e}_{11} , \dot{e}_{12} and \dot{e}_{22} , we obtain

$$\dot{e}_{11}^* = \frac{E[\beta_2]}{E[\beta_2] + E[\hat{\alpha}_{12}] - E[\beta_1]}, \quad (3.55a)$$

$$\dot{e}_{12}^* = 0, \quad (3.55b)$$

$$\dot{e}_{22}^* = \frac{E[\hat{\alpha}_{12}] - E[\beta_1]}{E[\beta_2] + E[\hat{\alpha}_{12}] - E[\beta_1]}, \quad (3.55c)$$

if $E[\hat{\alpha}_{12}], E[\beta_2] > E[\beta_1]$, otherwise the relay is not used $\dot{e}_{12}^* = 1$, $\dot{e}_{11}^* = 0$, and $\dot{e}_{22}^* = 0$.

Finally, provided that if $E[\hat{\alpha}_{12}], E[\beta_2] > E[\beta_1]$, we have $\bar{\eta} = \dot{C}_{E_1}(\dot{\mathbf{e}}^*) = \dot{C}_{E_2}(\dot{\mathbf{e}}^*)$, the maximum RPE with a relay in HD or FD mode is given by

$$\bar{\eta} = \begin{cases} \frac{E[\hat{\alpha}_{12}]E[\beta_2]}{E[\beta_2] + E[\hat{\alpha}_{12}] - E[\beta_1]} & \text{if } E[\hat{\alpha}_{12}], E[\beta_2] > E[\beta_1], \\ E[\beta_1] & \text{otherwise} \end{cases} \quad (3.56)$$

with $\hat{\alpha}_{12} = \alpha_{12} + \beta_1$ for the CB and $\hat{\alpha}_{12} = \alpha_{12}$ for DF.

3.8.4 Slope of the Spectral Efficiency

The maximum RPE has not revealed the potential gain of the FD capability at the relay nor the impact of the distribution of the channel coefficients. Moreover, obtaining the maximum RPE is possible even without optimizing the time-sharing factors τ_1 and τ_2 and assuming a linear dependence of the power allocation as a function of the total power $\mathbf{E}(E) = \dot{\mathbf{e}}^* E$. Thus, we turn our attention to the analysis of the slope. This metric allows us to compare transmission schemes with equal maximum RPE and determines the use made of the bandwidth.

The slope of the spectral efficiency can be computed as (3.17). The first-order derivative $\dot{R}^*(0)$ was already computed in the previous section and thus, we only need to obtain $\ddot{R}^*(0)$. To obtain $\ddot{R}^*(0)$, we solve the problem in (3.51).

For a relay in FD mode, substituting the functions g_{E_i} in (3.46) into (3.49b), the second-order derivative of the rate constraints at $E = 0$ read

$$\ddot{C}_{E_1}(\ddot{\mathbf{e}}) = E[\hat{\alpha}_{12}] \ddot{e}_1 - E[(\dot{g}_{E_1}(\dot{\mathbf{e}}^*))^2], \quad (3.57a)$$

$$\ddot{C}_{E_2}(\ddot{\mathbf{e}}) = E[\beta_1] \ddot{e}_1 + E[\beta_2] \ddot{e}_2 - E[(\dot{g}_{E_2}(\dot{\mathbf{e}}^*))^2] \quad (3.57b)$$

with, after substituting the solution to $\dot{\mathbf{e}}^*$ found in (3.53)

$$\mathbb{E} [(\dot{g}_{E_1}(\dot{\mathbf{e}}^*))^2] = \mathbb{E} [(\hat{\alpha}_{12}\dot{e}_1^*)^2] = \kappa_{12}\bar{\eta}^2, \quad (3.58a)$$

$$\begin{aligned} \mathbb{E} [(\dot{g}_{E_2}(\dot{\mathbf{e}}^*))^2] &= \mathbb{E} [(\beta_1\dot{e}_1^* + \beta_2\dot{e}_2^*)^2], \\ &= [1 + (\kappa_1 - 1)\Theta^2 + (\kappa_2 - 1)(1 - \Theta)^2] \bar{\eta}^2 \end{aligned} \quad (3.58b)$$

with $\Theta = \frac{\mathbb{E}[\beta_1]}{\mathbb{E}[\hat{\alpha}_{12}]}$ and $\kappa_{12} = \frac{\mathbb{E}[(\hat{\alpha}_{12})^2]}{(\mathbb{E}[\hat{\alpha}_{12}])^2}$, $\kappa_1 = \frac{\mathbb{E}[(\beta_1)^2]}{(\mathbb{E}[\beta_1])^2}$ and $\kappa_2 = \frac{\mathbb{E}[(\beta_2)^2]}{(\mathbb{E}[\beta_2])^2}$ are the kurtosis of the channel coefficients. Here, we have use of the fact that β_1 and β_2 are independent r.v. and $\mathbb{E}[\beta_1\beta_2] = 0$.

By substituting (3.57) into (3.51), and solving the resultant problem over \ddot{e}_1, \ddot{e}_2 , we obtain

$$\ddot{e}_1^* = \frac{\mathbb{E} [(\dot{g}_{E_1}(\dot{\mathbf{e}}^*))^2] - \mathbb{E} [(\dot{g}_{E_2}(\dot{\mathbf{e}}^*))^2]}{\mathbb{E} [\hat{\alpha}_{12}] - \mathbb{E} [\beta_1] + \mathbb{E} [\beta_2]}, \quad (3.59a)$$

$$\ddot{e}_2^* = -\ddot{e}_1^* \quad (3.59b)$$

if $\mathbb{E} [\hat{\alpha}_{12}], \mathbb{E} [\beta_2] > \mathbb{E} [\beta_1]$ (the relay is used) and $\ddot{e}_1^* = 1, \ddot{e}_2^* = 0$ otherwise. Substituting, this solution into (3.57) we have $\ddot{R}^*(0) = \ddot{C}_{E_1}(0) = \ddot{C}_{E_2}(0)$ and the slope (3.17) reads

$$\begin{aligned} \frac{2}{\bar{S}_{FD}} &= 1 + (\kappa_{12} - 1)(1 - \Gamma) \\ &+ (\kappa_1 - 1)\Gamma\Theta^2 + (\kappa_2 - 1)\Gamma(1 - \Theta)^2. \end{aligned} \quad (3.60)$$

with $\Gamma = \frac{\bar{\eta}}{\mathbb{E}[\beta_2]}$.

Instead, if the power allocation is restricted to be linear in E , $E_1 = \dot{e}_1^*E$, $E_2 = \dot{e}_2^*E$, then substituting $\ddot{e}_2^* = \ddot{e}_1^* = 0$ into (3.57), we have

$$\ddot{R}^*(0) = -\max_{i \in \{1,2\}} \mathbb{E} [(\dot{g}_{E_i}(\dot{\mathbf{e}}^*))^2] \quad (3.61)$$

with $\mathbb{E} [(\dot{g}_{E_i}(\dot{\mathbf{e}}^*))^2]$ in (3.58). Substituting (3.61) into the slope definition (3.17), we obtain

$$\frac{2}{\bar{S}_{FD_e}} = \max (\kappa_{12}, [1 + (\kappa_1 - 1)\Theta^2 + (\kappa_2 - 1)(1 - \Theta)^2]). \quad (3.62)$$

This last result was first found in [61, eq. 33].

For a relay in HD mode, substituting the functions g_{E_i} in (3.47) into (3.49b), the second-order derivative of the rate constraints at $E = 0$ read

$$\begin{aligned} \ddot{C}_{E_1}(\ddot{\mathbf{e}}, \mathbf{t}) &= \mathbb{E} [\hat{\alpha}_{12}] \ddot{e}_{11} + \mathbb{E} [\beta_1] \ddot{e}_{12} \\ &- \frac{\mathbb{E} [(\dot{g}_{E_{11}}^*(\dot{\mathbf{e}}^*))^2]}{t_1} - \frac{\mathbb{E} [(\dot{g}_{E_{21}}^*(\dot{\mathbf{e}}^*))^2]}{t_2}, \end{aligned} \quad (3.63a)$$

$$\begin{aligned} \ddot{C}_{E_2}(\ddot{\mathbf{e}}, \mathbf{t}) &= \mathbb{E} [\beta_1] \ddot{e}_{11} + \mathbb{E} [\beta_1] \ddot{e}_{12} + \mathbb{E} [\beta_2] \ddot{e}_{22} \\ &- \frac{\mathbb{E} [(\dot{g}_{E_{12}}^*(\dot{\mathbf{e}}^*))^2]}{t_1} - \frac{\mathbb{E} [(\dot{g}_{E_{22}}^*(\dot{\mathbf{e}}^*))^2]}{t_2} \end{aligned} \quad (3.63b)$$

with, after substituting the solution to $\dot{\mathbf{e}}^*$ found in (3.55)

$$\mathbb{E} \left[(\dot{g}_{E_{11}}^* (\dot{\mathbf{e}}^*))^2 \right] = \mathbb{E} [(\hat{\alpha}_{12})^2] (\dot{e}_{11}^*)^2 = \kappa_{12} \bar{\eta}^2, \quad (3.64a)$$

$$\mathbb{E} \left[(\dot{g}_{E_{21}}^* (\dot{\mathbf{e}}^*))^2 \right] = \mathbb{E} [(\beta_1)^2] (\dot{e}_{12}^*)^2 = 0, \quad (3.64b)$$

$$\mathbb{E} \left[(\dot{g}_{E_{12}}^* (\dot{\mathbf{e}}^*))^2 \right] = \mathbb{E} [(\beta_1)^2] (\dot{e}_{11}^*)^2 = \kappa_1 \Theta^2 \bar{\eta}^2, \quad (3.64c)$$

$$\mathbb{E} \left[(\dot{g}_{E_{22}}^* (\dot{\mathbf{e}}^*))^2 \right] = \mathbb{E} [(\beta_2)^2] (\dot{e}_{22}^*)^2 = \kappa_2 (1 - \Theta)^2 \bar{\eta}^2. \quad (3.64d)$$

Substituting (3.63) into (3.51), and solving the resultant problem, first over $\ddot{e}_{11}, \ddot{e}_{12}, \ddot{e}_{22}$ assuming constant \mathbf{t} , we obtain (notice that the resultant problem is equivalent to that for constant channels in (3.38))

$$\ddot{e}_{12}^{A*} = 0, \ddot{e}^{R*} = -\ddot{e}_{11}^*, \quad (3.65a)$$

$$\hat{\alpha}_{12} \frac{\hat{\beta}_2}{\eta} \ddot{e}_{11}^* = \frac{\mathbb{E} \left[(\dot{g}_{E_{11}}^* (0))^2 \right] - \mathbb{E} \left[(\dot{g}_{E_{12}}^* (0))^2 \right]}{t_1} - \frac{\mathbb{E} \left[(\dot{g}_{E_{22}}^* (0))^2 \right]}{t_2}, \quad (3.65b)$$

and

$$\begin{aligned} \ddot{R}^* (\mathbf{t}) &= \ddot{C}_{E_1} (\ddot{\mathbf{e}}^*, \mathbf{t}) = \ddot{C}_{E_1} (\ddot{\mathbf{e}}^*, \mathbf{t}) \\ &= -\frac{(\bar{\Psi}_1)^2}{t_1} - \frac{(\bar{\Psi}_2)^2}{t_2} \end{aligned} \quad (3.66)$$

with

$$(\bar{\Psi}_1)^2 = (1 - \Gamma) \kappa_{12} \bar{\eta}^2 + \Gamma \kappa_1 \Theta^2 \bar{\eta}^2, \quad (3.67a)$$

$$(\bar{\Psi}_2)^2 = \Gamma \kappa_2 (1 - \Theta)^2 \bar{\eta}^2. \quad (3.67b)$$

Maximizing (3.66) over \mathbf{t} we get $\frac{1}{t_1^*} = 1 + \frac{\Psi_2}{\Psi_1}$ which substituted into (3.66) yields $\ddot{R}^* (0) = -(\Psi_1 + \Psi_2)^2$ and the slope is

$$\frac{2}{\bar{S}_{HD}} = \left(\sqrt{\kappa_{12} (1 - \Gamma) + \kappa_1 \Gamma \Theta^2} + \sqrt{\kappa_2 \Gamma (1 - \Theta)^2} \right)^2. \quad (3.68)$$

Instead, if the power allocation is restricted to be linear in E , $E_{11} = \dot{e}_{11}^* E$, $E_{12} = 0$, and $E_{22} = \dot{e}_{22}^* E$, then substituting $\ddot{e}_{11}^* = \ddot{e}_{12}^* = \ddot{e}_{22}^* = 0$ into (3.63), we have

$$\ddot{C}_{E_1} (\mathbf{0}, \mathbf{t}) = -\frac{\kappa_{12} \bar{\eta}^2}{t_1}, \quad (3.69a)$$

$$\ddot{C}_{E_2} (\mathbf{0}, \mathbf{t}) = -\frac{\kappa_1 \Theta^2 \bar{\eta}^2}{t_1} - \frac{\kappa_2 (1 - \Theta)^2 \bar{\eta}^2}{t_2}. \quad (3.69b)$$

Now, we substitute (3.69) into (3.51), and solve the resultant problem only over \mathbf{t} . By substituting $\mathbf{t} = [t_1, 1 - t_1]$ into (3.69b) it is easy to show that $-\ddot{C}_{E_2} (\mathbf{0}, \mathbf{t})$ has a unique minimum over $t_1 \in (0, 1)$ at $t_1 = t_1^{c2}$

$$\frac{1}{t_1^{c2}} = 1 + \frac{1 - \Theta}{\Theta} \sqrt{\frac{\kappa_2}{\kappa_1}} \quad (3.70)$$

at this point, we have

$$\ddot{C}_{E_2}(\mathbf{0}, \mathbf{t}^{c_2}) = - \left(\sqrt{\kappa_1 \Theta^2} + \sqrt{(1-\Theta)^2 \kappa_2} \right)^2 \bar{\eta}^2 \quad (3.71)$$

if $\ddot{C}_{E_1}(\mathbf{0}, \mathbf{t}^{c_2}) > \ddot{C}_{E_2}(\mathbf{0}, \mathbf{t}^{c_2})$ or equivalently

$$\kappa_{12} - \kappa_1 \Theta^2 < (1-\Theta) \Theta \sqrt{\kappa_1 \kappa_2} \quad (3.72)$$

then $\ddot{R}(0) = \ddot{C}_{E_2}(\mathbf{0}, \mathbf{t}^{c_2})$, otherwise $\ddot{R}(0) = \ddot{C}_{E_1}(\mathbf{0}, \mathbf{t}^{c_1})$ where \mathbf{t}^{c_1} is found by setting $\ddot{C}_{E_1}(\mathbf{0}, \mathbf{t}) = \ddot{C}_{E_2}(\mathbf{0}, \mathbf{t})$ at

$$\frac{1}{t_1^{c_1}} = 1 + \frac{\kappa_2 (1-\Theta)^2}{\kappa_{12} - \kappa_1 \Theta^2}. \quad (3.73)$$

Finally, substituting $\ddot{R}(0)$ into the slope definition, we obtain

$$\frac{2}{\bar{S}_{HD_e}} = \begin{cases} \left(\sqrt{\kappa_1 \Theta^2} + \sqrt{(1-\Theta)^2 \kappa_2} \right)^2 & \text{if } \frac{\kappa_{12} - \kappa_1 \Theta^2}{(1-\Theta) \Theta \sqrt{\kappa_1 \kappa_2}} < 1, \\ \kappa_{12} \left(1 + \frac{\kappa_2 (1-\Theta)^2}{\kappa_{12} - \kappa_1 \Theta^2} \right) & \text{otherwise} \end{cases}. \quad (3.74)$$

This last result was first found in [61, Proposition 4].

Consider, now, that the time-sharing factors are fixed (independent of the channel gains) $\mathbf{t}_0 = [\frac{1}{2}, \frac{1}{2}]$ but the energies \ddot{e} are optimally allocated. It is direct from (3.66) that

$$\ddot{R}^*(\mathbf{t}_0) = -2(\Psi_1)^2 - 2(\Psi_2)^2 \quad (3.75)$$

and the slope is

$$\frac{1}{\bar{S}_{HD_\tau}} = \kappa_{12} (1-\Gamma) + \kappa_1 \Gamma \Theta^2 + \kappa_2 \Gamma (1-\Theta)^2. \quad (3.76)$$

Finally, consider that, the power allocation is linear and the time-sharing factors are fixed $\mathbf{t} = \mathbf{t}_0$. In this case, we have

$$\ddot{C}_{E_1}(0, \mathbf{t}_0) = -2\kappa_{12} \bar{\eta}^2, \quad (3.77a)$$

$$\ddot{C}_{E_2}(0, \mathbf{t}_0) = -2\kappa_1 \Theta^2 \bar{\eta}^2 - 2\kappa_2 (1-\Theta)^2 \bar{\eta}^2 \quad (3.77b)$$

and $\ddot{R}^*(0) = \min_{i \in \{1,2\}} \ddot{C}_{E_i}(0, \mathbf{t}_0)$. Then, the slope decreases to

$$\frac{1}{\bar{S}_{HD_{\tau,e}}} = \max (\kappa_{12}, \kappa_1 (\Theta)^2 + \kappa_2 (1-\Theta)^2). \quad (3.78)$$

From this result, we can state the following conclusions for ergodic fading channels.

- The optimal power allocation is not linear in the total power E as $\ddot{e}^* \neq \mathbf{0}$ for both, HD nodes (3.65) and FD nodes (3.59).
- For a relay in HD mode, regardless of the channel distribution, the source never transmits in the second interval ($\dot{e}_{12}^* = \dot{e}_{12}^* = 0$) $\lim_{E \rightarrow 0} E_{12}(E) = \dot{e}_{12}^* E + \ddot{e}_{12}^* \frac{E^2}{2} + o(E^3) = o(E^3)$. Therefore, orthogonal transmissions are optimal in the low power regime in terms of maximum RPE and maximum slope of the spectral efficiency.

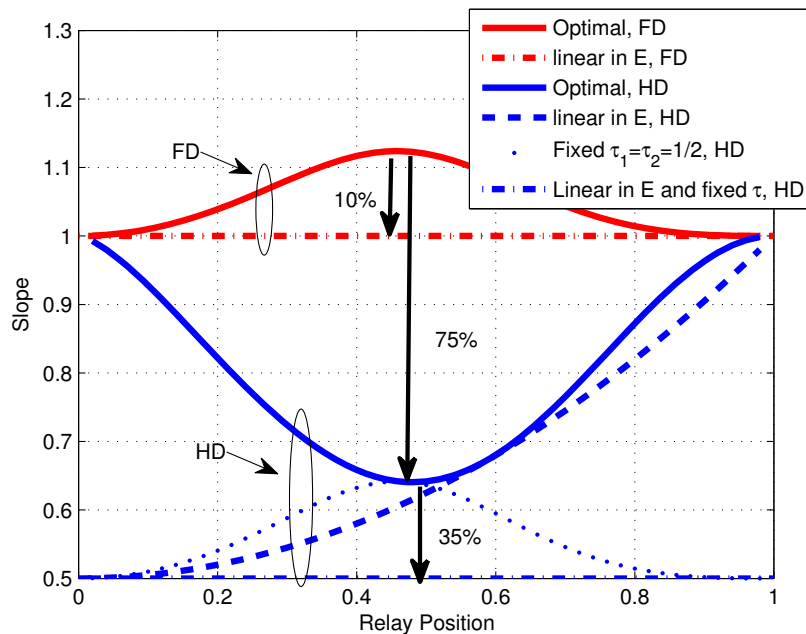


Figure 3.8: Maximum slope versus source to relay distance over Rayleigh fading $\kappa = 2$.

3.8.5 Numerical Results

In this section, we present numerical results to show the performances losses incurred by the HD transmission mode and the suboptimal resource allocation solutions.

The slope of the spectral efficiency depends on the mean of the channel fading and the kurtosis of the fading coefficients. We consider Rayleigh fading channels; i.e. $\alpha_{12}, \beta_1, \beta_2$ are exponential distributed random variables. Thus, the kurtosis of the channel coefficients is $\kappa = 2$. The relay is placed on the line connecting the source and the transmitters, and the path-loss exponent is $\nu = 2$. The mean of β_1 is normalized to $E[\beta_1] = 1$, then $E[\alpha_{12}] = d^{-\nu}$ and $E[\beta_2] = (1 - d)^{-\nu}$ where d is the distance from the source to the relay. In Fig. 3.8, we depict the slope of the spectral efficiency as a function of the distance from the source to the relay. The figure includes all the scenarios under analysis: the relay in FD or HD modes and the optimal or the approximated resource allocation solutions. For a relay in FD mode, the slope obtained with the linear power allocation approximation does not depend on the distance d , note that substituting $\kappa = \kappa_{12} = \kappa_1 = \kappa_2$ into (3.62), we obtain $\frac{2}{S_{FDe}} = k_{12}$ if $E[\beta_1] < E[\hat{\alpha}_{12}]$, which is always the case if the relay cooperates. Although, an efficient use of the bandwidth is done if the relay is near to the source or the destination, if the relay is located in the middle the linear approximation requires 10% more of the minimum bandwidth. Compared to the FD mode, a relay in HD mode, requires up to 75% more of the minimum bandwidth, when the relay is in the middle point between the source and the destination. For a relay in HD mode, the bandwidth losses incurred by suboptimal resource allocation solutions depend strongly on the distance d . If the relay is near to the destination, the best suboptimal solution is to only allocate the time-sharing factor. However, if the relay is in the middle point, the best option is

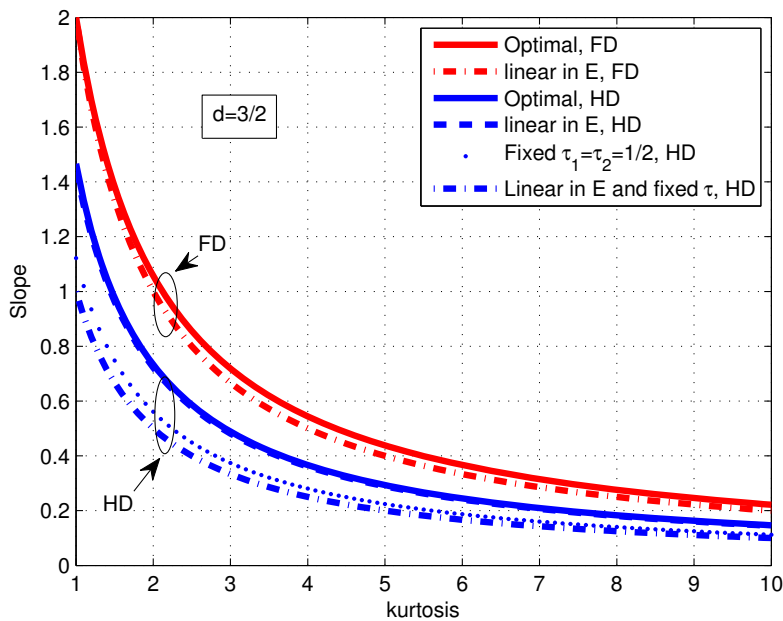


Figure 3.9: Maximum slope versus the kurtosis of the channel coefficients at $d = 2/3$. For a relay in FD and HD modes with DF and different resource allocation policies.

to consider fixed time-sharing factors but optimal power allocation. If both approximation are taken the system requires 35% more of the minimum possible bandwidth with a HD relay.

Finally, in Fig. 3.9, we show the slope as a function of the kurtosis of the channel coefficients for each of the scenarios under consideration. In this case, the relay is located near the destination at $d = 2/3$.

3.8.6 Conclusions

We studied the spectral efficiency of relayed transmissions over ergodic channels in the power efficient regime. The study includes DF relaying and the CB on the relay channel capacity, with relays in, both, full duplex or half duplex modes. We found the optimal resource allocation that maximizes the spectral efficiency at $E = 0$ and computed the maximum RPE and the slope of the spectral efficiency with the $\frac{E_b}{N_0}$. We showed that a linear power allocation, as assumed in previous works [61] is not sufficient to characterize the slope of the spectral efficiency. It is found that, whereas the maximum RPE does not depend on the duplexing capability, the slope reveals that the HD mode requires up to 75% more of the minimum bandwidth under Rayleigh fading channels. Besides, we showed that for a relay in HD mode, orthogonal transmissions are optimal in the low power regime.

3.9 Extension to Non-Regenerative Relaying Techniques

In this section, we explore the energy efficient regime of non-regenerative relaying strategies such as *amplify and forward* and *compress and forward*. For these strategies, hard decisions are only taken at the destination, while the relay transmits information about the received signal, including the noise, rather than the message it carries. It was shown in [43, 64] that the energy efficient regime for these strategies is no longer the low power regime, namely, when the total power E , as well as the spectral efficiency $R(E)$ go to 0. The reason is that, in the low power regime, these strategies suffer a large noise amplification at the relay, that strongly limits their performance.

As a consequence, the wide-band or low power regime tools developed in [1] are, here, not useful to analyze the energy efficient regime. In particular, to compute the maximum RPE (η) the useful equivalence ($\eta = \dot{R}(0)$) can no longer be used. Furthermore, the slope of the spectral efficiency when $\frac{E_b}{N_0} \rightarrow \frac{E_b}{N_{0 \min}}$, is no longer a useful metric. In fact, we show later on that the slope is always $S \rightarrow \infty$ at $\frac{E_b}{N_0} = \frac{E_b}{N_{0 \min}}$.

In this section, we restrict ourselves to orthogonal transmissions. After presenting and numerically computing the spectral efficiency as function of the total power for these non-regenerative techniques, we observe that the spectral efficiency is not a monotonically concave function of the total power. We show that for any interval where the spectral efficiency function is convex, we can always find a better strategy by time-sharing that improves the spectral efficiency in this interval. This new spectral efficiency is concave for all E and thus, achieves the maximum RPE in the low power regime. However, we show that the original maximum RPE can not be increased. Finally, we compare the energy efficient regime (maximum RPE) obtained with the non-regenerative techniques with the one for DF as a function distance from the source to the relay.

3.9.1 Spectral Efficiency

Previous to studying the maximum RPE, we present the spectral efficiency as a function of the total power E for AF and CF. In both cases, we consider Gaussian signalling. The transmission is divided in two intervals of duration τ_1, τ_2 with $\tau_1 + \tau_2 = 1$. The source transmits with power P_1 during τ_1 and the relays transmits with power P_2 during τ_2 .

For AF, the achievable rate can be found in [9] to be

$$R_{AF}(P_1, P_2) = \frac{1}{2} \log \left(1 + \beta_1 P_1 + \frac{\alpha_{12} \beta_2 P_1 P_2}{1 + \alpha_{12} P_1 + \beta_2 P_2} \right) \quad (3.79)$$

with a total power $E = \frac{1}{2} P_1 + \frac{1}{2} P_2$ and $P_1, P_2 > 0$.

For CF, an achievable rate for half duplex nodes was found in [20]. Particularizing for orthogonal transmissions, the achievable rate is

$$R_{CF}(P_1, P_2, \tau_1, \tau_2) = \tau_1 \log \left(1 + \beta_1 P_1 + \frac{\alpha_{12}}{1 + \sigma_\omega^2} P_1 \right) \quad (3.80)$$

where σ_ω^2 is the ‘‘compression’’ noise and depends on the resources as

$$\sigma_\omega^2(P_1, P_2, \tau_1, \tau_2) = \left(1 + \frac{\alpha_{12} P_1}{1 + \beta_1 P_1} \right) \frac{1}{(1 + \beta_2 P_2)^{\frac{\tau_2}{\tau_1}} - 1} \quad (3.81)$$

with total power $E = \tau_1 P_1 + \tau_2 P_2$, $P_1, P_2, \tau_1, \tau_2 \geq 0$ and $\tau_1 + \tau_2 = 1$.

The rate as a function of the total power can be computed by solving the optimal resource allocation problem for all E , namely

$$\begin{aligned} R(E) &= \max_{\tau_1, \tau_2, P_1, P_2} R(P_1, P_2, \tau_1, \tau_2) \\ E &= \tau_1 P_1 + \tau_2 P_2, \\ 1 &= \tau_1 + \tau_2, \\ P_1, P_2, \tau_1, \tau_2 &\geq 0 \end{aligned} \quad (3.82)$$

where $R(P_1, P_2, \tau_1, \tau_2)$ is given by (3.79) for AF (with $\tau_1 = \tau_2 = \frac{1}{2}$) and by (3.80) for CF.

We are unable to solve this problem for all E in close form. Instead, we solve (3.82) numerically. In Fig. 3.10, assuming that the relay is very near to the destination, we depict the rate as a function of the total power for the AF scheme. We observe that the spectral efficiency function is convex for $E < P_{vex}$ and concave otherwise. Consequently, the necessary and sufficient condition *ii*) in Proposition 3.1 ($R(E) \leq E\dot{R}(0)$) is clearly not satisfied for all E and thus, the maximum RPE is not obtained in the low power regime.

3.9.2 Time Sharing On-Off

The rate functions $R(E)$ for AF and CF, since are convex in a certain interval of the total power $E < P_{vex}$, can be always outperformed by an ON-OFF strategy or equivalently a time-sharing between remaining silent (OFF) during a fraction τ_1 and transmitting with power $P_2^* = \frac{E}{\tau_2}$ during a fraction τ_2 . See Fig. 3.10 for a graphical illustration.

Assume that there is only one convex interval. Let us denote as $R_{vex}(E)$ the rate as a function of the total power for AF or CF. Then, the achievable rate by the ON-OFF strategy is the solution to

$$R_{on-off}(E) = \max_{\tau_2, P_2} (\tau_2 R_{vex}(P_2)) \quad (3.83)$$

with $\tau_2 P_2 = E$ and $0 \leq \tau_2 \leq 1$. Solving (3.83), we obtain

$$R_{on-off}(E) = \begin{cases} \eta_{vex} E & \text{if } P_2^* > E \\ R_{vex}(E) & \text{if } P_2^* < E \end{cases} \quad (3.84)$$

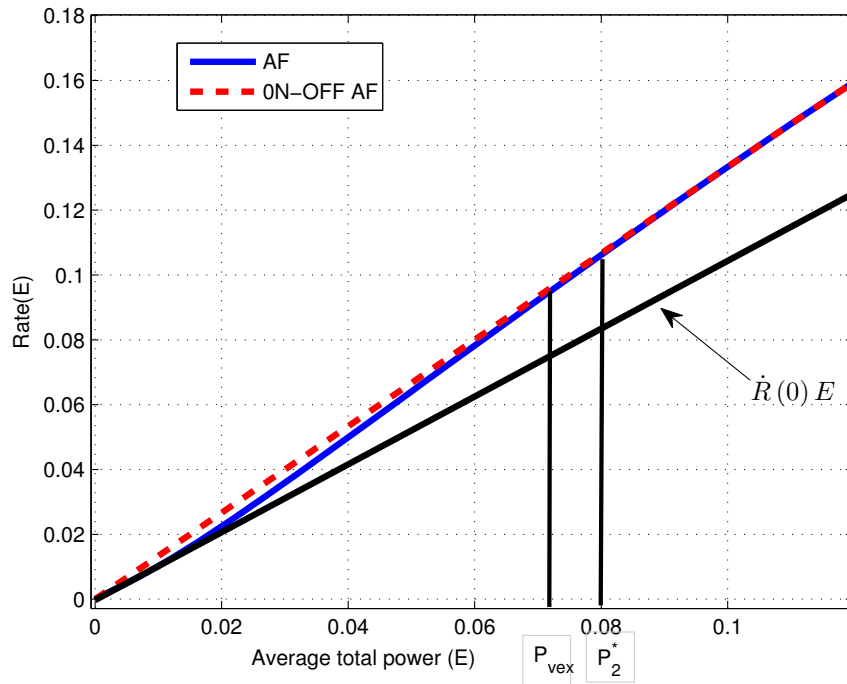


Figure 3.10: Achievable rate as a function of the total power, $R(E)$ for AF and ON-OFF AF.

where P_2^* is the solution to $\eta_{vex} = \max_{P_2} \frac{R_{vex}(P_2)}{P_2}$ and thus, η_{vex} is the maximum RPE for AF or CF without time-sharing.

The resultant time-sharing rate $R_{on-off}(E)$ not only outperforms $R_{vex}(E)$ but is also linear (concave) in the whole interval $0 \leq E \leq P_2$. Consequently, $R_{on-off}(E)$ satisfies the condition *ii*) in Proposition 3.1 and thus, obtains the maximum RPE in the low power regime.

The diversity gain in the low power regime for this time sharing strategy was studied in [59], (there referred to as, *bursty AF*). It is shown there, that $R_{on-off}(E)$ achieves the optimal diversity gain. On the contrary, here we show that, under the maximum RPE criteria, this strategy never improves the one without time-sharing (the maximum RPE remains unchanged).

The maximum RPE is thus given by

$$\eta_{on-off} = \dot{R}_{on-off}(0), \quad (3.85a)$$

$$= \eta_{vex} \quad (3.85b)$$

Given that $R_{on-off}(E)$ is linear at $E \rightarrow 0$, then $\ddot{R}_{on-off}(0) = 0$ and the slope is

$$S = \frac{2 \left(\dot{R}_{on-off}(0) \right)^2}{-\ddot{R}_{on-off}(0)} \rightarrow \infty \quad (3.86)$$

This result is illustrated in Fig. 3.11, where the rate $R\left(\frac{E_b}{N_0}\right)$ as a function of the $\frac{E_b}{N_0}$ is plotted for AF and ON-OFF AF. Note that, since the spectral efficiency is not concave for all E , it is

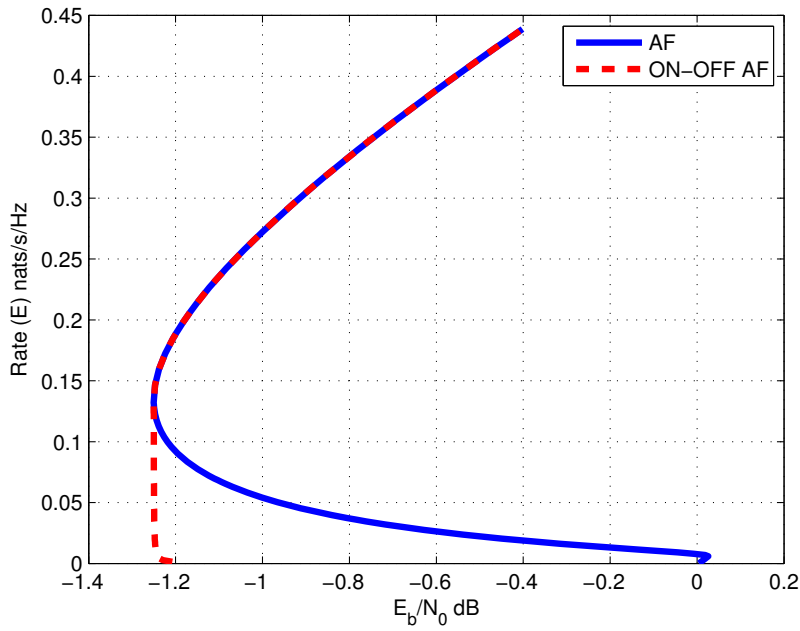


Figure 3.11: Achievable rate as a function of the $\frac{E_b}{N_0}$, $R\left(\frac{E_b}{N_0}\right)$ for AF and ON-OFF AF.

possible to find the same ratio $\frac{E_b}{N_0}$ at different spectral efficiencies R , namely, $\frac{R(E')}{E'} = \frac{R(E'')}{E''}$ with $E' \neq E''$.

3.9.3 Generalized Time-Sharing Strategy

In general, we can obtain a time sharing rate R_{TS} by using a transmission strategy with a concave rate function R_{cave} for all E and another with a rate function R_{vex} convex in a certain interval, as

$$R_{TS}(E) = \max_{\tau_1, \tau_2, E_1, E_2} \tau_1 R_{cave}(P_1) + \tau_2 R_{vex}(P_2) \quad (3.87)$$

with $E_1 + E_2 = E$, $E_1 = \tau_1 P_1$, $E_2 = \tau_2 P_2$ and $\tau_1 + \tau_2 = 1$.

The resultant rate function $R_{TS}(E)$ can be shown to be concave for all E and thus, obtains the maximum RPE in the low power regime. However, it is easy to show that this strategy never improves the maximum RPE obtained by the best of the individual strategies

$$\eta_{TS} = \max_{\tau_1, \tau_2, E_1, E_2} \frac{\tau_1 R_{cave}(P_1) + \tau_2 R_{vex}(P_2)}{E}, \quad (3.88a)$$

$$= \max_{E_1, E_2, P_1, P_2} \frac{R_{cave}(P_1) E_1}{P_1 E} + \frac{R_{vex}(P_2) E_2}{P_2 E}, \quad (3.88b)$$

$$\leq \max_{0 \leq x \leq 1} (x \eta_{cave} + (1-x) \eta_{vex}), \quad (3.88c)$$

$$= \max(\eta_{cave}, \eta_{vex}). \quad (3.88d)$$

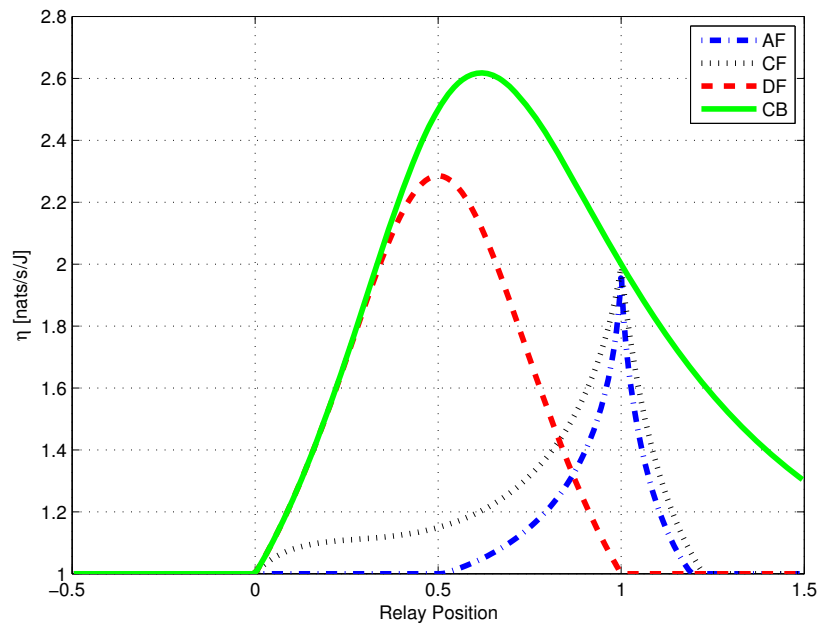


Figure 3.12: Maximum RPE as a function of the relay position for CB, DF, CF and AF.

To obtain the equality (3.88b), we use $\tau_1 = \frac{E_1}{P_1}$, $\tau_2 = \frac{E_2}{P_2}$. Then, the maximization is with respect to E_1, E_2, P_1, P_2 constrained to $E_1 + E_2 = E$ and $\frac{P_1}{E_1} + \frac{P_2}{E_2} < 1$. Denoting, $x = \frac{E_1}{E}$ and maximizing with respect to P_1 and P_2 , separately, we obtain the inequality (3.88c).

3.9.4 Comparison with Regenerative Strategies

In Fig. 3.12, we depict the maximum RPE obtained, numerically, for AF and CF with the ones obtained for DF and the CB, as a function of the distance from the source to the relay. It is interesting to note that the non-regenerative strategies are useful only if the relay is near to the destination, no matter if the relay is farther from the source than the destination. In addition, CF always outperforms AF, and is always better than the direct transmission.

In Fig. 3.13, we depict the transmitted power during the (ON) transmission interval to achieve the maximum RPE. It is remarkable that for CF the power needed is 10 times lower than for AF.

3.10 Chapter Summary and Conclusions

In this chapter, we have studied the energy efficient regime for the relay channel. First, we have shown that the low power regime is the energy efficient regime for a fairly general AWGN multi-hop channels under duplexing and synchronism constraints. Using this result, it has

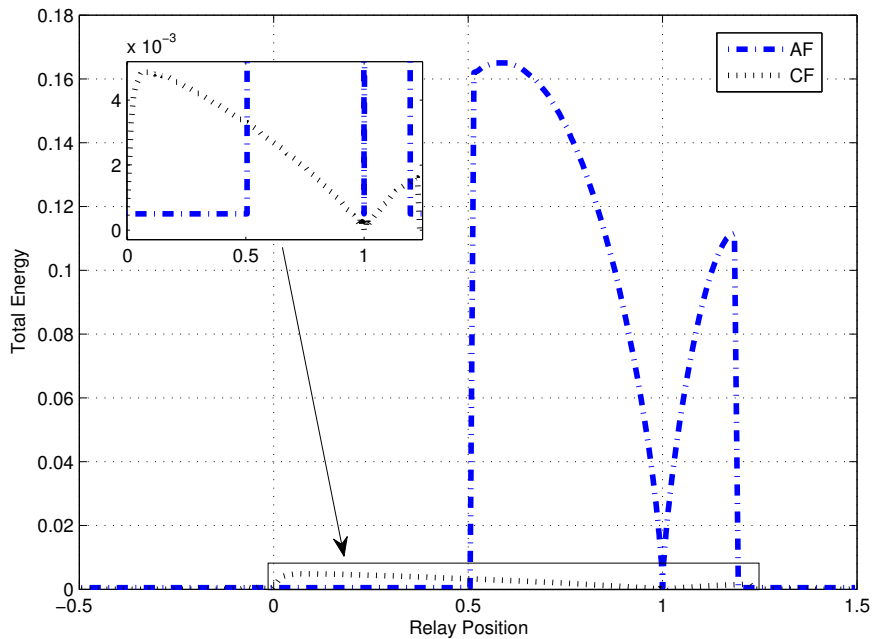


Figure 3.13: Total power at which the maximum RPE is achieved for AF and CF.

been shown that the energy efficient regime for decode and forward and the cut-set bound is the low power regime. Thus, the low power analysis tools were applied to investigate the gains provided by synchronism, duplexing and the optimal allocation of the network resources. We showed that synchronous transmissions are necessary to obtain the maximum RPE but can be achieved also with half duplex nodes, without optimizing the time-sharing factors and only considering a linear dependence of the power allocation as a function of the total power. Furthermore, we showed that for *asynchronous* transmissions, the orthogonal access to the channel is sufficient and for the *synchronous* transmissions, the HD mode is sufficient to obtain the maximum RPE. The suboptimality of the orthogonal transmissions, the *half duplex* mode and the suboptimal resource allocation were determined computing the slope of the spectral efficiency with the $\frac{E_b}{N_0}$. Then, numerical results have been used to show that the low power analysis can be used to: design power allocation and relay selection strategies. The study was then extended to ergodic fading channels. It was shown, how the spectral efficiency is affected by the peakiness (kurtosis) of the channel amplitude. Finally, the analysis is extended to non-regenerative relaying strategies such as amplify and forward and compress and forward. It was shown that for these strategies the energy efficient regime is no longer the low power regime and the suitability of these techniques in the energy efficient regime has been discussed in detail.

Appendix 3.A Derivatives of the Rate Constraints

Here we compute the first and second-order derivatives with respect to the total power E of the rate constraints in (3.11) evaluated at $E \rightarrow 0$. Consider that \mathbf{E} and $\boldsymbol{\tau}$ are function of E , then

$$C_{E_i}(E) = C_i(\boldsymbol{\tau}(E), \mathbf{E}(E)), \quad (3.89a)$$

$$= \sum_{j=1}^2 \tau_j(E) \log \left(1 + \frac{g_{E_{ji}}(E)}{\tau_j(E)} \right). \quad (3.89b)$$

Let us assume that $\mathbf{E}(E)$ and $\boldsymbol{\tau}(E)$ are twice differentiable functions of E and define $\dot{\mathbf{e}} \triangleq \dot{\mathbf{E}}(0)$, $\ddot{\mathbf{e}} \triangleq \ddot{\mathbf{E}}(0)$, $\mathbf{t} \triangleq \boldsymbol{\tau}(0)$, $\dot{\mathbf{t}} \triangleq \dot{\boldsymbol{\tau}}(0)$ and $\ddot{\mathbf{t}} \triangleq \ddot{\boldsymbol{\tau}}(0)$.

For the first-order derivative, we have $\dot{C}_{E_i}(E) = \sum_{j=1}^2 \dot{C}_{E_{ji}}(E)$ with

$$\dot{C}_{E_{ji}}(E) = \dot{\tau}_j(E) \log \left(1 + \frac{g_{E_{ji}}(E)}{\tau_j(E)} \right) + \frac{\tau_j(E)}{1 + \frac{g_{E_{ji}}(E)}{\tau_j(E)}} \left(\frac{\dot{g}_{E_{ji}}(E)\tau_j(E) - \dot{\tau}_j(E)g_{E_{ji}}(E)}{(\tau_j(E))^2} \right), \quad (3.90a)$$

$$= \dot{\tau}_j(E) \log \left(1 + \frac{g_{E_{ji}}(E)}{\tau_j(E)} \right) + \frac{\tau_j(E) \dot{g}_{E_{ji}}(E) - \dot{\tau}_j(E) g_{E_{ji}}(E)}{\tau_j(E) + g_{E_{ji}}(E)}. \quad (3.90b)$$

At $E = 0$, $g_{E_{ji}}(0) = 0$ and the first-order derivative $\dot{g}_{E_{ji}}(0)$ only depends on $\dot{\mathbf{e}}$. Then, $\dot{C}_{E_{ji}}(0)$ is

$$\dot{C}_{E_{ji}}(0) = \dot{g}_{E_{ji}}(\dot{\mathbf{e}}) \quad (3.91)$$

For the second-order derivative, we have

$$\begin{aligned} \ddot{C}_{E_{ji}}(E) &= \ddot{\tau}_j(E) \log \left(1 + \frac{g_{E_{ji}}(E)}{\tau_j(E)} \right) + \frac{\dot{\tau}_j(E)}{\tau_j(E) + g_{E_{ji}}(E)} \left(\dot{g}_{E_{ji}}(E) - \frac{\dot{\tau}_j(E)}{\tau_j(E)} g_{E_{ji}}(E) \right) \\ &\quad + \frac{(\tau_j(E) \ddot{g}_{E_{ji}}(E) - \ddot{\tau}_j(E) g_{E_{ji}}(E))}{(\tau_j(E) + g_{E_{ji}}(E))} \\ &\quad - \frac{(\dot{\tau}_j(E) + \dot{g}_{E_{ji}}(E)) (\tau_j(E) \dot{g}_{E_{ji}}(E) - \dot{\tau}_j(E) g_{E_{ji}}(E))}{(\tau_j(E) + g_{E_{ji}}(E))^2}. \end{aligned} \quad (3.92)$$

At $E = 0$, $g_{E_{ji}}(0) = 0$ and $\ddot{g}_{E_{ji}}(0)$ only depends on $\dot{\mathbf{e}}$ and $\ddot{\mathbf{e}}$. Then, $\ddot{C}_{E_{ji}}(0)$ is

$$\ddot{C}_{E_{ji}}(0) = \ddot{g}_{E_{ji}}(\dot{\mathbf{e}}, \ddot{\mathbf{e}}) - \frac{(\dot{g}_{E_{ji}}(\dot{\mathbf{e}}))^2}{t_j}. \quad (3.93)$$

Chapter 4

Cooperative Multiple Access Channel

This chapter addresses the energy efficiency analysis of the two-user cooperative multiple-access channel (CMAC) under additive white Gaussian noise (AWGN). In this scenario, two nodes cooperate with each other in transmitting information to a common destination. This channel captures the essence of user cooperation, and jointly with the relay channel (RC) serves as one of the primary building block for cooperation on a larger scale (multiple-source multiple-destination cooperative scenarios).

In this chapter, we continue the analysis of the energy efficiency gains associated with the different capabilities at terminals. The capabilities here studied are basically the ones addressed for the RC in the previous chapter, see Table 4.1: *i*) the users *multiple access channel* via superposition or time division *ii*) the *full duplex* (FD) capability at user terminals, *iii*) the *synchronization* of the transmissions and *iv*) the optimal *resource allocation*. In addition, we also investigate *v*) the gain of transmitting jointly (*joint coding* (JC) via e.g. superposition) the own generated data and the cooperative data, instead of transmitting them using different degrees of freedom via data flow-separation (FS). Notice that in the RC, the relay never transmits new information and thus, this capability was not addressed.

Table 4.1: Terminal constraints for RC, MAC and CMAC.

CMAC	RC	MAC	Channel Access	Superposition		
			Duplexing	X	HD	FD
			Synchronism	Async.	Sync./Async.	Sync./Async.
			Cod./Dec. Complexity	FS	JC/FS	JC/FS

4.1 Related Work and Contributions

Depending on the terminals capabilities, different communication scenarios/strategies have to be addressed/designed. The CMAC generalizes the multiple-access channel (MAC) and the relay channel (RC). For each of these channels, the constraints considered in this chapter are detailed in the following and summarized in Table 4.1.

4.1.1 MAC

The energy efficient regime analysis for the MAC was addressed in [42]. In this channel, two sources transmit information messages (ω_1, ω_2) within independent codebooks $\mathcal{X}_1(\omega_1)$, $\mathcal{X}_2(\omega_2)$. From several standpoints, the main issue of implementation complexity at terminals is due to how the channel is shared, the **channel access**. If the receiver is able to cope with inter-user interference, then both users can transmit simultaneously, so that their transmitted signals arrive superposed at the destination. If not, then the sources transmissions must be orthogonal, i.e. time-division multiple-access (TDMA).

The TDMA achieves the maximum rate per energy (RPE) pair equal to that of superposition. The strict suboptimality of TDMA was demonstrated in [42] by computing slope regions of spectral efficiencies.

4.1.2 RC

For the RC, only the source node transmits information to the destination whereas the relay node sole purpose is to assist the communication. Again, both nodes share the same medium and thus, the channel access is still an issue. Besides, as simultaneous transmissions are possible, then duplexing and synchronism capabilities become the new complexity issues. If the relay has **full duplex** capabilities, then this node receives and transmits simultaneously on the same frequency channel. In such a case, the signal transmitted by the relay interferes with its own received signal. In practice, however, any error in interference cancelation (e.g. due to quantization and finite-precision processing effects) can be catastrophic because the transmit-

ted signal is typically 100-150dB stronger than the received signal [9]. If FD operation is not possible, the relay works in half duplex (HD) mode, which consists of a relay transmitting and receiving using different degrees of freedom, e.g. the transmission can be divided into two consecutive time intervals. During the first interval, the source transmits while the relay receives. During the second interval, both nodes transmit simultaneously. Concerning the **synchronization**, given that, the source terminal knows, partially or completely, the signal transmitted by the relay. If, additionally, local oscillators are synchronized and the phases of the channels between the source and the destination and between the relay and the destination are known, the transmitted signals can add coherently at the receiver. This seems highly unrealistic. Left by themselves, the drift of the oscillators makes synchronization impossible. However, some distributed carrier synchronization and channel feedback techniques are currently available. An excellent overview of the state of the art can be found in [27].

We studied the impact of the *duplexing* and *synchronism* constraints in Chapter 3. It was there shown that synchronous transmissions are necessary to obtain the maximum RPE but can be achieved with HD nodes. The suboptimality of the HD nodes was determined by the study of slope of the spectral efficiency. However, it was shown that, for asynchronous nodes in HD mode, time-division multiple access is sufficient to obtain the maximum slope.

4.1.3 CMAC

The multiple-access channels with generalized feedback was first examined in [56, 57, 67]. Considering the source messages as feedback information allows the sources to act as relays for one another. The study of these coding schemes introducing multipath fading into the model has been recently addressed in [2, 68], there referred to as *user cooperation diversity*. The **cooperative coding** is the new complexity issue we consider for the CMAC. In cooperative systems, transmitting simultaneously typically requires complex coding schemes and challenging code construction. For instance, in the RC to take advantage of the full duplex capability at the relay, block Markov coding (BMC) is needed. In the CMAC, additionally, joint coding techniques are needed to transmit simultaneously the own generated and the relayed data. Joint encoding can be done with multiplexing coding or superposition coding. Multiplexed codes are difficult to build, see [30]. With superposition coding, for each jointly encoded message, a different and independent codebook is used. In addition, the decoding of simultaneously received or jointly encoded messages requires high complexity receivers.

For the CMAC in the low power regime, the diversity gain of cooperation over Rayleigh fading channels not known at the transmitter has been addressed in [30, 46, 59]. Instead, we consider fixed channel gains that are known at the user terminals. Thus, our main focus is on the gains of user cooperation due to an efficient use of the available network resources.

We organize our contributions as follows:

- We assume that cooperation among users is based on decode and forward (DF) and that the network resources are optimally allocated among nodes to enhance the rate region according to the channel state information (CSI). In that case, as shown in the previous chapter, the energy efficient regime is the low power regime. Thus, the low power analysis tools [1] are used to study energy efficient regime of the CMAC. First, we particularize and define the low power metric to the CMAC. Unlike the RC, where we have a rate from the source to the destination, for the CMAC, we have a rate region. Thus, in the low power regime, we are interested in computing the maximum RPE region that both user can achieve simultaneously and the slope region of spectral efficiencies with respect to the energy per user bit.
- Previous to consider more advanced joint coding strategies. We investigate the direct extension of the RC to the CMAC. The total transmission time is divided into two intervals each one entirely dedicated to transmit or relay the data flow of one user. Thus, in a given transmission interval each node can act as a relay or as a source but not as both simultaneously. We label this strategy as flow-separation (FS-CMAC).
- Then, to introduce the JC capability of the CMAC and also accommodate the RC terminal capabilities studied in the previous chapter, we design new coding schemes and find the associated rate regions. This is possible by introducing orthogonal intervals on which either: *i*) jointly encoding the own and the cooperative data is not allowed FS-CMAC, *ii*) users can not transmit and receive simultaneously (*duplexing*), or *iii*) only one user can access to the channel but can jointly encode the own and the cooperative data (*time-division with jointly-coding*).
- Then, we study the energy efficiency of the rate regions with joint coding to assess the impact of the energy efficiency of the above mentioned terminal capabilities. To that end, we compute the maximum RPE region and the slope region of spectral efficiencies with respect to the energy per user bit.
- Finally, numerical results are presented.

The remainder of the chapter is organized as follows. First the CMAC model is presented in Section 4.2, after which, in Section 4.3, we introduce the low power analysis tools particularized to this channel. Then, as a baseline for comparison and to discuss the suboptimality of simpler resource allocation strategies, the low power regime analysis is first conducted for the flow-separation transmission strategy in Section 4.4. Then, in Section 4.5, achievable rate regions that use joint coding techniques are presented. For these regions, the maximum rate per energy pair is computed in Section 4.6 and the slope region, in Section 4.7. Finally, simulation results are given in Section 4.8 and conclusions are drawn in Section 4.9.

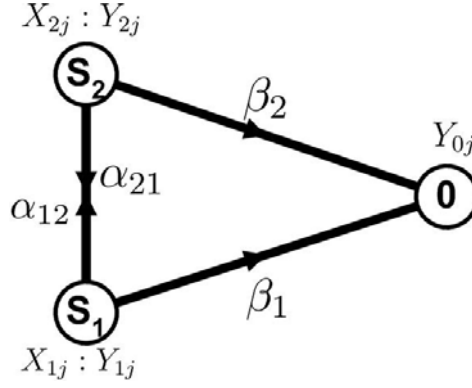


Figure 4.1: Cooperative multiple-access channel model (CMAC).

4.2 Channel Model

Consider the AWGN cooperative multiple-access channel model depicted in Fig. 4.1. Due to the duplexing or coding complexity requirements, the channel degrees of freedom (time / bandwidth) must be shared and assigned. Without loss of generality hereafter we consider a fixed total bandwidth and we assign the transmission time degree of freedom. Thus, the communication may be divided into orthogonal transmission intervals. This division is indicated with the index $j \in \{1, \dots, M\}$, where M is the total number of orthogonal transmissions. The received signals, during interval j , at each source Y_{1j}, Y_{2j} and at the destination Y_{0j} are:

$$\begin{aligned} Y_{1j} &= \sqrt{\alpha_{21}}X_{2j} + Z_{1j}, \\ Y_{2j} &= \sqrt{\alpha_{12}}X_{1j} + Z_{2j}, \\ Y_{0j} &= \sqrt{\beta_1}X_{1j} + \sqrt{\beta_2}X_{2j} + Z_{0j}. \end{aligned} \quad (4.1)$$

We assume, without claim of optimality, that the signals transmitted by each source X_{1j}, X_{2j} are Gaussian distributed with zero mean and power P_{1j}, P_{2j} , respectively. The noise process at the sources Z_{1j}, Z_{2j} and at the destination Z_{0j} are independent white Gaussian, each with zero mean and variance $E[|Z_{ij}|^2] = N_0 = 1$ for all i and j . The channel gains between sources are denoted by α_{12}, α_{21} , and from each source to destination by β_1, β_2 . Each orthogonal transmission uses a fraction $\tau_j T$ out of the total transmission period T , with $\sum_{j \in \{1, M\}} \tau_j = 1$. The power allocated to user $l \in \{1, 2\}$ during the interval j is denoted as $E_{lj} = \tau_j P_{lj}$ (if there is no channel division, then index j is dropped). Notice that E_{lj} is still power, (not energy) since τ_j is a time-sharing factor. As outlined previously, in each orthogonal transmission interval users may divide its power to jointly (i.e. superposition) transmit several messages within independent signals. We use letter upper-indices to designate the power assigned to each signal contribution. In Fig. 4.2, an example of the power allocation is depicted. User 2, working in HD mode, cooperates in the second transmission interval with user 1 by jointly encoding via superposition its own new (N) data with a Gaussian signal of power P_{22}^N and the cooperative (C) data with a Gaussian signal of power P_{22}^C , with $P_{22} = P_{22}^N + P_{22}^C$.

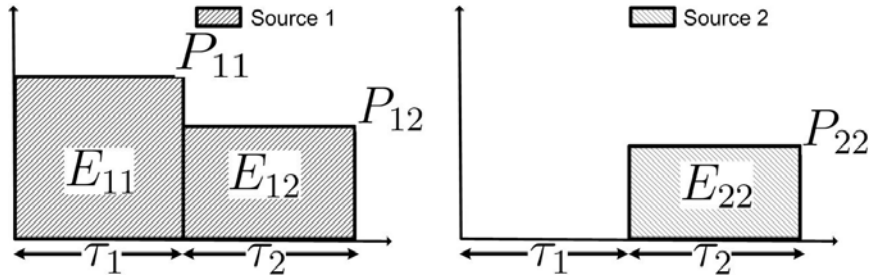


Figure 4.2: Power allocation among sources. User 2 cooperates with user 1 in HD mode.

4.3 The Energy Efficiency Analysis

The low power analysis developed in [1] and introduced in Chapter 2 is here briefly reviewed and then particularized to address the energy efficient regime for the CMAC.

When studying the energy efficiency of a communication system, we aim at determining the spectral efficiency $C\left(\frac{E_b}{N_0}\right)$ (bits per second per hertz) as a function of the transmitted energy per information bit relative to the noise spectral level $\frac{E_b}{N_0}$. In the energy efficient regime, there are two metrics of special interest [1]: the minimum energy per bit $\frac{E_b}{N_{0\min}}$ or, equivalently, maximum rate per energy and the slope of the spectral efficiency. If the spectral efficiency $C(\text{SNR})^1$ bit/s/Hz is a monotonically increasing concave function in the signal to noise ratio (SNR), the minimum values of energy per bit are obtained in the low SNR regime as

$$\frac{E_b}{N_{0\min}} = \lim_{\text{SNR} \rightarrow 0} \frac{\text{SNR}}{C(\text{SNR})}, = \frac{\log_e 2}{\dot{C}(0)} \quad (4.2)$$

where $\dot{C}(0)$ is the derivative at 0 of $C(\text{SNR})$ but computed in nats. Note that, the $\frac{E_b}{N_{0\min}}$ is obtained in the limit of infinite bandwidth or zero power $\text{SNR} \rightarrow 0$, and therefore imply zero spectral efficiency $C(0) = 0$. Thus, the computation of $\frac{E_b}{N_{0\min}}$ gives no indication about the *bandwidth-power* tradeoff in the channel. The key performance measure then is the slope S of the spectral efficiency vs $\frac{E_b}{N_0}$ curve (bit/s/Hz/3 dB) at $\frac{E_b}{N_{0\min}}$ expressed in [1] as

$$S = \frac{2 \left[\dot{C}(0) \right]^2}{-\ddot{C}(0)} \quad (4.3)$$

where $\ddot{C}(0)$ is the second-order derivative at 0 of $C(\text{SNR})$ computed in nats. This metric determines the bandwidth efficiency of the communication system.

In the following, we particularize the low power analysis to the AWGN CMAC

- Unlike the single-user case, we consider two users that cooperatively transmit two data flows. Different definitions for the energy per bit are possible depending on the considered energy cost of the communication and to whom the energy belongs. We consider

¹The choice of C and \mathcal{C} avoids the abuse of notation that assigns the same symbol to the spectral efficiency function of SNR and $\frac{E_b}{N_0}$.

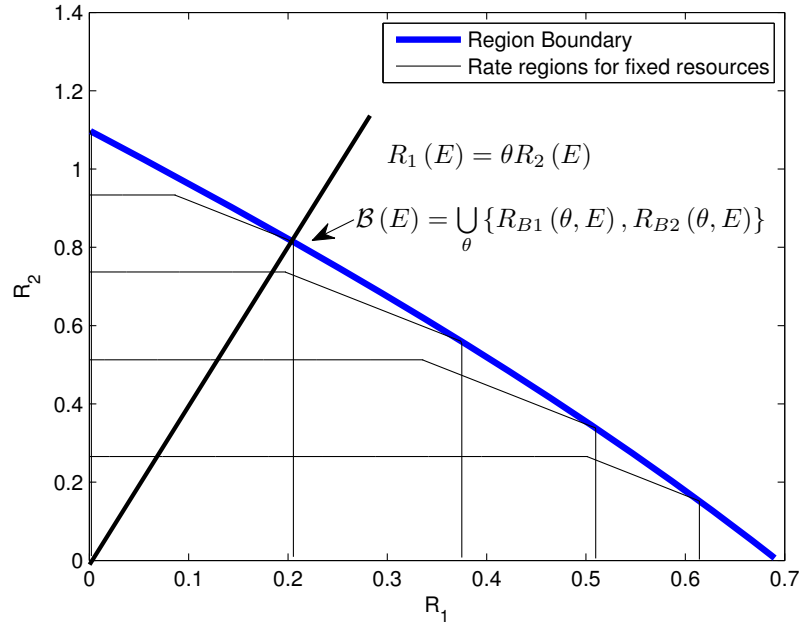


Figure 4.3: Computation of the boundary points of the rate region.

that the energy belongs to the “network” and is optimally allocated among nodes and flows. Then, the network energy per bit of user l is defined as $E_{bl} = \frac{E}{R_l(E)}$, where $E = \sum_{l \in \{1,2\}} \sum_{j \in \{1,M\}} E_{lj}$ and $R_l(E)$ is the spectral efficiency of user l in bits.

- For notation convenience, we replace the $\text{SNR} = \frac{E}{N_0}$ by the total power E . Then, the spectral efficiency expressions $R(E)$ in bits/dimension are expressed as functions of the total power E instead of a function of the SNR, $C(\text{SNR})$. Unless otherwise indicated, all the logarithms are in base 2, i.e., all the rates (also referred to as spectral efficiencies) $R(E)$ are in bits. Nevertheless, the derivatives of the rates with respect to the total power E , $\dot{R}(E)$ and $\ddot{R}(E)$ are computed in nats.
- For the cooperative MAC, instead of the rate R as a function of E , we have a rate region $\mathcal{R}_F(\boldsymbol{\tau}, \mathbf{E})$ which depends on fixed resources $\boldsymbol{\tau} = \{\tau_j\}_{j=1}^M$, $\mathbf{E} = \{\{E_{lj}\}_{l=1}^2\}_{j=1}^M$. Then, the rate region as a function of the total power $\mathcal{R}(E)$ is obtained as the union of rate regions $\mathcal{R}_F(\boldsymbol{\tau}, \mathbf{E})$, over all the possible resource allocation policies

$$\mathcal{R}(E) = \left\{ (R_1, R_2) \in \bigcup_{\boldsymbol{\tau} \in \Xi, \mathbf{E} \in \Sigma} \mathcal{R}_F(\boldsymbol{\tau}, \mathbf{E}), \right. \quad (4.4a)$$

$$\Xi = \left\{ \boldsymbol{\tau} : \tau_j \geq 0 \forall j \in \{1, 2, \dots, M\}, \sum_{j=1}^M \tau_j = 1 \right\}, \quad (4.4b)$$

$$\Sigma = \left\{ \mathbf{E} : E_{lj} \geq 0 \forall l \in \{1, 2\}, \forall j \in \{1, 2, \dots, M\}, \sum_{l \in \{1,2\}} \sum_{j=1}^M E_{lj} = E \right\}. \quad (4.4c)$$

For the energy efficiency analysis, we focus on the boundary points of this region $\mathcal{B}(E) = \bigcup_{\theta} \{R_{B1}(\theta, E), R_{B2}(\theta, E)\}$. These points can be found, as illustrated in Fig. 4.3, by first forcing a fixed relation between the user rates $R_1 = \theta R_2$ and then, optimally allocating the resources to maximize the boundary point. Note that after forcing the ratio between the rates it is equivalent to maximize R_1 , R_2 or even the sum rate R_S .

$$R_S = R_2 + R_1 = \frac{1 + \theta}{\theta} R_1. \quad (4.5)$$

We keep this ratio fixed for all E

$$R_1(E) = \theta R_2(E) \quad (4.6)$$

Then, the set of achievable rate pairs for given total power per user bit is given by

$$\mathcal{R}_{\theta} \left(\frac{E_{b1}}{N_0} \right) = \left\{ R_1 \in \mathbb{R}_+ : \left(R_1, \frac{R_1}{\theta} \right) \in \mathcal{R}(E), \frac{E}{N_0 R_1(E)} = \frac{E_{b1}}{N_0} \right\}. \quad (4.7)$$

where $\frac{E_{b1}}{N_0} = \frac{E}{N_0 R_1(E)}$ is the total network power per user bit normalized by the noise spectral level. Note that, because of the fixed ratio between rates (4.6), it is enough to consider the achievable segments of rates for user 1.

- We define the rate of user l per total power normalized by the noise spectral level as

$$RPE_l \triangleq N_0 \log_e 2 \frac{R(E)}{E}. \quad (4.8)$$

If the energy efficient regime is the low power regime, using (4.2), the maximum RPE_l for user l can be obtained as

$$\eta_l = \max_E RPE_l = \frac{\log_e 2}{\frac{E_{bl}}{N_0 \min}} = \dot{R}_{Bl}(0) \quad (4.9)$$

with $R_{Bl}(E)$ computed in bits and $\dot{R}_{Bl}(0)$ computed in nats.

Note that, due to the fixed relation for all E , we can establish the following relations

$$\eta_2 = \dot{R}_{B2}(0) = \frac{\dot{R}_{B1}(0)}{\theta} = \frac{\eta_1}{\theta}. \quad (4.10)$$

Likewise, the slopes in the boundary points of the region (S_{B1}, S_{B2}) satisfy

$$S_{B2} = -2 \frac{[\dot{R}_{B2}(0)]^2}{\ddot{R}_{B2}(0)} = \frac{S_{B1}}{\theta}. \quad (4.11)$$

The slope region $\mathbf{S}(\theta)$ is, then, the set of slope pairs

$$\mathbf{S}(\theta) = \left\{ (S_1, S_2) \in \mathbb{R}_+^2 : S_l \leq S_{Bl}, S_{B1} = \theta S_{B2}, S_{Bl} = \frac{2 [\dot{R}_{Bl}(0)]^2}{-\ddot{R}_{Bl}(0)}, l \in \{1, 2\} \right\} \quad (4.12)$$

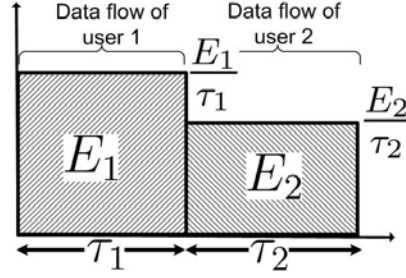


Figure 4.4: Power allocation among flows.

4.4 Cooperative Multiple-Access Channel with FS

Previous to consider more advanced strategies. We investigate the energy efficiency of the direct extension of the RC to the CMAC. The transmission is divided into two orthogonal transmission intervals $f = \{1, 2\}$. At each interval one node acts as a source (node f) and the other as a dedicated relay (node \bar{f}). Thus, the data originated at one user is never jointly encoded (JC) with the cooperative data (data decoded from the transmission of a different user). We label this strategy as flow-separation cooperative multiple-access channel (FS-CMAC). The power allocation among flows is depicted in Figure 4.4. We use τ_f, E_f to denote the fraction of the channel and power dedicated to the data flow (f). Notice that, if we consider also half duplex relaying, then each of these intervals is further divided into two orthogonal intervals.

To study this user cooperation strategy, we reuse all the results obtained in the previous chapter for the RC. Thus, regardless of the duplexing or synchronism capabilities assumed, each flow interval is treated as a black box from which we know, the spectral efficiency as a function of the transmitted power and the low power regime metrics (maximum RPE and slope).

4.4.1 Rate Region

Within each interval we have a dedicated relay channel. Let us denote as $R'_f(E'_f)$ the rate of the dedicated relay channel for user f as a function of the total power dedicated to this data flow E'_f . Given that only a fraction τ_f of the total transmission time is dedicated to each flow f , the spectral efficiency of the relay channel used to transmit data flow f can work at the power level $E'_f = \frac{E_f}{\tau_f}$. By doing so, the average power used for data flow f in the total transmission time satisfies $E_f = \tau_f E'_f + \tau_{\bar{f}} \times 0$. Then, the rate region achievable by FS-CMAC is

$$\mathcal{R}(E) = \left\{ (R_1, R_2) \in \bigcup_{\tau \in \Xi, \mathbf{E} \in \Sigma} R_f \leq \tau_f R'_f(E'_f), E'_f = \frac{E_f}{\tau_f}, f = \{1, 2\}, \right. \quad (4.13a)$$

$$\Xi = \{\tau : \tau_1 + \tau_2 = 1, \tau_1, \tau_2 \geq 0\}, \quad (4.13b)$$

$$\left. \Sigma = \{\mathbf{E} : E_1 + E_2 = E, E_1, E_2 \geq 0\} \right\}. \quad (4.13c)$$

4.4.2 Maximum Rates Per Energy

The FS-CMAC consists of two dedicated RC that share the total power and the communication channel. The maximum RPE for the dedicated RC under duplexity and synchronous constraints is studied in Chapter 3. There, we have shown that DF and the cut-set bound (CB) can be studied together. Here, we make use of those results to obtain the bounds on the maximum RPE pair for the FS-CMAC scenario. The following theorem summarizes the obtained results.

Theorem 4.1 *Suppose that $\frac{R_1}{R_2} = \theta$, the maximum RPE pair (η_{FS}) for the FS-CMAC with DF or the CB can be written in a unified manner as*

$$\eta_{FS}(\theta) = \left\{ (\eta_1, \eta_2) \in \mathbb{R}_+^2 : \eta_1 = \theta\eta_2, \frac{\eta_1}{\hat{\eta}_1} + \frac{\eta_2}{\hat{\eta}_2} = 1 \right\} \quad (4.14)$$

where $\hat{\eta}_f$, $f = \{1, 2\}$ is the individual maximum RPE of node f using node \bar{f} as a dedicated relay. In Chapter 3, we have shown that $\hat{\eta}_f$ is given by

$$\hat{\eta}_f = \frac{\hat{\alpha}_{f\bar{f}}\hat{\beta}}{\hat{\alpha}_{f\bar{f}} + \hat{\beta} - \beta_f} \quad (4.15)$$

with $\hat{\beta} = \beta_1 + \beta_2$ for synchronous and $\hat{\beta} = \max(\beta_1, \beta_2)$ for asynchronous transmissions; and $\hat{\alpha}_{f\bar{f}} = \alpha_{f\bar{f}} + \beta_f$ for the cut-set bound and $\hat{\alpha}_{f\bar{f}} = \max(\alpha_{f\bar{f}}, \beta_f)$ for decode-and-forward. Notice that, the maximum RPE pair does not depend on the duplexity constraint.

Proof: To obtain the maximum RPE pair as defined in (4.9), we need to compute the first-order derivative of the users rates (4.13) at the boundary of the rate region $R_{Bf} = \tau_f R'_f \left(\frac{E_f}{\tau_f} \right)$, with respect to the total power and evaluate them at $E = 0$. These boundary rates are initially not available. Instead, we assume that the power dedicated to each data flow $E_f(E)$ as well as the time-sharing factor $\tau_f(E)$ are differentiable functions of the total power E and define:

- The time-sharing factor dedicated to each flow f and its first-order derivative at $E = 0$ are denoted as $t_f \triangleq \tau_f(0)$ and $\dot{t} \triangleq \dot{\tau}_f(0)$, respectively.
- The power allocated to each flow, the first and the second-order derivatives evaluated at $E = 0$ are denoted as $e_f \triangleq E_f(0)$, $\dot{e}_f \triangleq \dot{E}_f(0)$ and $\ddot{e}_f \triangleq \ddot{E}_f(0)$, respectively.

The maximum RPE for node f is then given by

$$\eta_f = \dot{R}_{Bf}(0), \quad (4.16a)$$

$$= \frac{d}{dE} \tau_f(E) R'_f \left(\frac{E_f(E)}{\tau_f(E)} \right) \Big|_{E=0}, \quad (4.16b)$$

$$= \dot{t}_f R'_f \left(\frac{e_f}{t_f} \right) + \dot{R}'_f \left(\frac{e_f}{t_f} \right) \left(\dot{e}_f - \frac{\dot{t}_f e_f}{t_f} \right), \quad (4.16c)$$

$$= \dot{R}'_f(0) \dot{e}_f, \quad (4.16d)$$

$$= \hat{\eta}_f \dot{e}_f. \quad (4.16e)$$

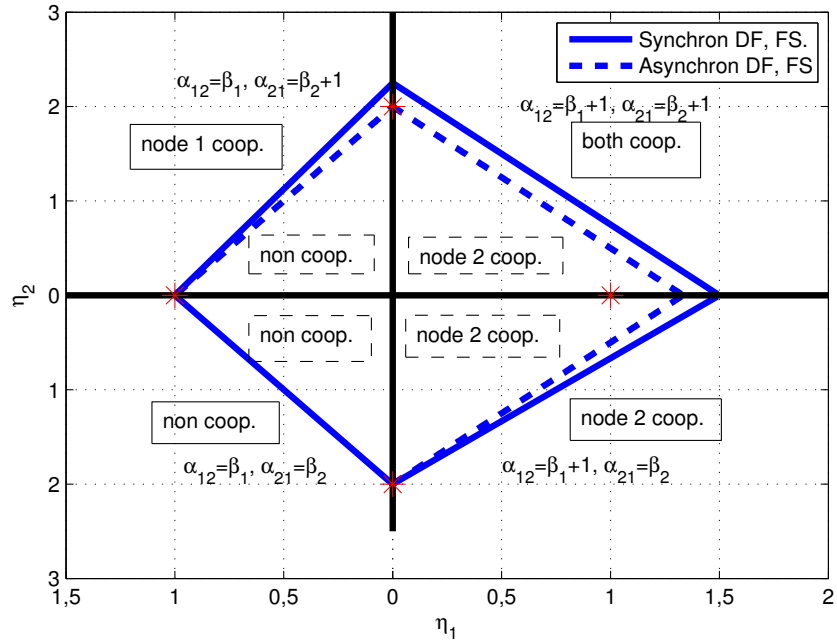


Figure 4.5: Maximum RPE pairs for the FS-CMAC with sync./async. transmissions.

To obtain (4.16d) notice that $e_f = E_f(0) = 0$ and $R'_f(0) = 0$. Equality (4.16e) follows from the definition of the maximum RPE for the dedicated relay channel $\hat{R}'_f(0) \triangleq \hat{\eta}_f$. The maximum RPE region in (4.14) can now be obtained by solving the linear system of equations build with η_f in (4.16e) which only depends on \dot{e}_f , the constraint $\dot{e}_1 + \dot{e}_2 = 1$ imposed by the total power constraint in (4.13c) and the constraint on the ratio of the rates $\eta_1 = \theta\eta_2$. ■

Likewise for the dedicated RC studied in Chapter 3, for the FS-CMAC the maximum RPE pair is not affected by duplexing. Thus, by now, only the synchronism gain can be devised. For the subsequent analysis, it is useful to identify the possible cooperation configurations that appear depending on the relative strength among channels. Each quadrant in Fig. 4.5 shows the maximum RPE pair obtained in a given configuration. The red star (★) indicates the maximum RPE given by direct transmission $\eta_f = \beta_f$. Without loss of generality, we assume $\beta_2 > \beta_1$.

For synchronous nodes there are four possible cooperative configurations (one per quadrant):

- i) both users cooperate, if $(\alpha_{12} > \beta_1 \text{ and } \alpha_{21} > \beta_2)$,
- ii) only the user 2 with “good” channel to destination cooperates, if $(\alpha_{12} > \beta_1 \text{ and } \alpha_{21} \leq \beta_2)$,
- iii) only the user 1 with “bad” channel to destination cooperates, if $(\alpha_{12} \leq \beta_1 \text{ and } \alpha_{21} > \beta_2)$,
- iv) no user cooperates (TDMA), if $(\alpha_{12} \leq \beta_1 \text{ and } \alpha_{21} \leq \beta_2)$.

For asynchronous nodes, there are only two possible scenarios: *i*) user 2 cooperates, if $(\alpha_{12} > \beta_1)$ or *ii*) no user cooperates, if $(\alpha_{12} \leq \beta_1)$.

4.4.3 Slope Region of Spectral Efficiencies

The study of the maximum RPE pair has not revealed the potential gain of incorporating FD capabilities at the terminals. The same maximum RPE pair is obtained with HD nodes. Moreover, obtaining the maximum RPE pair is possible even without optimizing the fraction of the channel dedicated to each data flow τ_f and just considering a linear dependence of the power allocation with respect to the total power ($E_f = \dot{e}_f E$). Thus, we turn our attention to the analysis of the slope region. This metric allows us to compare transmission schemes with equal maximum RPE pair. The next theorem summarizes the obtained results.

Theorem 4.2 *Let the rates vanish while keeping the relation $R_1 = \theta R_2$ constant. The slope region for the FS-CMAC can be written in a unified manner for DF and the CB as*

$$\mathbf{S}_{FS}(\theta) = \left\{ (S_1, S_2) \in \mathbb{R}_+^2 : S_1 \leq S_{B1}, S_2 \leq S_{B2}, S_{B1} = \theta S_{B2}, \right. \\ \left. \frac{2\hat{\beta}\theta}{\hat{\eta}_1} \frac{1}{S_{B1}} + \frac{2\hat{\beta}}{\hat{\eta}_2\theta} \frac{1}{S_{B2}} = (\Psi_1 + \Psi_2)^2 \right\} \quad (4.17)$$

with

$$(\Psi_1)^2 = \frac{2\hat{\beta}\theta}{\hat{S}_1\hat{\eta}_1}, \quad (\Psi_2)^2 = \frac{2\hat{\beta}}{\theta\hat{S}_2\hat{\eta}_2} \quad (4.18)$$

where $\hat{\eta}_f$ and \hat{S}_f are, respectively, the individual maximum RPE and the slope obtained by user f using \bar{f} as a dedicated relay. The individual maximum RPE is given in (4.15), the slope was found in Chapter 3 to be: for a FD relay $\hat{S}_f = 2$ and for a HD relay

$$\frac{\hat{S}_f\hat{\eta}_f}{2\hat{\beta}} = \left(\sqrt{\frac{\hat{\beta}}{\hat{\eta}_f} - 1 + \left(\frac{\beta_f}{\hat{\alpha}_{f\bar{f}}}\right)^2} + \sqrt{\left(1 - \frac{\beta_f}{\hat{\alpha}_{f\bar{f}}}\right)^2} \right)^{-2} \quad (4.19)$$

with $\hat{\beta}$ and $\hat{\alpha}_{f\bar{f}}$ as defined in Theorem 4.1.

If the power allocated to each flow is restricted to be linear in E but the time-sharing factors τ_1 and τ_2 are optimally assigned, the slope is

$$\mathbf{S}_{FS_e}(\theta) = \left\{ (S_1, S_2) \in \mathbb{R}_+^2 : S_1 \leq S_{B1}, S_2 \leq S_{B2}, S_{B1} = \theta S_{B2}, \frac{S_{B1}}{\hat{S}_1} + \frac{S_{B2}}{\hat{S}_2} = 1 \right\}. \quad (4.20)$$

Instead, if the time-sharing factors are fixed $\tau_1 = \tau_2 = \frac{1}{2}$ but the power is optimally allocated, then

$$\mathbf{S}_{FS_\tau}(\theta) = \left\{ (S_1, S_2) \in \mathbb{R}_+^2 : S_1 \leq S_{B1}, S_2 \leq S_{B2}, S_{B1} = \theta S_{B2}, \right. \\ \left. \frac{\theta}{\hat{\eta}_1} \frac{1}{S_{B1}} + \frac{1}{\hat{\eta}_2\theta} \frac{1}{S_{B2}} = \frac{2\theta}{\hat{\eta}_1\hat{S}_1} + \frac{2}{\theta\hat{\eta}_2\hat{S}_2} \right\}. \quad (4.21)$$

Note that, in all these cases, the maximum RPE pair is unchanged.

Proof: We need to compute the first and second-order derivatives of the user rates at the boundary of the rate region $S_{Bf} \triangleq \frac{2(\dot{R}_{Bf}(0))^2}{-\ddot{R}_{Bf}(0)}$. The first-order derivative is by definition $\dot{R}_{Bf}(0) \triangleq \eta_f$, already computed in the proof of Theorem 4.1. Using the notation there introduced, the second-order derivative can be shown to be

$$\ddot{R}_{Bf}(0) = \ddot{R}'_f(0) \frac{(\dot{e}_f)^2}{t_f} + \dot{R}'_f(0) \ddot{e}_f, \quad (4.22a)$$

$$= \frac{2(\eta_f)^2}{-\hat{S}_f} \frac{1}{t_f} + \hat{\eta}_f \ddot{e}_f. \quad (4.22b)$$

To obtain (4.22b), we have used the fact that $\dot{e}_f = \frac{\eta_f}{\hat{\eta}_f}$, see (4.16e). Likewise, from the dedicated RC we know that $\dot{R}'_f(0) = \hat{\eta}_f$ and $\ddot{R}'_f(0) = \frac{2(\hat{\eta}_f)^2}{-\hat{S}_f}$. Substituting (4.22b) into the slope definition for each user, we obtain

$$\frac{2(\eta_1)^2}{S_{B1}} = \frac{2(\eta_1)^2}{\hat{S}_1} \frac{1}{t_1} - \hat{\eta}_1 \ddot{e}_1, \quad (4.23a)$$

$$\frac{2(\eta_2)^2}{S_{B2}} = \frac{2(\eta_2)^2}{\hat{S}_2} \frac{1}{t_2} - \hat{\eta}_2 \ddot{e}_2. \quad (4.23b)$$

These equalities only depend on t_f and \ddot{e}_f . From the resource constraints in (4.13), we can obtain the following constraints on t_f and \ddot{e}_f

$$t_1 + t_2 = 1, \quad t_1, t_2 \geq 0 \quad (4.24a)$$

$$\ddot{e}_1 + \ddot{e}_2 = 0, \quad (4.24b)$$

$$\ddot{e}_f > 0 \text{ if } \dot{e}_f^* = 0 \text{ } f \in \{1, 2\}. \quad (4.24c)$$

The constraints in (4.24a) are those in (4.13b) evaluate at $E = 0$. The constraints (4.24b) and (4.24c) are due to the sum and positive power constraints in (4.13c). Note that, if $\dot{e}_f^* = 0$ then, the positive energy constraint imposes $\ddot{e}_f \geq 0$. Additionally, in the boundary of the rate region, due to the fixed ratio between rates we have $S_{B1} = \theta S_{B2}$, see (4.11).

Before maximizing the slopes in (4.23) subject to (4.24), let us consider two interesting special cases:

1. Consider the power allocation functions $E_f(E)$ to be linear in the total power E , namely $E_1(E) = \dot{e}_2 E$. Then, $\ddot{e}_1 = \ddot{e}_2 = 0$ and the slope boundary is given by insulating t_1, t_2 from (4.23) and forcing (4.24a), then

$$\frac{S_{B1}}{\hat{S}_1} + \frac{S_{B2}}{\hat{S}_2} = 1 \quad (4.25)$$

and the slope region is that in (4.20).

2. Consider the time-sharing factors dedicated to each data flow to be fixed e.g., $\tau_f(E) = t_f = \frac{1}{2}$. Then, the slope in the boundary of the region is obtained by isolating \ddot{e}_f from equations (4.23) and forcing (4.24b). By doing so, we obtain

$$\frac{\theta}{\hat{\eta}_1} \frac{1}{S_{B1}} + \frac{1}{\hat{\eta}_2 \theta} \frac{1}{S_{B2}} = \frac{2\theta}{\hat{\eta}_1 \hat{S}_1} + \frac{2}{\theta \hat{\eta}_2 \hat{S}_2} \quad (4.26)$$

and the slope region is that in (4.21).

Finally, let us consider the general problem. First, by substituting the total power constraint $\ddot{e}_2 = -\ddot{e}_1$ into (4.23b) and solving \ddot{e}_1 we can found the following condition on the slope region as a function of t_f

$$\frac{2\hat{\beta}\theta}{\hat{\eta}_1} \frac{1}{S_{B1}} + \frac{2\hat{\beta}}{\hat{\eta}_2 \theta} \frac{1}{S_{B2}} = \frac{(\Psi_1)^2}{t_1} + \frac{(\Psi_2)^2}{t_2} \quad (4.27)$$

with $(\Psi_1)^2 = \frac{2\hat{\beta}\theta}{\hat{\eta}_1 \hat{S}_1}$ and $(\Psi_2)^2 = \frac{2\hat{\beta}}{\theta \hat{\eta}_2 \hat{S}_2}$.

Since $S_{B1} = \theta S_{B2}$, the boundary of the slope region is obtained by minimizing the right hand side part of equation (4.27). Forcing $t_1 + t_2 = 1$ and minimizing over t_1 we found

$$\frac{1}{t_1} = 1 + \frac{\Psi_2}{\Psi_1}. \quad (4.28)$$

By substituting, (4.28) into (4.27) we get the slope region presented in Theorem 4.2. ■

In Theorem 4.2, we have also found the slope region: *i*) if the channel fraction remains fixed (4.20) and *ii*) if the power allocated to each data flow is restricted to be a linear function on E (4.21). For the later, the next remark points out the equivalence with an existent result.

Remark 4.1 *Let us consider the scenario where no node cooperates $\hat{S}_1 = \hat{S}_2 = 2$. Considering $\beta_1 > \beta_2$ the slope region in (4.20) can be rewritten as*

$$\left\{ (S_1, S_2) : 0 \leq S_1 \leq \frac{2\theta}{1+\theta}, 0 \leq S_2 \leq \frac{2}{1+\theta} \right\}. \quad (4.29)$$

This region is exactly the non-cooperative broadcast slope region found in [42, eq. (79)] for time-division transmissions. The broadcast channel (BC) is directly comparable to our MAC scenario since we consider a total power constraint and thus, the rate regions are dual [16]. Removing the linear assumption on the power allocation we have shown in Theorem 4.2 that the slope region is enhanced.

The required bandwidth for a system to achieve rate R with power E is [1]

$$B = \frac{R}{S} \frac{3\text{dB}}{\frac{E}{N_0 R} |_{\text{dB}} - \frac{E_b}{N_0 \min} |_{\text{dB}}}. \quad (4.30)$$

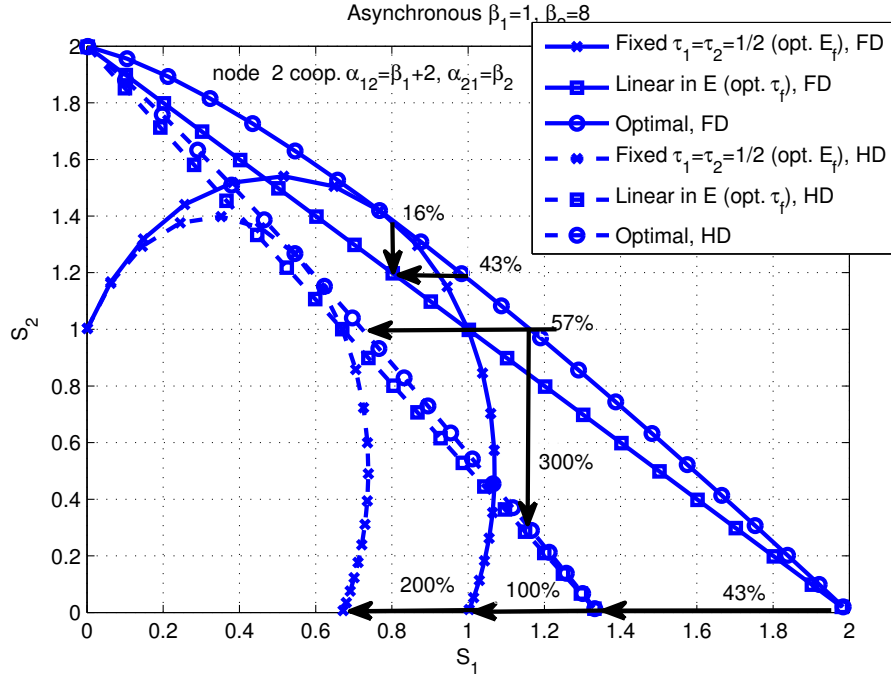


Figure 4.6: Slope regions in the FS-CMAC with asynchronous transmissions.

Figure 4.6 compares, for the cooperative scenario where only user 2 cooperates and transmissions are asynchronous, the slope regions obtained with HD and FD nodes under the discussed resource allocation strategies: *i*) the channel fraction is assumed constant (4.21), *ii*) the power allocation among data flows is restricted to be linear (4.20), and *iii*) the optimal slope region (4.17). All possible configurations obtain the same maximum RPE pair and thus, are comparable in terms of the slope region. Note that the FD capabilities and the optimization of the channel fraction dedicated to each data flow are mandatory requirements to obtain the maximum slope borders of the region $\theta \in \{0, \infty\}$ (where the cooperative node acts as a dedicated relay). At $\theta = \infty$, in the example of Fig. 4.6, we observe that user 1 working in HD mode needs up to

$$\frac{B_{HD1} - B_{FD1}}{B_{FD1}} \times 100 = \left(\frac{S_{FD1}}{S_{HD1}} - 1 \right) \times 100 = 43\% \quad (4.31)$$

more of the minimum bandwidth required with FD nodes. Moreover, fixing the channel fraction intervals to $\tau_1 = \tau_2 = \frac{1}{2}$ requires 100% more of the minimum bandwidth for FD nodes and 200% for HD nodes. As we go close to the middle point of the region, HD users require 57% (user 1) and 300% (user 2) more of the minimum bandwidth required with FD nodes. At this point, the linear energy allocation with optimal time-sharing factors has the worst bandwidth efficiency. If users work in FD mode then the linear energy allocation solution needs up to 43% (user 1) and 16% (user 2) more of the minimum bandwidth required with the optimal power allocation.

Table 4.2: BMC scheme for the FD relay channel.

FD	Block 1	Block 2	Block 3	Block 4
Source	$\mathcal{X}^R(\omega[1])$	$\mathcal{X}^R(\omega[2])$	$\mathcal{X}^R(\omega[3])$	$\mathcal{X}^R(1)$
Relay	$\mathcal{X}^C(1)$	$\mathcal{X}^C(\omega[1])$	$\mathcal{X}^C(\omega[2])$	$\mathcal{X}^C(\omega[3])$

Table 4.3: Coding scheme for the HD relay channel.

HD	Interval 1	Interval 2
Source	$\mathcal{X}^R(\omega_1^R)$	$\mathcal{X}^D(\omega_1^D)$
Relay	\emptyset	$\mathcal{X}^C(\omega_1^R)$

4.5 Rate Regions for the CMAC with Joint Coding

In the FS-CMAC scenario, the own and the decoded data are never transmitted simultaneously. In this section, we investigate the gain of jointly encoding this information. Joint encoding can be done, among others, using *superposition* or *multiplexing* coding, see [30, 69] for a detailed comparison in the CMAC. There it was shown that multiplexed codes improve superposition cooperation if there is no CSI at the transmitters. Then, the power allocation among the superposed message can not be adjusted, this is overcome by the multiplexed codes, since the transmitter encodes the two messages using a single codebook $\mathcal{X}(\omega_1, \omega_2)$. We consider the Gaussian CMAC with sum power constraint and CSI at transmitter side. In this case, both coding strategies achieve the same rate region and we focus on superposition coding.

In this section, after discussing the coding complexity for the flow-separation strategy, we first describe the rate region obtained with joint coding and FD or HD nodes. As expected, the joint coding and simultaneous transmissions gains are at the cost of high decoding complexity. Then, we propose a time-division (TD) strategy for which users jointly encode the own and the decoded messages but never transit simultaneously asynchronous signals.

4.5.1 Coding for the Flow-Separation Strategy

In the previous section, we have shown that due to FD operation at nodes, both users can transmit simultaneously during the whole communication. This significantly increases the spectral efficiency gains. However, besides of the practical difficulty of working in FD mode, FD relaying also increases the coding complexity, on which we are interested in this section. The coding complexity for the FS-CMAC is that of the dedicated relay channel:

- For the FD relay channel, the source divides the message into B blocks $\omega[1], \dots, \omega[B]$, and encodes each block separately [28] (block Markov coding). For asynchronous transmissions, the coding strategy is illustrated in Table 4.2. The source and the relay use

Table 4.4: BMC construction for the CMAC with JC and FD nodes.

	Block b
User 1	$\mathcal{X}_1^D(\omega_1^D[b]) + \mathcal{X}_1^R(\omega_1[b]) + \sqrt{\frac{P_1^S}{P_2^C}} \mathcal{X}_2^C(\omega_1[b-1]) + \mathcal{X}_1^C(\omega_2[b-1])$
User 2	$\mathcal{X}_2^D(\omega_2^D[b]) + \mathcal{X}_2^R(\omega_2[b]) + \mathcal{X}_2^C(\omega_1[b-1]) + \sqrt{\frac{P_2^S}{P_1^C}} \mathcal{X}_1^C(\omega_2[b-1])$

different codebooks: $\mathcal{X}^R(\cdot)$, $\mathcal{X}^C(\cdot)$. The destination decodes using several or all of its available output blocks.

- For HD nodes and asynchronous transmissions, the coding scheme proposed in [20] is illustrated in Table 4.3. The transmission is divided into two intervals. During the first interval, the source transmits alone the data to be relayed ω_1^R using the codebook $\mathcal{X}^R(\cdot)$. During the second interval, the relay cooperates by transmitting ω_1^R using an independent codebook $\mathcal{X}^C(\cdot)$. Simultaneously, the source transmits a message ω_1^D directly to the destination. In this case, block Markov transmissions are not needed and the decoding at the destination can be done using only these two output intervals. In the low power regime, the decoding complexity is further reduced. As we see in Chapter 3, the maximum RPE and slope are obtained without transmitting ω_1^D .

We consider that the synchronism gain does not impact on the decoding complexity. For the FD relay channel, to obtain synchronism gains, the source jointly encodes (i.e. superposition) the previous block message using the relay codebook as $\mathcal{X}(\omega[b], \omega[b-1]) = \mathcal{X}^R(\omega[b]) + \mathcal{X}^C(\omega[b-1])$. For a HD relay, in the second interval, the source transmits $\mathcal{X}(\omega_1^D, \omega_1^R) = \mathcal{X}^D(\omega_1^D) + \mathcal{X}^C(\omega_1^R)$. In both cases, the codeword $\mathcal{X}^C(\cdot)$ is transmitted from both nodes and arrives coherently added in amplitude at the receiver antenna, not requiring additional complexity to the decoder.

4.5.2 Joint Coding with Full Duplex Operation

The rate region for the *decode-and-forward* CMAC with FD nodes and receiver CSI was obtained in [56]. A more recent description based on [70] can be found in [2]. Authors used superposition block-Markov coding and backward decoding. Here, we first introduce this communication strategy and then, enhance the rate region by considering also transmitter CSI.

Each user $l = \{1, 2\}$ divides its message ω_l into two parts: a message ω_l^D of rate R_l^D sent directly to the destination and a message ω_l^R of rate R_l^R decoded first at the cooperative node. There are 3 Gaussian codebooks per user terminal: $\mathcal{X}_l^D(\cdot)$, $\mathcal{X}_l^R(\cdot)$ and $\mathcal{X}_l^C(\cdot)$. Following the BMC transmission scheme, the message is divided into B blocks, $\omega_l = (\omega_l[1], \dots, \omega_l[B])$. At each block b , the codebook is constructed via superposition coding as depicted in Table 4.4. User l transmits the messages $\omega_l^D[b]$ and $\omega_l^R[b]$ using, respectively, the codebooks $\mathcal{X}_l^D(\cdot)$ and

$\mathcal{X}_l^R(\cdot)$ with power P_l^D and P_l^R . Additionally, at the end of the previous block $b - 1$, each node l has decoded from the other user \bar{l} , the cooperative information $\omega_{\bar{l}}^R[b - 1]$ and transmits it, in block b , with the cooperative codebook $\mathcal{X}_l^C(\cdot)$ at power P_l^C . Using the same codebook but with power P_l^S , user \bar{l} retransmits its own message $\omega_{\bar{l}}^R[b - 1]$ to obtain synchronism gains. The total power dedicated by user l in block b to transmit the new information is denoted as $P_l^N = P_l^D + P_l^R$ and to retransmit the previous block information as $P_l^{CS} = P_l^C + P_l^S$.

If transmissions are synchronous, the achievable rate is the closure of the convex hull of all rate pairs (R_1, R_2) such that $R_1 = R_1^D + R_1^R$ and $R_2 = R_2^D + R_2^R$ with

$$R_1^R \leq \log \left(1 + \frac{\alpha_{12} P_1^R}{1 + \alpha_{12} P_1^D} \right), \quad (4.32a)$$

$$R_2^R \leq \log \left(1 + \frac{\alpha_{21} P_2^R}{1 + \alpha_{21} P_2^D} \right), \quad (4.32b)$$

$$R_1^D \leq \log (1 + \beta_1 P_1^D), \quad (4.32c)$$

$$R_2^D \leq \log (1 + \beta_2 P_2^D), \quad (4.32d)$$

$$R_1^D + R_2^D \leq \log (1 + \beta_1 P_1^D + \beta_2 P_2^D), \quad (4.32e)$$

$$R_1 + R_2 \leq \log \left(1 + \beta_1 P_1^N + \beta_2 P_2^N + \left(\sqrt{\beta_1 P_1^{CS}} + \sqrt{\beta_2 P_2^{CS}} \right)^2 \right). \quad (4.32f)$$

If transmissions are asynchronous, then $P_1^S = P_2^S = 0$. Each user l dedicates all the cooperative power P_l^{CS} to transmit the partner's message $\mathcal{X}_l^C(\omega_{\bar{l}}^R[b - 1])$. The cooperative signals are not added coherently at the destination and the sum rate condition (4.32f) is replaced by

$$R_1 + R_2 \leq \log (1 + \beta_1 (P_1^N + P_1^{CS}) + \beta_2 (P_2^N + P_2^{CS})). \quad (4.33)$$

The rate region in (4.32) can be enhanced if CSI is also available at the user terminals and the power resources are optimally allocated. In particular, in the following theorem we optimally allocate P_l^D, P_l^R to satisfy $P_l^N = P_l^D + P_l^R$ and P_l^{CS} to satisfy $P_1^{CS} + P_2^{CS} = P^C$.

Theorem 4.3 *For the decode-and-forward CMAC with FD nodes and transmitter CSI, if transmissions are synchronous, then*

- For $\alpha_{12} \leq \beta_1$ or $\alpha_{21} \leq \beta_2$, at most one node cooperates by fully decoding the partner's message. Denoting $\hat{\alpha}_{\bar{l}} = \max(\beta_l, \alpha_{\bar{l}})$ and $\hat{\beta} = \beta_1 + \beta_2$, the rate region can be written as

$$R_1 \leq \log (1 + \hat{\alpha}_{12} P_1^N), \quad (4.34a)$$

$$R_2 \leq \log (1 + \hat{\alpha}_{21} P_2^N), \quad (4.34b)$$

$$R_1 + R_2 \leq \log (1 + \beta_1 P_1^N + \beta_2 P_2^N + \hat{\beta} P^C). \quad (4.34c)$$

Table 4.5: Cooperative configurations for the CMAC with JC and FD terminals.

$\beta_2 > \beta_1$	Cooperative Configuration	
	Asynchronous	Synchronous
$\alpha_{12} \leq \beta_1$ and $\alpha_{21} \leq \beta_2$	No user coop.	
$\alpha_{12} \leq \beta_1$ and $\alpha_{21} \geq \beta_2$	No user coop.	User 1 coop. full DF
$\alpha_{12} \geq \beta_1$ and $\alpha_{21} \leq \beta_2$	User 2 coop. full DF	
$\alpha_{12} \geq \beta_1$ and $\alpha_{21} \geq \beta_2$	User 2 coop. full DF	Both users coop.

- For $\alpha_{12} \geq \beta_1$ and $\alpha_{21} \geq \beta_2$, optimizing only the cooperative powers P_1^{CS}, P_2^{CS} and rewriting the rate region in (4.32) as a union of rectangles we obtain

$$\bigcup_{0 \leq x \leq 1} \left\{ \begin{aligned} R_1 &\leq \log \left(1 + \frac{\alpha_{12} P_1^R}{1 + \alpha_{12} P_1^D} \right) \\ &+ x \log (1 + \beta_1 P_1^D) + (1 - x) \log \left(1 + \frac{\beta_1 P_1^D}{1 + \beta_2 P_2^D} \right), \\ R_2 &\leq \log \left(1 + \frac{\alpha_{21} P_2^R}{1 + \alpha_{21} P_2^D} \right) \\ &+ (1 - x) \log (1 + \beta_2 P_2^D) + x \log \left(1 + \frac{\beta_2 P_2^D}{1 + \beta_1 P_1^D} \right) \end{aligned} \right\}, \quad (4.35a)$$

$$R_1 + R_2 \leq \log \left(1 + \beta_1 P_1^N + \beta_2 P_2^N + \hat{\beta} P^C \right). \quad (4.35b)$$

If transmissions are asynchronous, only the node with better channel can cooperate by fully decoding the partner's message. The rate region is given by (4.34) with $\hat{\beta} = \max(\beta_2, \beta_1)$.

A summary of all the possible cooperative configurations is given in Table 4.5.

Proof: Let us first maximize the sum rate constraints (4.32f) and (4.33) by allocating P_1^{CS} and P_2^{CS} to satisfy $P_1^{CS} + P_2^{CS} = P^C$. The rest of rate constrains are not affected by this power allocation. If transmissions are synchronous, the coherent term $T_c = \left(\sqrt{\beta_1 P_1^{CS}} + \sqrt{\beta_2 P_2^{CS}} \right)^2$ is maximized by choosing

$$P_1^{CS} = \frac{\beta_1}{\beta_1 + \beta_2} P^C, \quad P_2^{CS} = \frac{\beta_2}{\beta_1 + \beta_2} P^C. \quad (4.36)$$

Then, $T_c = (\beta_1 + \beta_2) P^C$. If transmissions are asynchronous, the sum rate constraint is maximized by allocating the total power P^C to the user with better channel to destination, then $T_c = \max(\beta_1, \beta_2) P^C$. Note that if $\beta_2 > \beta_1$, then $P_1^C = 0$, $P_2^C = P^C$ and the user 1 never cooperates. Finally, the sum rate constraint can be compactly written using $\hat{\beta} = \beta_1 + \beta_2$ for synchronous and $\hat{\beta} = \max(\beta_1, \beta_2)$ for asynchronous transmissions as

$$R_1 + R_2 \leq \log \left(1 + \beta_1 P_1^N + \beta_2 P_2^N + \hat{\beta} P^C \right). \quad (4.37)$$

Let us now enhance the individual rate constraints on R_1, R_2 by allocating the powers P_l^D, P_l^R with $P_l^N = P_l^D + P_l^R$. Note that the sum rate constraints (4.32f) or (4.33) are not affected by this resource allocation. Adding together (4.32a) with (4.32c) and (4.32b) with (4.32d) we can found that the conditions on the individual rates $R_l = R_l^R + R_l^D, l \in \{1, 2\}$ are

$$R_l \leq \log \left(1 + \beta_1 P_1^D + \frac{1 + \beta_1 P_1^D}{1 + \alpha_{12} P_1^D} \alpha_{12} P_1^R \right). \quad (4.38)$$

These conditions are maximized at

$$(P_l^D, P_l^R) = \begin{cases} (P_l^N, 0) & \text{if } \beta_l > \alpha_{l\bar{l}}, \\ (0, P_l^N) & \text{if } \beta_l \leq \alpha_{l\bar{l}}. \end{cases} \quad (4.39)$$

If $\alpha_{12} \leq \beta_1$ or $\alpha_{21} \leq \beta_2$, substituting (4.39) into the rate constraints in (4.32), the constraint (4.32e) is automatically satisfied and using $\hat{\alpha}_{l\bar{l}} = \max(\beta_l, \alpha_{l\bar{l}})$ the individual rate constraints read

$$R_l \leq \log(1 + \hat{\alpha}_{l\bar{l}} P_l^N). \quad (4.40)$$

If $\alpha_{12} \geq \beta_1$ and $\alpha_{21} \geq \beta_2$, the power allocation in (4.39) is not valid since the constraint (4.32e) is not always satisfied. In that case, we rewrite the constraints on the direct rates (4.32c), (4.32d) and (4.32e) as a union of rectangles as

$$\bigcup_{0 \leq x \leq 1} \left\{ R_1^D \leq x \log(1 + \beta_1 P_1^D) + (1 - x) \log \left(1 + \frac{\beta_1 P_1^D}{1 + \beta_2 P_2^D} \right), \right. \quad (4.41a)$$

$$\left. R_2^D \leq (1 - x) \log(1 + \beta_2 P_2^D) + x \log \left(1 + \frac{\beta_2 P_2^D}{1 + \beta_1 P_1^D} \right) \right\}. \quad (4.41b)$$

Then, the region can be written as that in Theorem 4.3. ■

4.5.3 Joint Coding with Half Duplex Operation

The half duplex constraint is only relevant if the user cooperates and needs to be silent while listening to the partner's transmission. Depending on the cooperative scenario, we design two different communication strategies: *i*) only one user cooperates or *ii*) both users cooperate.

One User Cooperates

The communication strategy described here is built upon the one for the HD relay channel presented in [20] and summarized in Table 4.3, but considering that, the relay superposes its own message to the relayed message. Let us consider that only user 2 cooperates. The transmission protocol is summarized in Table 4.6. The total transmission period is divided into two intervals fractions τ_1 and τ_2 . The non-cooperative user (user 1) divides its message ω_1 into two parts: a

Table 4.6: Transmission strategy for the CMAC with JC and HD users if only user 2 cooperates.

	Interval 1	Interval 2
User 1	$\mathcal{X}_1^R(\omega_1^R)$	$\mathcal{X}_1^D(\omega_1^D) + \sqrt{\frac{P_1^S}{P_2^C}} \mathcal{X}_2^C(\omega_1^R)$
User 2	\emptyset	$\mathcal{X}_2^D(\omega_2) + \mathcal{X}_2^C(\omega_1^R)$

message ω_1^D of rate R_1^D sent, directly, to the destination and a message ω_1^R of rate R_1^R decoded first at the cooperative node. The message from the cooperative user ω_2 is sent directly to the destination at rate R_2 . There are 4 independent Gaussian codebooks: $\mathcal{X}_1^R(\cdot)$, $\mathcal{X}_1^D(\cdot)$, $\mathcal{X}_2^D(\cdot)$ and $\mathcal{X}_2^C(\cdot)$. During the first interval, the non-cooperative user (node 1) transmits the data to be relayed ω_1^R with the codebook $\mathcal{X}_1^R(\cdot)$ at power P_1^R . In the second interval, the cooperative user (user 2) uses superposition coding to transmit directly to the destination, its own data ω_2 with the codebook $\mathcal{X}_2^D(\cdot)$ at power P_2^D and the cooperative data ω_1^R within $\mathcal{X}_2^C(\cdot)$ at power P_2^C . User 1 uses its remaining power to transmit, simultaneously, a synchronous signal (by retransmitting ω_1^R) with the cooperative codebook $\mathcal{X}_2^C(\cdot)$ at power P_1^S and a new message direct to the destination ω_1^D within $\mathcal{X}_1^D(\cdot)$ at power P_1^D . For asynchronous transmissions assume $P_1^S = 0$.

From the point of view of user 1, the CMAC is a dedicated relay channel with the additional Gaussian noise $\mathcal{X}_2^D(\omega_2^D)$. Given that we are only interested in the energy efficient regime it is useful to outline the obtained results for the dedicated relay channel in Chapter 3. There we showed that, the maximum RPE and the maximum slope are obtained without transmitting ω_1^D in the second interval. Consequently, hereafter, we assume full decoding $R_1 = R_1^R$ and $P_1^D = 0$.

Optimally allocating P_2^C and P_1^S with $P^C = P_2^C + P_1^S$, the rate region is given in the following theorem.

Theorem 4.4 *For the decode-and-forward CMAC with HD nodes and transmitter CSI, if only node 2 cooperates, the following rate region is achievable*

$$R_1 \leq \tau_1 \log(1 + \alpha_{12} P_1^R), \quad (4.42a)$$

$$R_1 \leq \tau_1 \log(1 + \beta_1 P_1^R) + \tau_2 \log(1 + \hat{\beta} P^C), \quad (4.42b)$$

$$R_2 \leq \tau_2 \log(1 + \beta_2 P_2^D), \quad (4.42c)$$

$$R_1 + R_2 \leq \tau_1 \log(1 + \beta_1 P_1^R) + \tau_2 \log(1 + \beta_2 P_2^D + \hat{\beta} P^C) \quad (4.42d)$$

with $\hat{\beta} = \beta_2 + \beta_1$ if transmissions are synchronous and $\hat{\beta} = \beta_2$ if transmissions are asynchronous.

Proof: In the first interval, user 2 can decode the data from user 1 ω_1^R if

$$R_1 \leq \tau_1 \log(1 + \alpha_{12} P_1^R). \quad (4.43)$$

Table 4.7: Transmission strategy for the CMAC with JC and HD users if both users cooperate.

	Interval 1	Interval 2	Interval 3
User 1	$\mathcal{X}_1^R(\omega_1)$	\emptyset	$\sqrt{\frac{P_1^S}{P_2^C}} \mathcal{X}_2^C(\omega_1) + \mathcal{X}_1^C(\omega_2)$
User 2	\emptyset	$\mathcal{X}_2^R(\omega_2)$	$\mathcal{X}_2^C(\omega_1) + \sqrt{\frac{P_2^S}{P_1^C}} \mathcal{X}_1^C(\omega_2)$

The destination decodes ω_1^R from the received signals in both transmission intervals and ω_2 from the one received in the second interval. Assume that the message ω_1^R is decoded first considering $\mathcal{X}_2^D(\omega_2)$ as noise. Using the theory for parallel Gaussian channels [16] this is possible if

$$R_1 \leq \tau_1 \log(1 + \beta_1 P_1^R) + \tau_2 \log \left(1 + \frac{\left(\sqrt{\beta_1 P_1^S} + \sqrt{\beta_2 P_2^C} \right)^2}{1 + \beta_2 P_2^D} \right). \quad (4.44)$$

It then subtracts $\mathcal{X}_1^R(\omega_1^R)$ from the received signal in the second interval and decodes ω_2 if

$$R_2 \leq \tau_2 \log(1 + \beta_2 P_2^D). \quad (4.45)$$

For synchronous transmissions, the term $T_c = \left(\sqrt{\beta_1 P_1^S} + \sqrt{\beta_2 P_2^C} \right)^2$ in (4.44) can be maximized over P_1^S and P_2^C while satisfying $P^C = P_1^S + P_2^C$ obtaining $T_c = (\beta_1 + \beta_2) P^C$. For asynchronous transmissions, assume $P_1^S = 0$. Interchanging the decoding orders at the destination (first ω_2^D then ω_1^R) we obtain the other MAC corner point. Finally, the rate region in Theorem 4.4 is obtained by time-sharing of both corner points. ■

Both Users Cooperate

If both users cooperate, to maintain the HD constraint each user needs to be silent while listening to the partner's transmission. Consider the transmission scheme represented in Table 4.7. We assume full *decode-and-forward*. The rate region can be enhanced if users also superpose information only decoded at the destination (partial *decode-and-forward*). However, such a strategy reduces to the full *decode-and-forward* in the low power regime and is not considered here. We divide the total communication time into three intervals. The time-sharing factors are τ_1 , τ_2 and τ_3 . Each user $l = \{1, 2\}$ transmits a message ω_l at rate R_l which is decoded at the other user. In this case, we use 4 independent Gaussian codebooks: $\mathcal{X}_1^R(\cdot)$, $\mathcal{X}_2^R(\cdot)$, $\mathcal{X}_1^C(\cdot)$ and $\mathcal{X}_2^C(\cdot)$. During the first two intervals, each user l transmits its own message ω_l within $\mathcal{X}_l^R(\cdot)$ at power P_l^R . During the third interval, each user l , uses superposition coding to jointly transmit the cooperative information $\omega_{\bar{l}}$ within $\mathcal{X}_{\bar{l}}^C(\cdot)$ at power $P_{\bar{l}}^C$ and its own information ω_l with $\mathcal{X}_l^C(\cdot)$ at power P_l^S to obtain synchronism gains. For asynchronous transmissions, assume $P_l^S = 0$.

4.5. Rate Regions for the CMAC with Joint Coding

By optimally allocating $P_2^C, P_2^S, P_1^C, P_1^S$ with $P_1^{CS} = P_1^C + P_2^S, P_2^{CS} = P_2^C + P_1^S$, and $P^C = P_1^{CS} + P_2^{CS}$ this strategy achieves the rate region described in the following theorem.

Theorem 4.5 *For the decode-and-forward CMAC with HD nodes and transmitter CSI, if both nodes cooperate, the following rate region is achievable*

$$R_1 \leq \tau_1 \log(1 + \alpha_{12} P_1^R), \quad (4.46a)$$

$$R_2 \leq \tau_2 \log(1 + \alpha_{21} P_2^R), \quad (4.46b)$$

$$R_1 \leq \tau_1 \log(1 + \beta_1 P_1^R) + \tau_3 \log(1 + \hat{\beta}_1 P_1^{CS}), \quad (4.46c)$$

$$R_2 \leq \tau_2 \log(1 + \beta_2 P_2^R) + \tau_3 \log(1 + \hat{\beta}_2 P_2^{CS}), \quad (4.46d)$$

$$R_1 + R_2 \leq \tau_1 \log(1 + \beta_1 P_1^R) + \tau_2 \log(1 + \beta_2 P_2^R) + \tau_3 \log(1 + \hat{\beta} P^C) \quad (4.46e)$$

with $\hat{\beta} = \hat{\beta}_1 = \hat{\beta}_2 = \beta_1 + \beta_2$ for synchronous transmissions. For asynchronous transmissions, consider $\hat{\beta}_1 = \beta_1, \hat{\beta}_2 = \beta_2$ and replace the sum rate constraint (4.46e) by

$$R_1 + R_2 \leq \tau_1 \log(1 + \beta_1 P_1^R) + \tau_2 \log(1 + \beta_2 P_2^R) + \tau_3 \log(1 + \beta_1 P_1^{CS} + \beta_2 P_2^{CS}). \quad (4.47)$$

Proof: During the first two intervals, the decoding at the user terminals is possible if

$$R_1 \leq \tau_1 \log(1 + \alpha_{12} P_1^R), \quad (4.48a)$$

$$R_2 \leq \tau_2 \log(1 + \alpha_{21} P_2^R). \quad (4.48b)$$

During the third interval, using the theory for parallel Gaussian channels and time division between the decoding orders $\{\omega_1, \omega_2\}$ and $\{\omega_2, \omega_1\}$ the destination can decode both messages if

$$R_1 \leq \tau_1 \log(1 + \beta_1 P_1^R) + \tau_3 \log\left(1 + \left(\sqrt{\beta_1 P_1^S} + \sqrt{\beta_2 P_2^C}\right)^2\right), \quad (4.49a)$$

$$R_2 \leq \tau_2 \log(1 + \beta_2 P_2^R) + \tau_3 \log\left(1 + \left(\sqrt{\beta_1 P_1^C} + \sqrt{\beta_2 P_2^S}\right)^2\right), \quad (4.49b)$$

$$R_1 + R_2 \leq \tau_1 \log(1 + \beta_1 P_1^R) + \tau_2 \log(1 + \beta_2 P_2^R) + \tau_3 \log\left(1 + \left(\sqrt{\beta_1 P_1^C} + \sqrt{\beta_2 P_2^S}\right)^2 + \left(\sqrt{\beta_1 P_1^S} + \sqrt{\beta_2 P_2^C}\right)^2\right). \quad (4.49c)$$

For asynchronous transmissions, assume $P_1^S = P_2^S = 0$. For synchronous transmissions, forcing $P_1^{CS} = P_1^C + P_2^S, P_2^{CS} = P_2^C + P_1^S$, and $P^C = P_1^{CS} + P_2^{CS}$ the coherent terms can be maximized by transmitting fully correlated signals obtaining the rate region in Theorem 4.5. ■

Table 4.8: Transmission strategy for the CMAC with TD and FD users.

	Block b	
	Interval 1	Interval 2
User 1	$\mathcal{X}_1^R(\omega_1(b)) + \mathcal{X}_1^C(\omega_2[b-1])$	$\sqrt{\frac{P_1^S}{P_2^C}} \mathcal{X}_2^C(\omega_1[b])$
User 2	$\sqrt{\frac{P_2^S}{P_1^C}} \mathcal{X}_1^C(\omega_2[b-1])$	$\mathcal{X}_2^R(\omega_2[b]) + \mathcal{X}_2^C(\omega_1[b])$

4.5.4 Joint Coding with TDMA

For the FS-CMAC with FD nodes, both users transmit, simultaneously, during the whole communication time. Compared to the joint coding strategies previously described the coding complexity is reduced since users transmit, separately, the own and the relayed information. In this case, unlike the FS, we consider joint encoding the own and the relayed information but force time-division (TD) among user's transmissions. Nevertheless, we allow the simultaneous transmissions of synchronous signals. These signals arrive added coherently in amplitude at the receiver antenna, not requiring additional complexity to the decoder stage.

Again, we assume that users cooperate by fully decoding the partner's message. In addition, we consider that: *i*) nodes are FD, *ii*) transmissions are synchronous and, *iii*) both nodes cooperate. For all the other possible scenarios, as is shown later on in Remark 4.2, the transmission strategy reduces to a previously considered one. In this case, we need to use the BMC transmission scheme to jointly encode messages transmitted in different blocks or intervals. The main difference with the dedicated relay BMC is that now, each node can only use a fraction of each block to transmit its own data. The transmission is divided into B blocks, and each block is further divided into two intervals with time-sharing factors τ_1 and τ_2 . Each user l divides its message ω_l of rate R_l into B blocks, $\omega_l[1], \dots, \omega_l[B]$ and encodes each block separately. There are 2 Gaussian codebooks per user terminal: $\mathcal{X}_l^R(\cdot)$ and $\mathcal{X}_l^C(\cdot)$. Let us assume that at the beginning of block b , user 1 has decoded the message transmitted by user 2 in the previous block $\omega_2[b-1]$. During the first interval of block b , user 1 uses superposition coding to transmit its own data $\omega_1[b]$ with the codebook $\mathcal{X}_1^R(\cdot)$ at power P_1^R and the cooperative information, decoded in the previous block $\omega_2[b-1]$, with the codebook $\mathcal{X}_1^C(\cdot)$ at power P_1^C . To obtain synchronism gains, node 2, simultaneously, transmits $\mathcal{X}_1^C(\omega_2[b-1])$ with power P_2^S . In the next interval, node 2 uses superposition coding to transmit its own data $\omega_2[b]$ with the codebook $\mathcal{X}_2^R(\cdot)$ at power P_2^R and cooperative information $\omega_1[b]$ with the codebook $\mathcal{X}_2^C(\cdot)$ at power P_2^C . Again, to obtain synchronism gains node 1, simultaneously, transmits $\mathcal{X}_2^C(\omega_1[b])$ at power P_1^S . For asynchronous transmissions, assume $P_l^S = 0$.

By optimally allocating $P_2^C, P_2^S, P_1^C, P_1^S$ with $P_1^{CS} = P_1^C + P_2^S, P_2^{CS} = P_2^C + P_1^S$ and $P^C = P_1^{CS} + P_2^{CS}$ this strategy achieves the rate region described in the following theorem.

Theorem 4.6 *For the decode-and-forward CMAC with FD nodes and transmitter CSI, the fol-*

lowing rate region is achievable

$$R_1 \leq \tau_1 \log(1 + \alpha_{12} P_1^R), \quad (4.50a)$$

$$R_2 \leq \tau_2 \log(1 + \alpha_{21} P_2^R), \quad (4.50b)$$

$$R_1 \leq \tau_1 \log(1 + \beta_1 P_1^R) + \tau_2 \log(1 + \hat{\beta}_2 P_2^{CS}), \quad (4.50c)$$

$$R_2 \leq \tau_2 \log(1 + \beta_2 P_2^R) + \tau_1 \log(1 + \hat{\beta}_1 P_1^{CS}), \quad (4.50d)$$

$$R_2 + R_1 \leq \tau_1 \log(1 + \beta_1 P_1^R + \hat{\beta}_1 P_1^{CS}) + \tau_2 \log(1 + \beta_2 P_2^R + \hat{\beta}_2 P_2^{CS}) \quad (4.50e)$$

with $\hat{\beta}_2 = \hat{\beta}_1 = \beta_2 + \beta_1$ for synchronous and $\hat{\beta}_2 = \beta_2, \hat{\beta}_1 = \beta_1$ for asynchronous transmissions.

Proof: At the end of the first interval see Table 4.8, node 2 can decode $\omega_1[b]$ if

$$R_1 \leq \tau_1 \log(1 + \alpha_{12} P_1^R). \quad (4.51)$$

At the end of the second interval, node 1 can decode $\omega_2[b]$ if

$$R_2 \leq \tau_2 \log(1 + \alpha_{21} P_2^R). \quad (4.52)$$

At the end of each interval within a block, the destination decodes the message of one user. The message of user 2, $\omega_2[b-1]$ is decoded at the end of the first interval of block b . In the second interval, the message of user 1, $\omega_1[b]$ is decoded. Assume $\omega_2[b-1]$ is known at the end of block b , it then can decode $\omega_1[b]$ using the signals received in block b and considering $\mathcal{X}_2^R(\omega_2[b])$ as noise. Using the theory for parallel Gaussian channels, this is possible if

$$R_1 \leq \tau_1 \log(1 + \beta_1 P_1^R) + \tau_2 \log\left(1 + \frac{(\sqrt{\beta_1 P_1^S} + \sqrt{\beta_2 P_2^C})^2}{1 + \beta_2 P_2^R}\right). \quad (4.53)$$

To decode $\omega_2[b]$, the destination waits until the end of the first interval of block $b+1$. Then, $\omega_1[b]$ is known. Using the signal received in the second interval of block b and in the first interval of block $b+1$ and, considering $\mathcal{X}_1^R(\omega_1[b+1])$ as noise the destination can decode $\omega_2[b]$ if

$$R_2 \leq \tau_2 \log(1 + \beta_2 P_2^R) + \tau_1 \log\left(1 + \frac{(\sqrt{\beta_2 P_2^S} + \sqrt{\beta_1 P_1^C})^2}{1 + \beta_1 P_1^R}\right). \quad (4.54)$$

For asynchronous transmission, assume $P_2^S = P_1^S = 0$. For synchronous transmissions, maximizing the coherent terms with $P_1^{CS} = P_1^C + P_2^S$, $P_2^{CS} = P_2^C + P_1^S$ and $P^C = P_1^{CS} + P_2^{CS}$. The rate region can be written as in Theorem 4.6. ■

Remark 4.2 The rate region in Theorem 4.6 assumes that both users cooperate and terminals are FD. If terminals are HD, the time division between users can not be satisfied while also

obtaining synchronism gains. Likewise, if transmissions are asynchronous $P_2^S = P_1^S = 0$, then the FD capability is not required. Finally, if only one node cooperates (node 2), then $P_1^C = P_2^S = 0$. Again, the FD capability is not required and the strategy reduces to the one presented in Theorem 4.4 for HD nodes.

4.5.5 Summary of Cooperative Configurations

Table 4.9: Summary of transmission strategies.

		Synchronous	Asynchronous
Both users coop.	FD	FS FD/JC FD/TD	FS FD/JC FD
	HD	FS HD/JC HD_2/—	FS HD/JC HD_2/TD
One user coop.	FD	FS FD/JC FD/—	FS FD/JCFD
	HD	FS HD/JC HD_1=TD	FS HD/JC HD_1=TD
No user coop.	HD	—	FS HD=TD/JC FD

In Table 4.9, we summarize the cooperative strategies proposed in this section depending on the user terminals capabilities. The following notation is used:

- FS HD or FS FD designate the FS strategies studied in Section 4.4 with nodes working in HD or FD, respectively.
- JC FD designates the joint coding strategy described in Theorem 4.3 for nodes working in FD mode.
- JC HD_1 or JC HD_2 designates the joint coding strategy presented in Theorem 4.4 and in Theorem 4.5 for nodes working in HD mode.
- TD designates the joint coding strategy presented in Theorem 4.6 for nodes that access to the channel in time-division manner.

We indicate that two different strategies obtain the same rate region for a particular configuration with “=”, otherwise we use “/”.

4.6 Maximum Rates Per Energy

In this section, we compute the maximum RPE pair (η_1, η_2) for each of the rate regions presented in the previous section. The study of the low power regime for the FS-CMAC has shown that HD and FD user terminals obtain the same maximum RPE pair. Here, we show that joint coding can neither improve that result. As for the duplexing gain, the joint coding gain appears

with the study of the slope region conducted in the next Section. This result is stated in the next Theorem.

Theorem 4.7 *For the decode-and-forward CMAC, the use of joint coding techniques under any of the duplexity or synchronism capabilities cannot increase the flow-separation maximum RPE pair presented in Theorem 4.1.*

Proof: The following sections are devoted to prove this result. First, in Section 4.6.1 the notation employed is introduced and the computation of the maximum RPE pair for the joint coding rate regions presented in the previous section is formulated in a unified manner as a linear problem. Then, in subsequent sections, the maximum RPE pair problem is particularized and solved for each of the rate regions. For nodes working in FD mode, the problem is solved in Section 4.6.2, in Section 4.6.3 for nodes in HD mode and in Section 4.6.4 for nodes transmitting in a time-division fashion. ■

4.6.1 Preliminaries

All the rate regions obtained in the previous section for fixed resources $\mathcal{R}(\boldsymbol{\tau}, \mathbf{E})$ are defined constraints on each individual rate and on the sum rate as

$$R_1 \leq C_1, R_2 \leq C_2, R_1 + R_2 \leq C_3. \quad (4.55)$$

For the sake of simplicity, now we assume that there is only one rate condition per individual or sum rate. The extension to more conditions is direct. Due to the duplexing or coding complexity requirements, the communication has been divided into up to M orthogonal transmission intervals. With the exception of the rate region in (4.35), which is considered apart, the rate conditions $C_l, l \in \{1, 2, 3\}$ can be always written as

$$C_l(\boldsymbol{\tau}, \mathbf{E}) = \sum_{j=1}^M \tau_j \log \left(1 + \frac{g_{l,j}(\mathbf{E})}{\tau_j} \right) \quad (4.56)$$

where the functions $g_{l,j}(\mathbf{E})$ are concave for a linear power allocation in E .

As described in the preliminaries, the boundaries of the rate region $\mathcal{R}(E)$ as a function of the total power E can be found by forcing a fixed relation between the user rates $R_1(E) = \theta R_2(E)$ and maximizing the rate for user 1 as

$$R_{B1}(E) = \max_{\boldsymbol{\tau}, \mathbf{E}} \min \left(C_1, \theta C_2, \frac{\theta}{1 + \theta} C_3 \right) \quad (4.57)$$

with $\boldsymbol{\tau}, \mathbf{E}$ satisfying the resource constraints.

For a rate defined as in (4.57), we show in Chapter 3 that the maximum RPE is always obtained at $E = 0$ and thus, we can use the low power regime tools developed in [1] to study the energy efficiency of these strategies.

As we have seen in Section 4.3, to obtain the maximum RPE pair we need to compute the first-order derivative of the user rates $R_{Bl}(E)$ and particularize them at $E = 0$. This may not be obtained explicitly. In the following, we formulate the computation of $\dot{R}_{Bl}(0)$ as a function of the derivatives of the rate constraints in (4.56).

Consider that the resource allocation solution to (4.57) can be any pair of differentiable functions of E $\boldsymbol{\tau}(E)$ and $\mathbf{E}(E)$.

- The vector of time-sharing factors and its first-order derivative evaluate at $E = 0$ are denoted as $\mathbf{t} \triangleq \boldsymbol{\tau}(0)$ and $\dot{\mathbf{t}} \triangleq \dot{\boldsymbol{\tau}}(0)$, respectively (recall that we assume differentiability of $\boldsymbol{\tau}(E)$).
- The first and second-order derivatives of the power allocation vectors evaluated at $E = 0$ are denoted as $\dot{\mathbf{e}} \triangleq \dot{\mathbf{E}}(0)$ and $\ddot{\mathbf{e}} \triangleq \ddot{\mathbf{E}}(0)$, respectively (recall that we assume differentiability of $\mathbf{E}(E)$).
- After substituting the resource functions $\boldsymbol{\tau}(E)$ and $\mathbf{E}(E)$ into (4.56), we define
 - The functions $C_l(\boldsymbol{\tau}, \mathbf{E})$ as a function of E as $C_{E_l}(E) \triangleq C_l(\boldsymbol{\tau}(E), \mathbf{E}(E))$.
 - The functions $g_{lj}(\mathbf{E})$ as a function of E as $g_{E_{lj}}(E) \triangleq g_{lj}(\mathbf{E}(E))$.

Using the above definitions, to find the maximum rate per energy pair (η_1, η_2) , we just need to force $\eta_2 = \theta\eta_1$ and maximizing η_1 over $\dot{\mathbf{e}}$ as

$$\eta_1 = \dot{R}_{B1}(0) = \max_{\dot{\mathbf{e}}} \eta_1 \quad (4.58a)$$

$$\eta_1 = \theta\eta_2, \quad (4.58b)$$

$$\eta_1 \leq \dot{C}_{E_1}(\dot{\mathbf{e}}), \quad (4.58c)$$

$$\eta_2 \leq \dot{C}_{E_2}(\dot{\mathbf{e}}), \quad (4.58d)$$

$$\eta_1 + \eta_2 \leq \dot{C}_{E_3}(\dot{\mathbf{e}}), \quad (4.58e)$$

$$1 = \sum_{j=1, \dots, M} [\dot{\mathbf{e}}]_j, \quad (4.58f)$$

$$[\dot{\mathbf{e}}]_j \geq 0 \quad j = 1, \dots, M. \quad (4.58g)$$

where $[\mathbf{x}]_j$ denotes the j th element in the vector \mathbf{x} . The constraints (4.58c), (4.58d), and (4.58e) are obtained by taking the first-order derivative at both sides of the rate constraints that define the rate regions (4.55). For the left-hand side, by definition the derivative satisfy $\dot{R}_{Bl}(0) = \eta_l$ and thus, the sum rate $R_{BS}(E) = R_{B1}(E) + R_{B2}(E)$ satisfy $\dot{R}_{BS}(0) = \eta_1 + \eta_2$. For the

right-hand side, the first-order derivative of the functions $C_{E_l}(E)$ evaluated at $E = 0$ are

$$\dot{C}_{E_l}(E)|_{E=0} = \sum_{j=1}^M \dot{g}_{E_l,j}(\dot{e}). \quad (4.59)$$

Notice that given (4.59) it is clear that $\dot{C}_{E_l}(E)|_{E=0} = \dot{C}_{E_l}(\dot{e})$ and $g_{E_l,j}(E)|_{E=0} = \dot{g}_{E_l,j}(\dot{e})$ only depend on \dot{e} . Finally, the constraint in (4.58f) and (4.58f) are obtained by taking derivatives to the total power constraint and the positive power constraint, respectively.

4.6.2 Joint Coding with Full Duplex Operation

In this section, we particularize the problem in (4.58) to the rate region of the CMAC with *decode-and-forward* and FD nodes given in Theorem 4.3. Without loss of generality assume $\beta_2 \geq \beta_1$.

- For asynchronous transmissions or for synchronous transmissions with $\alpha_{12} \leq \beta_1$ or $\alpha_{21} \leq \beta_2$, the rate region is given in (4.34). According to (4.59), the first-order derivative of the rate constraints evaluated at $E = 0$ are given by

$$\dot{C}_{E_1}(\dot{e}) = \dot{g}_{E_1}(\dot{e}) = \hat{\alpha}_{12} \dot{e}_1^N, \quad (4.60a)$$

$$\dot{C}_{E_2}(\dot{e}) = \dot{g}_{E_2}(\dot{e}) = \hat{\alpha}_{21} \dot{e}_2^N, \quad (4.60b)$$

$$\dot{C}_{E_3}(\dot{e}) = \dot{g}_{E_3}(\dot{e}) = \beta_1 \dot{e}_1^N + \beta_2 \dot{e}_2^N + \hat{\beta} \dot{e}^C. \quad (4.60c)$$

Additionally, the positive and the total power constraints require that

$$\dot{e}_1^N + \dot{e}_2^N + \dot{e}^C = 1, \quad (4.61a)$$

$$\dot{e}_1^N, \dot{e}_2^N, \dot{e}^C > 0. \quad (4.61b)$$

By substituting (4.61a) into the sum rate constraint (4.60c), the maximum RPE pair is found maximizing η_1 over \dot{e} while satisfying

$$\eta_1 \leq \hat{\alpha}_{12} \dot{e}_1^N, \quad (4.62a)$$

$$\eta_2 \leq \hat{\alpha}_{21} \dot{e}_2^N, \quad (4.62b)$$

$$\eta_1 + \eta_2 \leq \hat{\beta} - \left(\hat{\beta} - \beta_1 \right) \dot{e}_1^N - \left(\hat{\beta} - \beta_2 \right) \dot{e}_2^N. \quad (4.62c)$$

- For synchronous transmissions, given that $\hat{\beta} > \beta_1, \beta_2$ and $0 \leq \dot{e}_1^N, \dot{e}_2^N \leq 1$. Constraints (4.62a) and (4.62b) increase with \dot{e}_1^N and \dot{e}_2^N , respectively, while (4.62c) decreases. Then, the maximum RPE pair is obtained if all three constraints are satisfied with equality

$$\dot{e}_1^{N*} = \frac{\eta_1}{\hat{\alpha}_{12}}, \quad \dot{e}_2^{N*} = \frac{\eta_2}{\hat{\alpha}_{21}}. \quad (4.63)$$

By substituting (4.63) into (4.62c), and using $\hat{\eta}_l$ in (4.15), the maximum RPE pair satisfy

$$\frac{\eta_2}{\hat{\eta}_2} + \frac{\eta_1}{\hat{\eta}_1} = 1. \quad (4.64)$$

- For asynchronous transmissions, we have $\hat{\beta} = \beta_2$. Then, the sum rate constraint (4.62c) does not depend on \dot{e}_2^N . Given that $0 \leq \dot{e}_2^N \leq 1$ the constraint (4.62b) is always less restrictive than (4.62c) and can be omitted. Then, the maximum RPE pair is given by (4.62a) and (4.62c) satisfied with equality

$$\dot{e}_1^{N*} = \frac{\eta_1}{\hat{\alpha}_{12}}. \quad (4.65)$$

By substituting (4.65) into (4.62c) the maximum RPE pair can be written as (4.64) with $\hat{\eta}_1 = \frac{\hat{\alpha}_{12}\hat{\beta}}{\hat{\alpha}_{12}+\hat{\beta}-\beta_1}$ and $\hat{\eta}_2 = \hat{\beta} = \beta_2$.

- For synchronous transmissions with $\alpha_{12} \geq \beta_1$ and $\alpha_{21} \geq \beta_2$, the rate region is described by (4.35). In this case, both nodes cooperate. The sum rate constraint is the same as in the previous case (4.60c). The individual rate constraints do not admit the general rate constraint representation in (4.56). The first-order derivatives are computed in the Appendix 4.A obtaining

$$\dot{C}_{E_1}(\dot{\mathbf{e}}) = \alpha_{12}\dot{e}_1^N + (\beta_1 - \alpha_{12})\dot{e}_1^D, \quad (4.66a)$$

$$\dot{C}_{E_2}(\dot{\mathbf{e}}) = \alpha_{21}\dot{e}_2^N + (\beta_2 - \alpha_{21})\dot{e}_2^D. \quad (4.66b)$$

Given that $\alpha_{12} \geq \beta_1$ and $\alpha_{21} \geq \beta_2$, these derivatives are always maximized by choosing $\dot{e}_1^D = \dot{e}_2^D = 0$. Then, the maximum RPE problem reduces to that in (4.62) with $\hat{\alpha}_{12} = \alpha_{12}$ and $\hat{\alpha}_{21} = \alpha_{21}$.

4.6.3 Joint Coding with Half Duplex Operation

In this case, since the rate region with FD nodes is always larger than with HD nodes, to shorten the proof, we check that the same maximum RPE pair is achieved with HD nodes.

The rate region for the CMAC using JC and HD nodes is given in Theorem 4.4 if only one node (node 2) cooperates and in Theorem 4.5 if both nodes cooperate.

- If only one node cooperates, the first-order derivatives of the rate constraints (4.42) evaluated at $E = 0$, are

$$\dot{C}_{E_{1,1}}(\dot{\mathbf{e}}) = \alpha_{12}\dot{e}_1^R, \quad (4.67a)$$

$$\dot{C}_{E_{1,2}}(\dot{\mathbf{e}}) = \beta_1\dot{e}_1^R + \hat{\beta}\dot{e}^C, \quad (4.67b)$$

$$\dot{C}_{E_{2,1}}(\dot{\mathbf{e}}) = \beta_2\dot{e}_2^D, \quad (4.67c)$$

$$\dot{C}_{E_{3,1}}(\dot{\mathbf{e}}) = \beta_1\dot{e}_1^R + \beta_2\dot{e}_2^D + \hat{\beta}\dot{e}^C. \quad (4.67d)$$

Additionally, the positive and the total power constraints require that

$$\dot{e}_1^R + \dot{e}_2^D + \dot{e}^C = 1, \quad (4.68a)$$

$$\dot{e}_1^R, \dot{e}_2^D, \dot{e}^C > 0. \quad (4.68b)$$

The individual rate constraints (4.67a) and (4.67b) are, jointly, more restrictive than the sum rate constraint (4.67d) which can be thus omitted. Then, the maximum RPE pair is found maximizing η_1 over $\dot{e} = [\dot{e}_1^R, \dot{e}_2^D, \dot{e}^C]$ while satisfying

$$\eta_1 \leq \alpha_{12}\dot{e}_1^R, \quad (4.69a)$$

$$\eta_1 \leq \beta_1\dot{e}_1^R + \hat{\beta}\dot{e}^C, \quad (4.69b)$$

$$\eta_2 \leq \beta_2\dot{e}_2^D, \quad (4.69c)$$

$$\eta_1 + \eta_2 \leq \beta_1\dot{e}_1^R + \beta_2\dot{e}_2^D + \hat{\beta}\dot{e}^C. \quad (4.69d)$$

We divide the problem (4.69) into two single source problems and maximizing η_1 and η_2 separately

$$\begin{aligned} \eta_1 &\leq \alpha_{12}\dot{e}_1^R, & \eta_2 &\leq \beta_2\dot{e}_2^D, \\ \eta_1 &\leq \beta_1\dot{e}_1^R + \hat{\beta}\dot{e}^C, & & \\ \dot{e}_1^R + \dot{e}^C &= \dot{e}_1, & \dot{e}_2^D &= \dot{e}_2. \end{aligned} \quad (4.70)$$

with $\dot{e}_1 + \dot{e}_2 = 1$.

The conditions imposed to (η_1) and (η_2) in each of these separated problems are more restrictive than the original ones (4.69). Thus, the solution is only valid if the final maximum RPE pair is the same as the one for FD nodes, which is always an upper-bound.

For the cooperative node (node 2) solving ((4.70) it is direct that

$$\dot{e}_2^{D*} = \frac{\eta_2}{\hat{\eta}_2} \quad (4.71)$$

with $\hat{\eta}_2 = \beta_2$. For node 1, this division results in a dedicated relay problem whose solution can be shown to be

$$\dot{e}_1^{R*} = \frac{\eta_1}{\alpha_{12}}, \quad \dot{e}^{C*} = \frac{\alpha_{12} - \beta_1}{\alpha_{12}\hat{\beta}_2}\eta_1. \quad (4.72)$$

Then, $\eta_1 = \hat{\eta}_1\dot{e}_1^{R*}$ with

$$\hat{\eta}_1 = \frac{\hat{\alpha}_{12}\hat{\beta}}{\hat{\alpha}_{12} + \hat{\beta} - \beta_1}, \quad (4.73)$$

Finally, using the sum power constraint, the maximum RPE pair can be expressed as in (4.64). For completeness, as we need them in Section 4.7 to compute the slope regions, we give the derivatives at $E = 0$ of the functions $g_{E_{l,i,j}}(E)$

$\dot{C}_{E_{l,i}}(\dot{\mathbf{e}}^*)$	$\dot{g}_{E_{l,i,1}}^*(\dot{\mathbf{e}}^*)$	$\dot{g}_{E_{l,i,2}}^*(\dot{\mathbf{e}}^*)$
$\dot{C}_{E_{1,1}}(\dot{\mathbf{e}}^*)$	η_1	0
$\dot{C}_{E_{1,2}}(\dot{\mathbf{e}}^*)$	$\frac{\beta_1}{\alpha_{12}}\eta_1$	$\frac{\alpha_{12} - \beta_1}{\alpha_{12}}\eta_1$
$\dot{C}_{E_{2,1}}(\dot{\mathbf{e}}^*)$	0	η_2
$\dot{C}_{E_{3,1}}(\dot{\mathbf{e}}^*)$	$\frac{\beta_1}{\alpha_{12}}\eta_1$	$\eta_2 + \frac{\alpha_{12} - \beta_1}{\alpha_{12}}\eta_1$

(4.74)

- If both nodes cooperate, the first-order derivatives of the rate constraints in (4.46), evaluated at $E = 0$ are

$$\dot{C}_{E_{1,1}}(\dot{\mathbf{e}}) = \alpha_{12}\dot{e}_1^R, \quad (4.75a)$$

$$\dot{C}_{E_{1,2}}(\dot{\mathbf{e}}) = \beta_1\dot{e}_1^R + \hat{\beta}\dot{e}_2^{CS}, \quad (4.75b)$$

$$\dot{C}_{E_{2,1}}(\dot{\mathbf{e}}) = \alpha_{21}\dot{e}_2^R, \quad (4.75c)$$

$$\dot{C}_{E_{2,2}}(\dot{\mathbf{e}}) = \beta_2\dot{e}_2^R + \hat{\beta}\dot{e}_1^{CS}, \quad (4.75d)$$

$$\dot{C}_{E_{3,1}}(\dot{\mathbf{e}}) = \beta_1\dot{e}_1^R + \beta_2\dot{e}_2^R + \hat{\beta}\dot{e}^C. \quad (4.75e)$$

Additionally, the positive and the total power constraints require that

$$\dot{e}_1^R + \dot{e}_2^R + \dot{e}_1^{CS} + \dot{e}_2^{CS} = 1, \quad (4.76a)$$

$$\dot{e}_1^{CS} + \dot{e}_2^{CS} = \dot{e}^C, \quad (4.76b)$$

$$\dot{e}_1^R, \dot{e}_2^R, \dot{e}_1^{CS}, \dot{e}_2^{CS} > 0. \quad (4.76c)$$

The individual constraints (4.75b) and (4.75d) are jointly more restrictive than the sum constraint (4.75e) which can be, thus, omitted. Again, we can define a more restrictive maximum RPE pair by dividing the problem into two single source problems and maximizing η_1 and η_2 separately

$$\begin{aligned} \eta_1 &\leq \alpha_{12}\dot{e}_1^R, & \eta_2 &\leq \alpha_{21}\dot{e}_2^R, \\ \eta_1 &\leq \beta_1\dot{e}_1^R + \hat{\beta}\dot{e}_2^{CS}, & \eta_2 &\leq \beta_2\dot{e}_2^R + \hat{\beta}\dot{e}_1^{CS}, \\ \dot{e}_1^R + \dot{e}_2^{CS} &= \dot{e}_1, & \dot{e}_2^R + \dot{e}_1^{CS} &= \dot{e}_2. \end{aligned} \quad (4.77)$$

with $\dot{e}_1 + \dot{e}_2 = 1$. The solution to these problems are given by

$$\begin{aligned} \dot{e}_1^{R*} &= \frac{\eta_1}{\alpha_{12}}, & \dot{e}_2^{R*} &= \frac{\eta_2}{\alpha_{21}}, \\ \dot{e}_2^{CS*} &= \frac{\alpha_{12} - \beta_1}{\alpha_{12}\hat{\beta}_2}\eta_1, & \dot{e}_1^{CS*} &= \frac{\alpha_{21} - \beta_2}{\alpha_{21}\hat{\beta}_1}\eta_2. \end{aligned} \quad (4.78)$$

Then, $\eta_l = \hat{\eta}_l \dot{e}_l^*$ with $\hat{\eta}_l$ given in (4.15). Finally, using the sum power constraint, again, the maximum RPE pair can be expressed as in (4.64). For completeness, the derivatives of $g_{E_{l,i,j}}(E)$ evaluated at $E = 0$, are given

$\dot{C}_{E_{l,i}}(\dot{\mathbf{e}}^*)$	$\dot{g}_{E_{l,i,1}}^*(\dot{\mathbf{e}}^*)$	$\dot{g}_{E_{l,i,2}}^*(\dot{\mathbf{e}}^*)$	$\dot{g}_{E_{l,i,3}}^*(\dot{\mathbf{e}}^*)$
$\dot{C}_{E_{1,1}}(\dot{\mathbf{e}}^*)$	η_1	0	0
$\dot{C}_{E_{1,2}}(\dot{\mathbf{e}}^*)$	$\frac{\beta_1}{\alpha_{12}}\eta_1$	0	$\frac{\alpha_{12} - \beta_1}{\alpha_{12}}\eta_1$
$\dot{C}_{E_{2,1}}(\dot{\mathbf{e}}^*)$	0	η_2	0
$\dot{C}_{E_{2,2}}(\dot{\mathbf{e}}^*)$	0	$\frac{\beta_2}{\alpha_{21}}\eta_2$	$\frac{\alpha_{21} - \beta_2}{\alpha_{21}}\eta_2$
$\dot{C}_{E_{3,1}}(\dot{\mathbf{e}}^*)$	$\frac{\beta_1}{\alpha_{12}}\eta_1$	$\frac{\beta_2}{\alpha_{21}}\eta_2$	$\frac{\alpha_{21} - \beta_2}{\alpha_{21}}\eta_2 + \frac{\alpha_{12} - \beta_1}{\alpha_{12}}\eta_1$

(4.79)

4.6.4 Joint Coding with TDMA

We show that the maximum RPE pair for the CMAC with TDMA is the same as in the previous cases. As discussed in Remark 4.2, we only consider that both nodes cooperate and have FD capabilities.

4.7. The Slope Region

In addition, we only consider synchronous transmissions and the channel gains satisfying $\alpha_{21} > \beta_1$ and $\alpha_{21} > \beta_2$ as the cooperation of both users only obtains the maximum RPE pair in that case as illustrated in Fig. 4.5. The rate region is then given by the rate constraints in (4.50). The first-order derivatives evaluated at $E = 0$ read

$$\dot{C}_{E_{1,1}}(\dot{\mathbf{e}}) = \alpha_{12}e_1^R, \quad (4.80a)$$

$$\dot{C}_{E_{2,1}}(\dot{\mathbf{e}}) = \alpha_{21}e_2^R, \quad (4.80b)$$

$$\dot{C}_{E_{1,2}}(\dot{\mathbf{e}}) = \beta_1e_1^R + \hat{\beta}_2e_2^{CS}, \quad (4.80c)$$

$$\dot{C}_{E_{2,2}}(\dot{\mathbf{e}}) = \beta_2e_2^R + \hat{\beta}_1e_1^{CS}, \quad (4.80d)$$

$$\dot{C}_{E_{3,1}}(\dot{\mathbf{e}}) = \beta_1e_1^R + \hat{\beta}_1e_1^{CS} + \beta_2e_2^R + \hat{\beta}_2e_2^{CS}. \quad (4.80e)$$

Additionally, the positive and the total power constraints require that

$$\dot{e}_1^R + e_2^R + \dot{e}_1^{CS} + \dot{e}_2^{CS} = 1, \quad (4.81a)$$

$$\dot{e}_1^R, e_2^R, \dot{e}_1^{CS}, \dot{e}_2^{CS} > 0. \quad (4.81b)$$

The individual constraints (4.80c) and (4.80d) are, jointly, more restrictive than the sum constraint (4.80e) which can be thus omitted. Again, we can define a more restrictive maximum RPE pair by dividing the problem into two single source problems and maximizing η_1 and η_2 separately

$$\begin{aligned} \eta_1 &\leq \alpha_{12}e_1^R, & \eta_2 &\leq \alpha_{21}e_2^R, \\ \eta_1 &\leq \beta_1e_1^R + \hat{\beta}_2e_2^{CS}, & \eta_2 &\leq \beta_2e_2^R + \hat{\beta}_1e_1^{CS}, \\ \dot{e}_1^R + \dot{e}_1^{CS} &= \dot{e}_1 & \dot{e}_2^R + \dot{e}_2^{CS} &= \dot{e}_2 \end{aligned} \quad (4.82)$$

with $\dot{e}_1 + \dot{e}_2 = 1$. For each user l , the solution is $\eta_l = \hat{\eta}_l \dot{e}_l^*$ with $\hat{\eta}_l$ given in (4.15). Finally, using the sum power constraint, the maximum RPE pair can be expressed as in (4.64). For completeness, the derivatives of the functions $g_{l,i,j}(E)$ evaluated at $E = 0$ are given

$\dot{C}_{E_{l,i}}(\dot{\mathbf{e}}^*)$	$\dot{g}_{l,i,1}(\dot{\mathbf{e}}^*)$	$\dot{g}_{l,i,2}(\dot{\mathbf{e}}^*)$
$\dot{C}_{E_{1,1}}(\dot{\mathbf{e}}^*)$	η_1	0
$\dot{C}_{E_{1,2}}(\dot{\mathbf{e}}^*)$	$\frac{\beta_1}{\alpha_{12}}\eta_1$	$\frac{\alpha_{12}-\beta_1}{\alpha_{12}}\eta_1$
$\dot{C}_{E_{2,1}}(\dot{\mathbf{e}}^*)$	0	η_2
$\dot{C}_{E_{2,2}}(\dot{\mathbf{e}}^*)$	$\frac{\alpha_{21}-\beta_2}{\alpha_{21}}\eta_2$	$\frac{\beta_2}{\alpha_{21}}\eta_2$
$\dot{C}_{E_{3,1}}(\dot{\mathbf{e}}^*)$	$\frac{\beta_1}{\alpha_{12}}\eta_1 + \frac{\alpha_{21}-\beta_2}{\alpha_{21}}\eta_2$	$\frac{\beta_2}{\alpha_{21}}\eta_2 + \frac{\alpha_{12}-\beta_1}{\alpha_{12}}\eta_1$

(4.83)

4.7 The Slope Region

In the previous section, we showed that the maximum RPE pair remains unaltered regardless of the duplexing or joint coding capabilities. We turn now our attention to study the slope region.

First, in Section 4.7.1, by using the notation introduced in Section 4.6.1, the computation of the slope region for all the joint coding rate regions is formulated in a unified manner. Then, in

subsequent sections, the slope region problem is particularized and solved for each case. For nodes working in FD mode, the problem is solved in Section 4.7.2, in Section 4.7.3 for nodes in HD mode and in Section 4.7.4 for nodes transmitting in a time-division fashion. Simulation results are shown in Section 4.8.

4.7.1 Preliminaries

As we have seen in Section 4.3, to obtain the slope region (S_1, S_2) we need to compute the maximum slope pair in the boundary of the rate region

$$S_{Bl} \triangleq \frac{2 \left(\dot{R}_{Bl}(0) \right)^2}{-\ddot{R}_{Bl}(0)}. \quad (4.84)$$

Once the maximum RPE pair is obtained, we have $\dot{R}_{Bl}(0) = \eta_l$. Then, the slope of user l , (S_{Bl}) can be obtained by computing $\ddot{R}_{Bl}(0)$.

The $\ddot{R}_{Bl}(0)$ or slopes in the boundary of the rate region can be computed by forcing $S_{B1} = \theta S_{B2}$, and maximizing S_{B1} over \mathbf{t} and $\ddot{\mathbf{e}}$, while satisfying

$$\max_{\mathbf{t}, \ddot{\mathbf{e}}} S_{B1} \quad (4.85a)$$

$$S_{B1} = \theta S_{B2}, \quad (4.85b)$$

$$\frac{(\eta_1)^2}{S_{B1}} \geq -\ddot{C}_{E_1}(\mathbf{t}, \ddot{\mathbf{e}}), \quad (4.85c)$$

$$\frac{(\eta_2)^2}{S_{B2}} \geq -\ddot{C}_{E_2}(\mathbf{t}, \ddot{\mathbf{e}}), \quad (4.85d)$$

$$\frac{(\eta_1)^2}{S_{B1}} + \frac{(\eta_2)^2}{S_{B2}} \geq -\ddot{C}_{E_3}(\mathbf{t}, \ddot{\mathbf{e}}), \quad (4.85e)$$

$$\sum_{\forall j} [\mathbf{t}]_j = 1, \quad (4.85f)$$

$$\sum_{\forall j} [\ddot{\mathbf{e}}]_j = 0, \quad (4.85g)$$

$$[\ddot{\mathbf{e}}]_j \geq 0 \text{ if } [\dot{\mathbf{e}}^*]_j = 0 \forall j. \quad (4.85h)$$

The constraints (4.85c), (4.85d), and (4.85e) are obtained by taking second-order derivative at both sides of the rate constraints that define the rate regions (4.55). For the left-hand side, by definition the derivative of the individual rates satisfy

$$-\ddot{R}_{Bl}(0) = \frac{2(\eta_l)^2}{S_{Bl}}. \quad (4.86)$$

The sum rate $R_{BS} = R_1 + R_2$ satisfies

$$-\ddot{R}_{BS}(0) = \frac{2(\eta_1)^2}{S_{B1}} + \frac{2(\eta_2)^2}{S_{B2}}. \quad (4.87)$$

For the right-hand side, the second-order derivative of the functions $C_{E_l}(E)$ evaluated at $E = 0$ are

$$\ddot{C}_{E_l}(0) = \sum_{j=1}^M \ddot{g}_{E_l,j}(\ddot{\mathbf{e}}) - \frac{(\dot{g}_{E_l,j}(\dot{\mathbf{e}}))^2}{t_j}. \quad (4.88)$$

From the previous section, we already know $\dot{\mathbf{e}}^*$, thus given (4.88), $\ddot{C}_{E_l}(0) = \ddot{C}_{E_l}(\mathbf{t}, \ddot{\mathbf{e}})$ only depends on $\ddot{\mathbf{e}}$ and \mathbf{t} . The constrain in (4.85f) is the time-sharing constraint evaluate at $E = 0$ and the constraints in (4.85g) and (4.85h) are obtained by taking derivatives to the total power constraint and the positive power constraint, respectively. Notice that if any element j of $\dot{\mathbf{e}}$, satisfies $\dot{e}_j = 0$, then E_j satisfies

$$\lim_{E \rightarrow 0} E_j(E) = \frac{\ddot{e}_j}{2} E^2 + o(E^3). \quad (4.89)$$

Consequently, the positive power constraint ($E_j(E) > 0$) forces $\ddot{e}_j \geq 0$.

4.7.2 Joint Coding with Full Duplex Operation

The next theorem unifies the obtained results with joint coding and full duplex terminals.

Theorem 4.8 *Let the rates vanish while keeping $R_1 = \theta R_2$, the CMAC slope region (S_1, S_2) with joint coding and full duplex nodes is*

$$\mathcal{S}_{JC_{FD}}(\theta) = \left\{ (S_1, S_2) \in \mathbb{R}_+^2 : S_1 \leq S_{B1}, S_2 \leq S_{B2}, \right. \\ \left. S_{B1} = \theta S_{B2}, \frac{\hat{\beta}\theta}{\hat{\eta}_1} \left(\frac{2}{S_{B1}} - 1 \right) + \frac{\hat{\beta}}{\hat{\eta}_2\theta} \left(\frac{2}{S_{B2}} - 1 \right) = 2 \right\} \quad (4.90)$$

where $\hat{\eta}_1, \hat{\eta}_2$ are defined in (4.15) and with $\hat{\beta}$ as defined in Theorem 4.1.

Proof: The rate region for the CMAC using JC and FD nodes is given in Theorem 4.3.

- For any asynchronous scenario and for synchronous transmissions with $\alpha_{12} \leq \beta_1$ or $\alpha_{21} \leq \beta_2$, the rate region is defined by the rate constraints in (4.34). Using (4.88), the second-order derivatives of these constraints, evaluated at $E = 0$, are

$$-\ddot{C}_{E_1}(\ddot{\mathbf{e}}) = (\hat{\alpha}_{12}\dot{e}_1^{N*})^2 - \hat{\alpha}_{12}\ddot{e}_1^N, \quad (4.91a)$$

$$-\ddot{C}_{E_2}(\ddot{\mathbf{e}}) = (\hat{\alpha}_{21}\dot{e}_2^{N*})^2 - \hat{\alpha}_{21}\ddot{e}_2^N, \quad (4.91b)$$

$$-\ddot{C}_{E_3}(\ddot{\mathbf{e}}) = \left(\beta_1\dot{e}_1^{N*} + \beta_2\dot{e}_2^{N*} + \hat{\beta}\dot{e}^{C*} \right)^2 - \left(\beta_1\ddot{e}_1^N + \beta_2\ddot{e}_2^N + \hat{\beta}\ddot{e}^C \right). \quad (4.91c)$$

Additionally, the total power constraint requires that

$$0 = \ddot{e}_1^N + \ddot{e}_2^N + \ddot{e}^C. \quad (4.92)$$

After including total power constraint $\ddot{e}^C = -(\ddot{e}_1^N + \ddot{e}_2^N)$ into the sum rate constraint (4.91c), and plugging into (4.91) the solution to \dot{e}_1^{N*} , \dot{e}_2^{N*} and \dot{e}^{C*} that maximizes the RPE, which was obtained in (4.63) for synchronous transmissions and in (4.65) for asynchronous transmissions. The slopes in the boundary of the rate region can be found by forcing $S_{B1} = \theta S_{B2}$ and maximizing S_{B1} over $\ddot{e} = [\ddot{e}_1^N, \ddot{e}_2^N]$ while satisfying

$$\frac{2(\eta_1)^2}{S_{B1}} \geq (\eta_1)^2 - \hat{\alpha}_{12}\ddot{e}_1^N, \quad (4.93a)$$

$$\frac{2(\eta_2)^2}{S_{B2}} \geq (\eta_2)^2 - \hat{\alpha}_{21}\ddot{e}_2^N, \quad (4.93b)$$

$$\frac{2(\eta_1)^2}{S_{B1}} + \frac{2(\eta_2)^2}{S_{B2}} \geq (\eta_1 + \eta_2)^2 + (\hat{\beta} - \beta_1)\ddot{e}_1^N + (\hat{\beta} - \beta_2)\ddot{e}_2^N. \quad (4.93c)$$

- For synchronous transmissions, given that $\hat{\beta} > \beta_1, \beta_2$ the right-hand side of (4.93c) increases with \ddot{e}_1^N and \ddot{e}_2^N while the right-hand side of (4.93a) and (4.93b) decreases. Thus, in the boundary, all three constraints are satisfied with equality. Isolating \ddot{e}_1^N and \ddot{e}_2^N from (4.93a) and (4.93b), respectively, and plugging them into (4.93c) we obtain

$$\begin{aligned} \left(1 + \frac{\hat{\beta} - \beta_1}{\hat{\alpha}_{12}}\right) \frac{2(\eta_1)^2}{S_{B1}} + \left(1 + \frac{\hat{\beta} - \beta_2}{\hat{\alpha}_{21}}\right) \frac{2(\eta_2)^2}{S_{B2}} &= \\ &= (\eta_1 + \eta_2)^2 + \frac{\hat{\beta} - \beta_1}{\hat{\alpha}_{12}}(\eta_1)^2 + \frac{\hat{\beta} - \beta_2}{\hat{\alpha}_{21}}(\eta_2)^2. \end{aligned} \quad (4.94)$$

Forcing $\eta_1 = \theta\eta_2$ the slope region can be finally written as in Theorem 4.8.

- For asynchronous transmissions, in the previous section we have seen that the rate constraint $C_{E_2}(E)$ is not satisfied with equality in the boundary of the rate region since $\dot{C}_{E_2}(\dot{e}) \neq \eta_2$. Consequently, the slope condition on $-\ddot{C}_{E_2}(\ddot{e})$ (4.93b) is omitted in this case. In addition, given that $\hat{\beta} = \beta_2$ the sum rate constraint (4.93c) does not depend on \ddot{e}_2^N . Thus, in the boundary, constraints (4.93a) and (4.93c) are satisfied with equality

$$\left(1 + \frac{\hat{\beta} - \beta_1}{\hat{\alpha}_{12}}\right) \frac{2(\eta_1)^2}{S_{B1}} + \frac{2(\eta_2)^2}{S_{B2}} = (\eta_1 + \eta_2)^2 + \frac{\hat{\beta} - \beta_1}{\hat{\alpha}_{12}}(\eta_1)^2. \quad (4.95)$$

Forcing $\eta_1 = \theta\eta_2$ the slope region can be finally written as in Theorem 4.8.

- For synchronous transmissions with $\alpha_{12} \geq \beta_1$ and $\alpha_{21} \geq \beta_2$, the rate region is given by (4.35). The constraint on $\ddot{C}_{E_{12}}(\ddot{e})$ is the same as that in (4.91c). The second-order derivatives of the individual rate constraints are computed in Appendix 4.A obtaining

$$\begin{aligned} -\ddot{C}_{E_1}(\ddot{e}) &= -\alpha_{12}\ddot{e}_1^R - \beta_1\ddot{e}_1^D + 2\alpha_{12}\dot{e}_1^D\alpha_{12}\dot{e}_1^R + 2(1-x_0)\beta_2\dot{e}_2^D\beta_1\dot{e}_1^D + \\ &\quad + (\alpha_{12}\dot{e}_1^R)^2 + (\beta_1\dot{e}_1^D)^2, \end{aligned} \quad (4.96a)$$

4.7. The Slope Region

$$- \ddot{C}_{E_2}(\ddot{\mathbf{e}}) = -\alpha_{21}\ddot{e}_2^R - \beta_2\ddot{e}_2^D + 2\alpha_{21}\dot{e}_2^D\alpha_{21}\dot{e}_2^R + 2x_0\beta_1\dot{e}_1^D\beta_2\dot{e}_2^D + (\alpha_{21}\dot{e}_2^R)^2 + (\beta_2\dot{e}_2^D)^2 \quad (4.96b)$$

with $x_0 \underset{E \rightarrow 0}{=} x(E)$. Additionally, the positive and the total power constraints require that

$$0 = \ddot{e}_1^D + \ddot{e}_2^D + \ddot{e}_1^R + \ddot{e}_2^R + \ddot{e}^C, \quad (4.97a)$$

$$\ddot{e}_1^N = \ddot{e}_1^D + \ddot{e}_1^R, \quad \ddot{e}_2^N = \ddot{e}_2^D + \ddot{e}_2^R, \quad (4.97b)$$

$$0 \leq \ddot{e}_1^D, \ddot{e}_2^D. \quad (4.97c)$$

After substituting the maximum RPE pair solution $\dot{e}_2^{D*} = \dot{e}_1^{D*} = 0$ and $\dot{e}_l^{N*} = \dot{e}_l^{R*} = \frac{\eta_l}{\alpha_{12}}$, the slopes in the boundary of the rate region can be found by forcing $S_{B1} = \theta S_{B2}$ and maximizing S_{B1} over $\ddot{\mathbf{e}} = [\ddot{e}_1^N, \ddot{e}_2^N, \ddot{e}_1^D, \ddot{e}_2^D]$ while satisfying

$$\frac{2(\eta_1)^2}{S_{B1}} \geq (\eta_1)^2 - \alpha_{12}\ddot{e}_1^N + (\alpha_{12} - \beta_1)\ddot{e}_1^D, \quad (4.98a)$$

$$\frac{2(\eta_2)^2}{S_{B2}} \geq (\eta_2)^2 - \alpha_{21}\ddot{e}_2^N + (\alpha_{21} - \beta_2)\ddot{e}_2^D, \quad (4.98b)$$

$$\frac{2(\eta_1)^2}{S_{B1}} + \frac{2(\eta_2)^2}{S_{B2}} \geq (\eta_1 + \eta_2)^2 + (\hat{\beta} - \beta_1)\ddot{e}_1^N + (\hat{\beta} - \beta_2)\ddot{e}_2^N. \quad (4.98c)$$

Provided that it is required that $\ddot{e}_1^D, \ddot{e}_2^D \geq 0$, see (4.97c) and $\alpha_{12} \geq \beta_1$ and $\alpha_{21} \geq \beta_2$, the right-hand side of (4.98a) and (4.98b) are always minimized by choosing $\ddot{e}_1^{D*} = \ddot{e}_2^{D*} = 0$. Then, the maximum slope problem reduces to that in (4.93) with $\hat{\alpha}_{12} = \alpha_{12}$, $\hat{\alpha}_{21} = \alpha_{21}$ and the solution is given by (4.95). ■

Remark 4.3 In [42], the slope region for the non-cooperative MAC is derived. Opposite to our work, there the power constraint was individual for each user, while in our case is global. In fact, our non-cooperative slope region ($\hat{\alpha}_{12} = \beta_1$ and $\hat{\alpha}_{21} = \beta_2$) is the dual slope region of the non-cooperative BC, also derived in [42], but taking into account that they consider $\beta_1 > \beta_2$.

4.7.3 Joint Coding with Half Duplex Operation

For this configuration, we have provided in Section 4.5 two rate regions:

- i) if at most one user (user 2) cooperates, the rate region is given in Theorem 4.4,
- ii) if both nodes cooperate, the rate region is given in Theorem 4.5.

The selection of the scenario of cooperation was solved in the previous section. It was found that two nodes cooperate to maximize the RPE pair, if and only if transmissions are synchronous and the channel gains satisfy ($\alpha_{12} > \beta_1$ and $\alpha_{21} > \beta_2$) otherwise only one or no user cooperates. The associated slopes regions are given in the following theorem.

Theorem 4.9 *Let the rates vanish while keeping $R_1 = \theta R_2$.*

Case i): If node 2 cooperates with node 1, the CMAC slope region (S_1, S_2) with joint coding and half duplex nodes is

$$\mathcal{S}_{JCHD_1}(\theta) = \left\{ (S_1, S_2) \in \mathbb{R}_+^2 : S_1 \leq S_{B1}, S_2 \leq S_{B2}, \right. \\ \left. S_{B1} = \theta S_{B2}, \frac{2\hat{\beta}\theta}{\hat{\eta}_1} \frac{1}{S_{B1}} + \frac{2\hat{\beta}}{\hat{\eta}_2\theta} \frac{1}{S_{B2}} = (\Psi_1 + \Psi_2)^2 \right\} \quad (4.99)$$

where

$$(\Psi_1)^2 = \left(\frac{\hat{\beta}}{\hat{\eta}_1} - 1 \right) \theta + \left(\frac{\beta_1}{\alpha_{12}} \right)^2 \theta, \quad (4.100a)$$

$$(\Psi_2)^2 = \left(\left(1 - \frac{\beta_1}{\alpha_{12}} \right) \sqrt{\theta} + \frac{1}{\sqrt{\theta}} \right)^2 + \left(\frac{\hat{\beta}}{\hat{\eta}_2} - 1 \right) \frac{1}{\theta} \quad (4.100b)$$

with $\hat{\eta}_1 = \frac{\alpha_{12}\hat{\beta}}{\alpha_{12} + \hat{\beta} - \beta_1}$, $\hat{\eta}_2 = \beta_2$ and $\hat{\beta} = \beta_2 + \beta_1$ for synchronous transmissions and $\hat{\beta} = \beta_2$ for asynchronous transmissions.

Case ii): If both nodes cooperate, the slope region obtained is the same as for the FS-CMAC with nodes in HD mode given in (4.17), namely $\mathcal{S}_{JCHD_2}(\theta) = \mathcal{S}_{FSHD}(\theta)$

Proof:

- If only one node cooperates, after computing the second-order derivatives of the rate constraints in (4.42) evaluated at $E = 0$, the slopes in the boundary of the rate region can be found by forcing $S_{B1} = \theta S_{B2}$ and maximizing S_{B1} over $\ddot{\mathbf{e}} = [\ddot{e}_1^R, \ddot{e}_2^D, \ddot{e}^C]$ and $\mathbf{t} = [t_1, t_2]$ while satisfying

$$\frac{2(\eta_1)^2}{S_{B1}} \geq \frac{(\dot{g}_{1,1,1}^*)^2}{t_1} - \alpha_{12}\ddot{e}_1^R, \quad (4.101a)$$

$$\frac{2(\eta_1)^2}{S_{B1}} \geq \frac{(\dot{g}_{1,2,1}^*)^2}{t_1} + \frac{(\dot{g}_{1,2,2}^*)^2}{t_2} - \beta_1\ddot{e}_1^R - \hat{\beta}\ddot{e}^C, \quad (4.101b)$$

$$\frac{2(\eta_2)^2}{S_{B2}} \geq \frac{(\dot{g}_{2,1,2}^*)^2}{t_2} - \beta_2\ddot{e}_2^D, \quad (4.101c)$$

$$\frac{2(\eta_2)^2}{S_{B2}} + \frac{2(\eta_1)^2}{S_{B1}} \geq \frac{(\dot{g}_{3,1,1}^*)^2}{t_1} + \frac{(\dot{g}_{3,1,2}^*)^2}{t_2} - \beta_1\ddot{e}_1^R - \beta_2\ddot{e}_2^D - \hat{\beta}\ddot{e}^C \quad (4.101d)$$

4.7. The Slope Region

with $\dot{g}_{l,i,j}^*$ given in (4.74). Additionally, the resource constraints require that

$$\ddot{e}_1^R + \ddot{e}^C + \ddot{e}_2^D = 0, \quad (4.102a)$$

$$t_1 + t_2 = 1. \quad (4.102b)$$

Including $\ddot{e}^C = -(\ddot{e}_1^R + \ddot{e}_2^D)$ into (4.101b) and (4.101d), these constraints can be rewritten as

$$\frac{2(\eta_1)^2}{S_{B1}} \geq \frac{(\dot{g}_{1,2,1}^*)^2}{t_1} + \frac{(\dot{g}_{1,2,2}^*)^2}{t_2} + (\hat{\beta} - \beta_1) \ddot{e}_1^R + \hat{\beta} \ddot{e}_2^D, \quad (4.103a)$$

$$\frac{2(\eta_2)^2}{S_{B2}} + \frac{2(\eta_1)^2}{S_{B1}} \geq \frac{(\dot{g}_{3,1,1}^*)^2}{t_1} + \frac{(\dot{g}_{3,1,2}^*)^2}{t_2} + (\hat{\beta} - \beta_1) \ddot{e}_1^R + (\hat{\beta} - \beta_2) \ddot{e}_2^D \quad (4.103b)$$

Let us first fix t_1 and t_2 and maximize the slope region over \ddot{e}_1^R and \ddot{e}_2^D . Note that the right-hand side of (4.101a) and (4.101c) linearly decrease with \ddot{e}_1^R and \ddot{e}_2^D , respectively, whereas the right-hand side of constraints in (4.103) linearly increase with both \ddot{e}_1^R and \ddot{e}_2^D . Consequently, the maximum slope pair is obtained with the constraints (4.101a) and (4.101c) satisfied with equality. Isolating \ddot{e}_1^R from (4.101a) and \ddot{e}_2^D from (4.101c) and plugging them into (4.103) we get

$$\left(1 + \frac{\hat{\beta} - \beta_1}{\alpha_{12}}\right) \frac{2(\eta_1)^2}{S_{B1}} + \frac{\hat{\beta}}{\beta_2} \frac{2(\eta_2)^2}{S_{B2}} \geq \frac{(\Psi_{1,1})^2}{t_1} + \frac{(\Psi_{2,1})^2}{t_2}, \quad (4.104a)$$

$$\left(1 + \frac{\hat{\beta} - \beta_1}{\alpha_{12}}\right) \frac{2(\eta_1)^2}{S_{B1}} + \frac{\hat{\beta}}{\beta_2} \frac{2(\eta_2)^2}{S_{B2}} \geq \frac{(\Psi_{1,2})^2}{t_1} + \frac{(\Psi_{2,2})^2}{t_2} \quad (4.104b)$$

with

$$(\Psi_{1,1})^2 = (\dot{g}_{1,2,1}^*)^2 + \frac{\hat{\beta} - \beta_1}{\alpha_{12}} (\dot{g}_{1,1,1}^*)^2, \quad (4.105a)$$

$$(\Psi_{1,2})^2 = (\dot{g}_{12,1,1}^*)^2 + \frac{\hat{\beta} - \beta_1}{\alpha_{12}} (\dot{g}_{1,1,1}^*)^2, \quad (4.105b)$$

$$(\Psi_{2,1})^2 = (\dot{g}_{1,2,2}^*)^2 + \frac{\hat{\beta}}{\beta_2} (\dot{g}_{2,1,2}^*)^2, \quad (4.105c)$$

$$(\Psi_{2,2})^2 = (\dot{g}_{12,1,2}^*)^2 + \left(\frac{\hat{\beta} - \beta_2}{\beta_2}\right) (\dot{g}_{2,1,2}^*)^2. \quad (4.105d)$$

Replacing $\dot{g}_{l,i,j}^*$ obtained in (4.74), it can be shown that $(\Psi_{1,1})^2 \leq (\Psi_{1,2})^2$ and $(\Psi_{2,1})^2 \leq (\Psi_{2,2})^2$. Consequently, (4.104b) is more restrictive than (4.104a), which can be, thus, omitted. Now, minimizing the right-hand side of the slope constraint (4.104b) over t_1 we obtain

$$\frac{1}{t_1^*} = 1 + \frac{\Psi_{2,2}}{\Psi_{2,1}} \quad (4.106)$$

which substituted into (4.104b) and using $\eta_1 = \theta\eta_2$ provides the slope region in (4.99).

- If both users cooperate, computing the second-order derivative of the rate constraints in (4.46), evaluated at $E = 0$, we can write the following constraints on the maximum slope pairs

$$\frac{2(\eta_1)^2}{S_{B1}} \geq \frac{(\dot{g}_{1,1,1}^*)^2}{t_1} - \alpha_{12}\ddot{e}_1^R, \quad (4.107a)$$

$$\frac{2(\eta_2)^2}{S_{B2}} \geq \frac{(\dot{g}_{2,1,2}^*)^2}{t_2} - \alpha_{21}\ddot{e}_2^R, \quad (4.107b)$$

$$\frac{2(\eta_1)^2}{S_{B1}} \geq \frac{(\dot{g}_{1,2,1}^*)^2}{t_1} + \frac{(\dot{g}_{1,2,3}^*)^2}{t_3} - \beta_1\ddot{e}_1^R - \hat{\beta}\ddot{e}_1^{CS}, \quad (4.107c)$$

$$\frac{2(\eta_2)^2}{S_{B2}} \geq \frac{(\dot{g}_{2,2,2}^*)^2}{t_2} + \frac{(\dot{g}_{2,2,3}^*)^2}{t_3} - \beta_2\ddot{e}_2^R - \hat{\beta}\ddot{e}_2^{CS}, \quad (4.107d)$$

$$\frac{2(\eta_1)^2}{S_{B1}} + \frac{2(\eta_2)^2}{S_{B2}} \geq \frac{(g_{3,1,1}^*)^2}{t_1} + \frac{(g_{3,1,2}^*)^2}{t_2} + \frac{(g_{3,1,3}^*)^2}{t_3} - \beta_1\ddot{e}_1^R - \beta_2\ddot{e}_2^R - \hat{\beta}\ddot{e}^C. \quad (4.107e)$$

with $\dot{g}_{i,i,j}^*$ given in (4.79). Additionally, the resource constraints require that

$$\ddot{e}_1^R + \ddot{e}_1^{CS} + \ddot{e}_2^{CS} + \ddot{e}_2^R = 0, \quad (4.108a)$$

$$\ddot{e}_1^{CS} + \ddot{e}_2^{CS} = \ddot{e}^C, \quad (4.108b)$$

$$t_1 + t_2 + t_3 = 1. \quad (4.108c)$$

Including $\ddot{e}^C = -(\ddot{e}_1^R + \ddot{e}_2^R)$ into constraint (4.107e), this constraint can be rewritten as

$$\frac{2(\eta_1)^2}{S_{B1}} + \frac{2(\eta_2)^2}{S_{B2}} \geq \frac{(g_{3,1,1}^*)^2}{t_1} + \frac{(g_{3,1,2}^*)^2}{t_2} + \frac{(g_{3,1,3}^*)^2}{t_3} + (\hat{\beta} - \beta_1)\ddot{e}_1^R + (\hat{\beta} - \beta_2)\ddot{e}_2^R. \quad (4.109)$$

Again, let us first fix t_1 , t_2 and t_3 and maximize the slope pair (S_{B1}, S_{B2}) over $\ddot{\mathbf{e}} = [\ddot{e}_1^R, \ddot{e}_2^R, \ddot{e}_1^{CS}, \ddot{e}_2^{CS}]$. The constraints (4.107c) and (4.107d) can be omitted since \ddot{e}_1^{CS} and \ddot{e}_2^{CS} can be made arbitrarily large without having any affect on the other constraints. Then, the region is defined by (4.107a), (4.107b) and (4.109). Note that the right-hand side of (4.107a) and (4.107b) linearly decrease with \ddot{e}_1^R and \ddot{e}_2^R , respectively, whereas the right-hand side of (4.109) linearly increases with both \ddot{e}_1^R and \ddot{e}_2^R . Consequently, the maximum slopes in the boundary of the rate region are obtained with the constraints (4.107a), (4.107b) and (4.109) satisfied with equality. Solving the resultant system of equations, replacing the functions $\dot{g}_{i,i,j}^*$ obtained in (4.79), and using the equivalence $\eta_1 = \theta\eta_2$, we obtain

$$\frac{2\hat{\beta}\theta}{\hat{\eta}} \frac{1}{S_{B1}} + \frac{2\hat{\beta}}{\hat{\eta}_2\theta} \frac{1}{S_{B2}} = \frac{(\Psi_1)^2}{t_1} + \frac{(\Psi_2)^2}{t_2} + \frac{(\Psi_3)^2}{t_3} \quad (4.110)$$

with

$$(\Psi_1)^2 = \left(\frac{\hat{\beta}}{\hat{\eta}_1} - 1 \right) \theta + \left(\frac{\beta_1}{\alpha_{12}} \right)^2 \theta, \quad (4.111a)$$

$$(\Psi_2)^2 = \left(\frac{\hat{\beta}}{\hat{\eta}_2} - 1 \right) \frac{1}{\theta} + \left(\frac{\beta_2}{\alpha_{21}} \right)^2 \frac{1}{\theta}, \quad (4.111b)$$

and

$$(\Psi_3)^2 = (\Psi_{31} + \Psi_{32})^2, \quad (4.111c)$$

$$\Psi_{31} = \left(1 - \frac{\beta_1}{\alpha_{12}}\right) \sqrt{\theta}, \quad (4.111d)$$

$$\Psi_{32} = \left(1 - \frac{\beta_2}{\alpha_{21}}\right) \sqrt{\frac{1}{\theta}}. \quad (4.111e)$$

The slopes (S_{B1}, S_{B2}) can be maximized by minimizing the right-hand side of (4.110) over $\mathbf{t} = [t_1, t_2, t_3]$ while satisfying $t_1 + t_2 + t_3 = 1$. By doing so, we get

$$\frac{1}{t_2^*} = \left(1 + \frac{\Psi_3}{\Psi_2}\right) \frac{1}{1 - t_1}, \quad \frac{1}{t_1^*} = 1 + \frac{\Psi_2 + \Psi_3}{\Psi_1} \quad (4.112)$$

which substituted into (4.110) provides the slope pair

$$\frac{2\hat{\beta}\theta}{\hat{\eta}_1} \frac{1}{S_{B1}} + \frac{2\hat{\beta}}{\hat{\eta}_2\theta} \frac{1}{S_{B2}} = (\Psi_{13} + \Psi_{23})^2 \quad (4.113)$$

with $\Psi_{13} = \Psi_1 + \Psi_{31}$ and $\Psi_{23} = \Psi_2 + \Psi_{32}$ which, after few manipulations, can be shown to be equal to the FS region in (4.17) for the case where both nodes cooperate. ■

4.7.4 Joint Coding with TDMA

As discussed in the previous section, in this case we only consider that both nodes cooperate, transmissions are synchronous and have FD capabilities. In addition, the channel gains are assumed to satisfy $\alpha_{21} > \beta_1$ and $\alpha_{12} > \beta_2$ as the cooperation of both users only obtains the maximum RPE pair in that case. The rate region is described by the rate constraints in (4.50).

Theorem 4.10 *Let the rates vanish while keeping $R_1 = \theta R_2$, the CMAC slope region (S_1, S_2) if both users cooperate by time-division, with FD terminals and synchronous transmissions is*

$$\mathcal{S}_{JCTD}(\theta) = \left\{ (S_1, S_2) \in \mathbb{R}_+^2 : S_1 \leq S_{B1}, S_2 \leq S_{B2}, \right. \\ \left. S_{B1} = \theta S_{B2}, \frac{2\hat{\beta}\theta}{\hat{\eta}_1} \frac{1}{S_{B1}} + \frac{2\hat{\beta}}{\hat{\eta}_2\theta} \frac{1}{S_{B2}} = (\Psi_1 + \Psi_2)^2 \right\} \quad (4.114)$$

with

$$(\Psi_1)^2 = \left(\frac{\beta_1}{\alpha_{12}} \sqrt{\theta} + \left(1 - \frac{\beta_2}{\alpha_{21}}\right) \frac{1}{\sqrt{\theta}} \right)^2 + \left(\frac{\hat{\beta}}{\hat{\eta}_1} - 1 \right) \theta, \quad (4.115a)$$

$$(\Psi_2)^2 = \left(\frac{\beta_2}{\alpha_{21}} \frac{1}{\sqrt{\theta}} + \left(1 - \frac{\beta_1}{\alpha_{12}}\right) \sqrt{\theta} \right)^2 + \left(\frac{\hat{\beta}}{\hat{\eta}_2} - 1 \right) \frac{1}{\theta} \quad (4.115b)$$

where $\hat{\eta}_1 = \frac{\alpha_{12}\hat{\beta}}{\alpha_{12} + \hat{\beta} - \beta_1}$, $\hat{\eta}_2 = \frac{\alpha_{21}\hat{\beta}}{\alpha_{21} + \hat{\beta} - \beta_2}$ and with $\hat{\beta}$ as defined in Theorem 4.1.

Proof: The second-order derivatives of the rate constraints in (4.46), evaluated at $E = 0$, provide the following constraints on the slope pairs in the boundary of the rate region

$$\frac{2(\eta_1)^2}{S_{B1}} \geq \frac{(\dot{g}_{1,1,1}^*)^2}{t_1} - \alpha_{12}\ddot{e}_1^R, \quad (4.116a)$$

$$\frac{2(\eta_2)^2}{S_{B2}} \geq \frac{(\dot{g}_{2,1,2}^*)^2}{t_2} - \alpha_{12}\ddot{e}_2^R, \quad (4.116b)$$

$$\frac{2(\eta_1)^2}{S_{B1}} \geq \frac{(\dot{g}_{1,2,1}^*)^2}{t_1} + \frac{(\dot{g}_{1,2,2}^*)^2}{t_2} - \beta_1\ddot{e}_1^R - \hat{\beta}_2\ddot{e}_2^{CS}, \quad (4.116c)$$

$$\frac{2(\eta_2)^2}{S_{B2}} \geq \frac{(\dot{g}_{2,2,1}^*)^2}{t_1} + \frac{(\dot{g}_{2,2,2}^*)^2}{t_2} - \beta_2\ddot{e}_2^R - \hat{\beta}_1\ddot{e}_1^{CS}, \quad (4.116d)$$

$$\frac{2(\eta_2)^2}{S_{B2}} + \frac{2(\eta_1)^2}{S_{B1}} \geq \frac{(\dot{g}_{3,1,1}^*)^2}{t_1} + \frac{(\dot{g}_{3,1,2}^*)^2}{t_2} - \beta_1\ddot{e}_1^R - \hat{\beta}_1\ddot{e}_1^{CS} - \beta_2\ddot{e}_2^R - \hat{\beta}_2\ddot{e}_2^{CS} \quad (4.116e)$$

with \dot{g}^* given in (4.83). Additionally, the resource constraints require that

$$\ddot{e}_1^R + \ddot{e}_1^{CS} + \ddot{e}_2^{CS} + \ddot{e}_2^R = 0, \quad (4.117a)$$

$$\ddot{e}_1^{CS} + \ddot{e}_2^{CS} = \ddot{e}^C, \quad (4.117b)$$

$$t_1 + t_2 = 1. \quad (4.117c)$$

Plugging $\ddot{e}^C = -(\ddot{e}_1^R + \ddot{e}_2^R)$ into the sum rate constraint (4.116e), we can rewrite it as

$$\frac{2(\eta_2)^2}{S_{B2}} + \frac{2(\eta_1)^2}{S_{B1}} \geq \frac{(\dot{g}_{3,1}^*)^2}{t_1} + \frac{(\dot{g}_{3,2}^*)^2}{t_2} + (\hat{\beta} - \beta_1)\ddot{e}_1^R + (\hat{\beta} - \beta_2)\ddot{e}_2^R. \quad (4.118)$$

Let us first fix t_1 and t_2 and maximize the slopes over $\ddot{\mathbf{e}} = [\ddot{e}_1^R, \ddot{e}_2^R, \ddot{e}_1^{CS}, \ddot{e}_2^{CS}]$. The constraints (4.116c) and (4.116d) can be omitted since \ddot{e}_1^{CS} and \ddot{e}_2^{CS} can be arbitrarily large without having any effect on the other constraints. Then, the region is defined by (4.116a), (4.116b) and (4.118). Note that the right-hand side of (4.116a) and (4.116b) linearly decrease with \ddot{e}_1^R and \ddot{e}_2^R , respectively, whereas the right-hand side of the constraint (4.118) linearly increases with both, \ddot{e}_1^R and \ddot{e}_2^R . Consequently, the maximum slope pair is obtained with the constraints (4.116a), (4.116b) and (4.118) satisfied with equality. Solving the resultant linear system of equations, using the equivalence $\eta_1 = \theta\eta_2$, and substituting the functions \dot{g}^* found in (4.83) we obtain

$$\frac{2\hat{\beta}\theta}{\hat{\eta}_1} \frac{1}{S_{B1}} + \frac{2\hat{\beta}}{\hat{\eta}_2\theta} \frac{1}{S_{B2}} = \frac{(\Psi_1)^2}{t_1} + \frac{(\Psi_2)^2}{t_2} \quad (4.119)$$

with Ψ_1 and Ψ_2 given in (4.115). Minimizing the right-hand side of (4.119) over t_1 , the slope region is maximized at

$$\frac{1}{t_1^*} = 1 + \frac{\Psi_2}{\Psi_1} \quad (4.120)$$

which substituted into (4.119) provides the slope region in Theorem 4.10. \blacksquare

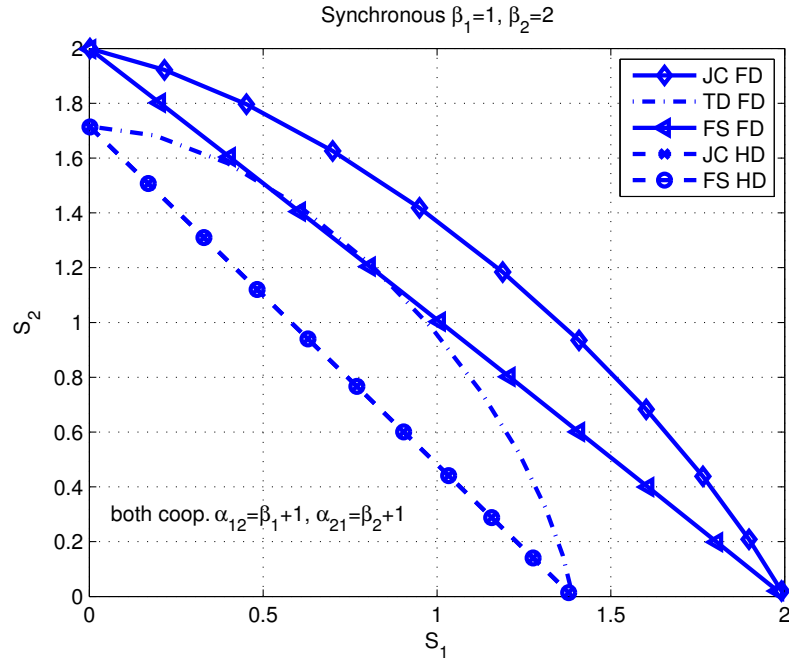


Figure 4.7: Slope regions if both users cooperate.

4.8 Numerical Results

In Section 4.6, we have seen that neither the duplexing nor the joint coding capabilities can improve the maximum RPE pair attained by flow-separation with HD terminals. Thus, all the proposed strategies need to be compared in terms of the slope region. We use the notation of Table 4.9 to designate each of the possible configuration. Depending on the relative channel strengths among nodes, four possible cooperative scenarios appear:

Both Users Cooperate

In this chapter, we have considered a total power constraint and transmitter CSI. As shown in Section 4.6, under these conditions, both nodes cooperate to obtain the maximum RPE pair if and only if: *i*) the channel gains satisfy ($\alpha_{12} \geq \beta_1$ and $\alpha_{21} \geq \beta_2$) and *ii*) transmissions are synchronous. In Fig. 4.7, we compare the five proposed transmission strategies, according to Table 4.9. It is possible to observe that the full duplex capability provides higher gains than those provided by the joint coding capability. In fact, FD terminals and simultaneous transmissions are necessary requirements to obtain the maximum slope in the corner points of the region (where the cooperative node is dedicated relay). Moreover, as we have shown in Theorem 4.9, for HD nodes there is no slope gain by using JC techniques, even though the number of transmission intervals has been reduced from 4 with FS to 3. The JC gain can only be observed whenever the terminals work in FD mode. Considering only FD terminals, the importance of simultaneous transmissions is especially remarkable in the corner point of the

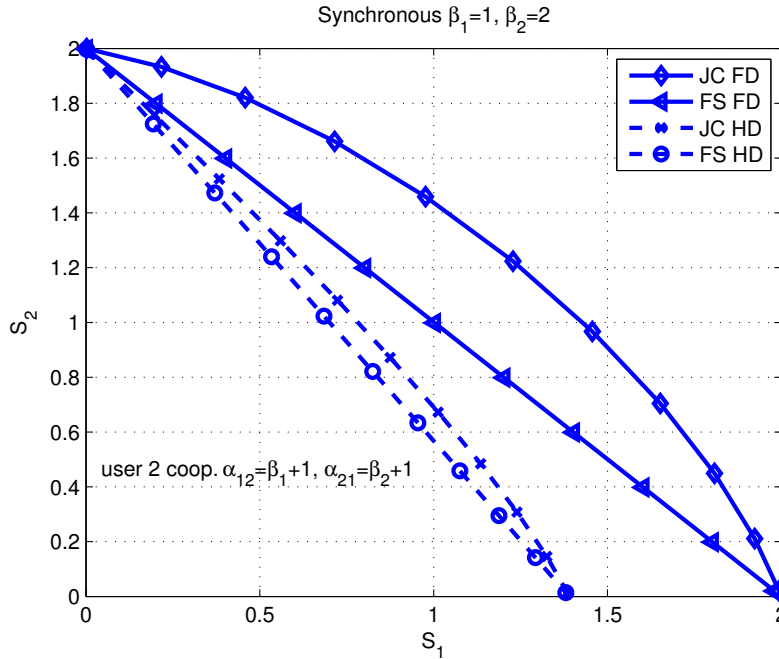


Figure 4.8: Slope regions if only user 2 cooperates.

region. There, the FS strategy reduces to the dedicated FD relay one, while the TD strategy reduces to the dedicated HD relay one, losing the advantage of working in FD mode. For any other point of the region, depending on the particular channel gain conditions, the TD strategy can outperform FS.

Only User 2 Cooperates

For this cooperative scenario, the cooperative user is the node experiencing the most favorable channel condition to the destination ($\beta_2 > \beta_1$). To obtain the maximum RPE pair it is also required that $\alpha_{12} > \beta_1$, see Fig. 4.5. Under these conditions, we depict in Fig. 4.8 the four proposed strategies. We have only focused on synchronous transmission, although the same conclusions are valid for asynchronous ones. Again, the slope region enhancement is mainly due to the full duplex capabilities at the cooperative terminals *i.e.* it allows node 2 to obtain the maximum slope ($S = 2$) in the corner point. For HD terminals, joint coding reduces the required transmission intervals from 3 with FS to 2. There exist some joint coding gains with HD nodes, however these gains are significantly smaller than the ones obtained with FD terminals.

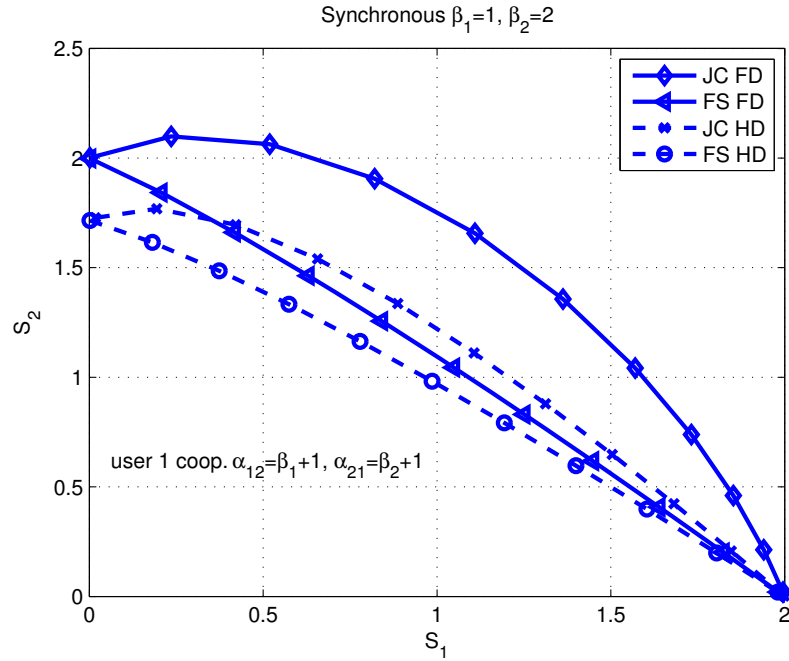


Figure 4.9: Slope regions if only user 1 cooperates.

Only user 1 cooperates

For this cooperative scenario, the cooperative user is the node experiencing the worst channel condition to the destination ($\beta_2 > \beta_1$). As for the scenario where both nodes cooperate, under the total power constraint and CSI at the transmitters this scenario only obtains the maximum RPE pair if transmissions are synchronous and ($\alpha_{21} > \beta_2, \alpha_{12} < \beta_1$), see Fig. 4.5. Under these conditions, we depict in Fig. 4.9 the four strategies proposed. Again, the FD capability is necessary to obtain the slope in the edges of the region. Nevertheless, in this case the use of joint coding with HD nodes, can outperform the FS strategy with FD terminals in most of the slope region.

No User Cooperates

If the channel gains satisfy ($\beta_1 > \alpha_{12}$ and $\beta_2 > \alpha_{21}$) then, the maximum RPE pair even with synchronous transmissions, is obtained without user cooperation, see Fig. 4.5. In addition, the FD capability is not required since nodes do not listen to each other. In Fig. 4.10, we compare the slope region obtained with simultaneous transmissions using joint coding and with time-division between users.

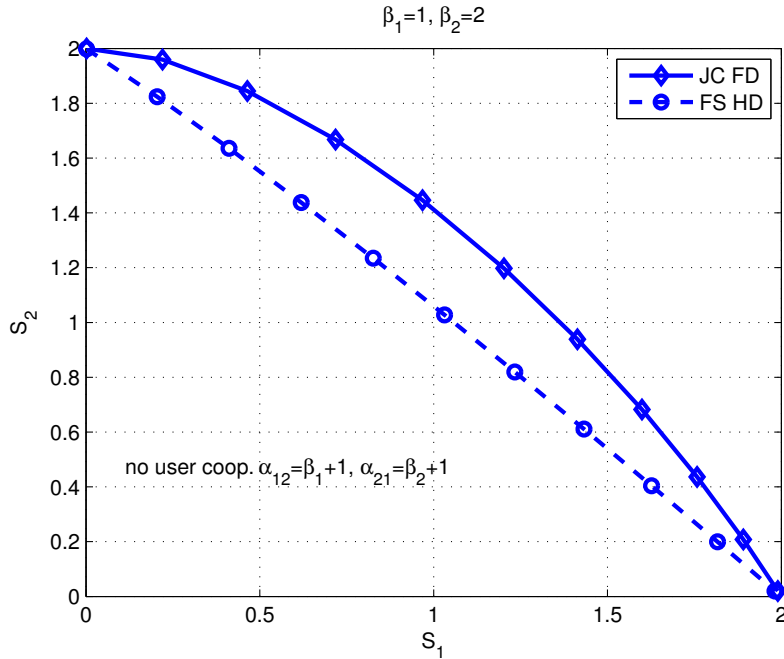


Figure 4.10: Slope regions if no user cooperates.

4.9 Chapter Summary and Conclusions

In this chapter, we have studied the energy efficient regime for the multiple-access channel with cooperative users. Cooperation is built upon *decode-and-forward*. We have discussed the gains provided by synchronism, optimal resource allocation, full duplex, joint coding and simultaneous transmissions capabilities at terminals. To that end, achievable rate regions for each of the possible cooperative scenarios have been proposed and compared in the energy efficient regime. We showed that only synchronism can enhance the maximum RPE pair. The gains obtained by duplexing, optimal resource allocation, joint coding, and simultaneous transmissions capabilities are studied by computing the slopes of the users spectral efficiencies with the energy per bit. We found that, whenever we need orthogonal transmission intervals, a system that does not optimize the fraction of the channel dedicated to each interval requires up to 100% more of the minimum bandwidth. In addition, we found that the bandwidth losses incurred by the suboptimal linear power allocation is much more relevant for FD than for HD nodes. Regarding duplexing and joint coding capabilities, it has been shown that, while joint coding only provides significant gains combined with the full duplex capability, the full duplex capability always provides important gains.

Appendix 4.A Derivatives of the Rate Constraints

Here, we compute, at $E = 0$, the first and second-order derivatives with respect to the total power of the individual rate constraints in (4.35). Let us consider the power $\mathbf{E}(E)$, and the time sharing parameter $x(E)$ as functions of the total power E , $\dot{\mathbf{e}} \triangleq \dot{\mathbf{E}}(0)$, $\ddot{\mathbf{e}} \triangleq \ddot{\mathbf{E}}(0)$ and $\tau(0) \triangleq \mathbf{t}$. Hereafter, for the ease of notation, we remove the explicit dependence on E in all the functions and in its derivatives. The individual rate constraints in (4.35) can be generally written as

$$R_l(E) \leq \sum_{j=1}^3 C_{E_{l,j}}(E) \quad (4.121)$$

with

$$C_{E_{l,j}}(E) = \tau_j(E) \log(1 + g_{E_{l,j}}(E)). \quad (4.122)$$

and $g_{E_{l,j}}(E) = g_{l,j}(\mathbf{E}(E))$. Computing the first-order derivative of (4.122), we obtain

$$\dot{C}_{E_{l,j}}(E) = \dot{\tau}_j(E) \log(1 + g_{E_{l,j}}(E)) + \frac{\tau_j \dot{g}_{E_{l,j}}(E)}{1 + g_{E_{l,j}}(E)}. \quad (4.123)$$

At $E = 0$, $g_{E_{l,j}}(0) = 0$ and the first-order derivative $\dot{g}_{E_{l,j}}(0)$ only depends on $\dot{\mathbf{e}}$. Then, $\dot{C}_{E_{l,j}}(0)$ is

$$\dot{C}_{E_{l,j}}(0) = t_j \dot{g}_{E_{l,j}}(\dot{\mathbf{e}}). \quad (4.124)$$

Computing the second-order derivative of (4.122), we obtain

$$\begin{aligned} \ddot{C}_{E_{l,j}}(E) &= \frac{\dot{\tau}_j(E) \dot{g}_{E_{l,j}}(E)}{1 + g_{E_{l,j}}(E)} + \ddot{\tau}_j(E) \log(1 + g_{E_{l,j}}(E)) \\ &+ \frac{[\dot{\tau}_j \dot{g}_{E_{l,j}}(E) + \tau_j(E) \ddot{g}_{E_{l,j}}(E)] (1 + g_{E_{l,j}}(E)) - (\dot{g}_{E_{l,j}}(E))^2 \tau_j(E)}{(1 + g_{E_{l,j}}(E))^2}. \end{aligned} \quad (4.125)$$

At $E = 0$, $g_{E_{l,j}}(0) = 0$ and $\ddot{g}_{E_{l,j}}(0)$ only depends on $\dot{\mathbf{e}}$ and $\ddot{\mathbf{e}}$. Then, $\ddot{C}_{E_{l,j}}(0)$ is

$$\ddot{C}_{E_{l,j}}(0) = 2\dot{t}_j \dot{g}_{E_{l,j}}(\dot{\mathbf{e}}) + t_j [\ddot{g}_{E_{l,j}}(\dot{\mathbf{e}}, \ddot{\mathbf{e}}) - (\dot{g}_{E_{l,j}}(\dot{\mathbf{e}}))^2]. \quad (4.126)$$

Finally, particularizing for the individual rate conditions in (4.35). We obtain the result in (4.96a) with $\mathbf{E} = [P_1^R, P_1^D, P_2^D]$, $g_{1,1} = \frac{\alpha_{12} P_1^R}{1 + \alpha_{12} P_1^D}$, $g_{1,2} = \beta_1 P_1^D$, $g_{1,3} = \frac{\beta_1 P_1^D}{1 + \beta_2 P_2^D}$ and $\tau_1 = 1$, $\tau_2 = x_0$, $\tau_3 = 1 - x_0$. The second-order derivative in (4.96b) is obtained with $\mathbf{E} = [P_2^R, P_2^D, P_1^D]$, $g_{1,1} = \frac{\alpha_{21} P_2^R}{1 + \alpha_{21} P_2^D}$, $g_{1,2} = \beta_2 P_2^D$, $g_{1,3} = \frac{\beta_2 P_2^D}{1 + \beta_1 P_1^D}$ and $\tau_1 = 1$, $\tau_2 = 1 - x_0$, and $\tau_3 = x_0$.

Chapter 5

The Multiple Relay Multi-Hop Channel

In this chapter, we address the multi-hop multiple relay channel also referred to as the cooperative multi-hop (CMH) channel. This channel consists of a single source that communicates with a single destination assisted by several relay nodes that listen to all the transmissions. This channel model includes, as a special case, the parallel or two-hop multiple relay channel in which relays only listen to the source transmission.

Introducing relay capabilities in a network has a strong effect on the information flow that extends to all communication levels, from the achievable rate to the routing strategy. A fundamental understanding of the role that relays play in wireless networks is of paramount importance to design efficient protocols for future communication systems.

With this purpose, in this chapter, we address the study of the CMH channel in the energy efficient regime. Opposite to previous chapters, in this case we only conduct the first-order analysis of the spectral efficiency, i.e., the maximum rate per energy (RPE). The slope of the spectral efficiency (second-order) is not addressed. Although, the slope was found useful in previous chapters to study the gains provided by transmitting simultaneously using full duplex nodes, each of the multi-hop strategies analyzed in this chapter obtain different maximum RPE and, thus, can not be compared in terms of the slope of the spectral efficiency.

In addition, the study is limited to the following scenario:

- *Constant channel gains*: The channel is assumed to remain constant over all the transmission and is frequency flat. The results we obtain here can be used as a first step towards the study of more involved time-varying channels.
- *Phase asynchronous transmissions*: We assume that signals do not arrive coherently combined to the receiving nodes. Synchronous transmissions need that separate microwave oscillators at different nodes are synchronized. It might be possible to couple oscillators, and very closely spaced nodes could even autocouple, but this requires non-trivial microwave innovation.
- *Orthogonal transmissions*: As shown in Chapter 3 if relays are *asynchronous*, the use of simultaneous transmissions by using *full duplex* terminals can not increase the maximum RPE. Thus, orthogonal transmissions are optimal in the maximum RPE sense.

By maximizing the RPE, we *analyze* different transmissions schemes and also provide a joint solution to a set of *design problems* that traditionally belong to different layers: power allocation (physical), relay selection, and routing (network).

Analysis: The energy efficiency or low power regime analysis for different multiple relay networks can be found in [71–74]. We use the energy efficiency analysis to discuss the impact of the accumulative capability and the decoding requirements imposed at terminals.

- Depending on the *receiving capability*, relays and destination can be *accumulative* (AC), if nodes use multiple received signals or *non-accumulative* (NAC) if only a single received signal is used. Two main accumulative approaches have been considered in the literature: energy or mutual-information accumulation. Energy accumulation can be performed at the receiving nodes, e.g., through space-time coding or repetition coding [75–77]. Mutual-information accumulation is proposed in [78, 79]. It can be realized using rateless codes of which fountain and raptor codes are two prominent examples.

Notice that at low signal-to-noise ratios, which is the focus of this thesis, energy accumulation is actually equivalent to mutual-information accumulation.

Accumulation mechanisms are considered in current and next generation standards. However, acting so at each node would inevitably consume a vast amount of resources. In a general wireless network, each node would need to store multiple signals of multiple sources simultaneously. Since nodes acting as relays cannot directly benefit from their transmission, in most of the cases, it is difficult to justify the huge amount of resources that the AC relays need. In some applications, the relays may have only limited memory and signal processing capability, and thus can not combine all these signals. In addition, the signals received from remote nodes bring insignificant information to the decoding of the message and it may not pay off to include these signals in the decoding of the message.

- Depending on the *decoding requirement* at the relays, the scenario can be *allcast*, where all the relays decode the complete source message or *unicast*, where only the destination recovers the message.

Design:

The network design is here addressed from the physical layer to the network layer. The study of wireless networks using information theory has led to novel network protocols [80–85] that are asymptotically order-optimal as the number of nodes goes to infinity. However, the gap between information-theoretic results and practical implementation can be huge. Likewise [86, 87], we focus on networks with a finite number of nodes and with an emphasis on the distributed implementation aspects. We maximize the spectral efficiency in the low power regime for a given total power. In doing so, we find optimal solutions to the power allocation, relay selection, and routing. These solutions give us useful guidelines on how to organize multi-hop communications: which relays will aid the communication, under what channel conditions do they it, and who decides (the mobiles themselves or the a central base station).

Given that the transmission scheme chosen strongly impacts on the resource allocation and routing solutions. Among all possibilities, we try to identify schemes for which the solution to the maximum RPE problem allows us to find a distributed solution to the power allocation and relay ordering (route). This distributed structure might be useful to design practical schemes.

5.1 Related Work and Contributions

Single relay: The optimal relaying strategy is still unknown even for the simple one-relay channel. In [28], the two basic relaying strategies were stated for the single relay network (hereafter referred to as *regenerative* and *non-regenerative*). In the case of regenerative strategies, each relay makes a hard decision about a previously transmitted codeword before transmitting. In the case of non-regenerative strategies such as, *amplify and forward* or *compress and forward*, hard decisions are only taken at the destination, while relays transmit information about the received signals, rather than the message they carry.

Two-hop multiple relay: In the two-hop multiple relay or multiple-parallel relay channel, the relays only listen to the source transmission. This channel was first studied in [88, 89]. For the particular case of orthogonal transmission, achievable rates can be found in [90] for decode and forward in [91] for amplify and forward.

Multiple relay: The extension of the results in [28] to multi-hop and multiple relays has recently attracted a lot of interest [54, 71, 80, 81, 84, 92]. Achievable rates with compress and forward and superposition coding schemes can be found in [84, Theorems 3 and 4]. In the particular case of multiple relay networks with regenerative relays, on which current work is

focused, there is no known strategy that consistently outperforms the others. The use of regenerative relays for multi-hop cooperative transmissions was initially conceived for allcast communications. In that case, an achievable rate was presented in [80] based on *irregular* encoding (parity forwarding) with successive decoding. This rate was enhanced in [71, 92] with a coding scheme based on *regular encoding* and *joint decoding*. By removing the allcast requirement, recently in [54], new achievable rates for multiple relay networks have been obtained that also generalize all previous results. The coding strategy derived in that work is based on irregular encoding with joint decoding.

We organize our contributions as follows:

- Before studying the general multi-hop multiple relay network, we address the particular case of the two-hop multiple relay network. In this scenario, the source transmission is listened to by multiple relay nodes. These nodes, only using the received signal from the source, transmit directly to the destination. We consider the achievable rate with decode and forward at the relays and the cut-set capacity upper bound (CB).
- Then, we study different multi-hop multiple relay achievable rates and capacity upper bounds, subject to different capabilities / requirements at terminals, which are summarized in Table 5.1:
 - First, the traditional multi-hop (TMH) network is studied as a benchmark scenario. Each node employs only the signal received from the immediately previous relay to decode the source-transmitted message before re-encoding and transmitting it.
 - Then, allcast cooperative multi-hop networks [81] with AC relays (ACMH) and with NAC relays (ACMH_{NAC}) are addressed:

For the ACMH scenario, relays are required to first, optimally combine all the received signals and then, fully decode the source message (allcast). Unfortunately, these two requirements do not allow a solution with a distributed structure. In [77], it was shown that for the ACMH scenario the optimal routing is an NP-complete problem. The optimal power allocation and route to achieve a certain fixed rate with a sum power constraint was studied in [93, 94]. There it was found that the optimal route is a sequential path, namely only one node uses the same previous transmission to decode the source message. For a given route, an optimal recursive power-filling procedure was presented. However only heuristic algorithms to find a good sequential path (route) from the source to the destination were found. We study this strategy in the low power regime, our analysis reveals the inherent structure of this communication strategy. Although the optimal route discovering algorithm found needs also exhaustive search, the algorithm presented can be used to design channel feedback signaling due to its *backward* nature (from the destination to the source) and to find suboptimal but distributed route discovering algorithms.

Table 5.1: Multi-hop multiple relay transmission strategies depending on the terminals capabilities and decoding requirements.

Relays Decoding Requirements	Receiving Capabilities (Relay/Destination)		
	NAC/NAC	NAC/AC	AC/AC
allcast	TMH	ACMH _{NAC}	ACMH
unicast	X	UCMH	CB/UP _R

The ACMH_{NAC} scenario was considered in [95]. Although the problem was simplified, only suboptimal conditions to improve a given route were derived. We here show that the optimal route can be found using the recursive and backward algorithm obtained for the unicast cooperative network.

- Then, we investigate the unicast cooperative multi-hop (UCMH) network with NAC relays. The UCMH network is shown to generalize TMH. In this scenario, relays do not need to decode the source message, but merely the message (*bin index*) transmitted by the immediately previous node. The achievable rate is enhanced, since only the first relay and the destination, after listening to all transmissions, are required to decode the source message (unicast).
- As shown in [54], in the context of regenerative relaying, there exist a huge number of possible coding schemes, each one providing a different achievable rate. We study an upper bound on any regenerative (*parity forwarding*) strategy.
- Finally, the cut-set upper bound is considered. This upper bound is valid for all type of relays and has been shown to be achievable in other communication scenarios [16].

The remainder of the chapter is organized as follows. First, we present the network model in Section 5.2. Then, in Section 5.3, we introduce the energy efficiency analysis particularized to multiple relay networks. Section 5.4 is devoted to the two-hop multiple relay network. In subsequent sections, we study the multi-hop multiple relay networks. The TMH network is studied in Section 5.5. The ACMH network is addressed in Section 5.6. The UCMH is investigated in Section 5.7. The upper bound on the regenerative strategy is studied in Section 5.8 and the CB is considered in Section 5.9. In Section 5.10, simulation results are provided and finally, concluding remarks are made in Section 5.11.

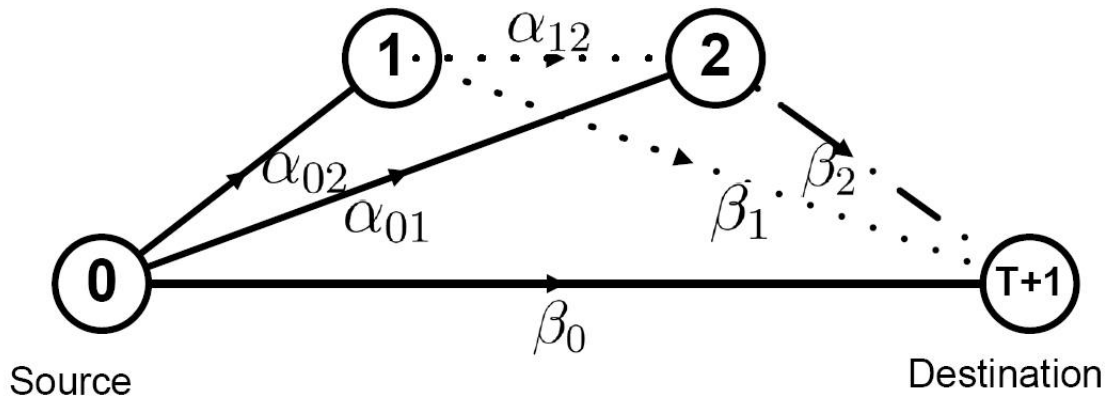


Figure 5.1: Two-relay network model.

5.2 Network Model

Consider a relay network where a single source communicates with a single destination assisted by up to T relays. The communication is divided into $T + 1$ orthogonal transmissions. Without loss of generality, hereafter, we consider a fixed total bandwidth and that the transmissions are orthogonal in time. In Fig. 5.1, the 2-relay scenario is depicted. The order of relay transmissions or the “route” from the source to the destination is denoted with the set π of cardinality $T = |\pi|$. For the sake of simplicity, we denote the source node as $i = 0$, the destination as $i = T + 1$ and the i -th relay in π as $[\pi]_i = i$. Let us also denote π_i as the ordered set of relays $(i, \dots, T]$, and π_i^C the ordered set of relays $[1, \dots, i]$.

The communication is organized as follows: the source transmits the signal X_0 to every node in the network. Each of the relay nodes that belong to the route $i \in \pi$ receives Y_i^j from the previous source and relay transmissions $j \in [0, 1, \dots, i - 1]$ and transmits X_i . The destination receives Y^j from all the transmissions $j \in [0, 1, \dots, T]$. The received symbols, from each orthogonal transmission $j \in [0, 1, \dots, T]$, at the relay $i \in \pi$ and at destination are

$$\begin{aligned} Y_i^j &= \sqrt{\alpha_{ji}} X_j + Z_{ij}, \quad j \in [0, 1, \dots, i - 1], \quad i \in \pi, \\ Y^j &= \sqrt{\beta_j} X_{j0} + Z_{T+1j}, \quad j \in [0, \dots, T]. \end{aligned} \quad (5.1)$$

We assume, without claim of optimality that the signals transmitted by the source X_0 and the relays X_i , are random variables independent, complex Gaussian with zero mean and power P_0 and P_i , respectively. The noise process at relays and destination Z_{ij} are complex independent white Gaussian, each one with zero mean and unit variance $\mathbb{E}[|Z_{ij}|^2] = N_0 = 1$. The channel gain from the relay node i to the destination is denoted as β_i , and the channel gain from the relay i to the relay j as $\alpha_{i,j}$. Each orthogonal transmission interval uses a fraction τ_j out of the total transmission time available with $\sum_{j=0}^T \tau_j = 1$. Then, the fraction of power assigned to node i during the time-sharing fraction τ_j is $E_i = \tau_j P_i$ if $j = i$ and 0 otherwise. Finally, the signal to noise ratio (SNR) is defined as $\text{SNR} \triangleq \frac{E}{N_0}$, where $E = \sum_{i=0}^T E_i$ is the total power constraint.

5.3 The Energy Efficiency Analysis

In this section, first we introduce the spectral efficiency functions considered in this chapter. Then, the energy efficiency analysis is particularized to these functions.

For notation convenience, the spectral efficiency expressions $R(E)$ are written as functions of the total power E instead of as function of the SNR. If the time-sharing fractions $\boldsymbol{\tau} = \{\tau_0, \dots, \tau_T\}$ and the user's power $\mathbf{E} = \{E_0, \dots, E_T\}$ are fixed, all the rates or spectral efficiency expressions $R_F(\boldsymbol{\tau}, \mathbf{E})$ that appear in this chapter can be written as the minimum of a set of rate limits as

$$R_F(\boldsymbol{\tau}, \mathbf{E}) = \min_l C_l(\boldsymbol{\tau}, \mathbf{E}) \quad (5.2)$$

where the rate limits C_l read

$$C_l(\boldsymbol{\tau}, \mathbf{E}) = \sum_{j=0}^T \tau_j \log \left(1 + \frac{g_{jl}(E_j)}{\tau_j} \right) \quad (5.3)$$

and all the functions $g_{jl}(E_j)$ are linear in E_j . Then, the spectral efficiency as a function of the total power E , denoted by $R^*(E)$, is the solution to the following problem for all E

$$R^*(E) = \max_{\boldsymbol{\tau}, \mathbf{E}} \min_l C_l(\boldsymbol{\tau}, \mathbf{E}) \quad (5.4a)$$

$$\sum_{j=0}^T \tau_j = 1, \quad \tau_j \geq 0 \quad j \in [0, \dots, T], \quad (5.4b)$$

$$\sum_{j=0}^T E_j = E, \quad E_j \geq 0 \quad j \in [0, \dots, T]. \quad (5.4c)$$

In the energy efficient regime, we are interested in studying the spectral efficiency $R\left(\frac{E_b}{N_0}\right)$ ¹ as a function of the energy we need to assign to each transmitted bit normalized by the noise spectral density N_0 , i.e., $\frac{E_b}{N_0}$. In this chapter, we focus only on the first-order analysis of the rate $R\left(\frac{E_b}{N_0}\right)$, namely, in computing the minimum value of energy per bit $\frac{E_b}{N_{0 \min}}$. In Chapter 3 we have shown that, for spectral efficiency functions defined by (5.4) and (5.3), the low power regime is the energy efficient regime and thus, the $\frac{E_b}{N_{0 \min}}$ can be computed as [1]

$$\frac{E_b}{N_{0 \min}} = \frac{\log_e 2}{\dot{R}^*(0)} \quad (5.5)$$

where $\dot{R}^*(0)$ is the derivative at 0 of $R^*(E)$ in nats. Equivalently, we compute here the maxi-

¹The choice of R and \mathbf{R} avoids the abuse of notation that assigns the same symbol to the spectral efficiency function of SNR or E and $\frac{E_b}{N_0}$.

imum rate per energy normalized by the noise spectral level (RPE), defined as

$$\eta \triangleq \max \text{RPE}, \quad (5.6a)$$

$$\triangleq \max_E N_0 \log_e 2 \frac{R(E)}{E}, \quad (5.6b)$$

$$= \frac{\log_e 2}{\frac{E_b}{N_0 \min}}, \quad (5.6c)$$

$$= \dot{R}^*(0), \quad (5.6d)$$

$$= \frac{\tilde{R}^*(E)}{E}. \quad (5.6e)$$

In definition (5.6b), we consider $R(E)$ in bits². The equality (5.6c) follows from the definition of energy per bit as $E_b = \frac{E}{R(E)}$. Then, equality (5.6d) follows from (5.5). Finally, in equality (5.6e), we use the first-order Taylor expansion of the spectral efficiency, in nats, at $E = 0$, which we denote as $\tilde{R}^*(E) = \dot{R}^*(0) \times E$.

To compute the maximum RPE as (5.6d) or (5.6e), we first need to obtain the rate as a function of the total power $R^*(E)$. However, we are unable to explicitly find the pair $\boldsymbol{\tau}$ and \mathbf{E} that maximizes the rate in (5.4) for all E . Instead, in the following we formulate the direct computation of $\tilde{R}^*(E)$. First, we introduce the notation used:

- We consider that the resource allocation solutions to (5.4) can be any pair of differentiable functions of E , namely $\boldsymbol{\tau}(E)$ and $\mathbf{E}(E)$.
- The first-order Taylor expansion at $E = 0$ of the power vector is given by $\tilde{\mathbf{E}} = [\tilde{E}_0, \dots, \tilde{E}_T]$.
- After substituting $\boldsymbol{\tau}(E)$ and $\mathbf{E}(E)$ into the rate limit function in (5.3), we define
 - The rate limits $C_l(\boldsymbol{\tau}, \mathbf{E})$ as a function of E as $C_{E_l}(E) \triangleq C_l(\boldsymbol{\tau}(E), \mathbf{E}(E))$.
 - The functions $g_{jl}(E_j)$ as a function of E as $g_{E_{jl}}(E) \triangleq g_{jl}(E_j(E))$.

The first-order Taylor expansion of the rate limits C_{E_l} is given by (see previous Chapters)

$$\tilde{C}_{E_l}(E) = \dot{C}_{E_l}(0) E, \quad (5.7a)$$

$$= \sum_{j=0}^T \dot{g}_{E_{jl}} \left(\dot{E}_j(0) \right) E \quad (5.7b)$$

Notice that given (5.7b) and the linearity of $g_{j,l}(E_j)$ in E_j it is clear that $\tilde{C}_{E_l}(E)$ only depends on $\tilde{\mathbf{E}} = [\dot{E}_0(0), \dots, \dot{E}_T(0)]E = [\tilde{E}_0, \dots, \tilde{E}_T]$.

Finally, to find $\tilde{R}^*(E)$, we solve the following problem over $\tilde{\mathbf{E}}$

$$\tilde{R}(E) = \max_{\tilde{\mathbf{E}}} \min_l \tilde{C}_{E_l}(E) \quad (5.8a)$$

$$\sum_{j=0}^T \tilde{E}_j = E, \quad \tilde{E}_j \geq 0 \quad j \in [0, \dots, T]. \quad (5.8b)$$

²However, the derivatives \dot{R} and the first-order Taylor approximations \tilde{R} are given in nats.

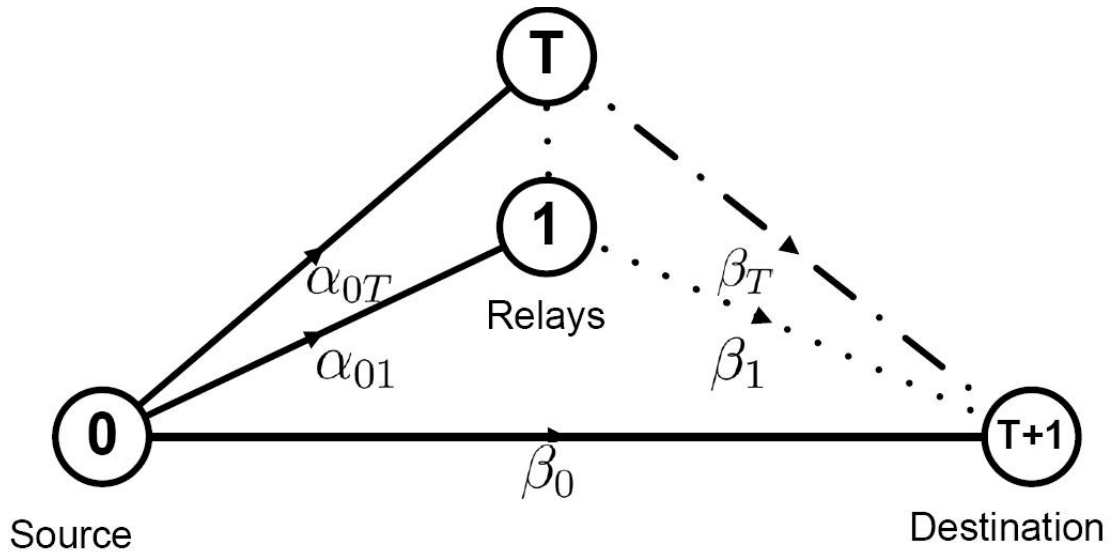


Figure 5.2: Two-hop multiple relay network model.

5.4 Two-Hop Multiple Relay Network

Before studying the general multi-hop multiple relay network, we address the particular case of the two-hop multiple relay network depicted in Fig. 5.2. In this scenario, the source transmission is listened to by multiple relay nodes. These nodes using only the received signal from the source, transmit to the destination according to the transmission order π . For this scenario, relays do not listen to each other or equivalently $\alpha_{ij} = 0$ for all i and j in π . In the following, we study the achievable spectral efficiency with decode and forward at the relays and the cut-set capacity upper bound in the energy efficiency regime.

5.4.1 Decode and Forward

In this case, only relays that are able to decode the source message are allowed to transmit to the destination. Let us denote as \mathcal{T} the non-ordered set of available relays and \mathcal{S} the subset of relays in \mathcal{T} that decode the source message. Then, the following rate is achievable

$$R_F(\boldsymbol{\tau}, \mathbf{E}) \leq \min(C_R, C_D) \quad (5.9)$$

with

$$C_R = \tau_0 \log \left(1 + \alpha_{0\mathcal{S}} \frac{E_0}{\tau_0} \right), \quad (5.10a)$$

$$C_D = \sum_{i \in \{0, \mathcal{S}\}} \tau_i \log \left(1 + \beta_i \frac{P_i}{\tau_i} \right) \quad (5.10b)$$

and $\alpha_{0\mathcal{S}} = \min_{i \in \mathcal{S}} \alpha_{0i}$. There are several coding strategies that achieves this rate. We focus on irregular encoding at the relays (*binnig*) with joint decoding at the destination. The source

broadcasts the message s_0 at a rate R_0 using a codebook $\mathcal{X}_0(\cdot)$ of size $|\mathcal{X}_0| = 2^{nR_0}$. The codewords of $\mathcal{X}_0(\cdot)$ have $\tau_0 n$ i.i.d elements according to a Gaussian distribution with power P_0 and thus uses a fraction τ_0 of the total channel. For a relay $i \in \mathcal{S}$ to successfully decode s_0 , the following inequality must hold:

$$R_0 \leq \frac{\tau_0 n}{n} I(X_0; Y_i) = \tau_0 \log(1 + \alpha_{0i} P_0) \quad \forall i \in \mathcal{S}. \quad (5.11a)$$

The rate is then limited by the relay with the worst source to relay channel state. Thus, we can write, equivalently, the condition in (5.10a). Each of the nodes in the decoding set \mathcal{S} makes an independent random partition of the source codebook \mathcal{X}_0 into $|\mathcal{X}_i| = 2^{nR_i}$ sets of size $|\mathcal{X}_0|/|\mathcal{X}_i| = 2^{n(R_0-R_i)}$. Each of these sets is then identified by a codeword $\mathcal{X}_i(s_i)$ in the relay codebook. Thus, each relay transmits at a rate R_i with an i.i.d Gaussian input $X_i(s_i)$, the bin index s_i identifying the set to which s_0 belongs. The destination makes use of all the received signals to decode the source message. First, it decodes each of the independent bin indices s_i using only the signal received from relay i . This is possible if the following statement holds:

$$R_i \leq \tau_i \log(1 + \beta_i P_i). \quad (5.12)$$

Then, the destination decodes s_0 using all the bin indices s_i . The intersection of all bins indexed by s_i with i in \mathcal{S} forces s_0 to be inside a bin of size $2^{n\left(R_0 - \sum_{i \in \mathcal{S}} R_i\right)}$. Consequently, s_0 can be successfully decoded if

$$R_0 - \sum_{i \in \mathcal{S}} R_i \leq \tau_0 \log(1 + \beta_0 P_0). \quad (5.13)$$

Finally, substituting (5.12) into (5.13) we obtain the rate condition (5.10b).

The achievable rate above assumes a predetermined set \mathcal{S} of active relays. Thus, we need to maximize over all the possible sets $\mathcal{S} \subseteq \mathcal{T}$. As discussed in Section 5.3, the maximum RPE can be computed as $\eta = \frac{\tilde{R}(E)}{E}$ (see (5.6e)). Particularizing the problem in (5.8) to this scenario, $\tilde{R}(E)$ is the solution to

$$\begin{aligned} \tilde{R}(E) &= \max_{\tilde{\mathbf{E}}, \mathcal{S} \subseteq \mathcal{T}} \min \tilde{C}_{E_R}, \tilde{C}_{E_D} \\ \text{s.t.} \quad &\sum_{i \in \{0, \mathcal{S}\}} \tilde{E}_i = E \\ &\tilde{E}_i \geq 0 \quad \forall i \in \{0, \mathcal{S}\} \end{aligned} \quad (5.14)$$

where \tilde{C}_{E_R} and \tilde{C}_{E_D} are the first-order Taylor approximations at $E = 0$ of the rate limits in (5.10). Using (5.7b), we obtain

$$\tilde{C}_{E_R} = \alpha_{0\mathcal{S}} \tilde{E}_0, \quad (5.15a)$$

$$\tilde{C}_{E_D} = \beta_0 \tilde{E}_0 + \sum_{i \in \mathcal{S}} \beta_j \tilde{E}_j. \quad (5.15b)$$

The solution to this problem is presented in the following Theorem.

Theorem 5.1 Given a set of available relays \mathcal{T} , the maximum RPE is obtained using only the best relay i^* and is given by

$$\eta_{DF_{2H}} = \begin{cases} \max_{i \in \mathcal{T}} \frac{\alpha_{0i} \beta_i}{\alpha_{0i} + \beta_i - \beta_0} & \text{if } \beta_{i^*}, \alpha_{0i^*} \geq \beta_0, \\ \beta_0 & \text{otherwise.} \end{cases} \quad (5.16)$$

Assume the best relay is $i^* = 1$. At $E = 0$, the first-order Taylor approximation of the optimal power allocations is given by

$$\begin{aligned} \tilde{E}_1 &= \frac{\alpha_{01} - \beta_0}{\beta_1} \tilde{E}_0, \\ \tilde{E}_0 &= \frac{\eta}{\alpha_{01}} E. \end{aligned} \quad (5.17)$$

Proof: Let us denote as $\tilde{E}_S = \sum_{i \in \mathcal{S}} \tilde{E}_i$ the sum of powers dedicated to the set \mathcal{S} of relays that decode the source message. It is easy to show that, the rate limit \tilde{C}_{E_D} is maximized by dedicating all the power \tilde{E}_S to the node in \mathcal{S} with the best channel gain to the destination $\beta_{i^*} = \max_{i \in \mathcal{S}} \beta_i$. Then

$$\tilde{C}_{E_D} = \beta_0 \tilde{E}_0 + \beta_{i^*} \tilde{E}_S. \quad (5.18)$$

Given that $\alpha_{0\mathcal{S}} = \min_{i \in \mathcal{S}} \alpha_{0i}$, the rate limit \tilde{C}_{E_R} is always maximized by choosing \mathcal{S} to contain only node i^* , namely $\mathcal{S} = i^*$ and $\alpha_{0i^*} = \alpha_{0\mathcal{S}}$. The problem then reduces to a single relay problem:

$$\begin{aligned} \tilde{R} &\leq \max_{\tilde{E}_0, \tilde{E}_S} \min \left(\alpha_{0i^*} \tilde{E}_0, \beta_0 \tilde{E}_0 + \beta_{i^*} \tilde{E}_S \right) \\ \tilde{E}_0 + \tilde{E}_{i^*} &= E. \end{aligned} \quad (5.19)$$

The solution to this problem was found in Chapter 3

$$\eta_{i^*} = \begin{cases} \frac{\alpha_{0i^*} \beta_{i^*}}{\alpha_{0i^*} + \beta_{i^*} - \beta_0} & \text{if } \beta_{i^*}, \alpha_{0i^*} \geq \beta_0, \\ \beta_0 & \text{otherwise.} \end{cases} \quad (5.20)$$

To find i^* , we only need to look for the best node in the scenario \mathcal{T} . Then $\eta_{DF_{2H}} = \max_{i^* \in \mathcal{T}} \eta_{i^*}$. ■

5.4.2 Cut-Set Bound

The cut-set upper bound on the achievable rate is addressed later on in Section 5.9 of this chapter for the general multi-hop multiple relay network. The two-hop multiple relay network is a particular case of this one. For comparison purposes, we introduce here the main results obtained. The reader can find the proofs of these results in Section 5.9.

We denote by \mathcal{T} the set no nodes that contains all the relays in the scenario. Additionally, we define the transmitter set $\mathcal{S} \subseteq \mathcal{T}$ as any of the 2^T possible not ordered subsets that can be created with up to T relays, and the receiver set \mathcal{S}^C as the complement of \mathcal{S} in \mathcal{T} . The rate upper bound is given by (see eq. (5.58)).

$$R_F(\boldsymbol{\tau}, \mathbf{E}) \leq \min_{\mathcal{S}} \tau_0 \log \left(1 + \frac{E_0}{\tau_0} \left(\beta_0 + \sum_{j \in \mathcal{S}^C} \alpha_{0,j} \right) \right) + \sum_{i \in \mathcal{S}} \tau_i \log \left(1 + \beta_i \frac{E_i}{\tau_i} \right). \quad (5.21)$$

The maximum RPE is provided in the following theorem.

Theorem 5.2 *The cut-set upper bound on the maximum RPE for the orthogonal two-hop additive white Gaussian noise (AWGN) channel is given by*

$$\eta_{CB_{2H}} = \frac{\beta_0 + \sum_{i \in \mathcal{S}^*} \alpha_{0i}}{1 + \sum_{i \in \mathcal{S}^*} \frac{\alpha_{0i}}{\beta_i}} \quad (5.22)$$

where \mathcal{S}^* is the subset of \mathcal{T} that satisfies $\mathcal{S}^* = \{i : \eta_{CB_{2H}} \leq \beta_i\}$.

The power allocation achieving (5.22) is given by

$$\begin{aligned} \tilde{E}_0 &= \frac{E}{1 + \sum_{i \in \mathcal{S}^*} \frac{\alpha_{0i}}{\beta_i}}, \\ \tilde{E}_i &= \frac{\alpha_{0i} \tilde{E}_0}{\beta_i} \quad \forall i \in \mathcal{S}^*. \end{aligned} \quad (5.23)$$

The set of active relays $\mathcal{S}^* = \{i : \eta_{CB_{2H}} \leq \beta_i\}$ can be found recursively as described below.

Proof: See the proof for the multi-hop multiple relay network in Theorem 5.8 particularized for $\alpha_{i,j} = 0$ for all i and j in \mathcal{T} . ■

The main conclusions about this result are summarized below:

- *The power allocation* at the relays depends only on local channel state information (CSI): the received power from the source $\alpha_{0i} \tilde{E}_0^*$ and the channel with destination β_i . However, the source requires not only local CSI α_{0i} , but also the channel to destination from all the nodes in \mathcal{S}^* . This power allocation has an intuitive interpretation, relay nodes must allocate as much power as needed to ensure that the destination receives the same power they have received from the source.
- *The set of active relays \mathcal{S}^** can be found recursively. However, the order on which these relays are discovered does not imply any order in the transmission scheduler. The *route-discovering* algorithm is as follows: Initially, we set the maximum RPE equal to that for direct transmission $\eta = \beta_0$. Among all the nodes in the network \mathcal{T} , at each iteration the algorithm discovers a new active relay and includes it in \mathcal{S}^* . This node i^* satisfies $\eta < \beta_{i^*}$ and has the best channel to the destination node of those in (\mathcal{T} subtracting those in \mathcal{S}^*) $i^* = \arg \max_{i \in \mathcal{T} - \mathcal{S}^*} \beta_i$. Then, the source computes the new maximum RPE using all the relays in \mathcal{S}^* as in (5.22). The algorithm finishes whenever the condition ($\eta < \beta_{i^*}$) is not satisfied for any node in $\mathcal{T} - \mathcal{S}^*$.

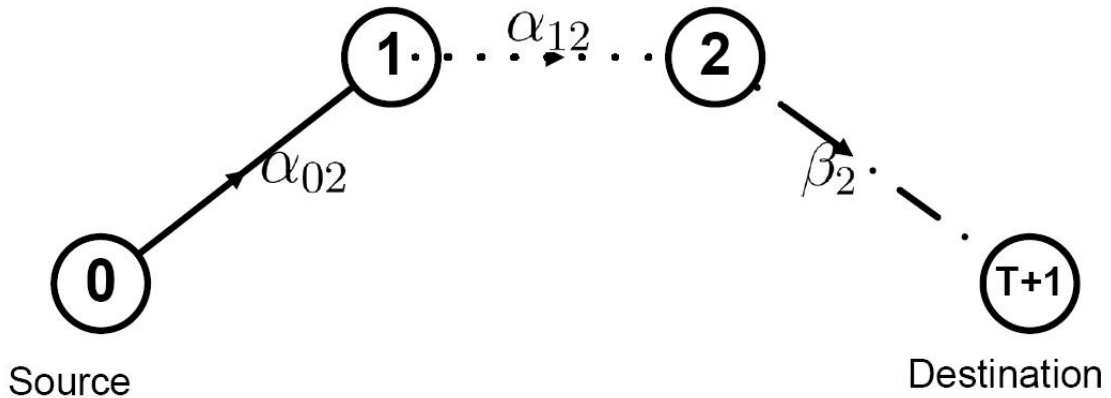


Figure 5.3: Two-relay TMH network model.

5.5 Traditional Multi-Hop Network

For the TMH network, given a relay order π (the route), the achievable rate is bounded by the minimum single-hop communication rate limit

$$R_F(\boldsymbol{\tau}, \mathbf{E}) \leq \min_{i \in \{0, \pi\}} \tau_i \log \left(1 + \alpha_{i, i+1} \frac{E_i}{\tau_i} \right). \quad (5.24)$$

The achievable rate above assumes a predetermined route π of relays. Thus, we need to maximize over all the possible routes. As discussed in Section 5.3, the maximum RPE can be computed as $\eta = \frac{\tilde{R}(E)}{E}$ (see (5.6e)). Particularizing the problem in (5.8) to this scenario, $\tilde{R}(E)$ is the solution to

$$\begin{aligned} \tilde{R} &= \max_{\pi, \tilde{\mathbf{E}}} \min_{i \in \{0, \pi\}} \tilde{C}_{E_i} \\ \text{s.t.} \quad &\sum_{i \in \{0, \pi\}} \tilde{E}_i = E, \\ &\tilde{E}_i \geq 0 \quad \forall i \in \{0, \pi\} \end{aligned} \quad (5.25)$$

where \tilde{C}_{E_i} for all $i \in \{0, \pi\}$ are the first-order Taylor approximations at $E = 0$ of the rate limits in (5.24). Using (5.7b), we obtain

$$\tilde{C}_{E_i} = \tilde{E}_i \alpha_{i, i+1}. \quad (5.26)$$

Before giving the solution to (5.25) in the next theorem, we introduce the notion of local RPE.

Definition 5.1 *The local RPE of node $i \in \pi$, denoted as η_{π_i} or η_i , is the maximum RPE between the relay node i and the destination using the nodes in $\pi_i = (i, \dots, T]$. In particular, if η_i has no dependence on previous nodes π_i^C , the maximum local RPE of node i can be seen, from the point of view of any other node that wants to relay information using this node, as the effective channel-to-destination of node i . Then, according to the equivalence in (5.6e), the first-order approximation of the rate of node i to the destination is $\tilde{R}_i = \eta_i \hat{E}_i$, where $\hat{E}_i \triangleq E - \sum_{j < i} \tilde{E}_j$ denotes the residual network power before relay i transmits.*

Theorem 5.3 *The maximum RPE achieved by the traditional multi-hop network is given by*

$$\frac{1}{\eta_{TMH}} = \sum_{i \in \{0, \pi^*\}} \frac{1}{\alpha_{i,i+1}} \quad (5.27)$$

or, alternatively, by computing the local RPE η_i for $i = T - 1, \dots, 0$ in the following way

$$\eta_i = \frac{\alpha_{i,i+1} \eta_{i+1}}{\alpha_{i,i+1} + \eta_{i+1}} \quad (5.28)$$

with $\eta_T = \alpha_{T,T+1}$ and π^* standing for the optimal relay ordered set.

The power allocation achieving (5.27) is given by

$$\tilde{E}_0 = \frac{E}{1 + \sum_{i \in \pi^*} \frac{\alpha_{0,1}}{\alpha_{i,i+1}}}, \quad (5.29a)$$

$$\tilde{E}_i = \frac{\alpha_{i-1,i}}{\alpha_{i,i+1}} \tilde{E}_{i-1} = \frac{\eta_i}{\alpha_{i,i+1}} \hat{E}_i, \quad i \in [1, \dots, T - 1], \quad (5.29b)$$

$$\tilde{E}_T = \frac{\alpha_{T-1,T}}{\alpha_{T,T+1}} \tilde{E}_{T-1}. \quad (5.29c)$$

The optimal relay order π^* is found recursively according to the algorithm in Table 5.3, which is described in the next section.

Proof: See the proof for the UCMH network in Theorem 5.6. There it is shown that the TMH network can be seen as a particular case of the UCMH network. ■

From the result in Theorem 5.3, the following conclusions can be drawn:

- The *power allocation* at the relays only requires local CSI: the received power from the previous relay $\alpha_{i-1,i} \tilde{E}_i$ and the channel with the following relay $\alpha_{i,i+1}$, see eq. (5.29b).
- *Rate flow symmetry*: if channel gains between two nodes are assumed symmetric $\alpha_{i,j} = \alpha_{j,i}$, the rate from source to destination coincides with that from destination to the source.

5.6 Allcast Multi-Hop Relay Network

For the allcast cooperative multi-hop network (ACMH), all the relays are required to first, optimally combine all the received signals from the source and previous relays and then, decode the source message. Two different allcast and regenerative techniques for multiple relay networks have been proposed in the literature, so far: *i*) a strategy based on codebook partitioning (*binning*) and successive decoding in [80], and *ii*) a different strategy [71, 92], on which we are instead focused, generally achieving larger rates, based on regular encoding and joint decoding.

In this case, we consider the network depicted in Fig. 5.1. For a given transmission order π , the allcast coding strategy presented in [92] achieves the rate

$$R_F(\boldsymbol{\tau}, \mathbf{E}) \leq \min_{i \in \{0, \pi\}} \tau_i \log \left(1 + \alpha_{i, i+1} \frac{E_i}{\tau_i} \right) + \sum_{j=0}^{i-1} \tau_j \log \left(1 + \alpha_{j, i+1} \frac{E_j}{\tau_j} \right). \quad (5.30)$$

To simplify the notation, we have here considered that $\alpha_{j, T+1} = \beta_j$. To compute the maximum RPE $\eta = \frac{\tilde{R}(E)}{E}$, we need to solve the problem in (5.25) with in this case

$$\tilde{C}_{E_i} = \sum_{j=0}^i \alpha_{j, i+1} \tilde{E}_j \quad \forall i \in [0, \pi]. \quad (5.31)$$

The solution to this problem is provided in the next theorem.

Theorem 5.4 *The maximum RPE for the ACMH network (η_{AC}) is given by $\eta_{AC} = \eta_0$, where η_0 is obtained by computing η_i for $i = T - 1, \dots, 0$ in the following way:*

$$\frac{\alpha_{i, i+1}}{\eta_i} = 1 - \sum_{j=i+1}^T \frac{\alpha_{i, j+1} - \alpha_{i, j}}{\eta_j} \quad (5.32)$$

with $\eta_T = \beta_T$. The power allocation achieving (5.32) is given by

$$\tilde{E}_0 = \frac{\eta_0}{\alpha_{0,1}} E, \quad (5.33a)$$

$$\tilde{E}_i = \frac{1}{\alpha_{i, i+1}} \sum_{0 \leq j \leq i-1} (\alpha_{j, i} - \alpha_{j, i+1}) \tilde{E}_j, \quad \forall i \in [1, T]. \quad (5.33b)$$

The optimal relay order π^* is found by exhaustive search over all the routes, see Table 5.2.

Proof: For a given set of relays π , the optimization problem (5.25) with \tilde{C}_{E_i} in (5.31) consists of a maximization over $\tilde{\mathbf{E}}$ of the minimum of a set of $T + 1$ linear functions \tilde{C}_{E_i} on $\tilde{\mathbf{E}}$ under a positive and total power constraint. The resultant convex problem can be written in a standard convex form using the auxiliary variable t as

$$\begin{aligned} & \min_{E_i} -t \\ & t - \tilde{C}_{E_i} \leq 0, \quad i \in \{0, \pi\}, \\ \text{s.t.} \quad & -\tilde{E}_i \leq 0, \quad i \in \{0, \pi\}, \\ & \sum E_i - E = 0. \end{aligned} \quad (5.34)$$

The Lagrangian function $\mathcal{L} \left(\left\{ \tilde{E}_j \right\}; \left\{ \lambda_j \right\}, \left\{ s_j \right\}, m \right)$ associated with this problem is given by

$$\mathcal{L} \triangleq -t + \sum_{j=0}^T \lambda_j \left(t - \tilde{C}_{E_j} \right) - \sum_{j=0}^T s_j \tilde{E}_j + m \left(\sum_{j=0}^T \tilde{E}_j - E \right) \quad (5.35)$$

where λ_j , m , and s_j are the Lagrangian multipliers associated with each rate limit, the total power and the positive power constraints, respectively. The corresponding Karush-Kuhn-Tucker (KKT) conditions the solution must satisfy are [96]: *i*) the primal: $\sum_{j=0}^T \tilde{E}_j = E$, $\tilde{E}_j \geq 0$ and $t \leq \tilde{C}_{E_j}$ for all j , *ii*) the dual: $\lambda_j \geq 0$, $s_j \geq 0$ for all j , *iii*) the complementary slackness: $\lambda_j (t - \tilde{C}_{E_j}) = 0$, $s_j \tilde{E}_j = 0$ for all j and, *iv*) the partial derivatives of the Lagrangian function with respect to the variable t and the powers \tilde{E}_i :

$$t : -1 + \sum_{j=0}^T \lambda_j = 0, \quad (5.36a)$$

$$\tilde{E}_i : -\sum_{j \geq i}^T \lambda_j \alpha_{i,j+1} - s_i + m = 0, \quad i \in \{0, \pi\}. \quad (5.36b)$$

We force all the relays in π to be active $\tilde{E}_j > 0$ for all j in $\{0, \pi\}$, then the complementary slackness condition $s_j \tilde{E}_j = 0$ forces $s_j = 0$ in (5.36b) for any j . By solving the $L + 1$ Lagrangian multipliers λ_i in (5.36), we obtain

$$\lambda_T = \frac{m}{\beta_T}, \quad \lambda_i = m \left(\frac{1}{\eta_i} - \frac{1}{\eta_{i+1}} \right), \quad i \in [0, 1, \dots, T-1] \quad (5.37)$$

with η_i given in (5.32). By substituting (5.37) into (5.36a) it can be shown that $m \neq 0$. In addition, provided that each η_i only depends on the channel gains, we can also assume that $\eta_{i+1} \neq \eta_i$ and thus, $\lambda_i > 0$ for every rate limit $i \in \{0, \pi\}$. Then using the complementary slackness condition $\lambda_i (t - \tilde{C}_{E_i}) = 0$, we can build the linear system of equations $\tilde{C}_{E_i} = \tilde{C}_{E_{i+1}}$ for $i = [0, 1, \dots, T-1]$ to find the optimal power allocation in Theorem 5.4. Notice that, the route π has a feasible solution to this problem only if the conditions $\eta_{i+1} > \eta_i$ are satisfied for all i in $[0, \pi]$. Finally, it only remains to check the positive power condition $\tilde{E}_i > 0$. ■

It is shown in [77] that for the ACMH scenario the optimal routing is an NP-complete problem and thus any *route-discovering* algorithm needs exhaustive search over all the possible routes. However, the conditions $\tilde{E}_i > 0$ and $\eta_{i+1} > \eta_i$ found here can be used to organize the *route-discovering* algorithm. An algorithm to find the optimal route is described below and summarized in Table 5.2. Once a source destination pair is chosen, let T be the number of relays in the network, then the number of possible routes is

$$N = \sum_{i=0}^T \binom{T}{i} i! = T! \sum_{i=0}^T \frac{1}{(T-i)!}. \quad (5.38)$$

The algorithm here presented needs an exhaustive search over all the possible orders of relays π such that $|\pi| = T$ which are $T!$ instead of N , defined in (5.38). For each of these orders, one-by-one, the algorithm finds the best subset π_i $i = [0, \dots, T]$ of π . Note that after all the orders π are evaluated, all the possible routes N have been considered. For a given order π , the algorithm is divided into two main stages: one stage is computed at each network nodes

Table 5.2: Allcast relay selection and ordering algorithm.

<p>Initialization: Choose a source destination pair.</p> <p>For each order of relays $\pi : \pi = T$ (there are $T!$)</p> <p>Set $\eta_\pi = \beta_0$, $\pi^* = [\emptyset]$ and $\eta_{T+1} = \infty$</p> <p>For node $i = T$ to 1 according to π:</p> <p>Node i: Consider node i as the source and the route π_i to destination</p> <ol style="list-style-type: none"> 1. Compute $\frac{\alpha_{i,i+1}}{\eta_i} = 1 - \sum_{j=i+1}^T \frac{\alpha_{i,j+1} - \alpha_{i,j}}{\eta_j}$. 2. if $\eta_i > \eta_{i+1}$ then this route is not feasible go to the next route π. Otherwise Communicate η_i to every node. <p>Centralized Entity: Consider the source and the route $[i, \pi_i]$</p> <ol style="list-style-type: none"> 1. if $\eta_i < \eta_\pi$ then this route is not feasible go to the next route π. Otherwise Compute $\frac{\alpha_{0,i}}{\eta_{\pi_i}} = 1 - \sum_{j=i}^T \frac{\alpha_{0,j+1} - \alpha_{0,j}}{\eta_j}$. 2. if $\eta_{\pi_i} > \eta_\pi$ and $\tilde{E}_i > 0, \forall i \in \pi^*$ then $\eta_\pi = \eta_{\pi_i}$ and $\pi^* = [i, \pi_i]$.
--

successively for $i = T$ to $i = 1$, and the other stage is computed at a central entity (the source). At network nodes, the local RPE (η_i) is computed considering the route π_i to the destination, if a feasible solution exists with $\eta_{i+1} > \eta_i$, then the resultant local RPE is communicated to the source and to all the previous nodes in the route π_i^C . After receiving η_i , the source computes the maximum RPE with the destination using the node i as the first relay in the route η_{π_i} . If the positive power constraint is satisfied and η_{π_i} improves the best previously computed one η_π , then the source stores $\eta_\pi = \eta_{\pi_i}$ and the route is $\pi^* = [i, \pi_i]$.

From the result in Theorem 5.4, the following conclusions can be stated:

- The *power allocation* at relay i requires:
 - i) local CSI: the received powers, namely $\alpha_{j,i} \tilde{E}_j$, from all the previous relays $j = [0, \dots, i - 1]$ and the channel with the following relay $\alpha_{i,i+1}$,
 - ii) global CSI: the received powers at the immediately following relay $i + 1$, namely $\alpha_{j,i+1} \tilde{E}_j$, from all the previous relays $j = [0, \dots, i - 1]$ (see eq. (5.33)).
- The *route-discovering* algorithm needs exhaustive search over all the ordered combinations of nodes. Furthermore, the route found is not optimal for the nodes inside the route.
- *Rate flow symmetry*: Unlike the TMH network, if channel gains between two nodes are symmetric $\alpha_{i,j} = \alpha_{j,i}$, the rate from source to destination in the ACMH network does not coincide with that from destination to the source.

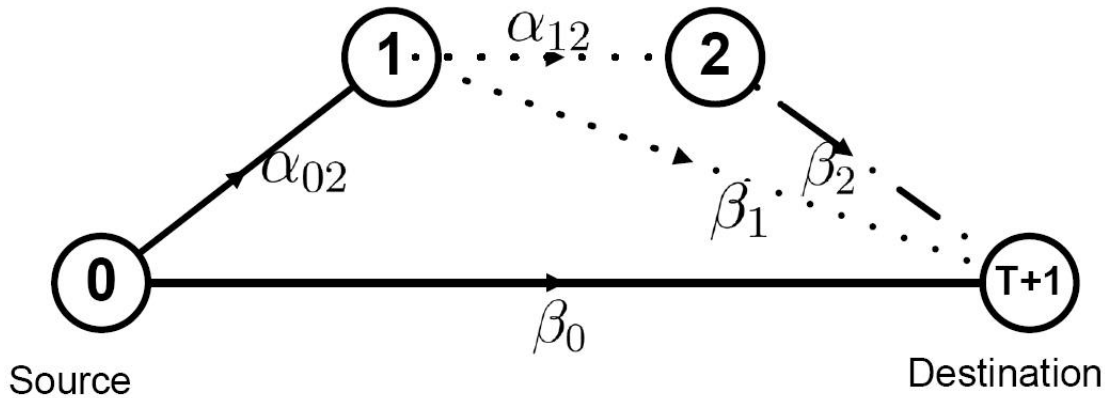


Figure 5.4: Two-relay UCMH network model.

5.7 Unicast Cooperative Multi-Hop Network

A unicast coding scheme for the two-relay network, where the second relay is only required to decode a bin index of the source transmitted message transmitted by the first relay, has recently shown to outperform allcast schemes when the channel from the source to the second relay is rather poor [97]. Under orthogonal transmission, we extend this coding scheme to an arbitrary number of nodes. For this strategy, each relay is only required to decode the bin index transmitted by the immediately previous node. After receiving the last transmission, the destination can recover the source message by successively decoding all the transmissions.

Before addressing the multiple relay UCMH network, the achievable rate for the one-relay AWGN channel with orthogonal transmissions is briefly reviewed. The one-relay scheme contains all the essential ideas and is the building block of the multiple relay extension conducted next.

5.7.1 One-Relay Network

The *binning* forwarding strategy was first shown in [28] to achieve the degraded relay channel capacity. For the AWGN channel, the achievable rate was shown to be maximized by choosing codebooks $\mathcal{X}_0(\cdot)$ and $\mathcal{X}_1(\cdot)$ with codewords jointly Gaussian (see [28, Theorem 5]). If orthogonal transmissions are used, the coding strategy is simpler since it is not necessary to use block-Markov coding as argued in [20]. The source transmits a message s_0 using a codebook $\mathcal{X}_0(\cdot)$ of size $|\mathcal{X}_0| = 2^{nR_0}$ at a rate R_0 . The codewords $\mathcal{X}_0(s_0)$ have $\tau_0 n$ i.i.d elements generated according to a Gaussian distribution with power P_0 and thus using a fraction τ_0 of the total transmission time. For the relay to successfully decode s_0 , the following inequality must hold:

$$R_0 \leq \frac{\tau_0 n}{n} I(X_0; Y_1^0) = \tau_0 \log(1 + \alpha_{01} P_0). \quad (5.39)$$

Consider now a random partition of the source codebook \mathcal{X}_0 into $|\mathcal{X}_1| = 2^{nR_1}$ sets of size $|\mathcal{X}_0|/|\mathcal{X}_1| = 2^{n(R_0-R_1)}$. Each set is identified by a bin index $s_1 = 1, \dots, |\mathcal{X}_1|$. The relay transmits s_1 to the destination. This transmission is done at a rate R_1 using a fraction τ_1 of the total transmission time. The codebook $\mathcal{X}_1(\cdot)$ contains codewords of length $\tau_1 n$ elements generated according to a Gaussian distribution with power P_1 . For the destination to successfully decode s_1 , the following statement must hold:

$$R_1 \leq \tau_1 \log(1 + \beta_1 P_1). \quad (5.40)$$

Now, the source codebook reduces to the $|\mathcal{X}_0|/|\mathcal{X}_1| = 2^{n(R_0-R_1)}$ codewords indexed by the bin index s_1 . For the destination to successfully decode s_0 , we need

$$R_0 - R_1 \leq \tau_0 \log(1 + \beta_0 P_0). \quad (5.41)$$

Finally, equations (5.39)-(5.41), give the achievable rate $R_F(\boldsymbol{\tau}, \mathbf{E}) = R_0$

$$R_F(\boldsymbol{\tau}, \mathbf{E}) \leq \min \left(\tau_0 \log \left(1 + \alpha_{01} \frac{E_0}{\tau_0} \right), \sum_{i \in \{0,1\}} \tau_i \log \left(1 + \beta_i \frac{E_i}{\tau_i} \right) \right). \quad (5.42)$$

5.7.2 Multi-Hop Multiple Relay Network

The *one-way relay protocol* presented in [97] for the two-relay network can be naturally extended to the multi-hop multiple relay network. The next theorem provides the achievable rate.

Theorem 5.5 *Consider a AWGN multiple relay network with orthogonal transmissions. Given a transmission order π , the UCMH network achieves the following rate*

$$R_F(\boldsymbol{\tau}, \mathbf{E}) \leq \min_{i \in \{0, \pi\}} \tau_i \log \left(1 + \alpha_{i, i+1} \frac{E_i}{\tau_i} \right) + \sum_{j=0}^{i-1} \tau_j \log \left(1 + \beta_j \frac{E_j}{\tau_j} \right). \quad (5.43)$$

Proof: The proof is a generalization of the two-relay network strategy presented in [97] particularized to orthogonal transmissions over the AWGN channel. Following the binning argument, given a transmission order π , each relay i uses the previous relay output to decode the transmitted index message s_{i-1} , which is transmitted at rate $R_{i-1} \geq R_i$. The relay i employs a random partition of the previous relay codebook \mathcal{X}_{i-1} in sets of size $|\mathcal{X}_{i-1}|/|\mathcal{X}_i| = 2^{n(R_{i-1}-R_i)}$ and transmits a bin index s_i at a rate R_i indexing the transmitted codeword s_{i-1} . The destination decodes successively and in a backward manner all the transmitted bin indices. In order to do that, the following inequalities must hold:

$$\begin{aligned} R_i &\leq \tau_i \log(1 + \alpha_{i, i+1} P_i) & i \in [0, 1, \dots, T], \\ R_i &\leq \tau_i \log(1 + \beta_i P_i) + R_{i+1} & i \in [0, 1, \dots, T-1] \end{aligned} \quad (5.44)$$

with $R_{T+1} = 0$. The first inequality ensures that relay $i + 1$ decodes the bin index transmitted by the previous relay i . The second inequality ensures *successive decoding* at the destination. Finally, eq. (5.43) is obtained by substituting R_{i+1} by its two possible values for $i = T, \dots, 0$. ■

Remark 5.1 *The UCMH network reduces to the TMH network if $\beta_i = 0$ for all i in $[0, T - 1]$.*

Remark 5.2 *Although relay i only uses the signal from the previous relay $i - 1$, this rate is not always lower than the one obtained by the best allcast strategy [92], where node i uses all the previous transmissions to decode the message. This can be verified by noting that the channel gains that contribute to each rate expression in (5.43) and (5.30) are different. While every rate limit (each i in (5.43)) depends on the channel gains β_j from previous nodes $j \in \pi_{i-1}^C$ to destination, the rate limits in (5.30) depend on the channel gains $\alpha_{j,i+1}$ from nodes $j \in \pi_{i-1}^C$ to the following node $i + 1$. Note that cuts only coincide, in both cases, for $i = \{0, 1, T\}$. As an example, for the two-relay network it is easy to verify that:*

- *The UCMH always outperforms the allcast network for NAC relays. In that case, $\alpha_{02} = 0$ and (5.43) is always larger than (5.30). This allcast scenario, in the energy efficient regime, was considered in [95] to obtain efficient but suboptimal routing schemes.*
- *The UCMH always outperforms the allcast network using AC relays if $\alpha_{02} < \beta_0$. In that case, the decoding requirement at the relay becomes too strong.*

The computation of $\tilde{R}(E)$ and hence of the maximum RPE is again formulated as the allcast problem (5.25), but with \tilde{C}_{E_i} given by

$$\tilde{C}_{E_i} = \alpha_{i,i+1}\tilde{E}_i + \sum_{j=0}^{i-1} \tilde{E}_j \beta_j. \quad (5.45)$$

The solution to this problem is provided in the next theorem.

Theorem 5.6 *Consider the same scenario as in Theorem 5.5. The maximum RPE is given by $\eta_{UCMH} = \eta_0$, where η_0 is obtained by computing η_i for $i = T - 1, \dots, 0$ in the following way:*

$$\frac{\alpha_{i,i+1}}{\eta_i} = 1 + \frac{\alpha_{i,i+1} - \beta_i}{\eta_{i+1}} \quad (5.46)$$

with $\eta_T = \beta_T$. The power allocation achieving (5.46) is given by

$$\tilde{E}_0 = \frac{\eta_0}{\alpha_{0,1}} E, \quad (5.47a)$$

$$\tilde{E}_i = \frac{\alpha_{i-1,i} - \beta_{i-1}}{\alpha_{i,i+1}} \tilde{E}_{i-1} = \frac{\eta_i}{\alpha_{i,i+1}} \hat{E}_i, \forall i \in [1, \dots, T - 1], \quad (5.47b)$$

$$\tilde{E}_T = \frac{\alpha_{T-1,N} - \beta_{T-1}}{\beta_T} \tilde{E}_{T-1}. \quad (5.47c)$$

The optimal relay order π^* is found recursively and in a distributed manner according to the algorithm in Table 5.3 described at the end of this section.

Proof: The problem is solved in two steps: first, the problem is solved for a fixed route π ; then, the optimal relay order is found (this second step is carried out in Appendix 5.A). If the route is given, the optimization problem consists of a maximization over \tilde{E}_i of the minimum of a set of linear functions (5.45), with a total power constraint. As showed in the previous section with the allcast network, if a feasible solution with $\tilde{E}_i > 0$ exists, then it is obtained when all the linear functions coincide. Jointly with the total power constraint, these constraints set a linear system with $T + 1$ equations, whose solution is provided in Theorems 5.3 and 5.6. Instead of solving this linear system directly, the rate expression (5.43) is first reformulated into a recursive one-hop representation. Denote R_i as the rate from relay i to the destination. Then, R_0 can be obtained by computing from $i = T - 1, \dots, 0$ as

$$R_i \leq \min (\tau_i \log (1 + \alpha_{i,i+1} P_i), \tau_i \log (1 + \beta_i P_i) + R_{i+1}) \quad (5.48)$$

with $R_{T+1} = 0$. Note that for the allcast rate in (5.30) such a reformulation is not possible since R_i also depends on previous transmissions.

Due to the recursive rate formulation in (5.48) and the notion of local RPE introduced in Definition 5.1 as $\tilde{R}_i = \eta_i \hat{E}_i$, the problem in (5.25) can be decomposed into T one-relay problems.

$$\tilde{R}_i = \max_{\tilde{E}_i, \hat{E}_{i+1}} \min \left(\alpha_{i,i+1} \tilde{E}_i, \beta_i \tilde{E}_i + \eta_{i+1} \hat{E}_{i+1} \right) \quad (5.49)$$

$$\tilde{E}_i + \hat{E}_{i+1} = \hat{E}_i.$$

These problems are solved from $i = T - 1, \dots, 0$. The solution to each problem is obtained when both terms inside the minimum coincide. Then, $\tilde{R}_i = \eta_i \hat{E}_i$ with η_i in (5.46). When the last one-hop problem is solved, then $\hat{E}_i = E$ and thus, $\eta_0 = \frac{\tilde{R}_0}{E}$ is the maximum RPE. ■

Remark 5.3 A more general scenario could be initially considered fulfilling the NAC requirement at the relays, where each relay does not use the immediately previous transmission, but any of the previous decoded ones. Such a scenario would reduce to the one considered here in the energy efficient regime. A detailed proof is given in Appendix 5.B.

Remark 5.4 If NAC relays and allcast transmissions are desired ($ACMH_{NAC}$), then the relays only listen to the immediately previous transmission $\alpha_{j,i} = 0$ for any $j < i - 1$. In that case, the local RPE in (5.32) is given by

$$\frac{\alpha_{i,i+1}}{\eta_i} = 1 + \frac{\alpha_{i,i+1}}{\eta_{i+1}} - \frac{\beta_i}{\eta_T}. \quad (5.50)$$

This scenario was considered in [95], but only suboptimal conditions to improve a given route were derived. Using the algorithm in Table 5.3, with the allcast non-accumulative local RPE in

Table 5.3: TMH and UCMH: Relay selection and ordering algorithm.

<p>Initialization:</p> <p>Set $i = T$, $\mathcal{N} = \mathcal{T}$ and $\mathcal{S} = \emptyset$.</p> <p>Let every node transmit directly to destination $\eta_n = \beta_n$, $\pi_n = [\emptyset]$.</p> <p>Centralized Entity:</p> <ol style="list-style-type: none"> 1. Choose the node $n^* = \arg \max_{n \in \mathcal{N}} \eta_n$. 2. Move node n^* from \mathcal{N} to node i in \mathcal{S}. <p>Set $\eta_i = \eta_{n^*}$ and $\pi_i^* = \pi_{n^*}$.</p> <p>if node i is the Source then STOP.</p> <p>Otherwise Communicate η_i to every node in \mathcal{N}.</p> <p>Each node in \mathcal{N}: Try to use node i to improve η_n and π_n as</p> <ol style="list-style-type: none"> 1. TMH: $\frac{1}{\eta_n^i} = \frac{1}{\alpha_{n,i}} + \frac{1}{\eta_i}$, UCMH: $\eta_n^i = \frac{\alpha_{n,i}\eta_i}{\alpha_{n,i} + \eta_i - \beta_n}$. 2. if $\eta_n^i > \eta_n$ then $\eta_n = \eta_n^i$, $\pi_n = [i, \pi_i^*]$. $i = i - 1$. 3. Communicate η_n to the central entity.

(5.50), we can find the optimal route. However, note that since it must be satisfied that $\eta_{i+1} < \eta_T$, the maximum RPE for the allcast network with non-accumulative relays ($\eta_{ACMH_{NAC}}$) is always lower than the unicast counterpart $\eta_{UCMH_{NAC}}$.

Remark 5.5 If the NAC requirement is removed, then hybrid schemes could be designed as pointed out in [97] and, more recently, formalized in [54]. Some relays would follow an allcast strategy while others would follow a unicast strategy. It would depend on what is required to each relay: to decode a message transmitted N hops apart using the N previous transmissions, or just the last previous transmission. Most likely, these strategies would not maintain the distributed nature of the UCMH and TMH networks. We study an upper bound on all these strategies in Section 5.8.

The route discovering algorithm is described in Table 5.3. Basically, the algorithm makes use of the recursive expression (5.28) for the TMH and (5.46) for the UCMH. At each iteration the algorithm discovers the optimal route to destination of the node n with the largest maximum RPE until the source is reached. At the expense of some abuse of notation we denote by π_n^* the optimal route to destination from node n , even though this node does not necessarily belong to the optimal route π^* of the target source. We denote \mathcal{T} as the set containing all nodes in the network, \mathcal{S} as the set containing the nodes that have already discovered π_n^* , and \mathcal{N} as the

set containing the remaining ones. The algorithm is divided into two main stages; one stage is computed at each network node $n \in \mathcal{N}$ and the other at a central entity. Define η_n^i as the maximum RPE of node n using node i as the following relay. At each iteration, each node $n \in \mathcal{N}$ computes and stores the maximum $\eta_n^{i^*}$ and the tentative route $\pi_n^{i^*} = [i^*, \pi_i^*]$ by finding the best next relay as $i^* = \arg \max_{i \in \mathcal{S}} \eta_n^i$ and communicates the result to the central entity. This entity decides at each iteration that the nodes n^* with maximum η_{n^*} , namely $n^* = \arg \max_{n \in \mathcal{N}} \eta_n$, should follow the proposed route $\pi_{n^*}^* = \pi_n^{i^*}$.

From results in Theorems 5.3 and 5.6, the following conclusions can be stated:

- The *power allocation* at the relays requires, along with the local CSI, some forward or backward CSI. For the UCMH network, observing the first equality in (5.47b), the backward CSI β_{i-1} is required; instead, observing the second equality in (5.47b), the forward CSI η_i is required. Note that in the later case, the local CSI including the received energy $\tilde{E}_j \alpha_{j,i}$ from all previous transmissions $j < i$ is sufficient to compute \hat{E}_i .
- Each network node n only needs to maintain a routing vector with two entries per destination, containing η_n and the next relay index i . The overall route is given by $\pi_n^* = [i, \pi_i^*]$.
- During the *route-discovery*, the source does not need to wait until the algorithm finishes. At each iteration, the source can improve its route by selecting the best next relay i among the available ones $i \in \mathcal{S}$. In addition, given a source-destination pair, every node with better η_{TMH} than that of the source also discovers its optimal route to destination.
- *Rate flow symmetry*: For the TMH, if channel gains between two nodes are assumed symmetric $\alpha_{i,j} = \alpha_{j,i}$, the rate from source to destination coincides with that from destination to the source. This is not the case for the UCMH network.

5.8 Upper Bound for Regenerative Networks

A more general view of regenerative techniques referred to as *parity forwarding* or *structured decode and forward* has recently been presented in [54]. This generalization liberates the relays nodes from decoding the source message. Nodes transmit a set of one or more bin indices to previous transmitted messages. Due to its great flexibility, this coding strategy achieves the highest known spectral efficiency for multi-hop networks with regenerative relays. However, the configuration of this coding strategy involves several choices. Given a relay order, it is necessary to define a message tree structure to characterize the encoding and decoding procedures and the dependencies between messages and their bin indices. For each tree structure, a different achievable rate is obtained. The unicast and allcast strategies can be viewed as particular tree structures. Unfortunately, there is not a tree structure which always outperforms the others

in all situations. Consequently, the huge number of possible coding schemes makes difficult the study of these schemes. Instead, we study an upper bound on all these schemes.

Theorem 5.7 Consider a network with T relays and orthogonal transmission over a Gaussian noise channel. Giving a transmission order π the following rate is an upper bound for parity forwarding techniques

$$R_F(\boldsymbol{\tau}, \mathbf{E}) \leq \min_{i \in \{0, \pi\}} C_i(\boldsymbol{\tau}, \mathbf{E}), \quad (5.51)$$

$$C_i(\boldsymbol{\tau}, \mathbf{E}) = \tau_i \log \left(1 + \alpha_{i, i+1} \frac{E_i}{\tau_i} \right) + \sum_{j=0}^{i-1} \tau_j \left(\log \left(1 + \alpha_{j, i+1} \frac{E_j}{\tau_j} \right) + \log \left(1 + \beta_j \frac{E_j}{\tau_j} \right) \right) \quad (5.52)$$

where, in this case $\alpha_{j, T+1} = 0$.

Proof: To obtain this upper bound, we allow each relay to use all the previous relay transmissions and only require them to decode the message transmitted by the previous relay. This message is assumed to be a bin index s_i of the message transmitted by the previous relay s_{i-1} , and thus is transmitted at a lower rate $R_i \leq R_{i-1}$. In this way, we obtain all the benefits of the allcast strategy (incorporate all the mutual information available in the received signals from all the previous relays transmissions) but also the decoding flexibility of the unicast scheme. In order to do that, given a route π , the following inequalities must hold:

$$R_i \leq \sum_{j=0}^i \tau_j \log \left(1 + \alpha_{j, i+1} P_j \right), \quad i \in [0, 1, \dots, T], \quad (5.53a)$$

$$R_i \leq \tau_i \log \left(1 + \beta_i P_i \right) + R_{i+1}, \quad i \in [0, 1, \dots, T]. \quad (5.53b)$$

The first inequality establishes the rate limit that allows the relay $i + 1$ to decode the bin index transmitted by the previous relay using all mutual information available in the previous transmissions. The second inequality follows from the successive decoding at the destination. Finally eq. (5.51) is obtained by substituting R_{i+1} by its two possible values for $i = T, \dots, 0$. ■

Notice that the rate limits in this upper bound are the union of contributions of the rate limit in (5.30) and (5.43).

The computation of $\tilde{R}(E)$ and, hence of the maximum RPE is again formulated as in (5.25) but, replacing \tilde{C}_{E_i} with

$$\tilde{C}_{E_i} = \sum_{j=0}^i \hat{\alpha}_{j, i+1} \tilde{E}_j, \quad (5.54)$$

where

$$\begin{aligned} \hat{\alpha}_{j, i+1} &= \alpha_{j, i+1} + \beta_j & j < i, \\ \hat{\alpha}_{j, i+1} &= \alpha_{j, i+1} & j = i. \end{aligned} \quad (5.55)$$

Since this problem is exactly the one solved for the allcast scenario, the maximum RPE η_{UPR} reads as that in Theorem 5.5 with $\alpha_{j, i+1}$ replaced by $\hat{\alpha}_{j, i+1}$.

5.9 Cut-Set Bound for Multi-Hop Networks

A capacity upper bound for relaying networks, referred to as *cut-set bound*, was derived in [98]. We use this result to establish an upper bound on the maximum RPE. Unlike the previous scenarios, here nodes are not required to decode any message before transmitting. In addition, relays and destination make use of multiple received signals.

Before formulating the problem, the cut-set bound [16] is introduced and particularized to the case of orthogonal transmissions over the AWGN channel. Denote \mathcal{T} as the set containing all relays in the scenario, transmitter set $\mathcal{S} \subseteq \mathcal{T}$ as any of the 2^T possible subsets that can be created with up to T relays, and receiver set \mathcal{S}^C as the complement of \mathcal{S} in \mathcal{T} . For the two-relay network in Fig. 5.1, there exist 4 possible cuts: $\mathcal{S} = \{\emptyset\}, \{1, 2\}, \{2\}, \{1\}$. For a given subset \mathcal{S} , let $X_{\mathcal{S}} = \{X_t : t \in \mathcal{S}\}$ and $Y_{\mathcal{S}} = \{Y_t : t \in \mathcal{S}\}$ be the transmitted and received signals at the relay nodes, respectively. Then, the transmission rate R_0 is upper bounded by

$$R_0 \leq \max_{p(x, x_1, \dots, x_T)} \min_{\mathcal{S} \subseteq \mathcal{T}} I(X, X_{\mathcal{S}}; Y_{\mathcal{S}^C}, Y \mid X_{\mathcal{S}^C}) \quad (5.56)$$

where $p(x, x_1, \dots, x_T)$ is the probability distribution function of the channel inputs and $I(X; Y)$ is the mutual information between X and Y . Now, consider the particular case where relays use different degrees of freedom to transmit, e.g. orthogonal transmission intervals, according to a transmission order π . Let us define the set $\mathcal{R}_i^C = \mathcal{S}^C \cap \pi_i$ as the subset of the receiver set \mathcal{S}^C that contains the nodes in π_i . The mutual information associated with a given *cut-set* \mathcal{S} is

$$I(X, X_{\mathcal{S}}; Y_{\mathcal{S}^C}, Y \mid X_{\mathcal{S}^C}) = I(X, X_{\mathcal{S}}; Y_{\mathcal{S}^C}, Y), \quad (5.57a)$$

$$= \sum_{i \in \{0, \mathcal{S}\}} \tau_i I(X_i; Y_{\mathcal{R}_i^C}^i, Y^i), \quad (5.57b)$$

$$\leq \sum_{i \in \{0, \mathcal{S}\}} \tau_i I(X_i; Y_{\mathcal{S}^C}^i, Y^i). \quad (5.57c)$$

The proof follows a similar argument as in [20, Appendix A]. By the orthogonality of the transmissions, mutual information can be rewritten as in (5.57a). Equality (5.57b) and inequality (5.57c) depend on the transmission causality requirement. When causality is required, nodes can only transmit based on previous transmissions (*time division* model). Once node i inside \mathcal{S} has transmitted, only the nodes inside \mathcal{S}^C which have not yet transmitted \mathcal{R}_i^C can contribute to the mutual information $I(X_i; Y_{\mathcal{R}_i^C}^i, Y^i)$. In that case, equality (5.57a) can be decomposed into a sum of $|\mathcal{S}| + 1$ broadcast single-input multiple-output channels with $|\mathcal{R}_i^C|$ channel outputs as shown in equality (5.57b). When causality is not required (*frequency or coded division* model) all relays can potentially make use of all transmissions. Then, $\mathcal{R}_i^C = \mathcal{S}^C$ and the mutual information achieves the inequality in (5.57c). Here, the analysis is conducted considering the non-causal scenario, a priori independent of the relaying order π . Surprisingly enough, the order constraint appears implicit in the solution and thus, results are also valid for causal transmissions.

Finally, if orthogonal transmission over AWGN are considered, the rate upper bound in (5.56) using (5.57c) with equality can be maximized employing independent Gaussian channel inputs as

$$R_F(\boldsymbol{\tau}, \mathbf{E}) \leq \min_{\mathcal{S}} \sum_{i \in \{0, \mathcal{S}\}} \tau_i \log \left(1 + \left(\beta_i + \sum_{j \in \mathcal{S}^C} \alpha_{i,j} \right) \frac{E_i}{\tau_i} \right). \quad (5.58)$$

Since there is no predetermined route π , the problem formulation is slightly different in this case.

To compute the first-order Taylor expansion at $E = 0$ of the rate as a function of the total power $\tilde{R}(E)$ we particularize the problem in (5.8), to this scenario as

$$\begin{aligned} \tilde{R}(E) = & \max_{\tilde{\mathbf{E}}} \min_{\mathcal{SCT}} \tilde{C}_{E_S} \\ \text{s.t.} & \sum_{i \in \{0, \mathcal{S}\}} \tilde{E}_i = E \\ & \tilde{E}_i \geq 0 \forall i \in \{0, \mathcal{S}\} \end{aligned} \quad (5.59)$$

where for each \mathcal{S} , \tilde{C}_{E_S} is the first-order Taylor approximation at $E = 0$ of the rate limits in (5.58), given by

$$\tilde{C}_{E_S} = \tilde{E}_0 \beta_0 + \tilde{E}_0 \sum_{i \in \mathcal{S}^C} \alpha_{0i} + \sum_{i \in \mathcal{S}} \tilde{E}_i \left(\beta_i + \sum_{j \in \mathcal{S}^C} \alpha_{i,j} \right). \quad (5.60)$$

The solution to this problem is provided in the following theorem.

Theorem 5.8 *The cut-set upper bound on the maximum RPE η_{CB} for the multi-hop AWGN channel with orthogonal transmissions is given by*

$$\eta_{CB} = \frac{\beta_0 + \sum_{i \in \pi^*} \alpha_{0i}}{1 + \sum_{i \in \pi^*} \frac{\alpha_{0i}}{\eta_i}} \quad (5.61)$$

where π^* is the optimal relay order set. The local RPE of the relay $[\pi^*]_i$ is given by

$$\eta_i \triangleq \frac{\beta_i + \sum_{j \in \pi_i^*} \alpha_{i,j}}{1 + \sum_{j \in \pi_i^*} \frac{\alpha_{i,j}}{\eta_j}}. \quad (5.62)$$

The optimal power allocation achieving (5.61) is given by

$$\begin{aligned} \tilde{E}_0 &= \frac{E}{1 + \sum_{i \in \pi^*} \frac{\alpha_{0i}}{\eta_i}}, \\ \tilde{E}_i &= \frac{\tilde{E}_0 \alpha_{0i} + \sum_{j \in \pi_i^{*C}} \tilde{E}_j \alpha_{j,i}}{\beta_i + \sum_{j \in \pi_i^*} \alpha_{i,j}} \quad \forall i \in \pi^*. \end{aligned} \quad (5.63)$$

The optimal relay order π^* implies a natural ordering of the transmissions which is found recursively and in a distributed manner according to the algorithm in Table 5.4 described below.

Table 5.4: CB upper bound: Relay selection and ordering algorithm.

<p>Initialization:</p> <p>Set $i = T$, $\mathcal{N} = \mathcal{T}$ and $\pi = \emptyset$.</p> <p>Let every node to transmit directly to destination $\eta_n = \beta_n$, $\pi_n = [\emptyset]$.</p> <p>Centralized Entity:</p> <ol style="list-style-type: none"> 1. Choose the node $n^* = \arg \max_{n \in \mathcal{N}} \eta_n$. 2. Remove n^* from \mathcal{N}. <p style="padding-left: 40px;">Set $[\pi^*]_i = n^*$.</p> <ol style="list-style-type: none"> 3. if node i is the Source then STOP otherwise communicate η_i to every node in \mathcal{N}. <p>Each node in \mathcal{N}: Use η_i and π^* to compute</p> <ol style="list-style-type: none"> 1. $\eta_n = \frac{\beta_n + \sum_{j \in \pi_i^*} \varsigma_{n,j}}{1 + \sum_{j \in \pi_i^*} \frac{\varsigma_{n,j}}{\eta_j}}$ $i = i - 1.$ 2. Communicate η_n to the central entity.

The optimal routing algorithm for the upper bound is described in Table 5.4. Like previous scenarios, the algorithm makes use of the recursive expression for the local RPE (5.62). Note that in this scenario, η_i is written as a function of the local RPE of all the subsequent relays in the route rather than just the following one. Again, the algorithm computes η_n and π_n^* of one node n in the network, iteratively, until the source is reached. However, in this case, all these nodes are included in the source route π^* . The set \mathcal{S} defined in Table 5.3 as the set containing all nodes that has already been computed η_n can be replaced by the source route π^* . The algorithm is divided into the same two stages. At each iteration each node $n \in \mathcal{N}$ computes η_n using η_i among all the following relays and communicates the result to the central entity. The central entity includes the node n^* with maximum η_n in the source route at position i .

Proof: We solve the optimization problem (5.59) in two steps. First, the problem is solved for a given set of active relays (not ordered) $\pi \subseteq \mathcal{T}$ with \tilde{E}_i strictly positive for all $i \in \pi$. Thus, we replace \mathcal{T} by π and consider $|\pi| = T$ in the problem formulation (5.59). Second, among all the sets π , the one with maximum RPE is found according to the algorithm in Table 5.4 (see Appendix 5.A). For the first step, we rewrite the convex problem (5.59) in a standard convex

form using the auxiliary variable t as

$$\begin{aligned}
 & \min_{\tilde{\mathbf{E}}} -t \\
 & t - \tilde{C}_{E_S} \leq 0, \forall \mathcal{S} \subseteq \pi, \\
 \text{s.t.} \quad & -\tilde{E}_i < 0, \forall i \in \pi, \\
 & \sum_{i \in \pi} \tilde{E}_i - E = 0.
 \end{aligned} \tag{5.64}$$

The Lagrangian function $\mathcal{L} \left(\left\{ \tilde{E}_i \right\}; \left\{ \lambda_{\mathcal{S}} \right\}, \left\{ s_i \right\}, m \right)$ associated with this problem is given by

$$\mathcal{L} \triangleq -t + \sum_{\mathcal{S} \subseteq \pi} \lambda_{\mathcal{S}} \cdot \left(t - \tilde{C}_{E_S} \right) - \sum_{i \in \pi} s_i \tilde{E}_i + m \cdot \left(\sum_{i \in \pi} \tilde{E}_i - E \right) \tag{5.65}$$

where $\lambda_{\mathcal{S}}$, m , and s_i are the Lagrangian multipliers associated with each capacity limits, the total power and the positive power constraints, respectively. The corresponding KKT conditions the solution must satisfy are [96]: *i*) the primal $\tilde{E}_i \geq 0, t \leq \tilde{C}_{E_S}, \sum \tilde{E}_i = E$, *ii*) the dual $\lambda_{\mathcal{S}} \geq 0, s_i \geq 0$, *iii*) the complementary slackness $\lambda_{\mathcal{S}} \left(t - \tilde{C}_{E_S} \right) = 0, s_i \tilde{E}_i = 0$ and, *iv*) the partial derivatives of the Lagrangian function with respect to the variable t and the powers \tilde{E}_i

$$-1 + \sum_{0 \leq j \leq |\pi|} \lambda_j = 0, \tag{5.66a}$$

$$- \sum_{i \leq j \leq |\pi|} \lambda_j \left(\beta_i + \sum_{k \in \pi_j} \alpha_{i,k} \right) + m = 0, \forall i \in \pi \tag{5.66b}$$

with subsets $\pi_T \subset \pi_{T-1}, \dots, \subset \pi_0$. Note that these expressions only depend on the Lagrangian multipliers λ_i associated with the sets π_i . Since $\tilde{E}_i > 0$ for all $i \in \pi$, the condition $s_i \tilde{E}_i = 0$ forces $s_i = 0$, for all $i \in \pi$. To show that the Lagrangian multipliers associated with the set $\mathcal{S} \neq \pi_i$ for all i are equal to zero we introduce the following lemma.

Lemma 5.1 *Two different capacity limits $\tilde{C}_{E_{S_1}}$ and $\tilde{C}_{E_{S_2}}$, with $\mathcal{S}_1, \mathcal{S}_2 \subseteq \pi$ can hold with equality if $\mathcal{S}_1 \subset \mathcal{S}_2$ or $\mathcal{S}_2 \subset \mathcal{S}_1$, i.e., one of the sets is included inside the other.*

Proof: The proof is provided in Appendix 5.C.1. ■

Corollary 5.1 *Transmissions are assumed orthogonal and, thus, no simultaneous transmissions are possible. Together with Lemma 5.1 this means that capacity limits-meeting cuts must increase one relay at a time. Let π_i denote the receiver set of the i th node in the route. Only the capacity cuts associated with the ordered receiving sets $\mathcal{S}^C = \pi_i$ with $\pi_T \subset \pi_{T-1}, \dots, \subset \pi_0$ can be satisfied with equality simultaneously.*

The slackness condition $\lambda_{\mathcal{S}} \left(t - \tilde{C}_{E_S} \right) = 0$ jointly with Lemma 2 forces that, only the capacity limits associated with the subsets π_i^C can satisfy $t = \tilde{C}_{E_S}$ with $\mathcal{S} = \pi_i^C$. Hence, $\lambda_{\mathcal{S}} = 0$ for any other set \mathcal{S} .

By solving the Lagrangian multipliers in (5.66a) and (5.66b), we obtain

$$\lambda_T = \frac{m}{\beta_T}, \quad (5.67a)$$

$$\lambda_i = m \left(\frac{1}{\eta_i} - \frac{1}{\eta_{i+1}} \right) \quad (5.67b)$$

with η_i given in (5.62). From these equations we can find the capacity limits \tilde{C}_{E_S} with $\mathcal{S} = \pi_i^C$ that are satisfied with equality (those for which λ_i is strictly positive). By substituting (5.67a) and (5.67b) into (5.66a) it can be shown that $m \neq 0$. Since η_i only depends on the channel gains we can assume that $\eta_{i+1} \neq \eta_i$ and thus, $\lambda_i > 0$ for every capacity limit. Then, a feasible solution exists only if $\eta_{i+1} > \eta_i$ for all $i \in [0, 1, \dots, T]$. The solution of the linear system of equations $\tilde{C}_{E_{S_0}} = \tilde{C}_{E_{S_i}}$, with $\mathcal{S}_0 = \pi^C$ and $\mathcal{S}_i = \pi_i^C$ for all $i \in [0, 1, \dots, T]$ provides the result in Theorem 5.8. It still remains to ensure that the condition $t < \tilde{C}_{E_S}$ is also satisfied for any other set \mathcal{S} different from π_i . This is carried out in Appendix 5.C.2. ■

The main conclusions about the result in Theorem 5.8 are summarized below:

- *Causality in relaying*: in previous scenarios, the decoding requirement imposes the causality in the route. However, for the cut-set bound, such a constraint has not been set. Surprisingly enough, the maximum RPE solution provides the optimal ordering among transmissions.
- *Relays reuse*: for this scenario, since any relay is able to decode the message, one may think that using relays more than once might be beneficial by improving the signal received at the relays and at the destination. However, the cut-set bound solution suggests that a relay should not transmit information about the received signal from relays that already use its transmitted signal. Like in previous scenarios, each relay transmits once at most.
- *The power allocation* at relays requires only local CSI: relay nodes allocate the amount of power for which its received power from source and *previous* relays coincides with the total power received, at the *subsequent* relays and at the destination. The power allocation at the source assumes knowledge of the local RPE from all relays in the route. The source and each relay i compute η_i using the local RPE from the i -th to the last relay in the route.
- Concerning *route-discovery*, the conclusions stated for previous scenarios are valid here. Again, when route discovery ends, all nodes inside π have discovered η_i and their route to destination π_i , but, in this case, all other nodes in \mathcal{N} have discovered part of the route, namely the part from the target source to the destination. Furthermore, all the relays that have obtained the route to destination belong to the source route.

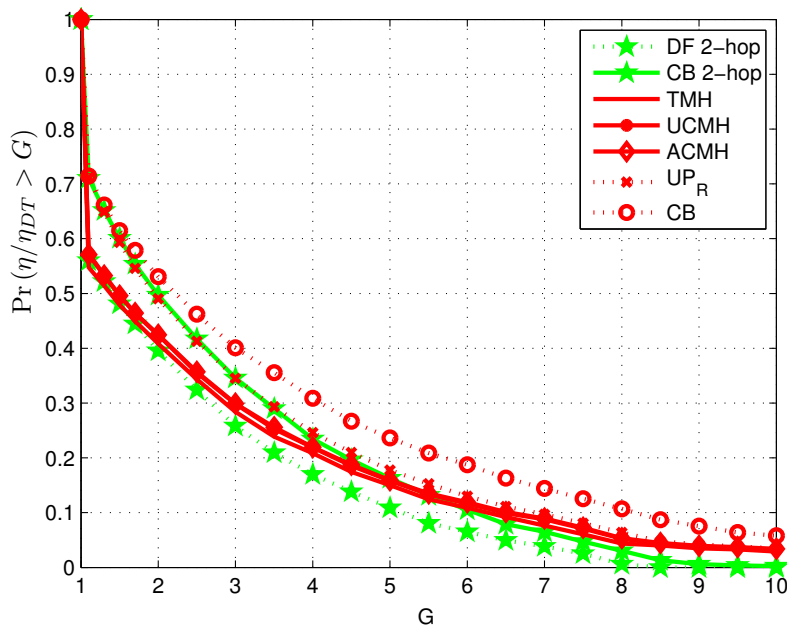


Figure 5.5: $\Pr(\eta/\eta_{DT} > G)$ for all the cooperative strategies studied in a scenario with 5 nodes (up to 4 hops) with a density of nodes of $1 \text{ nodes}/m^2$.

5.10 Simulation Results

In this section, we present numerical results to compare all the strategies described in terms of the maximum RPE (η). We generate $M = 1000$ independent scenarios. For each of these scenarios, we place N nodes randomly in a square plane of area $A = \sqrt{\frac{N}{\rho}}$, where ρ [nodes/m^2] stands for the density of nodes. We consider distance dependent channels, then the channel gain between nodes i and j is $\alpha_{ij} = d_{ij}^{-\nu}$ where d_{ij} is the distance between these two nodes and $\nu = 4$ is the path-loss exponent. Subsequently, we compute the maximum RPE from every network node $i = [1, \dots, N]$ to every node $j \neq i$ in the scenario, assuming that the rest of nodes are potential relays. Finally, we compute the cumulative density function (CDF) of the ratio η/η_{DT} between the maximum RPE (η) of any of the strategies described in this chapter and the maximum RPE obtained by direct transmission from the source to the destination (η_{DT}). Fig. 5.5 depicts, for each one of the strategies described above, the probability that the ratio η/η_{DT} is above a certain prescribed threshold gain G , i.e., $\Pr(\eta/\eta_{DT} > G) = 1 - CDF(\eta/\eta_{DT})$. The probability that a strategy strictly improves direct transmissions is given by $\Pr(\eta/\eta_{DT} > 1)$. At this point, $G \rightarrow 1$, all the upper bounds: the cut-set bound with two hops (CB 2-hop), the multi-hop cuts set bound (CB) and the upper bound for regenerative strategies (UP_R), obtain the highest gap with respect to the achievable strategies. As G increases, the CB upper bounds (multi-hop CB and the 2-hops CB) maintain most of the gap. However, the regenerative upper bound UP_R comes closer to all the achievable multi-hop strategies. The unicast cooperative multi-hop scenario (UCMH) is shown to improve the traditional multi-

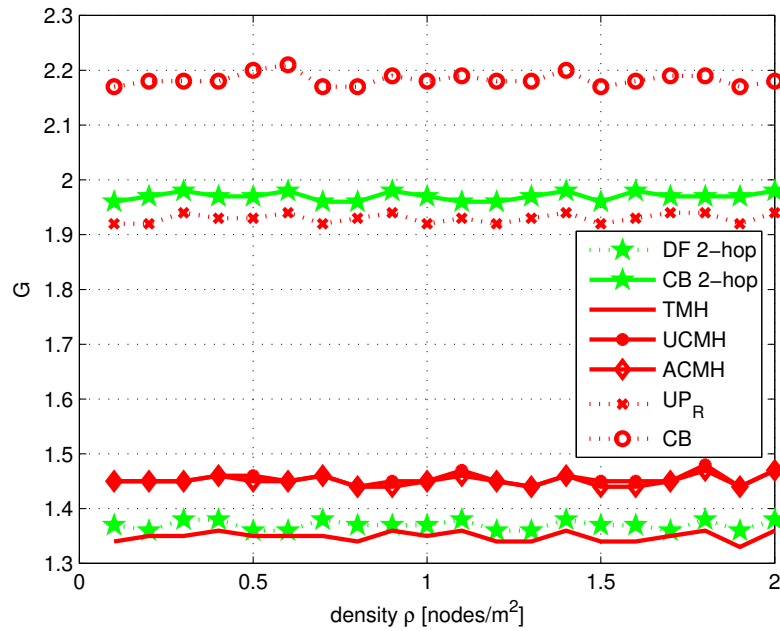


Figure 5.6: Gain ratio $G = \eta/\eta_{DT}$ as a function of the density of nodes ρ for a given $\Pr(\eta/\eta_{DF} > G) = 0.5$ and a fixed number of nodes $N = 5$.

hop (TMH) network with similar routing and power allocation complexity. Interestingly, the UCMH curve is extremely close to the allcast cooperative multi-hop (ACMH) one, for which exhaustive relay search and AC relays are needed. However, the cut-set bound (CB) remains far from the proposed regenerative techniques. In Fig. 5.6, for the same simulation set-up, we study the dependence of the gain G with respect to the density of nodes ρ . To that end, we vary the scenario size A , for a given $\Pr(\eta/\eta_{DT} > G) = 0.5$ and a fixed number of nodes $N = 5$. That is, with probability 0.5 the gain of the multi-hop strategy is G or greater. It is interesting to note that the gain is almost independent of the node density. This figure can be seen as a zoom of Fig. 5.5 at $\Pr(\eta/\eta_{DT} > 0.5)$. Here, the difference between the different multi-hop strategies is much clear. Note that at this point, choosing the best relay (DF-2hop) is even better than traditional multi-hop. Finally, in Fig. 5.7 we study the dependence of the gain G with respect to the number of nodes N , for a given $\Pr(\eta/\eta_{DT} > G) = 0.5$ and a constant density of nodes $\rho = 1$. In this case, as the number of nodes increases, we observe that while the cut-set bound (CB) maintain or even increases the gap with respect to the achievable strategies, the upper bound on multi-hop regenerative techniques UP_R converges to them.

5.11 Conclusions

In this chapter, we have studied the maximum rate per energy of cooperative two-hop and multi-hop networks over AWGN channels. For the two-hop network, we obtained one lower

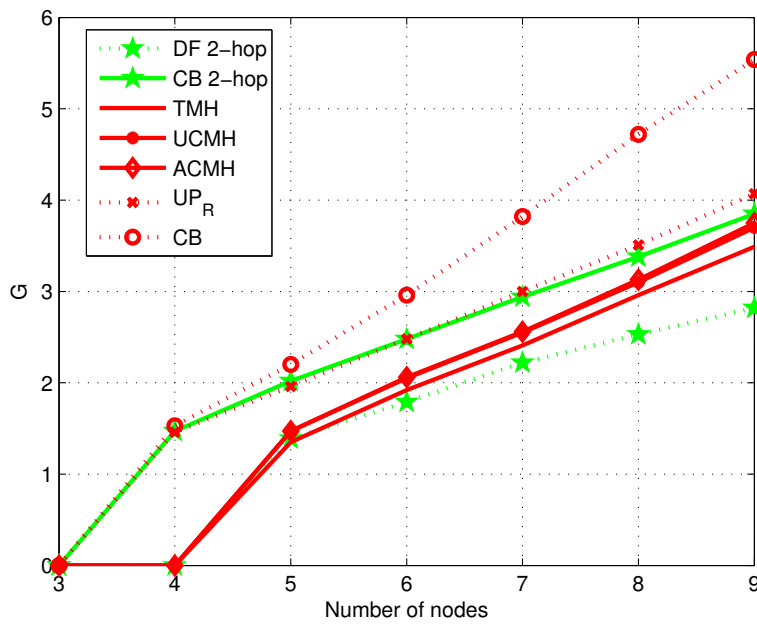


Figure 5.7: The gain ratio G as a function of the number of nodes N , for a given $\Pr(\eta/\eta_{DT} > G) = 0.5$ and $\rho = 1$.

bound on the maximum RPE by using regenerative relays and one upper bound based on the cut-set bound. For the multi-hop network, we obtained three lower bounds using *regenerative* relays and two upper bounds; one only valid for regenerative relays and the other, based on the CB, valid for all type of relays. The first multi-hop lower bound was obtained by solving the *traditional multi-hop network* (TMH). For this strategy, we showed that the power allocation among nodes that maximizes the RPE only requires *local channel information* at the relays and that the optimal route can be obtained in a distributed manner. However, the achievable rate for the TMH network is strongly limited by the worst link between two relays in the route. Then, the *allcast cooperative multi-hop network* is addressed. This strategy requires all relays to decode the source message, by properly combining all the received signals. Despite of the fact that this technique is known to achieve the *allcast* capacity, all relays requires *global network channel information* and does not admit a relay selection and routing solution with a distributed structure. To maintain the TMH distributed properties while obtaining the *accumulative* gain at destination, a *unicast* strategy with *non-accumulative* relays is investigated. We showed that, compared to *allcast* networks, the *unicast* network has similar performance while offering a more attractive distributed nature. More specifically, this strategy does not require global channel information at each relay to perform the power allocation solution, and also provides low complexity optimal relay selection and routing solutions. Interestingly, the upper bound based on the cut-set bound also presents such a distributed nature. Although the cut-set bound is shown to be far from being achievable with *regenerative* techniques, the upper bound obtained only for *regenerative* relays is shown to be very close to the *allcast* and *unicats* strategies and

so, small gains are expected by new multi-hop strategies with regenerative relays in this single source-destination pair network.

Appendix 5.A Optimality of the Routing Algorithms

In this appendix, the optimality of the routing algorithms in Tables 5.3 and 5.4 is proved. To that end it is sufficient to show that by choosing the node with larger local RPE at each route position i , for $i = T, \dots, 0$, as $n^* = \arg \max_{n \in \mathcal{N}} \eta_n$, the larger possible $\eta_0 = \eta$ is obtained. The proof is by contradiction. For a given order π with $|\pi| = T$, assume that there exists a node \check{i} which obtains, using the nodes in π_i , a local RPE larger than the one of node i , namely $\eta_{\check{i}} > \eta_i$. Then, it can be shown that by including this node in the route between node i and node $i + 1$ all the other nodes in positions $j \leq i$ can compute a new local RPE $\check{\eta}_j$ that satisfies $\check{\eta}_j > \eta_j$ and, thus also the first node $i = 0$ (the source) does $\check{\eta}_0 = \check{\eta}$, (in the particular case where this node is already in another position in π , the node is used twice). By selecting $n^* = \arg \max_{n \in \mathcal{N}} \eta_n$ at each route position, the route-discovering algorithm ensures that a node like \check{i} does not exist and $\check{\eta}_0$ cannot be further improved.

The rest of the proof is particularized for the cut-set bound (TMH and UCMH scenarios can be proved similarly). After including node \check{i} in the route, node i becomes the node immediately previous to node \check{i} . The new and the initial local RPE are then given by

$$\eta_i = \frac{N_i}{D_i}, \quad (5.68a)$$

$$\check{\eta}_i = \frac{N_i + \alpha_{i,\check{i}}}{D_i + \frac{\alpha_{i,\check{i}}}{\eta_{\check{i}}}} \quad (5.68b)$$

with $N_j = \beta_j + \sum_{j < l \leq T} \alpha_{j,l}$ and $D_j = 1 + \sum_{j < l \leq T} \frac{\alpha_{j,l}}{\eta_l}$.

From these definitions, a sufficient condition for $\eta_j < \check{\eta}_j$ is $\frac{N_i}{D_i} = \eta_i < \eta_{\check{i}}$, which is indeed satisfied by assumption. This argument can be repeated for all other positions $j < i$. For a general position j , assume that $\check{\eta}_l > \eta_l$ for $j < l \leq i$ has already been ensured. Then, at position j , since $\frac{\eta_l}{\check{\eta}_l} < 1$, the new local RPE can be bounded below as

$$\check{\eta}_j = \frac{N_j + \alpha_{j,\check{i}}}{\check{D}_j + \sum_{j < l \leq i} \frac{\alpha_{j,l}}{\check{\eta}_l} + \frac{\alpha_{j,\check{i}}}{\eta_{\check{i}}}}, \quad (5.69a)$$

$$= \frac{N_j + \alpha_{j,\check{i}}}{\check{D}_j + \sum_{j < l \leq i} \frac{\eta_l}{\eta_l} \frac{\alpha_{j,l}}{\check{\eta}_l} + \frac{\alpha_{j,\check{i}}}{\eta_{\check{i}}}}, \quad (5.69b)$$

$$\geq \frac{N_j + \alpha_{j,\check{i}}}{D_j + \frac{\alpha_{j,\check{i}}}{\eta_{\check{i}}}} \quad (5.69c)$$

with $\check{D}_j = 1 + \sum_{i < l \leq T} \frac{\alpha_{j,l}}{\eta_i}$. Comparing this local RPE with the initial one η_j , a sufficient condition for $\eta_j < \check{\eta}_j$ is $\eta_i < \eta_i$ which, again, is satisfied by assumption.

Appendix 5.B Proof of Remark 5.2

If there is a relay using the immediately previous transmission then, at least, two relays use the same transmission. Assume that there are two relays $i \in \{1, 2\}$ that aid the transmission between the relay n and the destination, since all relays are NAC both use different routes to reach the destination π_1 and π_2 , with local RPE η_1 and η_2 , respectively. Without loss of generality assume $\eta_1 > \eta_2$. To prove Remark 5.2, we show that the largest local RPE at node n is always obtained by selecting only the best relay. At hop n the optimization problem can be written as

$$\begin{aligned} R_n &= \max_{\tilde{E}_n, \hat{E}_1, \hat{E}_2} \min_{\tilde{E}_i} \left(\alpha_{n,1} \tilde{E}_n, \alpha_{n,2} \tilde{E}_n, \beta_n \tilde{E}_n + \eta_1 \hat{E}_1 + \eta_2 \hat{E}_2 \right) \\ \tilde{E}_n + \hat{E}_1 + \hat{E}_2 &= \hat{E}_n \end{aligned} \quad (5.70)$$

where $\alpha_{n,1} \tilde{E}_n, \alpha_{n,2} \tilde{E}_n$ are the decoding requirements at the relays and $\beta_n \tilde{E}_n + \eta_1 \hat{E}_1 + \eta_2 \hat{E}_2$ at the destination. This rate is always worse than the one given by

$$\begin{aligned} R_n^{UP} &= \max_{\tilde{E}_n, \tilde{E}_i} \min_{\hat{E}_i} \left(\alpha_{\min} \tilde{E}_n, \beta_n \tilde{E}_n + \eta_1 \tilde{E}_i \right) \\ \tilde{E}_n + \tilde{E}_i &= \hat{E}_n \end{aligned} \quad (5.71)$$

where $\alpha_{\min} = \min(\alpha_{n,i}, \alpha_{n,\check{i}})$, $\eta_1 = \max(\eta_1, \eta_2)$ and $\hat{E}_i = \hat{E}_1 + \hat{E}_2$. Solving this problem yields

$$\eta_{UP} = \frac{R_n}{\hat{E}_n} = \frac{\alpha_{\min} \eta_1}{\alpha_{\min} + \eta_1 - \beta_n} \quad (5.72)$$

which can be shown to be always worse than using the best next relay

$$\eta = \max_{i \in \{1,2\}} \frac{\alpha_{n,i} \eta_i}{\alpha_{n,i} + \eta_i - \beta_n}. \quad (5.73)$$

Note that η_{UP} is always equal or worse than η since $\alpha_{\min} \leq \alpha_{n,1}$.

Appendix 5.C Auxiliary Results for Proof of Theorem 5.8

We first introduce some notation needed to manipulate the capacity limits \tilde{C}_{E_S} , as defined in (5.60). Let \mathcal{X} and \mathcal{Y} denote two different relay sets and: $A_{\mathcal{X}} \triangleq \tilde{E}_0 \sum_{i \in \mathcal{X}} \alpha_{0i}$, $B_{\mathcal{X}} \triangleq \sum_{i \in \mathcal{X}} \tilde{E}_i \beta_i$ and $D_{\mathcal{X},\mathcal{Y}} \triangleq \sum_{i \in \mathcal{X}} \tilde{E}_i \sum_{j \in \mathcal{Y}} \alpha_{i,j}$. Then, the capacity associated with a given cut-set \mathcal{S} in (5.60) is written as

$$\tilde{C}_{E_S} = \tilde{E}_0 \alpha_0 + A_{\mathcal{S}^c} + B_{\mathcal{S}} + D_{\mathcal{S},\mathcal{S}^c}. \quad (5.74)$$

In order to operate with these definitions, the following notation is used:

$$\sum_{j \in \mathcal{X} - \mathcal{Y}} \alpha_{i,j} = \sum_{j \in \mathcal{X}} \alpha_{i,j} - \sum_{j \in \mathcal{Y}} \alpha_{i,j}. \quad (5.75)$$

5.C.1 Proof of Lemma 5.1

The proof consists of finding necessary conditions that allow two capacity limits $\tilde{C}_{E_{\mathcal{S}_1}}, \tilde{C}_{E_{\mathcal{S}_2}}$ in (5.59) with $\mathcal{S}_1, \mathcal{S}_2 \subseteq \mathcal{T}$ to hold with equality simultaneously. Consider that all the relays in $\mathcal{S}_1 \cup \mathcal{S}_2$ transmit power $\tilde{E}_i > 0$ and define the following sets: $\mathcal{X} = \mathcal{S}_1 \cap \mathcal{S}_2$, $\mathcal{Z} = \mathcal{S}_1 \cup \mathcal{S}_2$, $\Omega_1 = \mathcal{S}_1 \cap \mathcal{S}_2^C$ and $\Omega_2 = \mathcal{S}_2 \cap \mathcal{S}_1^C$. The condition on the capacity cuts in (5.59) requires

$$\tilde{C}_{E_{\mathcal{S}_1}} = \tilde{C}_{E_{\mathcal{S}_2}}, \quad (5.76a)$$

$$\tilde{C}_{E_{\mathcal{S}_1}} \leq \tilde{C}_{E_{\mathcal{Z}}}, \quad (5.76b)$$

$$\tilde{C}_{E_{\mathcal{S}_1}} \leq \tilde{C}_{E_{\mathcal{X}}}. \quad (5.76c)$$

Equation (5.76a) forces the conditions associated with \mathcal{S}_1 and \mathcal{S}_2 to hold with equality. Conditions (5.76b) and (5.76c) must be fulfilled, since $\mathcal{Z}, \mathcal{X} \subseteq \mathcal{T}$. From the equality condition (5.76a), we have

$$A_{\mathcal{S}_1^C - \mathcal{S}_2^C} + B_{\mathcal{S}_1 - \mathcal{S}_2} = D_{\mathcal{S}_2, \mathcal{S}_2^C} - D_{\mathcal{S}_1, \mathcal{S}_1^C}. \quad (5.77a)$$

Using equation (5.77a) and $\mathcal{Z} = \mathcal{S}_1 + \mathcal{S}_2 - \mathcal{X}$, inequality (5.76b) can be rewritten as

$$B_{\mathcal{S}_1 - \mathcal{X}} - A_{(\mathcal{S}_1 - \mathcal{X})} \geq D_{\mathcal{S}_2, \mathcal{S}_2^C} - D_{\mathcal{S}_1 + \mathcal{S}_2 - \mathcal{X}, T - (\mathcal{S}_1 + \mathcal{S}_2 - \mathcal{X})} \quad (5.78)$$

and inequality (5.76c) as

$$B_{\mathcal{S}_1 - \mathcal{X}} - A_{\mathcal{S}_1 - \mathcal{X}} \leq D_{\mathcal{X}, \mathcal{X}^C} - D_{\mathcal{S}_1, \mathcal{S}_1^C}. \quad (5.79)$$

Finally, since (5.78) and (5.79) should be accomplished it is necessary that

$$D_{\mathcal{X}, \mathcal{X}^C} - D_{\mathcal{S}_1, \mathcal{S}_1^C} \geq D_{\mathcal{S}_2, \mathcal{S}_2^C} - D_{\mathcal{S}_1 + \mathcal{S}_2 - \mathcal{X}, T - (\mathcal{S}_1 + \mathcal{S}_2 - \mathcal{X})}. \quad (5.80)$$

Using now auxiliary sets Ω_1, Ω_2 and replacing $\mathcal{S}_1 = \mathcal{X} + \Omega_1$ and $\mathcal{S}_2 = \mathcal{X} + \Omega_2$, these conditions can be fulfilled only if $0 \geq D_{\Omega_1, \Omega_2} + D_{\Omega_2, \Omega_1}$. This last condition implies that either relays in Ω_1, Ω_2 transmit no power, which cannot occur by the assumption $\tilde{E}_i > 0$, or that one of the sets Ω_1, Ω_2 is empty. In that case, \mathcal{S}_1 or \mathcal{S}_2 are one included, totally, inside the other.

5.C.2 Primal KKT Condition

In this section, we show that the primal KKT condition $t < \tilde{C}_{E_S}$ for all $S \subseteq \pi$ is satisfied. Let π be an ordered set with a feasible solution to $\tilde{C}_{E_{\mathcal{S}_0}} = \tilde{C}_{E_{\mathcal{S}_i}}$, with $\mathcal{S}_0 = \pi^C$ and $\mathcal{S}_i = \pi_i^C$ for

all $i \in [0, 1, \dots, T]$. We must show that for any set $\mathcal{S}^C \neq \pi_i^C$, the KKT condition $\tilde{C}_{E_{\mathcal{S}_0}} < \tilde{C}_{E_{\mathcal{S}^C}}$ is satisfied. Using the notation in (5.74), we have

$$A_{\mathcal{S}^C} < B_{\mathcal{S}^C} + D_{\mathcal{S}^C \mathcal{S}}, \quad (5.81a)$$

$$A_{\pi_i^C} = B_{\pi_i^C} + D_{\pi_i^C \pi}. \quad (5.81b)$$

Since $i = \pi_{i-1} \cap \pi_i$, with $\pi_{T+1} = \emptyset$ any set \mathcal{S} can be written as

$$\mathcal{S} = \bigcup_{i \in \mathcal{S}} (\pi_{i-1} \cap \pi_i) \quad (5.82)$$

or equivalently, using previous notation, $\mathcal{S} = \sum_{i \in \mathcal{S}} (\pi_{i-1} - \pi_i)$. Substituting (5.82) into (5.81a) we get

$$A_{\pi} - \sum A_{(\pi_{i-1} - \pi_i)} < B_{\pi} - \sum B_{(\pi_{i-1} - \pi_i)} + D_{\mathcal{S}^C \mathcal{S}}. \quad (5.83)$$

Using the equality (5.81b), and $\pi_{i-1} - \pi_i = i$ after some manipulations we get

$$\sum_{i \in \mathcal{S}} D_{\pi_i^C, i} - \sum_{i \in \mathcal{S}} D_{i, \pi_i} < D_{\mathcal{S}^C \mathcal{S}} \quad (5.84)$$

Using $D_{\mathcal{S}^C \mathcal{S}} = \sum_{i \in \mathcal{S}} D_{\mathcal{S}^C, i}$ and $\mathcal{S}^C = \pi - \mathcal{S}$, the inequality (5.84) reads

$$\sum_{i \in \mathcal{S}} D_{i, \mathcal{S}} < \sum_{i \in \mathcal{S}} D_{\pi_i, i} + \sum_{i \in \mathcal{S}} D_{i, \pi_i}. \quad (5.85)$$

Let i_{\min} denote the lowest element in \mathcal{S} according to π ; then the following equivalence exists

$$\sum_{i \in \mathcal{S}} D_{\pi_i, i} = \sum_{i \in \pi_{i_{\min}}^C} D_{i, \mathcal{S} \cap \pi_i^C}, \quad (5.86a)$$

$$> \sum_{i \in \mathcal{S}} D_{i, \mathcal{S} \cap \pi_i^C}. \quad (5.86b)$$

Using this equivalence, inequality (5.85) satisfies

$$\sum_{i \in \mathcal{S}} D_{i, \mathcal{S}} < \sum_{i \in \mathcal{S}} D_{i, (\mathcal{S} \cap \pi_i^C + \pi_i)}. \quad (5.87)$$

Finally, since $\mathcal{S} \cap \pi_i^C + \pi_i = \mathcal{S} \cap \pi_i^C + \pi_i \cap (\mathcal{S} + \mathcal{S}^C) = \mathcal{S} + \pi_i \cap \mathcal{S}^C \supset \mathcal{S}$, and all the nodes transmit power, condition (5.87) is always satisfied.

Chapter 6

Conclusions

This dissertation has studied cooperative wireless communications in the energy efficient regime. We have considered three basic channels: the relay channel, the cooperative multiple access channel, and the multi-hop multiple relay channel. These channels capture the essence of user cooperation and serve as primary building blocks for cooperation on a larger scale.

Even for the simplest one, the relay channel, the capacity is not known today. Therefore, we have mainly focused on studying spectral efficiencies achievable with decode and forward (DF) protocols and capacity upper bounds derived with the cut-set bound.

First, for each of the cooperative channels studied, we have designed several communication strategies to accommodate different capabilities or constraints at terminals, such as: the distributed *phase synchronization* among terminals, that allows terminals to transmit signals that add coherently at the destination; the *full-duplex* transmission mode, that allows a relay to transmit and receive simultaneously in the same bandwidth; the *channel access via superposition*, that jointly with a receiver able to cope with inter-user interference, allows the source and the relay to transmit simultaneously; and the *accumulative* capability, that allows receivers to use multiple received signals to decoded the message.

Then, the energy efficient regime of these transmission strategies was studied using the low power metrics introduced by Verdú in [1]: *i*) the maximum rate per energy (RPE) and *ii*) the slope of the spectral efficiency as a function of the energy per bit. The former indicates the

minimum energy we need to dedicate to each transmitted bit to have a reliable communication, whereas the later indicates the bandwidth efficiency of the communication strategy.

Using these metrics, we *analyzed* the benefits provided by each of the terminal capabilities considered and, *designed* the network resources and the transmission strategy degrees of freedom according to the channel state information (CSI). We have found solutions to: the power allocation among terminals, the relay selection and ordering (route).

Chapter 3, has studied the relay channel (RC), where a source communicates with a destination aided by a dedicated relay.

First, we found simple conditions to determine that the low power regime is the energy efficient regime for the capacity bounds studied. These conditions were shown to be sufficiently general to determine the energy efficient regime of more involved scenarios such as the cooperative multiple access channel in Chapter 4 or the multiple relay multi-hop channel in Chapter 5.

Then, the low power analysis tools were applied to the RC to investigate the gains provided by *synchronism*, *duplexing* and *superposition channel access* capabilities.

- i) We showed that *synchronous* transmissions are necessary to obtain the maximum RPE but can be achieved with a relay in *full duplex* (FD) or in *half duplex* (HD) mode. In addition, we observed that obtaining the maximum RPE is possible, even without optimizing the time-sharing degrees of freedom of the HD case and considering a linear dependence of the power allocated to each node as a function of the total power.
- ii) The suboptimality of the HD mode was determined computing the slope of the spectral efficiency. It was shown that a system in HD mode needs up to (50%) more of the minimum bandwidth needed in FD mode.
- iii) Regarding the *channel access*, we showed that for *asynchronous* transmissions, the orthogonal channel access is optimal in terms of the maximum RPE for FD and HD relays and also in terms of the slope for HD relays.

The analysis was extended to ergodic fading channels to assess the impact of the channel fading distribution. In particular, we showed, how the peakiness (kurtosis) of the channel amplitude impacts on the the spectral efficiency. Finally, the analysis was extended to non-regenerative relaying strategies such as *amplify and forward* and *compress and forward*. It was shown that for these strategies the energy efficient regime is no longer the low power regime and the suitability of using these techniques in the energy efficient regime was discussed in detail.

Chapter 4 has studied the multiple-access channel with cooperative users (CMAC), where two nodes cooperate with each other in transmitting information to a common destination.

In addition to the capabilities considered for the RC, we studied the gain provided by *jointly coding*, via superposition, the own generated data and the cooperative data, instead of transmitting them as separated data flows.

To introduce these capabilities into the CMAC, we have designed coding schemes and found the associated spectral efficiency regions. This was possible by introducing orthogonal transmission intervals on which either: *i) jointly encoding* the own and the cooperative data is not allowed (*data flow separation*), *ii) users can not transmit and receive simultaneously (duplexing)*, or *iii) only one user can use the channel but can jointly encode* the own and the cooperative data (*time-division with jointly-coding*).

The gains obtained by *joint coding* and simultaneous transmissions capabilities were found computing the slope of the users spectral efficiencies with the energy per bit. We found that, while *joint coding* only provides significant gains combined with the FD capability, the FD capability always pays off.

Finally, **Chapter 5** has studied the multi-hop multiple relay channel, where a source communicates with a destination aided by several relay nodes that listen to all the transmissions. In this case, we constrained the analysis to *asynchronous* and *orthogonal transmissions*.

We studied several DF-like protocols depending on whether all the relays decode the source message (*allcast*) or only the destination (*unicast*), and depending on whether nodes use multiple received signals (*accumulative*) or only one signal (*non-accumulative*) to decoded the message. For each of these possibilities, we computed the maximum RPE and provided a joint solution to a set of problems traditionally belonging to different layers: energy allocation (physical), relay selection, and routing (network).

In particular, we studied three achievable strategies and two upper bounds on the unknown capacity of this channel:

- i) The first strategy studied was the traditional multi-hop network (TMH). For this strategy, we showed that the optimal power allocation among nodes only requires local CSI at the relays and that the optimal route can be obtained in a distributed manner.
- ii) Then, a *allcast* and *accumulative* cooperative multi-hop strategy (ACMH), where all relays were required to decode the source message by properly combining all the received signals was studied. In this case, we found that all relays required global network CSI to optimally allocate the power resources. Furthermore, the relay selection and routing solutions found for this channel do not admit a distributed structure.
- iii) To maintain the TMH distributed properties while obtaining the *accumulative* gain at destination, a *unicast* strategy with *non-accumulative* relays was investigated (UCMH). We showed that, compared to *allcast* networks, the *unicast* network has similar performance

while offering a more attractive distributed nature. More specifically, we showed that this strategy does not require global CSI and has also low complexity optimal relay selection and routing solutions.

- iv) Then, we found an upper-bound only valid for DF-like protocols. The maximum RPE for this upper bound was shown to be very close to the one obtained for the *allcast* and *unicat* achievable strategies.
- v) Finally, a second upper bound, using the cut-set bound, valid for any type of relays, was studied. Interestingly, similar to TMH and UCMH networks, the maximum RPE solution to this upper bound presents a distributed nature.

6.1 Future Work

The most important extensions to the work conducted in this dissertation are discussed below. We identify two main branches: *i)* additional studies for the scenarios already addressed in this work: relay channel, cooperative MAC, and cooperative multi-hop and *ii)* applying the energy efficiency analysis to new cooperative scenarios.

6.1.1 Studied Scenarios

Non-Regenerative Forwarding Protocols

It is needed a better understanding of the energy efficient regime for non-regenerative forwarding protocols such as: compress and forward, amplify and forward and linear relaying [64,99]. An initial analysis of these strategies has been conducted in Chapter 3. However, the study developed there is limited to the relay channel and does not discuss the impact of the relay capabilities: duplexing, synchronism, etc...

To study the energy efficient regime of these strategies, the low power analysis tools are not helpful. As a result, we have not been able to find close form expression to the maximum RPE or to the optimal energy allocation as a function of the channel gains. Additional work is needed to find good approximations for the spectral efficiency of these communication schemes that capture the essence of these non-regenerative protocols while providing insightful solutions.

Multi-hop Forwarding Protocols

Even in the case of regenerative relays, further investigation is required to find better multi-hop coding strategies. An interesting starting point is the *structured decode and forward* group

of strategies presented in [54]. The study of these strategies would include: *i*) obtaining the maximum RPE for the up to N hops network, where each node listens up to N previous transmissions and *ii*) finding message tree structures with appealing energy allocation and routing solutions.

Channel Model and Degree of CSI

The extension of our work to more general channel models (ergodic and block fading) and degrees of CSI (global, local) was already discussed in the introduction Chapter 1.2.2 and is not repeated here. An additional extension, not included there, is the study of the robustness of cooperation against the channel state uncertainty at the transmitters. In Chapter 5, we have shown that the gains in maximum RPE obtained with sophisticated cooperative multi-hop strategies are relatively small with respect to the maximum RPE obtained by the simple traditional multi-hop strategy. The main reason is that we can allocate the resources perfectly. We believe that if the channel is not known perfectly at the transmitters, the additional number of links used in more advanced cooperative strategies should bring important gains to the system.

Validity of the Solution

For the three scenarios studied, we have found solutions to the resource allocation, relay selection and ordering. These solutions are valid for the regime where the energy goes to 0, $E \rightarrow 0$. The discussion of the validity of these solutions as the energy increases has been initiated for the relay channel in Chapter 3. We have shown that the results are valid for a wide-range of $\frac{E_b}{N_0}$. Nonetheless, for multi-hop relay networks several we do not know how does it change the resource allocation, node selection and optimal route as the energy increases. The tools used in [73] to study the spectral efficiency of multi-hop at low and high SNR could be useful for this purpose.

Practical Coding Strategies

We have assumed Gaussian signaling for the inputs to the channel. This choice is optimal for fixed channel gains in point to point communications [40] [13], and also for the relay channel under the decode and forward protocol [20]. The performance losses incurred by suboptimal BPSK and QPSK modulations schemes can be quantified using the low power analysis tools as shown in [1].

Of important interest is also the study of pragmatic code constructions for relaying and cooperation. Low Density Parity Check codes (LDPC), have recently attracted special interest [45, 100]. These codes emulate random coding strategies used in information theoretic

achievability proofs, have a simple factor graph representation, and low complexity belief propagation decoding.

6.1.2 New Scenarios

The Cooperative Broadcast Channel

The cooperative broadcast channel (CBC) is not specifically addressed in our work. The reason is that under the energy efficiency metrics employed this channel always reduces to either the non-cooperative broadcast channel or the relay channel studied in Chapter 3.

The three nodes CBC consists of one source transmitting a common message to two destinations terminals, which can cooperate. Compared to the (also three nodes) dedicated relay channel the differences strives in that:

- In the RC, the relay is not required to decode the source message entirely. Whereas, for the CBC both destinations have to decode the message completely.
- In the RC, there is always one node (the destination) that never cooperates. Whereas for the CBC both destinations can cooperate.

Our main focus is on regenerative relaying. In that case, the energy efficiency study conducted for the RC reveals that even if the relay is allowed to decode only a part of the source message¹ to cooperate, the relay is always required to either completely decode the source message or not cooperate at all.

The immediate consequence of these results is the differences between the RC and the CBC vanishes in the case of regenerative relaying. Although both destinations can cooperate in the CBC only one cooperates since cooperation implies decoding the message, and once a destination decodes the message the other destination can not aid the communication. Consequently, the CBC reduces to a relay channel if one destination cooperates and to the non-cooperative broadcast channel if non of the nodes cooperate.

It worth mentioning that, there are other cooperative broadcast channel that could certainly be of interest: *i*) the cooperative broadcast channel with common and individual information [101, 102] and *ii*) the cooperative broadcast channel with non-regenerative relaying strategies. In that case, technique based on successive refinement among the cooperative receivers can be useful [103].

¹Relaying by decoding only a part of the message instead of the complete message is possible with FD nodes by using the generalized block Markov strategy presented in [28] and studied in the energy efficiency in [64] and for HD nodes, by using the relaying strategy presented in [20] which we studied in Chapter 3.

Multi-Source, Multi-Destination, Multi-Relay Wireless Networks

The ultimate goal is to consider networks with multiple nodes that can work as sources, destinations or relays. The capacity of these networks has been investigated in several recent works [80, 81, 104–106].

Optimizing the transmission strategies for these general networks is a challenging problem. Initial scenarios towards the analysis of these general networks can be:

- The cooperative multi-access channel with N sources that cooperates to transmit their messages to a single destination. Probably, the simplest multiple cooperative sources scenario can be designed using the data flow separation strategy, that we introduce in Chapter 4. In this strategy, the total transmission slot is divided into multiple orthogonal transmissions. For each orthogonal transmission, there is only one source-destination pair and all the other nodes are potential relays. Any new transmission strategy designed for this channel should include simultaneous transmissions between sources: FD capabilities and *joint coding* techniques.
- The relay-interferer channel (RIC). In networks with multiple source-destination pairs, the channel output at any destination receiver consists of both the desired signal and interference. The RIC is the simplest network model that captures the impact of interference in relaying networks [107]. This channel consist a source, a destination, a relay and a interference from a known codebook listened to at the relay and the destination.

In addition, the power efficiency analysis of sensory and ad-hoc wireless networks with multiple sources and destinations has been initiated in [35]. Extensions of this work are possible by considering the advanced cooperative multi-hop techniques studied in Chapter 5.

Bibliography

- [1] S. Verdú, “Spectral efficiency in the wideband regime,” *IEEE Trans. Inform. Theory*, vol. 48, no. 8, pp. 1319–1343, June 2002.
- [2] A. Sendonaris, E. Erkip, and B. Aazhang, “User cooperation diversity-part I: System description,” *IEEE Trans. Commun.*, vol. 51, no. 11, pp. 1927–1938, Nov. 2003.
- [3] J. G. Proakis, *Digital Communications*, New York: MacGraw-Hill, 2001.
- [4] S. Alamouti, “A simple transmit diversity technique for wireless communications,” *IEEE J. Select. Areas Commun.*, vol. 16, no. 8, pp. 1451–1458, Oct 1998.
- [5] V. Tarokh, N. Seshadri, and A. Calderbank, “Space-time codes for high data rate wireless communication: performance criterion and code construction,” *IEEE Trans. Inform. Theory*, vol. 44, no. 2, pp. 744–765, Mar 1998.
- [6] V. Tarokh, H. Jafarkhani, and A. Calderbank, “Space-time block codes from orthogonal designs,” *IEEE Trans. Inform. Theory*, vol. 45, no. 5, pp. 1456–1467, Jul 1999.
- [7] E. Larsson and P. Stoica, *Space-Time Block Coding for Wireless Communications*, Cambridge University Press, 2003.
- [8] M. Dohler, *Virtual Antenna Arrays, PhD Dissertaion*, King’s College London, UK, 2003.
- [9] J. N. Laneman, D. N. C. Tse, and G. W. Wornell, “Cooperative diversity in wireless networks: Efficient protocols and outage behavior,” *IEEE Trans. Inform. Theory*, vol. 50, no. 12, Dec. 2004.
- [10] R. U. Nabar, H. Bölcskei, and F. W. Kneubühler, “Fading relay channels: Performance limits and space-time signal design,” *IEEE J. Select. Areas Commun.*, vol. 22, no. 6, pp. 1099–1109, Aug. 2004.
- [11] J. N. Laneman and G. W. Wornell, “Distributed space-time-coded protocols for exploiting cooperative diversity in wireless networks,” *IEEE Trans. Inform. Theory*, vol. 49, no. 10, pp. 2415–2425, 2003.

- [12] D. Tse and P. Viswanath, *Fundamentals of Wireless Communication*, Cambridge University Press, 2005.
- [13] I. E. Telatar., "Capacity of multi-antenna gaussian channels," *Europ. Transn. Telecommun.*, vol. 10, pp. 585–596, Nov. 1999.
- [14] A. Scaglione, D. Goeckel, and J. Laneman, "Cooperative communications in mobile ad hoc networks," *IEEE Signal Processing Mag.*, vol. 23, no. 5, pp. 18–29, 2006.
- [15] A. Nosratinia, T. Hunter, and A. Hedayat, "Cooperative communication in wireless networks," *IEEE Commun. Mag.*, vol. 42, no. 10, pp. 74–80, 2004.
- [16] T. Cover and J. A. Thomas, *Elements of Information Theory*, New York: Wiley, 1991.
- [17] M. Khojastepour, A. Sabharwal, and B. Aazhang, "Lower bounds on the capacity of gaussian relay channel," in *Proc. Conference on Information Science and Systems (CISS)*, Mar. 2004.
- [18] D. M. Pozar, *Microwave Engineering*, New York: Wiley, 1998.
- [19] S. Chen, M. Beach, and J. McGeehan, "Division-free duplex for wireless applications," *Electronics Letters*, vol. 34, no. 2, pp. 147–148, Jan 1998.
- [20] A. Host-Madsen and J. Zhang, "Capacity bounds and power allocation for the wireless relay channel," *IEEE Trans. Inform. Theory*, vol. 51, no. 6, pp. 2020–2040, June 2005.
- [21] M. Khojastepour, A. Sabharwal, and B. Aazhang, "On the capacity of "cheap" relay networks," in *Proc. Conference on Information Science and Systems (CISS)*, Mar. 2003.
- [22] H. Weingarten, Y. Steinberg, and S. Shamai, "The capacity region of the gaussian multiple-input multiple-output broadcast channel," *IEEE Trans. Inform. Theory*, vol. 52, no. 9, pp. 3936–3964, Sept. 2006.
- [23] L. Zheng, D. N. C. Tse, and M. Medard, "Channel coherence in the low-SNR regime," *IEEE Trans. Inform. Theory*, vol. 53, no. 3, pp. 976–997, Mar. 2007.
- [24] M. R. Bhatnagar and A. Hjørungnes, "Double differential modulation for decode-and-forward cooperative communications," *IEEE International Conference on Signal Processing and Communications (ICSPC)*, pp. 45–48, Nov. 2007.
- [25] B. Holchwald and W. Sweldens, "Differential unitary space-time modulation," *IEEE Trans. Commun.*, vol. 48, no. 12, pp. 2042–2052, Dec. 2000.
- [26] W. Shiroma and M. P. D. Lisio, *Quasioptical circuits*, New York: Wiley, 1999.

- [27] R. Mudumbai, D. Brown Iii, U. Madhow, and H. Poor, "Distributed transmit beamforming: challenges and recent progress," *IEEE Commun. Mag.*, vol. 47, no. 2, pp. 102–110, February 2009.
- [28] T. M. Cover and A. E. Gamal, "Capacity theorems for the relay channel," *IEEE Trans. Inform. Theory*, vol. 25, no. 5, p. 572, Sept. 1979.
- [29] Z. Zhang and T. Duman, "Capacity-approaching turbo coding and iterative decoding for relay channels," *IEEE Trans. Commun.*, vol. 53, no. 11, pp. 1895–1905, Nov. 2005.
- [30] G. Yue, X. Wang, Z. Yang, and A. Host-Madsen, "Coding schemes for user cooperation in low-power regimes," *IEEE Trans. Signal Processing*, vol. 56, no. 5, pp. 2035–2049, May 2008.
- [31] J. Andrews, S. Shakkottai, R. Heath, N. Jindal, M. Haenggi, R. Berry, D. Guo, M. Neely, S. Weber, S. Jafar, and A. Yener, "Rethinking information theory for mobile ad hoc networks," *IEEE Commun. Mag.*, vol. 46, no. 12, pp. 94–101, December 2008.
- [32] Z. Alliance, www.zigbee.org, latest version.
- [33] S. Valentin, H. S. Lichte, H. Karl, G. Vivier, S. Simoens, A. A. J. Vidal, and I. Aad, "Co-operative wireless networking beyond store-and-forward: Perspectives for phy and mac design," in *Proceedings of the 17th Wireless World Research Forum Meeting (WWRF)*, Nov. 2006.
- [34] A. Ephremides, "Energy concerns in wireless networks," *IEEE Trans. Wireless Commun.*, vol. 9, no. 4, pp. 48–59, Aug. 2002.
- [35] A. Dana and B. Hassibi, "On the power efficiency of sensory and ad hoc wireless networks," *IEEE Trans. Inform. Theory*, vol. 52, no. 7, pp. 2890–2914, July 2006.
- [36] A. Goldsmith and S. Wicker, "Design challenges for energy-constrained ad-hoc wireless networks," *IEEE Trans. Wireless Commun.*, vol. 9, no. 4, pp. 8–27, Aug. 2002.
- [37] Y. Zhang and H. Dai, "Energy-efficiency and transmission strategy selection in cooperative wireless sensor networks," *Journal of communications and networks*, vol. 9, no. 4, pp. 1–9, Dec. 2007.
- [38] Y. Yuan, M. Chen, and T. Kwon, "A novel cluster-based cooperative mimo scheme for multi-hop wireless sensor networks," *EURASIP Journal on Wireless Communications and Networking*, p. 9, 2006.
- [39] D. Chen and J. N. Laneman, "The diversity-multiplexing tradeoff for the multiaccess relay channel," in *Proc. Conference in Information Sciences and Systems*, Princeton, NJ, USA, Apr. 2006.

- [40] A. Goldsmith, *Wireless Communications*. Cambridge University Press, 2005.
- [41] L. Ford and D. Fulkerson, *Flows in Networks*, Princeton University Press, 1962.
- [42] G. Caire, D. Tuninetti, and S. Verdú, “Suboptimality of TDMA in the low power regime,” *IEEE Trans. Inform. Theory*, vol. 50, no. 4, pp. 608–620, Apr. 2004.
- [43] Y. Yao, X. Cai, and G. B. Giannakis, “On energy efficiency and optimum resource allocation in wireless relay transmissions,” *IEEE Trans. Wireless Commun.*, vol. 4, no. 6, pp. 2917–2927, Nov. 2005.
- [44] L. Ozarow, S. Shamai, and A. Wyner, “Information theoretic considerations for cellular mobile radio,” *Vehicular Technology, IEEE Transactions on*, vol. 43, no. 2, pp. 359–378, May 1994.
- [45] G. Yue, X. Wang, Z. Yang, and A. Host-Madsen, “Coding schemes for user cooperation in low-power regimes,” *Signal Processing, IEEE Transactions on*, vol. 56, no. 5, pp. 2035–2049, May 2008.
- [46] A. Avestimehr and D. Tse, “Outage capacity of the fading relay channel in the low-SNR regime,” *IEEE Trans. Inform. Theory*, vol. 53, no. 4, pp. 1401–1415, Apr. 2007.
- [47] A. Bletsas, A. Khisti, D. Reed, and A. Lippman, “A simple cooperative diversity method based on network path selection,” *IEEE J. Select. Areas Commun.*, vol. 24, no. 3, pp. 659–672, March 2006.
- [48] O. Kaya and S. Ulukus, “Power control for fading cooperative multiple access channels,” *IEEE Trans. Wireless Commun.*, vol. 6, no. 8, pp. 2915–2923, August 2007.
- [49] A. Lozano, A. Tulino, and S. Verdu, “Multiple-antenna capacity in the low-power regime,” *IEEE Trans. Inform. Theory*, vol. 49, no. 10, pp. 2527–2544, Oct. 2003.
- [50] C. Shannon, “A mathematical theory of communication,” *Bell System Technical Journal*, vol. 27, pp. 379–423, 623–656, July-Oct. 1948.
- [51] M. C. Valenti and Zhao, “Capacity approaching distributed turbo codes for the relay channel,” in *Proc 57th IEE Semiannual Vehicular Technology Conf: VTC’03-Spring*, Korea, Apr. 2003.
- [52] M. Costa, “Writing on dirty paper,” *IEEE Trans. Inform. Theory*, vol. 29, no. 3, pp. 439–441, May 1983.
- [53] M. Gastpar, G. Kramer, and P. Gupta, “The multiple-relay channel: Coding and antenna-clustering capacity,” in *IEEE Int. Symp. Information Theory (ISIT)*, Lausanne, Switzerland, July 2002, p. 136.

- [54] P. Razaghi and W. Yu, "Parity forwarding for multiple-relay networks," *IEEE Trans. Inform. Theory*, 2009.
- [55] S.-Y. Li, R. Yeung, and N. Cai, "Linear network coding," *IEEE Trans. Inform. Theory*, vol. 49, no. 2, pp. 371–381, Feb. 2003.
- [56] A. B. Carleial, "Multiple-access channels with different generalized feedback signals," *IEEE Trans. Inform. Theory*, vol. IT-28, no. 6, pp. 841–850, Nov. 1982.
- [57] F. Willems and E. van der Meulen, "The discrete memoryless multiple-access channel with cribbing encoders," *IEEE Trans. Inform. Theory*, vol. 31, no. 3, pp. 313–327, May 1985.
- [58] C.-M. Zeng, F. Kuhlmann, and A. Buzo, "Achievability proof of some multiuser channel coding theorems using backward decoding," *IEEE Trans. Inform. Theory*, vol. 35, no. 6, pp. 1160–1165, Nov 1989.
- [59] A. Avestimehr and D. Tse, "Outage-optimal relaying in the low SNR regime," in *Proc. IEEE Int. Symp. Information Theory*, Sept. 2005, pp. 941–945.
- [60] A. E. Gamal and S. Zahedi, "Minimum energy communication over a relay channel," in *Proc. IEEE Int. Symp. Information Theory*, Yokohama, Japan, June 2003.
- [61] X. Cai, Y. Yao, and G. Giannakis, "Achievable rates in low-power relay links over fading channels," *IEEE Trans. Commun.*, vol. 53, no. 1, pp. 184–194, Jan. 2005.
- [62] E. V. der Meulen, "Three-terminal communication channels," *Advanced Applied Probability*, vol. 3, pp. 120–154, Dec. 1971.
- [63] A. Reznik, S. R. Kulkarni, and S. Verdú, "Degraded Gaussian multirelay channel: capacity and optimal power allocation." *IEEE Trans. Inform. Theory*, vol. 50, no. 12, pp. 3037–3046, Dec. 2004.
- [64] A. E. Gamal, M. Mohseni, and S. Zahedi, "Bounds on capacity and minimum energy-per-bit for AWGN relay channels." *IEEE Trans. Inform. Theory*, vol. 52, no. 4, pp. 1545–1561, Apr. 2006.
- [65] G. Kramer, "Models and theory for relay channel with receive constraints," in *Proc. 42nd Allerton Conference on communications, Control and Computing*, Allerton, IL, Sept. 2004.
- [66] T. F. Wong, T. M. Lok, and J. M. Shea, "Half-duplex cooperative transmission for the relay channel with flow optimization," in *Proc. Conference on Information Science and Systems (CISS)*, Mar. 2007, pp. 402 – 407.

- [67] R. C. King, *Multiple access channels with generalized feedback*, Ph.D. Dissertation, Stanford Univ., Palo Alto, CA, 1978.
- [68] A. Sendonaris, E. Erkip, and B. Aazhang, "User cooperation diversity-part II: Implementation aspects and performance analysis," *IEEE Trans. Commun.*, vol. 51, no. 11, pp. 1939–1948, Nov. 2003.
- [69] Z. Yang and A. Host-Madsen, "Rateless coded cooperation for multiple-access channels in the low power regime," in *Information Theory, 2006 IEEE International Symposium on*, July 2006, pp. 967–971.
- [70] L. Ozarow, "The capacity of the white Gaussian multiple access channel with feedback," *IEEE Trans. Inform. Theory*, vol. 30, no. 4, pp. 623–629, July 1984.
- [71] A. Reznik, S. Kulkarni, and S. Verdú, "Broadcast-relay channel: capacity region bounds," in *Proc. IEEE Int. Symp. Information Theory*, 4-9 Sept. 2005, pp. 820–824.
- [72] I. Maric and R. Yates, "Efficient multihop broadcast for wideband systems," in *Proc. Allerton Conf. on Comm. Cont. Comp.*, Oct. 2002.
- [73] O. Oyman and S. Sandhu, "Non-ergodic power-bandwidth tradeoff in linear multi-hop networks," in *Proc. IEEE Int. Symp. Information Theory*, July 2006, pp. 1514–1518.
- [74] M. Sikora, J. Laneman, M. Haenggi, D. Costello, and T. Fuja, "Bandwidth- and power-efficient routing in linear wireless networks," *IEEE Trans. Inform. Theory*, vol. 52, no. 6, pp. 2624–2633, June 2006.
- [75] I. Maric and R. Yates, "Cooperative multihop broadcast for wireless networks," *IEEE J. Select. Areas Commun.*, vol. 22, no. 6, pp. 1080–1088, Aug. 2004.
- [76] ———, "Cooperative multihop broadcast for wireless networks," *IEEE J. Select. Areas Commun.*, vol. 22, no. 6, pp. 1080–1088, Aug. 2004.
- [77] J. Chen, L. Jia, X. Liu, G. Noubir, and R. Sundaram, "Minimum energy accumulative routing in wireless networks," in *Proc. IEEE Int. Conference on Computer Communications (INFOCOM)*, vol. 3, Mar. 2005, pp. 1875 – 1886.
- [78] A. Molisch, N. Mehta, J. Yedidia, and J. Zhang, "Cooperative relay networks using fountain codes," in *Global Telecommunications Conference, 2006. GLOBECOM '06. IEEE*, 27 2006-Dec. 1 2006, pp. 1–6.
- [79] J. Castura and Y. Mao, "Rateless coding over fading channels," *Communications Letters, IEEE*, vol. 10, no. 1, pp. 46–48, Jan 2006.
- [80] P. Gupta and P. R. Kumar, "Towards an information theory of large networks: An achievable rate region," *IEEE Trans. Inform. Theory*, vol. 49, no. 8, pp. 1877–1894, Aug. 2003.

- [81] ———, “A network information theory for wireless communication: Scaling laws and optimal operation,” *IEEE Trans. Inform. Theory*, vol. 50, no. 5, pp. 748–767, May 2004.
- [82] J. Boyer, D. Falconer, and H. Yanikomeroglu, “Multihop diversity in wireless relaying channels,” *IEEE Trans. Commun.*, vol. 52, no. 10, pp. 1820–1830, Oct. 2004.
- [83] A. Ribeiro, X. Cai, and G. Giannakis, “Symbol error probabilities for general cooperative links,” *IEEE Trans. Wireless Commun.*, vol. 4, no. 3, pp. 1264–1273, May 2005.
- [84] G. Kramer, M. Gastpar, and P. Gupta, “Cooperative strategies and capacity theorems for relay networks,” *IEEE Trans. Inform. Theory*, vol. 51, no. 9, pp. 3037 – 3063, Sept. 2005.
- [85] M. Gastpar and M. Vetterli, “On the capacity of large gaussian relay networks,” *IEEE Trans. Inform. Theory*, vol. 51, no. 3, pp. 765–779, Mar. 2005.
- [86] D. Chen, M. Haenggi, and J. Laneman, “Distributed spectrum-efficient routing algorithms in wireless networks,” *IEEE Trans. Wireless Commun.*, vol. 7, no. 12, pp. 5297–5305, December 2008.
- [87] O. Oyman, N. Laneman, and S. Sandhu, “Multihop relaying for broadband wireless mesh networks: From theory to practice,” *IEEE Commun. Mag.*, vol. 45, no. 11, pp. 116–122, Nov. 2007.
- [88] B. Schein and R. Gallager, “The gaussian parallel relay network,” in *Proc. IEEE International Symposium on Information Theory*, Sorrento, Italy, June 2000, p. 22.
- [89] B. Schein, *Distributed coordination in network information theory*, Phd Dissertation, Massachusetts Institute of Technology, 2003.
- [90] I. Maric and R. Yates, “Forwarding strategies for Gaussian parallel-relay networks,” in *Proc. International Symposium On Information Theory*, Chicago, IL, USA.
- [91] ———, “Bandwidth and power allocation for cooperative strategies in Gaussian relay networks,” in *Thirty-Eighth Asilomar Conference on Signals, Systems and Computers*, Nov. 2004, pp. 1912–1916.
- [92] L.-L. Xie and P. R. Kumar, “An achievable rate for the multiple-level relay channel,” *IEEE Trans. Inform. Theory*, vol. 51, pp. 1348 – 1358, Apr. 2005.
- [93] Z. Yang, J. Liu, and A. Host-Madsen, “Cooperative routing and power allocation in ad-hoc networks,” in *Global Telecommunications Conference. GLOBECOM '05. IEEE*, vol. 5, 28 Nov.-2 Dec 2005.

- [94] Z. Yang and A. Host-Madsen, "Routing and power allocation in asynchronous gaussian multiple-relay channels," *EURASIP Journal on Wireless Communications and Networking*, p. 11, 2006.
- [95] R. Yim, N. Mehta, A. F. Molisch, and J. Zhang, "Progressive accumulative routing in wireless networks," in *Proc. IEEE Global Communications Conference (GLOBECOM)*, Nov. 2006, pp. 1 – 6.
- [96] S. Boyd and L. Vandenberghe, *Convex optimization*. Cambridge, U.K.: Cambridge Univ. Press, 2004.
- [97] P. Razaghi and W. Yu, "Parity-forwarding for multiple-relay networks," in *Proc. IEEE Int. Symp. Information Theory (ISIT)*, July 2006, pp. 1678–1682.
- [98] A. A. E. Gamal, "On information flow in relay networks," in *Proc. IEEE National Telecommunications Conf.*, vol. 2, Miami, FL, Nov. 1981, pp. D4.1.1–D4.1.4.
- [99] A. del Coso and C. Ibars, "Linear relaying for the multiple-access and broadcast channels," *IEEE Trans. Wireless Commun.*, 2008, to appear.
- [100] P. Razaghi and W. Yu, "Bilayer low-density parity-check codes for decode-and-forward in relay channels," *IEEE Trans. Inform. Theory*, vol. 53, no. 10, pp. 3723–3739, Oct. 2007.
- [101] S. Bhaskaran, "Gaussian degraded relay broadcast channel," *IEEE Trans. Inform. Theory*, vol. 54, no. 8, pp. 3699–3709, Aug. 2008.
- [102] Y. Liang and V. V. Veeravalli, "Cooperative relay broadcast channels," *IEEE Trans. Inform. Theory*, vol. 53, no. 3, pp. 900–928, 2007.
- [103] W. Equitz and T. Cover, "Successive refinement of information," *IEEE Trans. Inform. Theory*, vol. 37, no. 2, pp. 269–275, Mar 1991.
- [104] A. Host-Madsen, "Capacity bounds for cooperative diversity," *IEEE Trans. Inform. Theory*, no. 4, pp. 1522–1544.
- [105] V. Stankovic, A. Host-Madsen, and Z. Xiong, "Cooperative diversity for wireless ad hoc networks," *IEEE Signal Processing Mag.*, vol. 23, no. 5, pp. 37–49, Sept. 2006.
- [106] L.-L. Xie and P. Kumar, "Multisource, multideestination, multirelay wireless networks," *IEEE Trans. Inform. Theory*, vol. 53, no. 10, pp. 3586–3595, Oct. 2007.
- [107] R. Dabora, I. Maric, and A. Goldsmith, "Interference forwarding in multiuser networks," in *Global Telecommunications Conference, 2008. IEEE GLOBECOM 2008. IEEE*, 30 2008-Dec. 4 2008, pp. 1–5.